Heparan Sulfate 3-O-sulfation in renal fibrosis

Laura Ferreras

A thesis submitted in fulfilment of the requirements for the degree of Doctor of Philosophy

Institute of Cellular Medicine
Newcastle University
November 2018

Abstract

Chronic kidney disease globally affects 10% of the population with fibrosis being one of the hallmarks of disease progression. Renal fibrosis is characterised by a change in the extracellular matrix (ECM) that can lead to tissue remodelling and organ loss. Throughout this process the kidney is exposed to damaging cytokines and growth factors. Heparan Sulfate (HS) proteoglycans present on the ECM and cell membranes play a crucial role in protecting, storing and presenting these cytokines and growth factors to the surrounding cells. This study focuses on HS sulfation and the enzymes modulating it, particularly HS 3-O-sulfotransferases (HS3ST), in the context of renal fibrosis.

Initially, this work used an *in vivo* murine model of renal fibrosis to assess changes in HS sulfation during disease progression. The amount of HS total O-sulfation and particularly 2-O-sulfation were increased. HS 3-O-sulfation was localised on the basal membrane of tubules and more intensively on blood vessels and the glomerulus. In this model, the level of mRNA encoding HS3ST1, Sulfatase 1 and HS2ST1 was increased, whilst HS3ST3A was decreased. Amongst all enzymes studied, HS3ST1 displayed the strongest correlation with collagen deposition during fibrosis. The generation of renal epithelial cells overexpressing HS3ST1 enabled the identification of a differential signalling pattern of Heparin Binding Epidermal Growth Factor like growth factor (HB-EGF) in cells with higher HS 3-O-sulfation. Additionally, this project found that pro-fibrotic factors downregulated HS3ST1 expression in human renal epithelial cells and rat renal fibroblasts.

Finally, this project attempted to generate competing peptides and peptoids for Fibroblast Growth Factor 2 (FGF2) binding to renal epithelial cells. Although peptides and peptoids were found to bind to heparin by isothermal titration calorimetry, no binding competition was observed *in vitro*. However, the peptides and peptoids studied did emphasise the importance of secondary structure in the binding of HS to protein.

Overall this highlights the complexity of HS modification during fibrosis. This work emphasises the need to study HS3ST in inflammation as it seems to be a potential marker of fibrosis.

Declaration

I declare that no portion of the work compiled in this thesis has been submitted in support of any other degree or qualification at Newcastle University or any other university or institute of learning. The work has been carried out by myself unless otherwise stated. All sources of information have been acknowledged accordingly by means of reference.

Table of contents

List of Abbreviations

AKI	Acute Kidney Injuries
Akt	Protein kinase B
Arg	Arginine
ATP	Adenosine Triphosphate
AMP	Ampicillin
aHS	anticoagulant Heparan Sulfate
AT	Antithrombin III
Arg/R	Arginine
BSA	Bovine Serum Albumin
CBC	Comparative Biology Centre
CD-numbers	Cluster of Differentiation
CD	Circular Dichroism
ChPF	Chondroitin Polymerising Factor
CHO	Chinese Hamster Ovarian cells
CKD	Chronic Kidney Diseases
CMV	Cytomegalovirus
CTL	Control
CS	Chondroitin Sulfate
DAPI	4, 6-Diamidino-2-Phenylindole
Db/db	Diabetic mice
DEAE	Diethylaminoethyl
Deg	Degrees
DEPC	Diethyl Percarbonate
DIC	Diisopropylcarbodiimide
DMEM	Dulbecco's Modified Eagle Medium
DMF	Dimethylformamide
DMSO	Dimethyl Sulfoxide
DNA	Deoxyribonucleic Acid
DS	Dermatan Sulfate
ECM	Extracellular Matrix

EDTA	Ethylenediamintetraacetic Acid
ELISA	Enzyme-Linked Immunosorbent Assay
ER	Endoplasmic Reticulum
ERK	Extracellular signal-Regulated Kinase
ESRD	Early Stage Renal Diseases
EXT	Exostosin
EXTL	Exostosin Like
FACS	Fluorescence-Activated Cell Sorting
FAM	Fluorescein
FBS	Fetal Bovine Serum
FGF	Fibroblast Growth Factor
FGFR	Fibroblast Growth Factor Receptor
FITC	Fluorescein isothiocyanate
Fmoc	Fluorenylmethyloxycarbonyl
FSC	Forward Scatter Channel
G418	Geneticin
GAG	Glycosaminoglycan
Gal	Galactose
gD	glycoprotein D
GBM	Glomerular Basement Membrane
GlcA	Glucuronic Acid
GlcN	Glucosamine
GlcNAc	N-acetyl Glucosamine
HA	Hyaluronan
HAc	Acetic Acid
HAS	Hyaluronan Synthase
H&E	Haematoxylin and Eosin
HB-EGF	Heparin Binding epidermal growth factor like Growth Factor
HCl	Hydrochloric Acid
HCV	Hepatitis C Virus
HIV	Human Immunodeficiency Virus

HLA	Human Leukocyte Antigen
H_2O	water
HOBt	1-hydroxybenzotriazole
HPLC	High-Performance Liquid Chromatography
HPRT	Hypoxanthine-guanine phosphoribosyltransferase
HS	Heparan Sulfate
HS2ST	Heparan Sulfate 2-O-sulfotransferase
HS3ST	Heparan Sulfate 3-O-sulfotransferase
HS6ST	Heparan Sulfate 6-O-sulfotransferase
HSPG	Heparan Sulfate Proteoglycan
HSV	Herpes Simplex Virus
HUVEC	Human Umbilical Vein Endothelial Cell
IdoA	Iduronic Acid
IFN	Interferon
IFTA	Interstitial Fibrosis Tubular Atrophy
IL	Interleukin
IRI	Ischemia Reperfusion Injury
ITC	Isothermal Titration Calorimetry
Jak/Stat	Janus kinase/Signal Transducer and Activator of Transcription
KS	Keratan Sulfate
KO	Knocked Out
lbAT	labelled Antithrombin III
LB	Lysogeny Broth
LPS	lipopolysaccharides
Lys	lysine
MS	Mass Spectrometry
MALDI	Matrix Assisted Laser Desorption/Ionisation
MC	Mean of Control
MeCN	Acetonitrile
MOPS	3-(N-morpholino)propanesulfonic acid
MT	Mutated

MWCO	Molecular Weight Cut Off
NaCl	Sodium chloride
NADPH	Nicotinamide adenine dinucleotide phosphate
NDST	N-deacetylase/N-sulfotransferase
Ob/Ob	Obese mice
PAPS	3'Phosphoadenosine 5'-Phosphosulfate
Pbf	2,2,4,6,7-pentamethyldihydrobenzofuran-5-sulfonyl
PBS	Phosphate buffered Saline
PCR	Polymerase Chain Reaction
PDGF	Platelet Derived Growth Factor
PG	Proteoglycans
PI3	Phosphatidylinositol-4,5-bisphosphate 3-kinase
PLC	Phospholipase C
PPlight	Plane Polarised Light
PTFE	Polytetrafluoroethene
PTX	Pentraxin-related protein
RNA	Ribonucleic Acid
RNS	Reactive Nitrogen Species
ROS	Reactive Oxygen Species
RPM	Rotation Per Minute
RP-HPLC	Reverse Phase High Performance Liquid Chromatography
RT-qPCR	Real Time quantitative Polymerase Chain Reaction
SAX	Strong Anion eXchange
SD	Standard Deviation
SDS	Sodium Dodecyl Sulfate
Ser	Serine
SLRP	Small Leucine-Rich Proteoglycans
SMA	Smooth Muscle Actin
SPPS	Solid Phase Peptide Synthesis
siRNA	Short Interfering RNA
SULF	6-O endosulfatase

SLE	Systemic Lupus Erythematosus
SPSS	Solid Phase Peptide Synthesis
SSC	Side Scatter Channel
STZ	Streptozotocin
TAE	Tris Acetate EDTA
TBST	Tris-buffered Saline Tween
TE	Tris EDTA
TEMED	Tetramethylethylenediamine
TFA	TriFluoroacetic Acid
TIPS	Triisopropylsilane
TGF-ß	Transforming Growth Factor beta
TNF	Tumour Necrosis Factor
TOF	Time Of Flight
UUO	Unilateral Ureteral Obstruction
UDP	Uridine Diphosphate
UG	Undergraduate
UA	Uronic Acid
UV	Ultraviolet radiation
VEGF	Vascular Endothelial Growth Factor
VSV	Vesicular Stomatitis Virus
WB	Western Blot
WT	Wild Type
Xyl	Xylose

Acknowledgments

Looking back at the past four years I spent in the U.K. and especially at Newcastle University makes me feel so grateful to everyone who has shared this incredible journey with me.

First, I would like to thank my main supervisor Prof Simi Ali for trusting me with this project and giving me the freedom to explore it my own way. It has been a challenging but wonderful adventure to do together. Thanks for your guidance and support in all the ups and downs that came on my way. Second, I would like to thank Prof Neil Sheerin for always pushing me forward and asking challenging questions. I have learnt a lot from you and appreciate the time you took to help me. My gratitude goes to Prof John Kirby for the support and encouragement given even during busy times. Your passion for science has always been an inspiration to me.

I would like to share my gratitude to everyone in the JK Lab for their kindness and help. It has been fantastic doing this PhD with all of you! I would especially thank staining lab Queen, Barbara for her help and dedication in all lab work aspects but also, on a more personal note, to have put a smile on my face when I needed it. I will greatly miss you. I would also like to thank all the PIs who helped me during my work. Thanks Dr Jem Palmer for teaching me protein labelling and for trying to elucidate some of the mysteries behind antithrombin and heparin binding. I have learnt so much from you, thanks for your wise advices and dedication. I would also like to extend my gratitude to everyone in Prof Neil Sheerin's laboratory and Dr Kevin Marchbank's laboratory. I would especially thank Dr Anna Moles who has been doing a fantastic job with the *in vivo* work but also for having so much fun talking about science together. I am also thankful to Dr Chris Ward and Dr Kevin Marchbank for being part of my panel and giving me lots of suggestions and encouragements. I am deeply grateful to Dr Chris Ward and Dr Sylvie Fournel-Gigleux for accepting to review this work. I would like to thank my funding body, the European Commission FP7 Marie Sklodowska-Curie actions.

This project would not have been the same without of course my Marie Curie fellows, thanks Bea for the countless brunch in town and Gabriel for our daily talks about politics and how we could change the world. To my lab mates or the Cleopatra girls, namely Shameem and Nina, I cannot thank you enough for all the love, happiness, craziness and laugh we shared together. I found true friendships in you and you will always have a special place in my heart. You left Newcastle before

me and I have been missing you ever since (despite the daily phone calls!) but I know we will meet again! I would also have to thank Avinash for all the great time in the lab, our nice talk and for your moral support. You have brought music to the lab and it was real fun doing this PhD with you, I will miss you too.

This work could not have been possible without my collaborators to whom I am deeply grateful. First, I would like to thank everyone I have met and work with at Durham University. As a biologist, I was quite scared about working in a chemistry lab but thanks to all PhD students, Post docs and supervisors I have met, it was an incredible and very rewarding experience. I would like to thank Dr Ehmke Pohl for the countless meetings in your office and for clarifying all the doubts I had during my work. Your support and encouragement always succeeded in pushing me forward. Thanks Dr Steven L Cobb for taking the time to teach me and Beatriz everything you knew about peptide synthesis and for all the help and support you provided from the first till the very last day of the project. I will extend my thanks to all the lab members of both Dr Pohl and Cobb's group with a special mention to Sam who has been amazing in helping me feel comfortable in the lab but also within the group. From Bergen University, I would like to thank Prof Marion Kusche-Gullberg for welcoming me in her group and helping me becoming a member of the "GAG family". I could not thank you enough for all the discussions and emails that helped me understand HS synthesis and become extremely curious about GAGs sequencing. All the lab members were very supportive, and I will always remember the unexpected hiking/boat trip I had in Bergen. Thanks Mona and Larry for making this collaboration such great fun! I would like to extend my thanks to Dr Romain Vives for a great collaboration! Our talks always helped me understand more the sulfotransferases and sulfatases.

To all the friends I have made in Newcastle, you deserve a massive thank you. Thanks Orla for showing me some of the best places in Newcastle and in this country. Time spent with you has always been memorable and you have always been very supportive. I am forever grateful to the lovely PhD students who finished their PhD with me in my second home, the graduate training suite, Soulaf and Zelal. You have been with me in wonderful days but also very difficult days of my life. You have been like family to me and I am looking forward to visiting you in the Middle East.

To all the people I lived with, you deserve a big thank you and potentially an apology for all the time I might have been too demanding. Thanks Samuel for being the best flat mate I could have imagined living with. Sharing “Crossley Terrace” with you for three years has changed me in so many ways. I will miss you greatly. Of course, I will have to thank Poonam, See, Maria, Yoga, for being great friends. I would like to thank everyone I have met in my outdoors activities and of course at Dance City where dancing became a delightful break from the lab and a good laugh too!

My deepest and special thanks go to my family and especially my parents who have given me so much but have seen so little of me in the last years. You have always been in my thoughts and heart. You are the foundation of the person I am today, and I could not have had better dad and mum than you. Thanks for everything and because we never say it enough, thanks for your love. I also thank my brother Christophe and his beautiful family. Coming back to France and spending time with Ethan and Elyna has always been a precious joy that kept me going. A very big and special thank you to my beloved grandparents or the famous “Mich et Pich” and Spanish grandma for their unconditional love. To all my funny uncles, aunts and cousins, thanks for making family matter and being always there for me and for continuously believing in me. Special thanks to Agnes and Denis for welcoming me to their family and for all their encouragements. My final and heartfelt thanks are for Thomas. You have been my best friend, partner and confident for the last 6 years and I have no word to thank you enough for all the sacrifices you have made and all the support you have provided me. I feel very lucky and blessed to have someone like you by my side. Thanks for filling my life with so much love.

List of Tables

List of Figures

1 General introduction

1.1 Rationale for this study

Healing processes allow the body to repair and regenerate itself in a well-orchestrated and coordinated manner involving actions of pro- and anti-inflammatory molecules. The extracellular matrix which surrounds and supports the cells within a tissue is in a dynamic equilibrium between synthesis and degradation. This balance is challenged during inflammation which can lead to the uncontrolled accumulation of extracellular matrix within an organ if unresolved. This process, called fibrosis, can develop in most organs and drive organ failure. To date, it is irreversible.

Renal fibrosis is one of the main features in chronic kidney diseases (CKD) and chronic graft rejection. Understanding and targeting it has therefore become one of the biggest challenges in modern medicine. Glycosaminoglycans (GAGs) which are carbohydrate molecules that are found on all cells membranes and matrices are important in cell to cell and cell-matrix interaction. Heparan Sulfate (HS) is a GAG that plays a pivotal role in the initiation of inflammation and fibrosis with the ability to trigger leukocyte attraction, chemokine and growth factor binding and signalling. The science of studying GAGs is complex and still emerging with the development of new analytical tools. This study was designed to improve understanding of the changes in HS in fibrosis and their potential use in therapy. The following introduction highlights first the basics about kidney structure/function and the development and management of CKD. Second, GAG synthesis and involvement in renal homeostasis is described with a focus on HS.

1.2 Renal homeostasis

1.2.1 Kidney: origin and structure

In human development, the urogenital system originates from the intermediate mesoderm. Kidney formation starts with two primitive forms, the pronephros and the mesonephros that develop in early stages, around day 22 and day 25 of gestation but regress later on (Gilbert, 2000). While the mesonephros degenerates completely in female, some parts of the male reproductive system are derived from mesonephric tubules (Michos, 2009). The metanephros represents the third and final stage of kidney development. It requires the interaction between the epithelial ureteric bud and the metanephric mesenchyme. Together they induce cell survival, specification and spatial

organisation. The metanephric mesenchyme will become the nephron while the ureteric bud will become the collecting duct (Lechner and Dressler, 1997). *In utero*, fetal kidneys become functional at about 14 weeks and produce 90% of the amniotic fluid after 20 weeks (Vanderheyden *et al.*, 2003).

Each kidney is surrounded by a fibrous capsule and adipose tissue for protection. Blood supply comes into the kidney via the abdominal aorta and leaves it via the inferior vena cava. The kidney is composed of 3 regions, the renal cortex which is the outer and darker area (due to increased perfusion representing 90% of renal blood flow), the renal medulla, composed of striated pyramids, and finally the renal pelvis where urine is collected and directed to the ureter. The renal structure is displayed Figure 1-1.

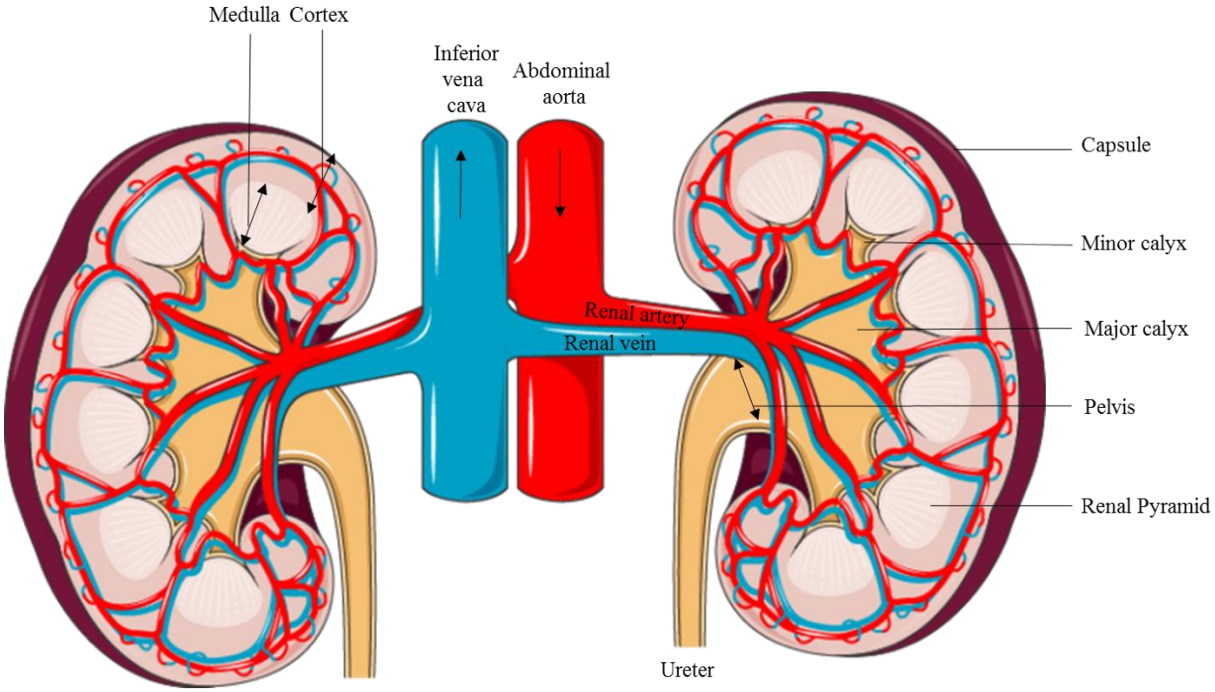

Figure 1-1: Kidney structure
Figure created using Servier Medical art.

1.2.2 Kidney function

Kidneys are responsible for urine production, fluid and electrolyte homeostasis. The functional unit of the kidney is called nephron. It is composed of the glomerulus and Bowman's capsule which plays a role in filtration and a renal tubule to collect and concentrate urine (see Figure 1-2). On

average, there are approximately 1 million nephrons per kidney but this number can vary up to 10 times between individuals (Bertram *et al.*, 2011). Blood reaches the nephron via the afferent arteriole. The arteriole subdivides into small capillaries where a permeable fenestrated endothelium initiates the filtration process. The glomerular epithelial cells are specialised cells named podocytes because of their elongated foot look like cytoplasm. The endothelial cells and podocytes share a basement membrane rich in fibers and proteoglycans (Haraldsson *et al.*, 2008). The glycocalyx on both cell types has been suggested to play a role in the filtration process. The efferent arteriole leaves the glomerulus but stays close to the nephron to reabsorb ions and water from the filtrate (vasa recta).

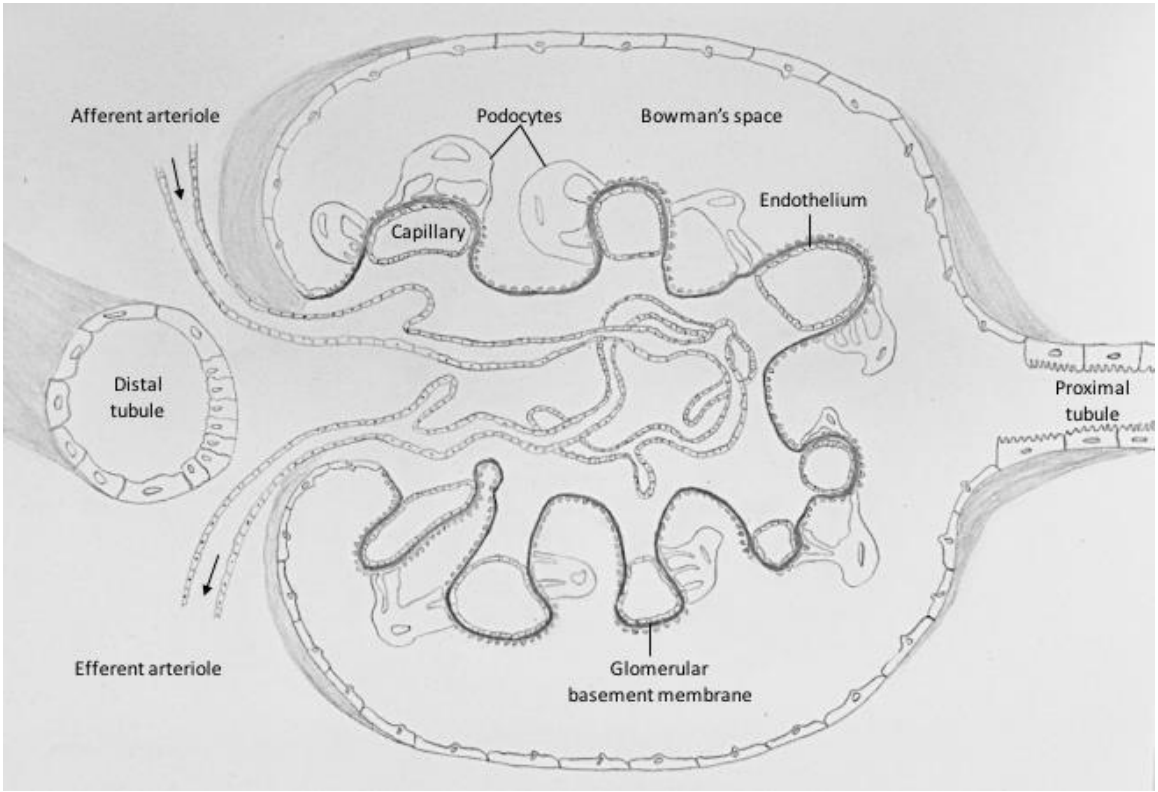

Figure 1-2: Glomerular structure
The glomerulus is the filtration unit of the kidney. Blood is reaching the glomerulus' capillaries via the afferent arteriole and leaves via efferent arterioles. Blood is filtered through a fenestred endothelium, reaches the Bowman's space and is further processed through the tubules. The endothelium and the glomerular epithelial cells, the podocytes, share the same basemement membrane enriched in proteoglycans and fibers.

Additionally, kidneys are in control of blood pressure, acid-base balance and vitamin D metabolism. They are responsible for the production and release of renin and erythropoietin which impact blood pressure and haematocrit respectively (Lote, 2013). The blood flow is important for

the glomerular filtration rate and is detected by specialised cells named juxtaglomerular cells. These cells secrete renin when blood flow is too low which leads to the activation of the Renin-Angiotensin system to regulate blood pressure.

1.2.3 Renal diseases

Kidney diseases can be acute or chronic depending on their duration. Even though Acute Kidney Injuries (AKI) can sometimes lead to the development of chronic diseases, AKI can be reversible if the cause of the damage is identified and treated. As seen Figure 1-3 it can start from diseases that are not initially related to the kidney.

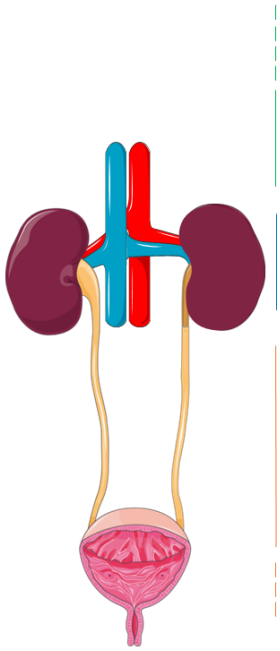

AKI origins	Causes	Examples
Prerenal injury **Alteration in renal flow**	hypovolemia	hemorrhage vomiting diarrhea oral intake burns sweating diuresis
	impaired cardiac function	heart failure decreased cardiac output
	vascular damages	renal vasodilatation renal vasoconstriction artery stenosis embolism
intrarenal injury	glomerulonephritis	idiopathic glomerulonephritis systemic diseases
	tubular necrosis >80%	ischemia nephrotoxicity
	interstitial nephritis	drugs allergies bacterial infection viral infection
	vascular damages	hypertension embolism blood disorder
Postrenal injury **Obstruction of the urinary tract**	cancer related	benign prostatic hyperplasia prostate cancer cervical cancer
	blockage	stones intratubular obstruction
	others	bladder dysfunction retroperitoneal dysfunction

Figure 1-3: Acute kidney injury causes and examples
Acute kidney injuries can be due to prerenal injuries as a consequence of a change in renal blood flow, due to postrenal injury with an obstructed urinary tract or due to intrarenal injury. Figure created using Servier Medical art.

Pre-renal injuries are caused by the obstruction or alteration of renal blood flow by hypovolemia (loss of fluid), impaired cardiac output and vascular damages. Post-renal injuries originates from the obstruction of the urinary tract by benign prostate hyperplasia, renal stones and intra-abdominal

tumors (Thadhani *et al.*, 1996; Basile *et al.*, 2012). Pre and post renal injuries can all lead to the development of intra kidney inflammation. Intrarenal injuries including glomerulonephritis, tubular necrosis, interstitial nephritis represent 35-70% of AKI and can be due to direct damage, inflammation, infection, drugs and auto immune diseases (Basile *et al.*, 2012).

On a cellular level, kidney injuries trigger cell stress and differentiation. Pathologies related to podocyte dysfunction can be observed by podocyte deficiency, foot process effacement, or podocyte dysfunction (Wiggins, 2007). Additionally, renal function correlates best to tubular integrity and the extent of tubulointerstitial fibrosis (Hewitson and Becker, 1995). Following an injury, tubular cells can undergo necrosis, apoptosis or an epithelial to mesenchymal transition-like process. The tubular epithelial cells proliferate migrate and contribute to disease progression (Liu, 2004). Furthermore, resident fibroblasts can transform into myofibroblasts and secrete pro fibrotic ECM components. Activated myofibroblast are a marker of disease progression (López-Novoa *et al.*, 2011).

1.2.4 Diagnosis and factors of risk

Early stage renal diseases are asymptomatic which makes them difficult to detect before late stages. The clinical signs only emerge when nephron function is lost, the glomerular filtration rate has dropped and urine outpout decreased. The body retains waste with an increase of urea in the blood (uremia) and there is protein loss in the urine (proteinuria).

A marker of reduced filtration is the presence of waste molecules in the blood such as creatinine, a molecule made during muscle activity. Additionally a good indicator of kidney function is the presence of essential molecules in the urine such as albumin, a protein found in the serum and essential for blood osmotic pressure (Baker, 1998). A screening programme would include a metabolic profile assessment, calculating glomerular filtration rate, and urinalysis (Woodhouse *et al.*, 2006). Kidney diseases can be classified by glomerular filtration rate (see Table 1-1) and urinary albumin to creatinine ratio.

Stage	Assessments	
Acute kidney injury	Serum Creatinine Concentration	Urine Output
1	1.5–1.9× baseline or ≥0.3 mg/dl above baseline	<0.5 ml/kg/hr for 6–12 hr
2	2.0–2.9× baseline	<0.5 ml/kg/hr for >12 hr
3	≥3.0× baseline, ≥4.0 mg/dl, or initiation of renal-replacement therapy	<0.3 ml/kg/hr for ≥24 hr or anuria for ≥12 hr
Chronic kidney disease	Definition	GFR
		ml/min/1.73 m²
1	Kidney damage with normal GFR	≥90
2	Kidney damage with mild decrease in GFR	60–89
3A	Mild-to-moderate decrease in GFR	45–59
3B	Moderate-to-severe decrease in GFR	30–44
4	Severe decrease in GFR	15–29
5	End-stage renal disease	<15

Table 1-1: Classification of AKI and CKD
From (Chawla *et al.*, 2014). A more accurate classification would include the urinary albumin to creatinine ratio. GFR: glomerular filtration rate.

Diabetes and hypertension are leading causes of end stage renal disease (Ghaderian *et al.*, 2015). Patients with hypertension have thicker vessels with a decreased luminal volume that diminish kidney blood flow. A reduced blood flow to the kidney leads to the activation of the renin angiotensin system which further increases hypertension. The resulting deprivation of blood supply to the kidney leads to a decrease in nutrients and oxygen and can generate ischemic injuries. As seen previously, ischemia is one of the main cause of intrarenal injuries. During renal injury, pro fibrotic growth factors such as Transforming Growth Factor β1 (TGFβ1) are secreted (Bobik, 2004) and stimulate production of extracellular matrix which generates scar tissue and causes tubulointerstitial fibrosis and glomerulosclerosis that diminish nephron function.

In diabetic patients, hyperglycemia and oxidative stress induce vascular remodelling and podocyte apoptosis (Susztak *et al.*, 2006). Furthermore, hyperglycemia generates advanced glycation end products which can alter the diabetic vessel wall composition and cause endothelial dysfunction.

These structural and cellular change can induce kidneys hypoperfusion and altered renal recovery from ischemia and can cause intrarenal damage (Spinetti *et al.*, 2008). Additionally, in the late 1990s smoking was found associated with high risks of early stage renal disease (ESRD) (Klag *et al.*, 1996).

Complications of CKD involve cardiovascular disorder mainly due to the development of hypertension and electrolytes abnormalities such as hyperkalemia which can cause cardiac arrhythmias. Furthermore, patients can develop hypocalcemia and have weak bones due to less activation of vitamin D (Nigwekar *et al.*, 2014). Toxin accumulation and anemia as CKD reduces erythropoietin synthesis can also be observed (Bello *et al.*, 2017).

1.3 Management of chronic kidney diseases

1.3.1 Early stages of chronic kidney diseases

For patients with hypertension, blood pressure and proteinuria can be controlled by anti-hypertensive drugs such as angiotensin-converting enzyme inhibitors, angiotensin receptors blockers or a change in diet. Overall, a change in patients life style can be recommended with a low protein diet, less salt, smoking cessation, more exercise and a moderate consumption of alcohol (Saweirs and Goddard, 2007). Furthermore, the control of glycaemia levels in diabetic patients and lipid-lowering therapy for patients that have not started dialysis are potential therapies (Kaysen, 2017). For patients with anemia, erythropoiesis-stimulating agents can be used. Unbalanced electrolytes such as phosphate can be overcome with the use of phosphate binders or a controlled diet.

1.3.2 Renal failure: dialysis and transplantation

Treatments of end stage renal disease, also called renal failure, are limited. Patients can undergo dialysis or kidney transplant. It was in 1944 that the first machine capable of blood filtration was created by Willem J. Kolff. There are now two types of dialysis, Hemodialysis and peritoneal dialysis (Queeley and Campbell, 2018). Even though patients' survival is increased with dialysis, there are lots of side effects and limitations to it. It is time consuming, tiring, associated with infections and cardiovascular disease.

The second option, renal transplantation, is generally accepted as the best option for better life quality with early graft survival improving over the last decades. The first successful kidney transplantation in animals were performed by Emerich Ullmann in 1902, Vienna with a dog autotransplant and a dog-to-goat xenograft (Ullman, 1914). It was 4 years later that the first transplantation in human was performed by Mathieu Jaboulay in Lyon with a pig and a goat kidney being grafted into the patients' fold of elbow (Jenkins, 1906). However, the grafts survived for only hours or few days and patients died quickly after. The development of our knowledge of immunology and rejection, with the first successful transplant performed in the mid-20th century, between twins and the introduction of immunosuppressive drug therapy were major advances and improved patients survival (Murray *et al.*, 1955, 1984).

In the UK, renal graft survival is 85-95% at one year, falling to 70-80% after 5 years. Improving long term graft survival is now the major challenge with survival only 50-60% after 15 years. In fact, ten years after transplantation, more than 50% of patients have progressive chronic renal graft dysfunction (Nankivell *et al.*, 2003). Due to graft rejection, it is not unusual for patients to need more than one transplant during their life. Despite the decrease in waiting time for patients in need of a transplant, there are still hundreds of patients dying while waiting (NHS Blood and transplantation data 2017). Preserving the donor kidney's integrity and limiting damage during transplantation would increase the patients' quality of life and help decrease the shortage in organs. New techniques to better assess kidney function and increase organ quality prior to transplant are being developed such as normothermic perfusion, a technique being explored at Newcastle University. This could allow more organs to be transplanted with potentially less complications (Hosgood *et al.*, 2018).

1.3.3 Origins of graft injury after transplantation

Integrity of the transplant organ depends firstly on the donor's health status and age. Additionally, surgical procedures can generate cellular stress. Damage from the time of retrieval, time outside the body, temperature, ischemia reperfusion injury and surgical complications are factors contributing to graft dysfunction. After transplantation, the kidney is still subject to injury from hemodynamic changes that lead to glomerular hypertension, urinary infection and drug toxicity all of which could impair kidney function. For example, the use of calcineurin inhibitors is pro-fibrotic. The recipient immune system is also a source of organ damage. Vascular insufficiency

can be caused by immune mediated injury due to reactivity against human leukocyte antigen (HLA) and non-HLA antigens on endothelial cells. Patients with anti-HLA antibodies are more likely to develop chronic rejection compared to renal transplant recipients without these antibodies (McKenna *et al.*, 2000; Süsal and Opelz, 2002).

1.3.4 Early events in transplantation

Organ retrieval triggers different types of stress in the kidney. First the kidney is subjected to ischemia as soon as the surgeon clamps the arterial blood supply. The decrease in oxygen and nutrients induces a decrease in the energy supplied to the cells and an increase in Reactive Oxygen Species (ROS). The activation of hypoxia induced factor mediates endothelial damages which can lead to cell death (Situmorang and Sheerin, 2018). Second, the organ is subjected to mechanical injuries during manipulation. These injuries generate an inflammatory response. Additionally, when the organ is transplanted, reperfusion which allows blood flow to go through the kidney generates an increase in Reactive Nitrogen Species (RNS) and ROS and opening of mitochondrial pore leading to cell death.

Therefore, when the graft is in place, the organ has been through a lot of physiological stresses and cytokines and growth factors that trigger inflammation have been released. They create a chemotactic environment and induce cell recruitment (Sherwood and Toliver-Kinsky, 2004). The first leukocytes to be recruited to the graft are neutrophils (de Oliveira *et al.*, 2016). They are the most abundant leukocytes in the blood and infiltrate injured area very quickly, followed by monocytes, which differentiate to become macrophages that start wound repair (Koh and DiPietro, 2011).

Multiple tissue remodeling factors (proteases, growth factors, matrix metalloproteinases), vascular mediators (prostaglandins) and cytokines are secreted by macrophages and contribute to wound repair by triggering cell infiltration, remodeling, and extracellular matrix (ECM) accumulation (Koh and DiPietro, 2011). Numerous cells, such as T cells, macrophages and mast cells, secrete pro-fibrotic factors (Meng *et al.*, 2014). Increased cell division can be observed in renal healing (Hewitson and Becker, 1995) that can be explained by the proliferation of fibroblasts inside the tissue to provide ECM proteins. This is called fibrogenesis and it takes place as long as the fibroblasts are present. If the inflammation is not stopped tissue destruction and scar tissue

accumulation will continue, leading to organ dysfunction and loss. The presence of inflammatory stimuli, pro-fibrotic factors, the continuous infiltration and/or the persistence of inflammatory cells prevent the termination of inflammation. What was an attempt from the body to heal transforms into an uncontrolled process leading to disruption of structure and function.

1.3.5 Acute and Chronic Rejection

The follow up after a transplantation needs to assess kidney function by analysing glomerular filtration rate (Kasiske *et al.*, 2002). Following transplantation, a biopsy of the organ provides histological information about vascular, tubular and glomerular inflammation, tubular atrophy and lymphocyte infiltration. The Banff classification can help determine the state of the organ. It is an international classification for renal transplant histology that looks at the evolution of graft inflammation. Since 2007 there are 5 categories (Table 1-2).

The new organ is seen as foreign material by the body and to prevent acute rejection, patients receive immunosuppressive treatment that target cytokine-mediated T cell and antigen presenting cell activation and proliferation; First, corticosteroids down-regulate IL2 and IL2 receptor expression in T cells (Daynes and Araneo, 1989; Paliogianni *et al.*, 1993) and IL1β, IL6 and TNFα expression in monocytes and macrophages (Breuninger *et al.*, 1993; Linden and Brattsand, 1994; Steer *et al.*, 1997). Calcineurin inhibitor and antiproliferative drugs are responsible for T cell inhibition.

1	normal	No rejection detected
2	Antibody mediated rejection	Antibody mediated graft injury with C4d staining in the glomerulus and peri-tubular capillaries. Associated with capillary vascular or glomerular inflammation, acute tubular necrosis or chronic injury (including IFTA).
3	Borderline changes	Interstitial lymphocyte infiltrates with minor tubulitis and no intimal arteritis
4	T cell mediated rejection	Significant interstitial, tubular inflammation and/or intimal inflammation. Chronic arteriopathy also included.
5	Interstitial fibrosis and tubular atrophy	In the absence of another pathology. Grade I mild 25% of cortical area, Grade II 26 to 50% cortical area and grade III when more of 50% of cortical area is affected.
6	Other	Changes that are not caused by rejection

Table 1-2: Classification of renal allograft rejection
From (Ferreras *et al.*, 2015) and (Solez *et al.*, 2008).

1.4 The Extracellular Matrix

The extracellular matrix (ECM) is acellular and functions as a mechanical support to all tissues. The composition and proportion of fibrous proteins and proteoglycans in the ECM determine its structure and is unique to every tissue (Frantz *et al.*, 2010). The body has to maintain a healthy balance between degradation and synthesis of the ECM components mediated by the activity of matrix metalloproteinases and their inhibitors. An abnormal overproduction of ECM leads to a stiff tissue that can lose its function (Figure 1-4). As mentioned previously, this process is called fibrosis and can affect almost all organs. In western countries, chronic fibro-proliferative diseases are responsible for about 45% of all deaths (Wynn, 2007). The main components that will be described in this section are collagens, elastin, glycoproteins and proteoglycans.

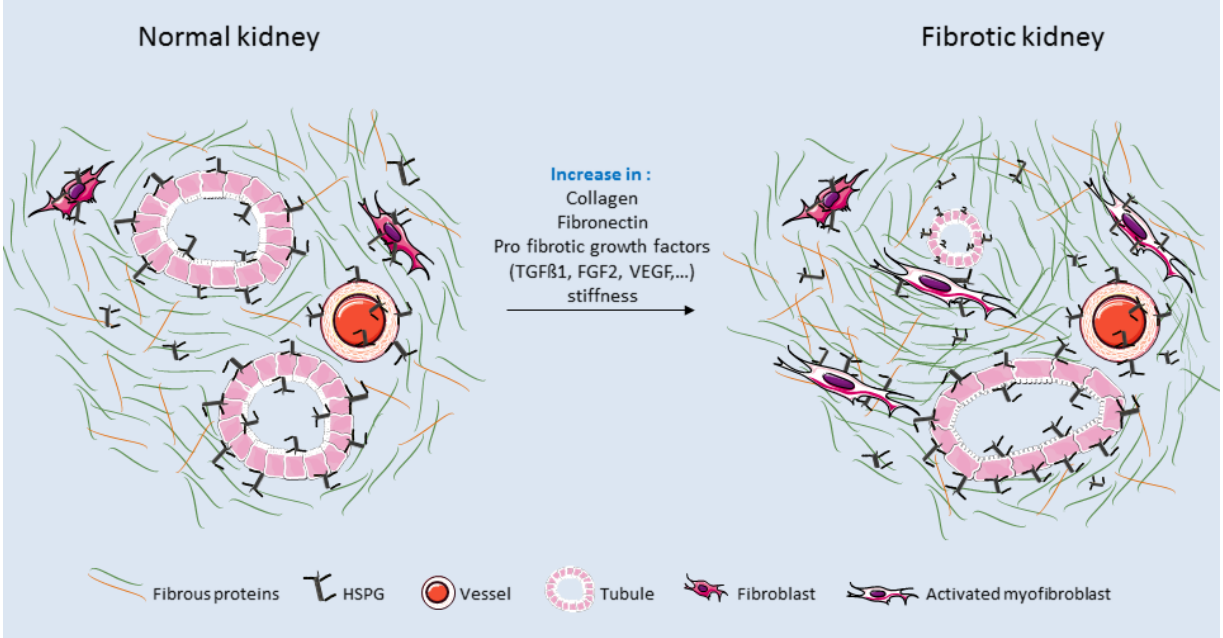

Figure 1-4: Matrix Remodelling during fibrosis
The process of fibrosis leads to the overproduction of ECM components such as fibrous proteins and HSPG generating a stiff environment within the organ. Dilated and/or atrophic tubules can be observed. Fibroblasts play an important role by becoming activated into myofibroblasts and secreting pro-fibrotic growth factors such as FGF2. Figure created using Servier Medical art.

1.4.1 Collagens and elastin

Collagens are the major fibrous glycoproteins with a characteristic triple helix representing 10 to 96% of their structure (Ricard-Blum, 2011). So far 28 types have been discovered. They can be classified as fibril-forming collagens (I, II, III, V, XI, XXIV, XXVII), fibril-associated collagens with interrupted triple helices (IX, XII, XIV, XVI, XIX, XX, XXI, XXII), network-forming collagens (IV, VIII, X) membrane collagens (XIII, XVII, XXIII, XXV), multiplexins (XV, XVIII) and collagen VI, VII, XXVI, XXVIII. In tissues the predominant collagen is fibrillary. Collagen is not only important for tissue structure but also for cell migration, differentiation and receptors activation (Hynes, 2009). Type IV collagen is the main component of the GBM (Miner, 1999). Urinary concentration of collagen IV is associated with kidney function in type 1 and type 2 diabetes (Okonogi *et al.*, 2001; Morita *et al.*, 2011). Furthermore collagen IV immunostaining is increased in chronic transplant nephropathy (Kawase *et al.*, 2001). The kidney interstitial ECM is mainly composed of collagen I, III, V, VI, VII and XV and the abnormal accumulation of collagen in the interstitium is one characteristic of renal fibrosis (Farris and Colvin, 2012) which will be further described later.

The ECM elasticity is mainly regulated by the presence of elastin, a protein synthesised and secreted as protoelastin and later cross-linked by lysyl oxidase to forms elastic fibers. In a uremic mouse model of CKD, elastin degradation was implicated in vascular calcification (Pai *et al.*, 2011) but these observations were not found in human patients (Schlieper *et al.*, 2010).

1.4.2 Glycoproteins and Proteoglycans

Glycoproteins are proteins bound to oligosaccharides. One important glycoprotein located in the ECM is fibronectin. It binds to collagen, heparin and cells receptors and is therefore important for cell migration (Yue, 2014). Fibronectin is secreted during the development of renal fibrosis and contributes to disease progression (Liu, 2015). Inhibiting fibronectin deposition has been shown to improve liver function in a murine model of liver fibrosis (Altrock *et al.*, 2015). Hence, fibronectin is a promising target for fibrosis treatment.

Proteoglycans (PG) are composed of a core protein covalently bound to glycosaminoglycans (GAGs). GAGs are linear polysaccharides made of repeating blocks (Esko *et al.*, 2009). PGs are considered as the reservoir of the ECM due to their ability to bind growth factors. They can create gradients and act as coreceptors which make them ideal targets for drug development. PGs can be divided into three groups: membrane bound, secreted and intracellular PGs.

Membrane-bound PGs include syndecans, Cluster of Differentiation CD44v3, CD47, betaglycan, neuropillin1, glypicans, Protein Tyrosine Phosphataseζ, thrombomodulin, neuron-glial antigen 2 and synaptic Vesicle protein 2. Secreted PGs include the aggrecan family, Small Leucine-Rich Proteoglycan family, collagen type IX, α2 chain, perlecan, agrin, collagen XVIII. Finally, intracellular PGs include serglycin which are found in granules of hematopoietic cells and can be secreted (Lindahl *et al.*, 2015). PGs generated from the binding of a core protein to Heparan Sulfate and their functions is shown Table 1-3.

PGs have multiple functions. They can facilitate the binding of FGF family members to receptors, bind to chemokines, enable cell adhesion and cell spreading (Iozzo, 2001; Ferreras *et al.*, 2015; Iozzo and Schaefer, 2015). They are also involved in the clearance of lipoproteins. Additionally, Proteoglycans can be internalised by endocytosis and degraded in the lysosome. This degradation is essential to maintain homeostasis. A lack of degrading enzymes can lead to diseases such as mucopolysaccharidosis.

PGs turnover happens by cleavage of the core protein through the activity of metalloproteases, by cleavage of HS by heparanase or membrane endosulfatases and by endocytosis. Most of the resulting glycans will be further degraded in lysosomes. It is hypothesised that heparanase and metalloprotease activities are implicated in ECM remodelling (Lindahl *et al.*, 2015).

The GAGs composing PGs are essential for their activities as they provide negative charges that are essential for protein binding. It is noteworthy that not all GAGs are bound to a protein.

HSPG	type	localisation	function
Perlecan	S	basement membranes, other ECM, cartilage	ECM assembly, cell migration, binds growth factors
Agrin	S	basement membranes, brain, neuromuscular junctions	neuromuscular junction, ligand
Collagen XVIII	S	basement membrane	basement membrane function
Syndecan (1-4)	M	most cells	cell adhesion, migration cytoskeletal organisation, ligand clearance
Betaglycan	M	fibroblasts	coreceptor, TGFß1 signalling
Glypican (1-6)	M	epithelial, mesenchymal cells, brain	coreceptor
CD44	M	most cells	hyaluronan and growth factor receptor
Serglycin	I	mast cells, leukocytes, endothelial cells	coagulation, wound repair, granule formation, support protease activity

Table 1-3: HSPGs localisation and function
Adapted from (Esko *et al.*, 2009) S: secreted, M: membrane, I: intracellular

1.5 Glycosaminoglycans

There are 6 different groups of GAGs, which are mostly linear and negatively charged. They are classified according to the monosaccharides composing their repeating disaccharides (Figure 1-5). It was in the early 20th century that Karl Meyer discovered hyaluronan (previously called hyaluronic acid) (Meyer and Palmer, 1934), dermatan sulfate (Meyer and Chaffee, 1941), keratan sulfate (Meyer *et al.*, 1953) and some forms of chondroitin sulfate (Meyer *et al.*, 1956) while Jorpes and Gardell identified heparin and heparan sulfate structures (Jorpes and Gardell, 1948). In the middle of the 20th century, isolation and analysis methods for proteoglycans allowed scientists to discover that proteoglycans are found in the ECM, inside the cell and on cell surfaces. GAGs are synthesised in the ER-Golgi system, except hyaluronan which is made at the plasma membrane. Even though the protein core of PG regulates localisation, quantity and time of expression, the presence of GAGs bearing negative charges is important for ligand interaction.

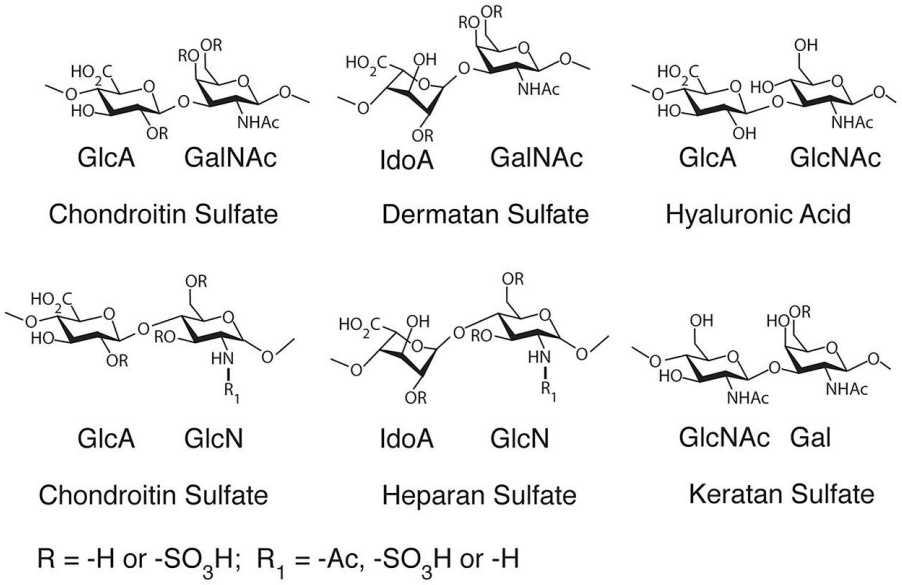

Figure 1-5: GAGs structure and features
From (Prestegard *et al.*, 2015) Iduronic acid (IdoA), N-acetylglucosamine (GlcNAc), N-acetylgalactosamine (GalNAc), Galactose (Gal), Glucuronic acid (GlcA).

1.5.1 Hyaluronan

Hyaluronan (previously named hyaluronic acid) was originally isolated from bovine vitreous (hualos glass in greek). Hyaluronan (HA) can be present in two forms, hyaluronic acid or as sodium hyaluronate in physiological conditions hence the new termination (Balazs *et al.*, 1986). Remarkably, amongst all GAGs, HA is the simplest of all with no sulfation, no core protein

attached and not being synthesised in the Golgi apparatus (Fraser *et al.*, 1997; Stern, 2004). HA binds to other components of the ECM or to cell surface receptor such as CD44. HA is mainly found in skin, synovial fluid, vitreous body, and muscles.

Three different hyaluronan synthase enzymes (HAS1, 2, 3) can independently synthesise hyaluronan at the plasma membrane and excrete it in the extracellular space, with HAS2 generating the largest hyaluronan molecules (Itano and Kimata, 2002). HA is composed of 250 to 25,000 repeating units of N-acetylglucosamine and D-glucuronic acid linked together with alternating glycosidic bonds GlcNAc-β-(1→4)-GlcA-β-(1→3). HA has a quick turnover with a half-life ranging from hours to several days (Fraser *et al.*, 1997). Its degradation occurs by endocytosis and lysosomal degradation via the activity of hyaluronidases (Stern, 2004). Because of its lengths and structure, hyaluronan is highly hydrophilic and lubricious and confers tissue hydration. Interestingly, when cells are exposed to stress they can secrete an unusual ECM structure with thick chains of HA (de La Motte *et al.*, 2003; Selbi *et al.*, 2006). This phenomenon is hypothesized to mediate leukocyte binding (Majors *et al.*, 2003; Petrey and de la Motte, 2014). Despite its simplicity, HA is involved in many physiological processes such as maintaining tissue hydration/integrity, wound healing (Monslow *et al.*, 2009), leukocyte trafficking and inflammation (Mack *et al.*, 2012). HA function depends on the polymer's length. High molecular weight HA has anti-inflammatory properties (Nakamura *et al.*, 2004) while during inflammation, HA fragmentation generates debris which have pro-inflammatory activity (Petrey and de la Motte, 2014).

HA is widely used in dermatology as a soft tissue-filler (Cohen *et al.*, 2013). In general, the use of HA in the clinic has many benefits. HA is non-immunogenic as it does not contain a core protein and it can be degraded by hyaluronidase (Hirsch *et al.*, 2007). HA injections to patients suffering from osteoarthritis provides pain relief and improved walking (Petrella and Wakeford, 2015). Regarding HA in kidney disease, hyaluronan was found in rejected human kidneys (Wells *et al.*, 1990), with an increased staining within the cortex and sclerotic vessels. In diabetic nephropathy, HA is increased at all stages of disease but not correlated with progression (Lewis *et al.*, 2008). HA can act as a sink for cells and proteins within a tissue and be both pro- and anti-inflammatory. Therefore, it is difficult to know if the increase in HA is detrimental or beneficial in these patients.

1.5.2 Chondroitin sulfate

Chondroitin Sulfate (CS) is a GAG mainly present within cartilage, bone, ligaments, tendons, blood vessels, brain and skin. CS provides strength and elasticity, hence providing resistance to mechanical stress (Henrotin *et al.*, 2010). CS is made of repeating disaccharides of a glucuronic acid and N-acetyl galactosamine GlcA-β-(1→3)-GalNAc-β-(1→4) and is synthesised in the endoplasmic reticulum/Golgi apparatus. The polymer bound to a core protein during synthesis and can be found in extracellular matrix, basement membrane where it can act as a cellular receptor.

Like other GAGs attached to a core protein, CS synthesis starts with the initiation step (Figure 1-6), a serine residue covalently linked to a linkage tetrasaccharide structure GlcA-β-(1→3)-Gal-β-(1→3)-Gal-β-(1→4)-Xyl-β-1→O-Ser. Xylose is added to serine residues located in the sequence "Glutamic acid/Aspartic Acid-X-Serine-Glycine" by xylosyltransferase (xylosyltransferases 1 and 2, XylT-1 and XylT2, XYLT1 and XYLT2). Gal residues are added by two different galactosyltransferases, β-1,4-galactosyltransferase 7 (β4GalT7, B4GALT7), β-1,3-galactosyltransferase 6 (β3GalT6, B3GALT6) and finally GlcA is added by a glucuronyltransferase β-1,3-glucuronyltransferase 1 (GlcAT-1, B3GAT3). The enzymes responsible for CS elongation are complex and have been studied *in vitro*. Three chondroitin synthase with two glycosyltransferase activities (GlcA and GalNAc) were identified (ChSy-1-3) with a chondroitin polymerising factor (ChPF) and two chondroitin GalNAc transferases (ChGn-2-2) (Silbert and Sugumaran, 2002; Mikami and Kitagawa, 2013).

For most GAGs, the synthesis is followed by the addition of sulfate groups by sulfotransferases. Their activity is essential for the overall final negative charge. They catalyse the addition of a sulfate group from the donor 3'-phosphoadenosine 5'-phosphosulfate (PAPS) to a GalNAc, GlcA and IdoA. CS is classified by its sulfation patterns; chondroitin sulfate unit A is sulfated at position C4, chondroitin sulfate unit C is sulfated at position C6. Additionally, the generation of disulfated units by the action of a 6-sulfotransferase and a uronyl 2-O-sulfotransferase generates the chondroitin sulfate D unit. Finally, a GalNAc4S-6S sulfotransferase generates the chondroitin sulfate E unit (Lindahl *et al.*, 2015).

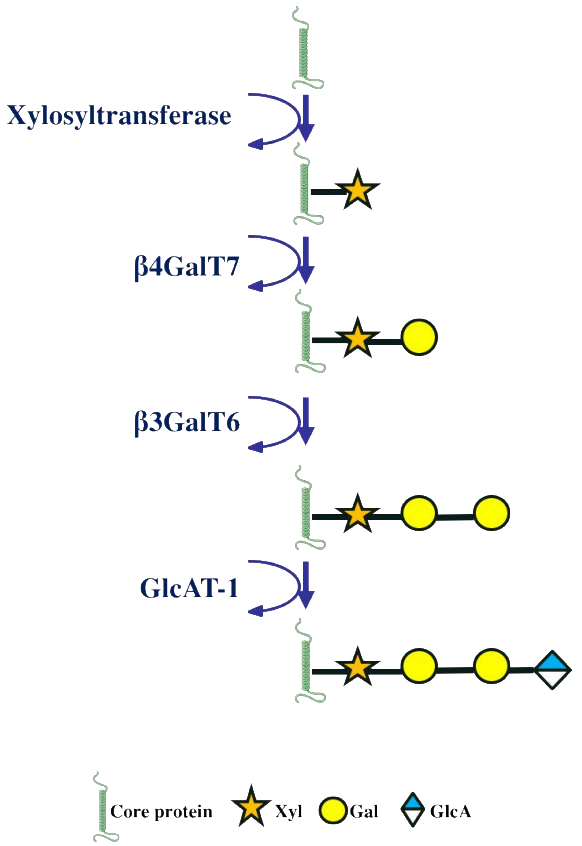

Figure 1-6: Initiation step: linkage tetrasaccharide synthesis to the core protein
For Chondroitin Sulfate, Dermatan Sulfate and Heparan Sulfate, synthesis begins with the assembly of a linkage tetrasaccharide to the core protein. Each sugar is added to the non-reducing end by specific enzymes (xylosyltransferases 1 and 2, XylT-1 and XylT2, XYLT1 and XYLT2), β-1,4-galactosyltransferase 7 (β4GalT7, B4GALT7), β-1,3-galactosyltransferase 6 (β3GalT6, B3GALT6), and β-1,3-glucuronyltransferase 1 (GlcAT-1, B3GAT3). Xyl: xylose, Gal: galactose, GlcA: glucuronic acid.

CS has anti-apoptotic, anti-inflammatory activities (Monfort *et al.*, 2008) and has been extensively used in clinical trials to treat osteoarthritis (Clegg *et al.*, 2006; Gabay *et al.*, 2011). It is actually recommended for osteoarthritis patients by the Osteoarthritis Research Society International (Zhang *et al.*, 2008). In the embryonic kidney, CS is the predominant GAG (representing 77%) but in adults the predominant GAG is HS and there are limited studies of CS function in kidney diseases (Steer *et al.*, 2004). Diabetic rats showed an abnormal distribution of CS proteoglycans (CSPG) in glomerular capillaries (McCarthy *et al.*, 1994). These results are consistent with the increase of CSPG NG2 in strepozotocin-induced diabetic rats with a potential role in mesanglial proliferation (Xiong *et al.*, 2007). However, Joladarashi *et al.* showed conflicting results in strepozotocin-induced diabetic rats (Joladarashi *et al.*, 2011). In this study, the CS content was decreased. The difference in findings can be explained by the difference in the model studied (Sprague Dawley rats vs Wistar) and the duration of strepozotocin treatment (2, 4 and 8 weeks vs 60 days

respectively). Furthermore, Joladarashi *et al.* studied CS by purification while Xiong *et al.* only studied one CSPG by mRNA and protein level assessment (Xiong *et al.*, 2007; Joladarashi *et al.*, 2011) It is possible that some CSPG are decreased while others are upregulated during inflammation and Joladarashi *et al.* looked at total CS modulation and no specific PGs (Joladarashi *et al.*, 2011). Nonetheless, these studies highlight a potential role of CSPGs in the development of glomerulosclerosis.

1.5.3 Dermatan sulfate

Dermatan Sulfate (DS) is a stereoisomer of chondroitin sulfate. Hence, the presence of CS/DS hybrids GAGs in some tissues. DS is ubiquitous and is predominant in the skin. It is involved not only in wound healing but also in development, infection and cancer. DS synthesis starts with CS synthesis in the endoplasmic reticulum/Golgi apparatus as detailed in section 1.5.2. It is the epimerisation of GlcA to IdoA in CS that generates DS. Therefore, DS is composed of repeated units of IdoA-β-(1→3)-GalNAc-β-(1→4) (Trowbridge and Gallo, 2002). DS can be monosulfated at position 4 by a specific sulfotransferase (Dermatan 4-sulfotransferase) and disulfated on position 4 and 6 by the same sulfotransferase as CS (GalNAc4S-6S sulfotransferase) and finally, 2-O sulfation is performed by the uronyl 2-O-sulfotransferase.

The most studied DS proteoglycan (DSPG) are small leucine-rich proteoglycans (SLRP) including decorin, and biglycan. SLRPs have been extensively studied in renal diseases (Schaefer, 2011). Decorin is the best studied SLRP and is expressed by renal fibroblast. During renal fibrosis, decorin accumulates in the interstitium where it interacts with collagen. An important function of decorin within the matrix is its ability to retain TGFβ and hence have anti-fibrotic activities (Border *et al.*, 1992). This was shown in a murine model of renal fibrosis where decorin -/- mice had more damaged tubules and leukocytes infiltration compared to WT after unilateral ureteral obstruction (Schaefer *et al.*, 2002). Interestingly, the kidney releases soluble biglycans after ischemia reperfusion injury (Moreth *et al.*, 2014). Biglycan is a ligand of toll like receptors 2/4 and can activate macrophages (Schaefer *et al.*, 2005; Babelova *et al.*, 2009). Therefore, biglycan plays an important role in pro-inflammatory responses. In line with these results, biglycan was increased in kidneys and plasma of patients with systemic lupus erythematosus (Moreth *et al.*, 2010). DSPGs play a central role in renal inflammation and fibrosis and further research may lead to the use of DSPG to regulate disease progression.

1.5.4 Keratan Sulfate

Keratan Sulfate (KS) is mainly found in the ECM of bones, cartilages, cornea and brain. This polymer differs from other GAGs as it does not have an acidic residue. KS structure is composed of the repeating disaccharides Gal-β-(1→4)-GlcNAc-β-(1→3) (Pomin, 2015). The attachment of KS chains to a core protein can be on asparagine residues by N-linkage (KSI) or on threonine and serine residues by O-linkage (KSII). KSI is mainly corneal while KSII is skeletal, shorter and more sulfated (Funderburgh, 2000). A third type of KS was found within the brain with a serine O-linked to a mannose (Krusius *et al.*, 1986). Not all enzymes involved in KS synthesis have been characterised. For what is known KS is synthesised by the activity of N-acetylglucosaminyltransferase, N-acetylglucosaminyl-6-sulfotransferase (GlcNAc6ST), Galactosyltransferase and KS galactosyl sulfotransferase (Caterson and Melrose, 2018).

KSs have been mainly studied in the cornea and the central nervous system where it has been found implicated in the development of macular dystrophy (Edward *et al.*, 1990) and Alzheimer's diseases (Lindahl *et al.*, 1996). In connective tissues, KS proteoglycans (KSPG) also contain CS and are important for tissue hydration (Caterson and Melrose, 2018). KS levels in the kidney are negligible.

1.5.5 Heparan sulfate and heparin

Heparan sulfate (HS) is a ubiquitous GAG synthesised by all mammalian cells. HS is present on the ECM, basement membranes and on cell surfaces. In contrast, heparin is mainly synthesised by mast cells and bipotential glial progenitor cells. Since its discovery in 1916, heparin has been intensively investigated for its anticoagulation activity (Esko and Selleck, 2002). HS also has anticoagulant activity but is less effective than heparin. Their anticoagulant activity is due to their ability to bind the serine protease inhibitor antithrombin III (AT). Heparin enhances antithrombin neutralisation of coagulation factors (Jordan *et al.*, 1980).

HS and heparin are made up of the repeat disaccharide unit containing an uronic acid (GlcA or IdoA) and a glucosamine. HS and heparin biosynthesis start with the initial disaccharide GlcNAc-α-(1→4)-GlcA-β-(1→4). This disaccharide can be modified by the activity of sulfotransferase and epimerase (discussed in section 1.6). Heparin, which is a highly sulfated form of HS, is extensively

modified with more than 80% of GlcNAc are modified to $GlcNSO_3$ and more than 70% of GlcA are IdoA residues (Lindahl *et al.*, 2015). Heparan sulfate biosynthesis and its biological significance is discussed in section 1.6.

1.6 Heparan Sulfate

1.6.1 HS synthesis

HS synthesis occurs in the endoplasmic reticulum (ER) and Golgi apparatus as described in Figure 1-6, where a uridine-diphospho-D-Xylose is attached to a serine residue of a core protein and two Gal molecules are added by the β-1,4-galactosyltransferase 7 (β4GalT7, B4GALT7) and β-1,3-galactosyltransferase 6 (β3GalT6, B3GALT6) respectively. Finally, GlcA is attached by a glucuronyltransferase β-1,3-glucuronyltransferase 1 (GlcAT-1, B3GAT3) creating what is named the GAG-protein linkage region (Breton *et al.*, 2012; Hull *et al.*, 2017).

Following synthesis of this tetrasaccharide linkage, the HS chain is ready to be extended by the addition of repeated glucuronic acid and glucosamine units. The polymerisation step, described in Figure 1-7, starts with addition of a GlcNAc by the GlcNAc transferase I enzyme (GlcNAcTI) and GlcA by GlcA transferase II. The next GlcNAc residue will be added by GlcNAc transferase II as GlcNAcTI is an initiating GlcNAc transferase and GlcNAcTII transfers to the elongating chain. The polymerisation continues with the alternate addition of GlcNAc and GlcA.

It is thought that the exostosin (EXT) gene family members are also involved in both initiation and elongation of the HS chain. The two enzymes EXT1 and EXT2 are known for their glycosyltransferase activity (Lind *et al.*, 1998). However, their mode of action is controversial as the two proteins form a hetero-oligomer directed to the Golgi. Overexpression of only one protein targets it to the ER. It is therefore speculated that the EXT1-EXT2 complex could be the functional form of the enzyme (Kobayashi *et al.*, 2000; McCormick *et al.*, 2000). The activity of EXT-like (EXTL) enzyme is less clear. Even though EXTL2 and EXTL3 have demonstrated to have GlcNAc transferase activity (Kitagawa *et al.*, 1999; Kim *et al.*, 2001), they do not seem to have the same mode of action. While EXTL3 can initiate the polymerisation by adding a GlcNAc to the linkage tetrasaccharide, EXTL2 is suggested to end the polymerisation process (Katta *et al.*, 2015). The precise role of the EXT family in HS elongation remains unclear.

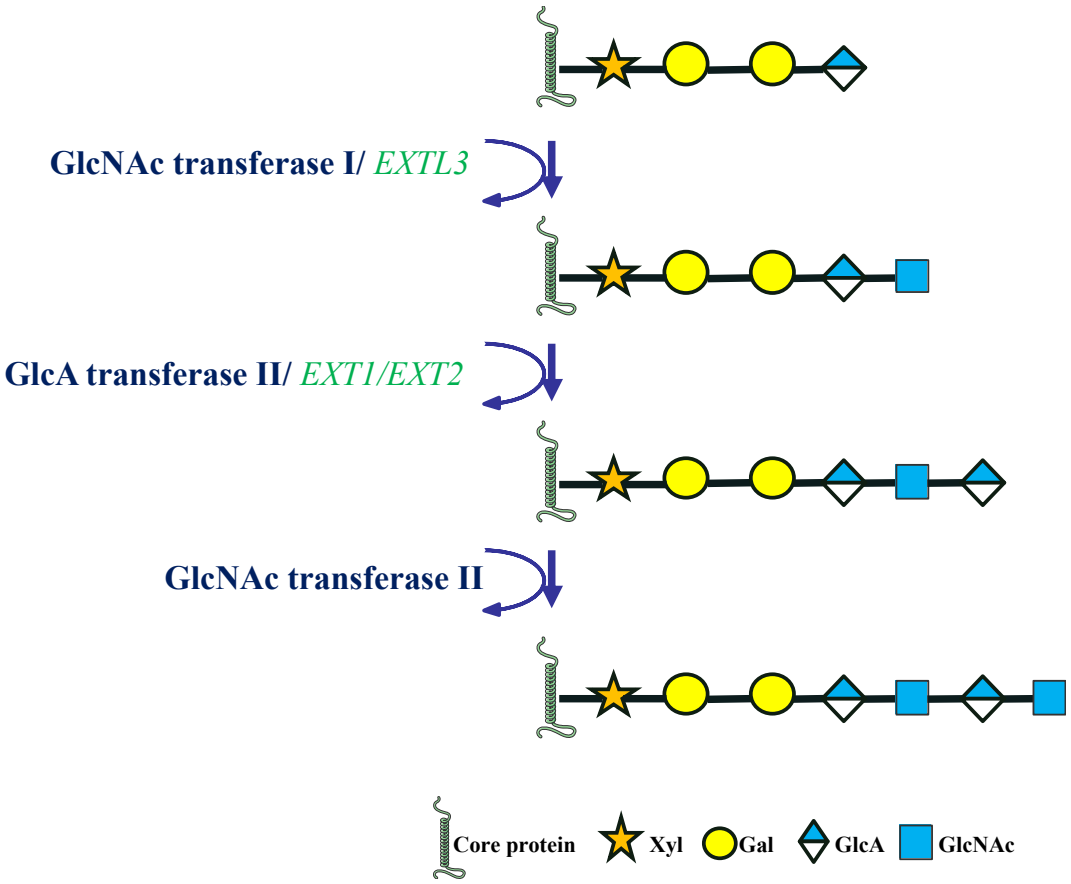

Figure 1-7: HS polymerisation step
Following the initiation step, GlcNAc transferase I initiates the HS polymerisation by adding a GlcNAc to the growing chain. The polymerisation process is catalysed by the alternating activities of GlcA transferase and GlcNAc transferase. Some of the enzymes involved in the polymerisation process are hypothesized to be members of the exostosin family and are highlighted in green. Xyl: xylose, Gal: galactose, GlcA: glucuronic acid, GlcNAc: N-acetylglucosamine.

1.6.2 HS modification

HS is implicated in chemokine and growth factor binding. However, it is not the HS backbone that is important for the binding, but the additional sulfation patterns. HS can be N, 2-O, 6-O and 3-O sulfated as described below.

First, GlcNAc can be deacetylated and N-sulfated (GlcNS) by a N-deacetylase/N-sulfotransferase. Second, GlcA can be transformed to IdoA by the C5-epimerase enzyme. Additionally, GlcNAc and GlcNS can be 6-O-sulfated (GlcNS(6S); GlcNAc(6S)) (Rabenstein, 2002; Li and Kusche-Gullberg, 2016; El Masri *et al.*, 2017). Glucuronic and iduronic acids can be 2-O-sulfated (GlcA(2S) and IdoA(2S) respectively), Ido(2S) is more abundant. One last modification that GlcA can undergo is a 3-O-sulfation on both GlcNS and GlcNS(6S) which finally gives GlcNS(3S) and

GlcNS(3,6S) (Rabenstein D.L., 2002). The enzymes responsible of Heparan Sulfate modification include:

-Four isoforms of N-deacetylase/N-sulfotransferase (NDST 1-4)

-One C5 epimerase

-One 2-O-sulfotransferase (HS2ST)

-Three isoforms of 6-O-sulfotransferase (HS6ST-1, 2, 3)

-Seven isoforms of 3-O-sulfotransferase (HS3ST 1-3A, 3B-6)

The activity of these enzymes is responsible for HS binding to many proteins involved in cell migration, cell adhesion and inflammation such as fibroblast growth factors, hepatocyte growth factor, chemokines, L and P selectins, fibronectin, TGFβ binding proteins, vascular endothelial growth factors (Esko and Linhardt, 2009). Modulating HS sulfation is important for protein binding and is a tool the body can use to increase cell signalling during inflammation. Recently, a study looking at tissue from idiopathic pulmonary fibrosis showed an increase in HS 2-O-sulfation (Westergren-Thorsson *et al.*, 2017). Therefore, research on HS modifying enzymes has focus on elucidating their mode of action and specificity to better understand what controls HS function.

1.6.3 HS modifying enzymes

All enzymes and all isoforms have their specificity and the knock-out of different isoforms does not lead to the same phenotype. Despite having the same function, some enzyme isoforms are lethal when others are not (Table 1-4).

It appears that controlling the enzyme responsible for these patterns is as important as the expression of a receptor on the cell surface. It is therefore essential to understand the mechanisms leading to these modifications and the potential physiological effects they have both in health and disease.

Enzyme studied	Model	Methods / Analysis	Observations	Ref
NDST (1-4) N-deacetylase-Sulfotransferase	Mice NDST1 -/- endothelial cell specific	Acute peritonitis, contact dermatitis	Impaired inflammatory responses. Decreased neutrophil infiltration	(Wang *et al.*, 2005)
	Mice NDST1-/- endothelial cell and leukocytes specific	Antiglomerular basement membrane nephritis	Decrease in granulocyte and macrophage influx. Improved renal function and reduced glomerular injuries (creatinine blood urea nitrogen; glomerular hyalinosis)	(Rops *et al.*, 2014)
		Acute inflammatory reaction (induced by IP thioglycollate); air pouch model	Decrease in chemokine presentation, migration and neutrophil influx	(Wang *et al.*, 2005)
		Repetitive allergen exposure Analyses of airway remodeling	Less macrophage infiltration and peribronchial fibrosis compared to WT	(Ge *et al.*, 2014)
	NDST1 -/- mice	Generation of NDST1 null mice	Non-viable, neonatal death due to lung defects	(Fan *et al.*, 2000)
	NDST2 -/- mice	Intraperitoneal injection of IgE followed by anti IgE antibodies injection	No significant difference in neutrophil influx in the peritoneum compared to NDST2 +/+ mice but have decreased number of connective tissue mast cells	(Forsberg *et al.*, 1999)
HS2ST 2-O-sulfotransferase	Mice HS2ST -/- endothelial cell specific	Acute peritonitis	Increase in neutrophils and monocyte infiltration, enhanced chemokine binding and number of neutrophils attached to the endothelial cell surface	(Axelsson *et al.*, 2012)
HS3ST 1-3A, 3B-6 3-O-sulfotransferase	HS3ST3B overexpression in pancreatic cell line	Analysis of epithelial-mesenchymal markers	EMT processes promoted	(Song *et al.*, 2011)
HS6ST-1,2,36-6-O-sulfotransferase	HS6ST1 overexpressing renal epithelial cells	Flow cytometry	Increased binding of FGF2	(Alhasan *et al.*, 2014)
Endosulfatases (SULF1,2)	Sulf2 KO type II alveolar epithelial cells	TGF beta stimulation	Increase in TGF-β1 target gene expression	(Yue *et al.*, 2013)
	Sulf1/2 double KO MEFs	FGF2 stimulation	Increase in FGF2 response compared to WT.	(Lamanna *et al.*, 2008)
Heparanase (hps)	Mice overexpressing hps	Neutrophil chemoattraction into cremaster muscle	Drop in leukocyte recruitment	(Massena *et al.*, 2010)
	Colon samples from ulcerative colitis; Hps tg mice	Histology, mouse model of colitis	Hps overexpression. Compared to WT, elevated hps in colonic epithelium have similar leukocyte infiltration during acute phase and increased mucosal infiltration during chronic phase	(Lerner *et al.*, 2011)
	Hps -/- mice	LPS injection	Inhibition of neutrophil adhesion to pulmonary microvasculature	(Schmidt *et al.*, 2012)
	Hps-silenced tubular cells	Pro-fibrotic stimulati	Reduced TGFβ synthesis, no change in EMT	(Masola *et al.*, 2014)
	Hps -/- effector T cells	Injection of Hps -/- effector T cells in WT mice with lymph node or skin inflammation	Hps not essential for lymphocyte extravasation through inflamed lymph nodes and inflamed skin vessels.	(Stoler-Barak *et al.*, 2015)
	Hps -/- mice	Zymosan induced peritonitis	Hps contributes to monocyte but not neutrophil entry to inflammation site	(Stoler-Barak *et al.*, 2015)

Table 1-4: HS modifying enzymes modulation and implication in development, inflammation and disease progression
WT: Wild Type; KO: Knock Out; IP: Intraperitoneal; LPS: Lipopolysaccharides. Adapted from (Ferreras *et al.*, 2015)

1.6.4 N-deacetylase/N-sulfotransferase

NDSTs are Golgi transmembrane proteins with two catalytic activities. They are capable of N-deacetylation and N-sulfation. The first deacetylation process removes the acetyl groups from GlcNAc and the NDST sulfotransferase activity then adds a sulfate group to GlcN. This modification is essential for HS synthesis as other modulating enzymes require GlcNS residues (Grobe *et al.*, 2002; Carlsson *et al.*, 2008). Vertebrates have 4 NDSTs but the reason for having 4 is still not clear. Their discovery is quite recent (Pettersson *et al.*, 1991; Hashimoto *et al.*, 1992; Aikawa and Esko, 1999), NDST1 and NDST2 are ubiquitous while NDST3 and 4 are mainly expressed during embryonic development. Modeling NDST sulfotransferase domains showed different substrate binding sequences. Furthermore, cells had higher N-sulfation patterns when transfected with NDST2 than NDST1 (Pikas *et al.*, 2000). Additionally, an increase in N-sulfation was accompanied by an increase in HS length. Hence NDSTs are important for N-sulfation and impact HS total length. NDST1-/- mice are non-viable and die from lung defects. However, NDST1-/- podocytes specific led to foot effacement with an abnormal cell-matrix interaction (Sugar 2014). Not only is NDST1 important for morphogenesis but it is also essential for inflammation processes. As seen Table 1-4, cell-specific NDST1-/- in murine models of dermatitis, nephritis and acute inflammation all showed a decrease in leukocyte infiltration (Wang *et al.*, 2005; Ge *et al.*, 2014; Rops *et al.*, 2014). HS is important for chemokines binding and leukocyte adhesion to the endothelium (see section 1.8). NDST2-/- mice are viable and do not show impaired leukocyte infiltration suggesting that NDST1 might me more important for HS biosynthesis.

1.6.5 C5-epimerase

After N-deacetylation-sulfation of the GlcNAc residue, the other component of the HS disaccharide is also modified. The action of C5-epimerase, a Golgi transmembrane protein, transforms GlcA into IdoA. This modification is important for flexible conformation and the activity of 2-O-sulfotransferase (Qin *et al.*, 2015). To date, only one C5-epimerase protein has been identified. C5-epimerase -/- mice are non-viable, they lack kidneys and show mild skeletal and lung malformations (Li *et al.*, 2003), with other organs not affected. The renal agenesis observed in these animals highlights a potential importance of 2-O-sulfation in renal development. Mice lacking HS2ST1 also lack kidneys (Bullock *et al.*, 1998). Some studies have shown that C5-epimerase and HS2ST1 interact *in vitro* and *in vivo* (Pinhal *et al.*, 2001; Préchoux *et al.*, 2015).

This interaction seems essential for their translocation within the Golgi apparatus. One concept about HS biosynthesis speculates that the modifying enzymes interact within the Golgi to form a physical complex named the "gagosome" (Esko and Selleck, 2002). However, further investigation will be required to validate this model.

1.6.6 Heparan Sulfate 2-O-sulfotransferase 1

In addition to N-sulfation and the generation of IdoA, HS can be O-sulfated. HS 2-O-sulfation is catalysed by only one enzyme, HS2ST1, a transmembrane Golgi protein. Surprisingly HS2ST1 has two substrates and is able to add a sulfate group to GlcA and preferentially to IdoA residues (Rong *et al.*, 2001). IdoAS is important for protein binding, including FGF2 (Maccarana *et al.*, 1993), lipoprotein lipase (Parthasarathy *et al.*, 1994), platelet derived growth factor (Feyzi *et al.*, 1997) and IL8 (Spillmann *et al.*, 1998).

Interestingly, endothelial cell specific HS2ST1 -/- resulted in an increase in leukocyte infiltration and an increase in chemokine and L-selectin binding (Axelsson *et al.*, 2012). This pro-inflamatory effect of HS2ST1 inactivation is unexpected as generally a decrease in sulfation inhibits protein binding. One explanation could be the increase in N- and 6-O-sulfation observed in the HS2ST1 -/- endothelial cells might be responsible for the enhanced inflammation. The same authors showed that the inactivation of HS2ST1 in a myeloid lineage did not have the same effect. Therefore, the decrease in 2-O-sulfation and its effect on inflammation is most important in the endothelium.

Additionally, HS 2-O-sulfation is crucial for renal development. Gene trap mutation of HS2ST in mice stopped kidney development and led to lethality (Bullock *et al.*, 1998). It is suggested that HS2ST impaired kidney development is due to a defect in metanephric mesenchyme induction (Shah *et al.*, 2010). A change in HS 2-O-sulfation can also be observed in pathological conditions. Immunostaining of HS 2-O-sulfation is increased during renal allograft rejection (Alhasan *et al.*, 2014).

1.6.7 Heparan Sulfate 6-O-sulfotransferases

HS 6-O-sulfation is generated by three different enzyme isoforms. HS6ST1, 2 and 3 are transmembrane Golgi proteins catalysing the addition of a sulfate group at the C6 of a GlcN.

HS6STs can be secreted to the extracellular space (Habuchi *et al.*, 1995) mediated by the activity of a β-secretase (Nagai *et al.*, 2007). This secretion can potentially be a regulatory mechanism of the cell to decrease the activity of HS6ST, hence, limit HS 6-O-sulfation. Each isoform has its preferential substrate. Habuchi *et al.* cloned all HS6STs in mice and observed that HS6ST1 catalysed the sulfation of IdoA-GlcNS residues (Habuchi *et al.*, 2000). However, IdoA seems to prevent HS6ST2 activity which preferentially modifies Glc-GlcNS. HS6ST3 can add a sulfate group to both IdoA-GlcNS and Glc-GlcNS with a preference to 2-O-sulfated residues (Jemth *et al.*, 2003). Murine and Human studies showed that three isoforms do not have the same pattern of expression in the body. HS6ST1 is mainly expressed in liver, kidney and intestine whereas HS6ST2 is predominantly found in brain, ovary, placenta and spleen. HS6ST3 is expressed ubiquitously but at low levels (Habuchi *et al.*, 2000, 2003).

HS6STs are important in development. HS6ST1-/- mice can be non-viable depending on the genetic background. The decrease of vascular endothelial growth factor in the placenta of null mice may explain this mortality. However, when viable, mice are smaller with abnormal skeletal development and abnormal eye and lung morphogenesis compared to WT mice (Habuchi *et al.*, 2007). In contrast, HS6ST2 -/- mice are viable and develop normally (Habuchi and Kimata, 2010). These observations suggest that HS6ST1 is more important than HS6ST2 in development.

HS 6-O-sulfation has been extensively studied for binding growth factor including FGF family. HS 6-O-sulfation is increased in idiopathic pulmonary fibrosis (Lu *et al.*, 2014; Westergren-Thorsson *et al.*, 2017) and in chronic renal rejection (Alhasan *et al.*, 2014). FGF2 binding to its receptor requires HS 6-O-sulfation. Hence the increase in 6-O-sulfation in fibrosis potentially increases FGF2 signalling and disease progression.

1.6.8 Heparan Sulfate 3-O-sulfotransferases

1.6.8.1 Catalytic activity, specificity and localisation

The addition of a sulfate group to the C3 position is catalysed by HS 3-O-sulfotransferases (HS3STs). HS3STs like other HS sulfotransferases are Golgi transmembrane proteins, with the exception of HS3ST1 which does not possess a transmembrane domain. The HS3ST family, with 7 members (HS3ST1, 2, 3A, 3B, 4, 5, 6), is the largest of all HS sulfotransferases. HS 3-O-sulfation is a rare modification and despite the number of enzymes involved in generating this pattern. HS

3-O-sulfated glucosamine residues represents around 1% in porcine endothelial cells (Marcum *et al.*, 1986) and 6% in follicles (De Agostini *et al.*, 2008). HS3STs are very well conserved within all vertebrates. However, invertebrates have less isoforms. Thacker et al. proposed that HS3ST originally emerged in a common ancestor of bilaterians (animals with bilateral symmetry) and cnidarians (see arrow, Figure 1-8) (Thacker *et al.*, 2014).

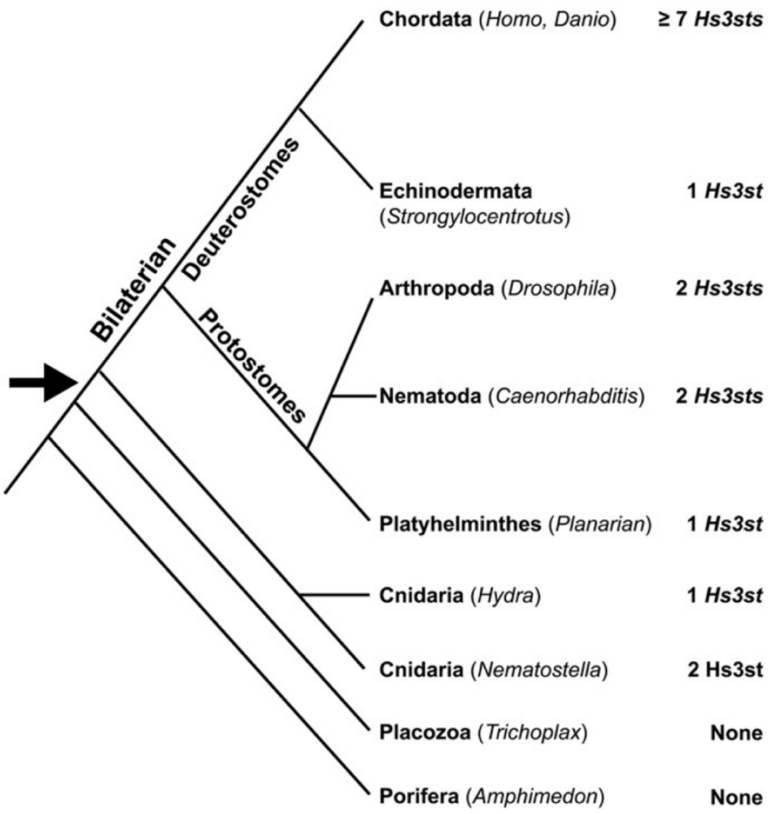

Figure 1-8: HS3ST evolution
HS3STs are well conserved amongst animals. It is hypothesised that the first HS3ST originates from a common ancestor of bilaterians and cnidarians (arrow). From (Thacker *et al.*, 2014).

HS3STs are heterogeneously expressed throughout the human body and vary from organ to organ, see Table 1-5. The most common forms are HS3ST1, HS3ST3A and HS3ST3B which are widely expressed. HS3ST5 is found in brain, spinal cord and skeletal muscle and HS3ST6 is mainly found in liver and kidney. Finally, HS3ST2 and HS3ST4 are predominantly expressed in the brain (Table 1-5).

	Intracellular localisation	Organ expression	Pattern generated
HS3ST1	luminal Golgi	**kidney, brain**, heart, lung, placenta, pancreas, stomach, small intestine, colon, testis, spleen	AT-type
HS3ST2	Transmembrane Golgi	**brain,** heart, placenta, lung and skeletal muscle	gD-type
HS3ST3A	Transmembrane Golgi	**heart, placenta**, liver, lung, pancreas, kidney, *spleen, stomach, small intestine, colon, testis*	gD-type
HS3ST3B	Transmembrane Golgi	**liver, placenta**, brain, heart, lung, skeletal muscle, kidney, *spleen, stomach, small intestine, colon, testis*	gD-type
HS3ST4	Transmembrane Golgi	**brain**	gD-type
HS3ST5	Transmembrane Golgi	brain, spinal cord, skeletal muscle	AT type and gD-type
HS3ST6	Transmembrane Golgi	**liver, kidney**, heart, brain, lung, testis	gD-type

Table 1-5: An overview of HS3STs localisation and types
Organs where the sulfotransferase is predominantly expressed are highlighted in bold. Research on HS3ST3A/B tissue expression used a probe detecting both isoforms, not discriminating them and giving limited information, hence the italic style (Shworak *et al.*, 1999; Xia *et al.*, 2002; Mochizuki *et al.*, 2003, 2008; Xu *et al.*, 2005).

Considering the rare occurrence of HS 3-O-sulfation, it could be suggested that all enzymes generate the same pattern. However, experiments show that this is not the case. Although they need the high energy sulfate donor PAPS (3'-phosphoadenosine 5'-phosphosulfate) for their activity, they do not have the same substrate specificity. Initial experiments showed that Chinese Hamster Ovarian (CHO) cells that do not have HS 3-O-sulfation, became sensitive to Herpes Simplex Virus-1 (HSV-1) after HS3ST3 transfection. However, when transformed with HS3ST1, the virus was not able to enter the CHO cells implying that these enzymes generate different 3-O-sulfation patterns (Shukla *et al.*, 1999). Additionally, HS3ST1 is known to generate an anticoagulant HS (Liu *et al.*, 1996). Consequently, HS3STs are classified in two different groups depending on their activity, the ones generating the antithrombin III binding site also named anticoagulant HS (AT-type) and the ones generating the herpes simplex virus type 1 glycoprotein D (gD-type) (Thacker *et al.*, 2014).

Isoforms 2,3A,3B 4 and 6 form herpes simplex virus binding sites (gD binding site) and have 80% sequence identity (Lawrence *et al.*, 2007). In contrast, HS3ST1 and 5, which have 71% sequence identity, generate anti-thrombin binding sites. HS3ST1 has a preferred target for GlcA-GlcN±6S and IdoA 2-O-sulfation prevents its action (Zhang *et al.*, 2001). HS3ST5 generates both AT-type

and gD-type and is not influenced by 2-O-sulfation patterns (Xia *et al.*, 2002). HS3ST1, 3 and 5 have been crystallised and their substrates, displayed Figure 1-9 have been extensively studied.

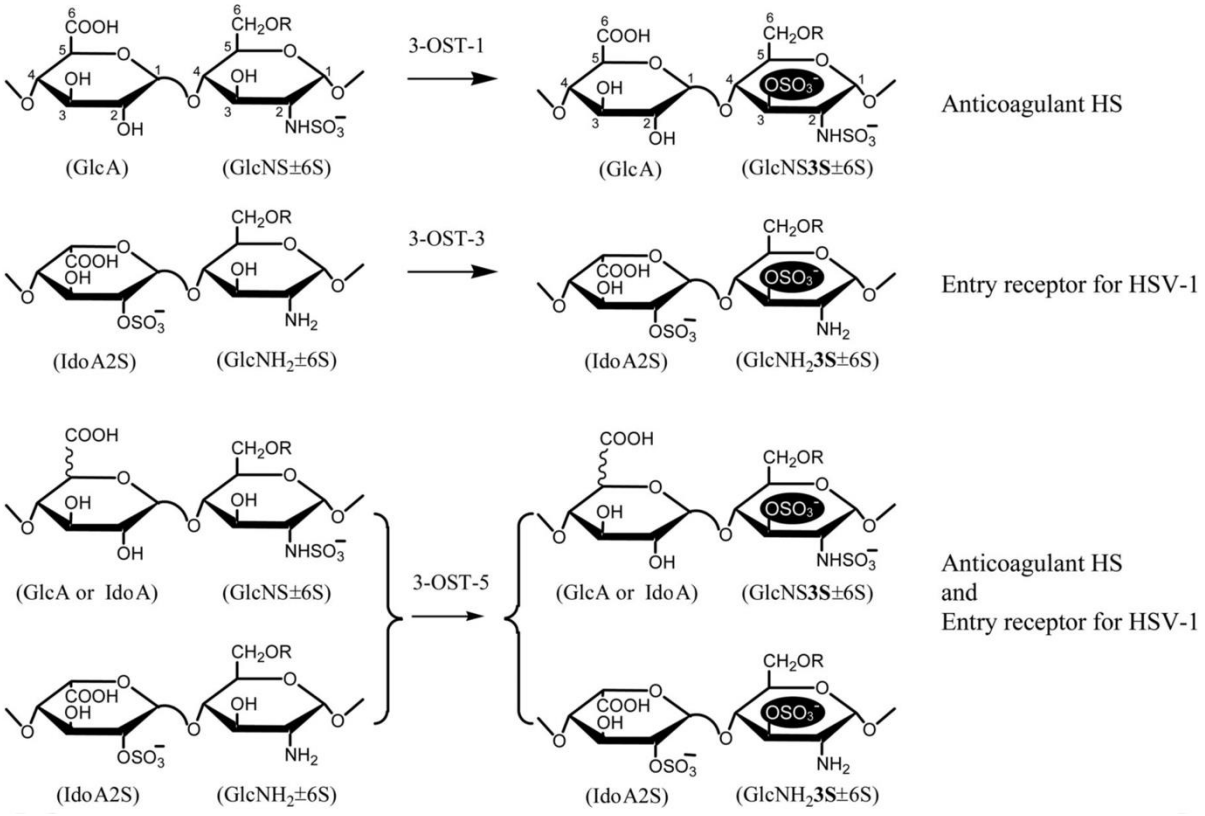

Figure 1-9: HS3ST1, 3 and 5 substrates specificity
HS3ST1 catalyses the addition of a sulfate group to GlcNS±6S and generates AT-type HS, GlcA-GlcNS3S±6S. HS3ST3 transfers a sulfate group to the residue GlcNH2±6S and generates gD-type HS, IdoA2S-GlcNH23S±6S, which is an entry receptor for HSV-1. HS3ST5 catalyse both reactions. R: H or SO_3^-. From (Xu *et al.*, 2005).

Recent research has addressed the difference in the isoforms' substrate. Previous work with computer modelling (Raman *et al.*, 2002) and recombinant protein experiments (Edavettal *et al.*, 2004) have provided information about the structure-function relationship. Moon and co-workers compared HS3ST1 and HS3ST3 conformations when binding oligosaccharides and discovered that their interactions were not similar. Interestingly, the IdoA2S was in a chair conformation when interacting with HS3ST1 while in a skew boat conformation in contact with HS3ST3 (Moon *et al.*, 2012). This change in conformation could explain why 2-O-sulfation prevents HS3ST1 action.

1.6.8.2 HS3STs in embryonic development

Recent research in mice showed that HS 3-O-sulfation plays a role in development by supporting stem cell differentiation (Hirano *et al.*, 2012). HS3STs were found to regulate axonal growth cone collapse (Thacker *et al.*, 2016a) and were expressed differentially during neuronal differentiation (Hasegawa and Wang, 2008). In addition, the study of null animals emphasised the role of HS3STs in organogenesis. Depending on the strain, HS3ST1-/- mice generation can be lethal or can induce growth retardation. These mice showed normal coagulation (HajMohammadi *et al.*, 2003), potentially due to the redundancy of the HS3STs function. The HS3ST1-/- mice developed a spontaneous eye degeneration which was not expected (Shworak *et al.*, 2003). Clark *et al.* showed that HS 3-O-sulfation was found on blood vessels and the membrane between retina and vitreous body within the human eye (Clark *et al.*, 2011). Furthermore, the dysregulation of factor H binding to HS is thought to play a role in the development of macular degeneration (Langford-Smith *et al.*, 2014). Therefore, one explanation could be the dysregulation of factor H binding in HS3ST1-/- mice causes eye degeneration due to an increase in complement activation. However, this is a hypothesis which stills requires testing. HS3STs are also important in non-mammalian animals where they are implicated in cilia function (Neugebauer *et al.*, 2013) and cardiac contractility (Samson *et al.*, 2013) of the zebrafish and neuronal development, neuronal branching of *Caenorhabditis elegans* (Tecle *et al.*, 2013). The role of HS3STs in human development is understudied but is better documented in physiological and pathological conditions.

1.6.8.3 HS3STs in cancer

Recently, there has been increasing interest in the function of HS3STs in cancer. In cancer evolution, three states can be observed: the primary tumor state, micro metastatic dissemination, when cancer cells migrate from the primary tumor to the circulation, and finally cell proliferation in distant organs (metastatic state). HSPGs are involved in cell contact, in cell motility and are crucial for growth factor-binding. It is therefore not surprising that they are implicated in cancer progression (Sasisekharan *et al.*, 2002). In the early stages of cancer progression, HS3ST3B promotes epithelial to mesenchymal transition in pancreatic cells with a potential role in cancer development (Song *et al.*, 2011). Additionally, Zhang *et al.* found that HS3ST3B increased tumor growth and angiogenesis (Zhang *et al.*, 2015). They suggested that this pro-oncogenic mechanism was induced by the activation of Vascular Endothelial Growth Factor (VEGF). HS3ST4 was shown

to inhibit the elimination of cancer cells by the innate immune system cells (Biroccio *et al.*, 2013). *In vitro*, HS3ST2, 3B and 4 increased breast cancer cell proliferation (Hellec *et al.*, 2018). In contrast, HS3ST2 is downregulated in primary breast cancer (Miyamoto *et al.*, 2003). This downregulation by gene methylation is thought to modulate cell invasiveness (Bui *et al.*, 2010; Kumar *et al.*, 2014). Furthermore, HS3ST3A displayed both anti- and pro-oncogenic activity depending on the breat cancer cell line studied *in vitro* and breast cancer subtype in patients (Mao *et al.*, 2016).

1.6.8.4 HS3STs in Alzheimer's disease

Alzheimer's disease is characterised by the accumulation of amyloid plaques and hyper phosphorylated tau proteins. Sulfated GAGs were found to promote tau protein and β-amyloid assembly into filaments (Goedert *et al.*, 1996; Castillo *et al.*, 1999). Additionally, HS3ST2 and HS3ST4 are overexpressed in patients with Alzheimer's disease (Sepulveda-Diaz *et al.*, 2015). 3-O-sulfated HS can bind to tau and Sepulveda-Diaz *et al.* suggested that HS3ST2 might regulate the abnormal phosphorylation of tau (Sepulveda-Diaz *et al.*, 2015).

1.6.8.5 HS3STs and viral infection

There is interest in the role of HS in viral infection. Because HS is present on all mammalian cells, viral particles with a HS binding site have an advantage for invading cells. For instance, Human immunodeficiency virus (HIV), Hepatitis C virus (HCV), dengue virus and herpes simplex virus (HSV) all use HS to bind their target cells (Liu and Thorp, 2002). The gD-type HS3STs generate the binding site of the viral glycoprotein gD required for the HSV viral envelope to fuse with the host cell membrane (Shukla *et al.*, 1999). A synthetic peptide binding 3-O-sulfated HS showed inhibition of HSV-2 infection in mice (Ali *et al.*, 2012). In line with these results, 3-O-sulfated octasaccharides can inhibit HSV-1 cell invasion *in vitro* (Copeland *et al.*, 2008). These observations highlight the need to understand and target HS3ST activity to generate new therapeuties in viral diseases.

1.6.8.6 HS3STs in ovulation

Human follicular fluid is rich in HS 3-O-sulfation (De Agostini *et al.*, 2008). The potential role for HS3ST in reproduction was initially proposed following the observation that HS3ST1-/- mice had impaired fertility. It was speculated that anticoagulant HS (aHS) may be essential for reproduction. The inner follicle contains the oocyte and granulosa cells (GC). GCs surround the oocyte and secrete hormones that influence oocyte maturation. Recent research showed that GCs synthesise aHS before and after ovulation to potentially protect the oocyte from proteolysis (Princivalle *et al.*, 2001; Hasan *et al.*, 2002; De Agostini, 2006). Hence, aHS seems important in maintaining a favourable environment to oocyte development during the ovulation cycle.

1.6.8.7 HS3STs in the kidney

In the kidney, HS 3-O-sulfation has been described in the glomerulus, tubular basement membrane and blood vessels (Girardin *et al.*, 2005). The Glomerular Basement Membrane (GBM) displayed an unusual disaccharide unit with a 3-O-sulfated GlcA without 6-O-sulfation (Edge and Spiro, 1990). The relevance of this finding is yet to be determined. Interestingly, HS3ST1 expression correlates with glomerular filtration rate (Bunnag *et al.*, 2009) and its expression was significantly modulated in kidney transplantation (Einecke *et al.*, 2010; Sagoo *et al.*, 2010). However, the mechanisms and consequences behind this change have not been described and require further investigation.

1.6.9 HS sulfatases and endosulfatases

Sulfatases are important as a mechanism to regulate HS on the cell surface and in the ECM.

6-O-sulfated HS is desulfated by the activity of two endosulfatases, SULF1 and SULF2. SULF1/2 are extracellular enzymes that preferentially remove a sulfate group from the trisulfated disaccharide IdoA2S-GlcNS6S (Frese *et al.*, 2009). SULF1-/- and SULF2-/- mice are viable (Lamanna *et al.*, 2006) but show structural abnormalities within the nervous system (Kalus *et al.*, 2009). These observations suggest that the SULFs and probably HS 6-O desulfation are essential to neuronal development. Additionally, the inactivation of SULF1 generated more HS structure modification compared to SULF2-/- with higher increase of trisulfated disaccharide IdoA2S-GlcNS6S and decrease in IdoA2S-GlcNS (Nagamine *et al.*, 2012). Because 6-O-sulfation is

important for growth factor binding and signalling, SULFs are essential regulators of cell proliferation, migration and differentiation. Their action can increase activity of some cytokines for example bone morphogenetic protein, or diminish activity of other such as FGF, VEGF and heparin-binding EGF-like growth factor (HB-EGF) (Nagamine *et al.*, 2012). Furthermore, SULF expression can be controlled by pro-fibrotic factors such as TGFβ1 (Yue *et al.*, 2008). All together these observations show that SULFs are important in inflammatory processes. In addition SULF2 is overexpressed in cancer and in idiopathic pulmonary fibrosis (Yue *et al.*, 2013; Vivès *et al.*, 2014) while SULF1 is downregulated in many cancers (Dai *et al.*, 2005).

Additionally, heparanase and three heparin lyases have endoglycosidase activity (Desai *et al.*, 1993). The three heparin lyase enzymes can cleave highly sulfated HS between 2-O-sulfated IdoA and GlcNS (Heparin Lyase I (heparinase) and II) and poorly sulfated HS between GlcA and either GlcNAc or GlcNS (Heparin Lyase II and III (heparitinase)). Nitrous acid can also cleave HS (Shively and Conrad, 1976).

Heparanase specificity has been widely studied and recently the cleavage sites of heparanase have been identified between GlcA and GlcNS3S or GlcNS6S but also between GlcA and GlcNS when there is a 2-O-sulfated GlcA2S next to the cleavage site. The repeating pattern of IdoA2S-GlcNS has an inhibiting action on the enzyme (Peterson and Liu, 2010). Heparanase has been widely studied in renal diseases (Van Den Hoven *et al.*, 2007; Masola *et al.*, 2015) and was overexpressed in the glomeruli of patients with overt diabetic nephropathy (Van Den Hoven *et al.*, 2006) and in rats with Adriamycin nephropathy (Kramer, 2006). In a murine model of diabetic nephropathy, heparanase -/- mice did not develop proteinuria and had unchanged urinary levels of albumin after streptozotocin injections (Gil *et al.*, 2012).

Additionally, heparanase plays a role in TGFβ1 expression in tubular cells (Masola *et al.*, 2014). Glycosidases are also important tools for us scientists to study the impact of HS cleavage in inflammation and fibrosis.

1.7 HS in renal development and renal diseases

The involvement of HS and HS modifying enzymes in renal development and disease progression have been discussed in section 1.6 and is summarised Table 1-6.

Interestingly, HS 2-O-sulfation seems crucial in renal development with C5-epimerase and HS2ST1 -/- mice developing renal agenesis (Bullock *et al.*, 1998; Li *et al.*, 2003). This agenesis could be due to an impaired ureteric bud branching, important in early stages of development as observed in rat embryos treated with heparitinase (Steer *et al.*, 2004). The changes in HS sulfation in kidney disease vary between diseases (Table 1-6).

However, the study of GAGs is very complex and the use of antibodies can be misleading as HS can be masked by attached cationic proteins.

.

	Model	Methods/analysis	Observations	References
In vivo models	rat embryos	treatment with heparitinase	impaired ureteric bud branching	(Steer *et al.*, 2004)
	HS2ST1-/- mice	morphological studies	renal agenesis	(Bullock *et al.*, 1998)
	NDST1-/- specific podocytes	functional studies	glomerular hypertrophy, increased albumin to creatinine ratio	(Sugar *et al.*, 2014)
	EXT1 -/- mice	morphological studies	hypertrophic glomeruli	(Chen *et al.*, 2008)
	C5-epimerase-/- mice	Morphological studies	Renal agenesis, lung and skeletal malformations	(Li *et al.*, 2003)
	Adriamycin nephropathy	staining	increase in heparanase	(Kramer *et al.*, 2006a)
	Heparanase -/-, STZ induced diabetic mice	functional and histological studies	decrease in albuminuria and renal damages	(Gil *et al.*, 2012)
	STZ induced diabetic mice and rats	staining, WB, mRNA level	increase in heparanase expression	(Van Den Hoven *et al.*, 2006)
Human studies	lupus nephritis	staining (JM403)	decrease in HS	(Van Den Born *et al.*, 1993)
	SLE nephritis	staining (EW3D10, GlcNS6S)	increase in HS N and 2-O-sulfation	(Rops *et al.*, 2007)
	glomerulonephritis	staining (JM403)	decrease in HS	(Van Den Born *et al.*, 1993)
	diabetic kidneys	disaccharide analysis	decrease in HS 3-O-sulfation	(Edge and Spiro, 2000)
	diabetic kidneys	staining (LKIV69, HS4C3)	increase in HS sulfation	(Wijnhoven *et al.*, 2006)
	diabetic nephropathy	staining	heparanase overexpression and HS loss	(Van Den Hoven *et al.*, 2006)
	diabetic nephropathy	staining (JM403)	decrease in HS	(Van Den Born *et al.*, 1993)
	minimal change nephrotic syndrome	staining (HS3A8, EW3D10, EW4G20)	no change	(Wijnhoven *et al.*, 2007)
	minimal change disease	staining (JM403)	decrease in HS	(Van Den Born *et al.*, 1993)
	Blood of tolerant transplanted patients	gene expression analysis	increase in HS3ST1 expression	(Sagoo *et al.*, 2010)
	kidney failing grafts	gene expression analysis	increase in HS3ST1 expression	(Einecke *et al.*, 2010)
	kidney transplant biopsies	gene expression analysis	HS3ST1 correlates with glomerular filtration rate	(Bunnag *et al.*, 2009)
	chronic rejection	staining (HS3A8)	increase in HS 2 and 6-O-sulfation	(Alhasan *et al.*, 2014)

Table 1-6: HS involvement in renal development and diseases
STZ: streptozotocin SLE: Systemic Lupus Erythematosus

Finally, HS is important in the GBM for the control of complement activation, an essential component of the innate immune system. The regulation of the complement system on the GBM is critical as it can trigger several kidney diseases. Briefly, the complement system has three pathways. The classic pathway mediated by immune complexes, the lectin pathway activated by glycans and the alternative pathway activated on the surface of pathogens. Activation of complement can mediate inflammation, clear cell debris and immune complexes (Borza, 2017) and is therefore tightly regulated. Factor H is a glycoprotein regulating the alternative pathway. Factor H can bind to HS of glomerular endothelial cells (Jokiranta *et al.*, 2005; Loeven *et al.*, 2016) and it is speculated that loss of HS on the GBM may compromise complement regulation by factor H (Borza, 2016). The alternative pathway of complement activation is implicated in lupus nephritis (Sato *et al.*, 2011) and anti-GBM disease (Ma *et al.*, 2014). Research on HS and the factor H interaction in renal diseases could identify new therapeutic avenues.

1.8 HS in inflammation

1.8.1 Chemotaxis

Inflammation is a rapid response to protect and heal the body. However, when uncontrolled, this process can lead to fibrosis in CKD and renal rejection following transplantation. To initiate inflammation, the access of leukocytes to the injured tissue requires migration through the blood vessel wall.

Leucocyte migration to injured tissue involves binding to the endothelium, degradation of the basement membrane and, finally, transmigration (Ferro, 2013) (Figure 1-10). HS on both the ECM and cell surface contributes to cell migration because of its binding to essential inflammatory proteins: chemokines. Chemokines are chemotactic cytokines.

It is widely accepted that leukocyte adhesion to endothelial cells is triggered by chemokines. Historically, it was believed that soluble chemokines triggered this attraction. However, they would be too easily removed by blood flow and circulating leukocytes would be activated which could be harmful. Therefore another hypothesis has emerged based on the observation that immobilised IL-8 attracts leukocytes *in vitro* (Rot, 1993) and that the immobilisation domain is required for transcytosis (Middleton *et al.*, 1997). HS can control the function of chemokines by preventing

their proteolysis, regulating receptor activation and immobilising them to create a gradient that attract leukocytes to injured tissue (see Figure 1-10). Originally this was a hypothetical function of chemokines and had never been demonstrated *in vivo*. The first time a chemokine gradient was demonstrated was in 2013 when Weber M *et al.* showed chemokine driven attraction of dendritic cells along lymphatic vessels in murine tissue (Weber *et al.*, 2013). Different models of inflammation in mice have been studied and correlated to HS enzymes (Table 1-4).

For neutrophil migration, L selectin and the expression of P and E selection on endothelial cells is also crucial (Figure 1-10). Recent studies investigating chemotaxis demonstrated that HS participates in L-selectin binding to leukocytes. Weak L selectin binding and increased rolling velocity are observed when HS biosynthesis is altered in mice lacking NDST1 enzyme (Wang *et al.*, 2005). This highlights the fact that leukocyte rolling is influenced by HS sulfation. It can be hypothesised that having under sulfated HS decreases chemokine presentation, chemokine gradient and L selectin binding impairing leukocyte entry to the injured tissue. Hence HS sulfation patterns could either become biomarkers or targets for inhibiting chemotaxis.

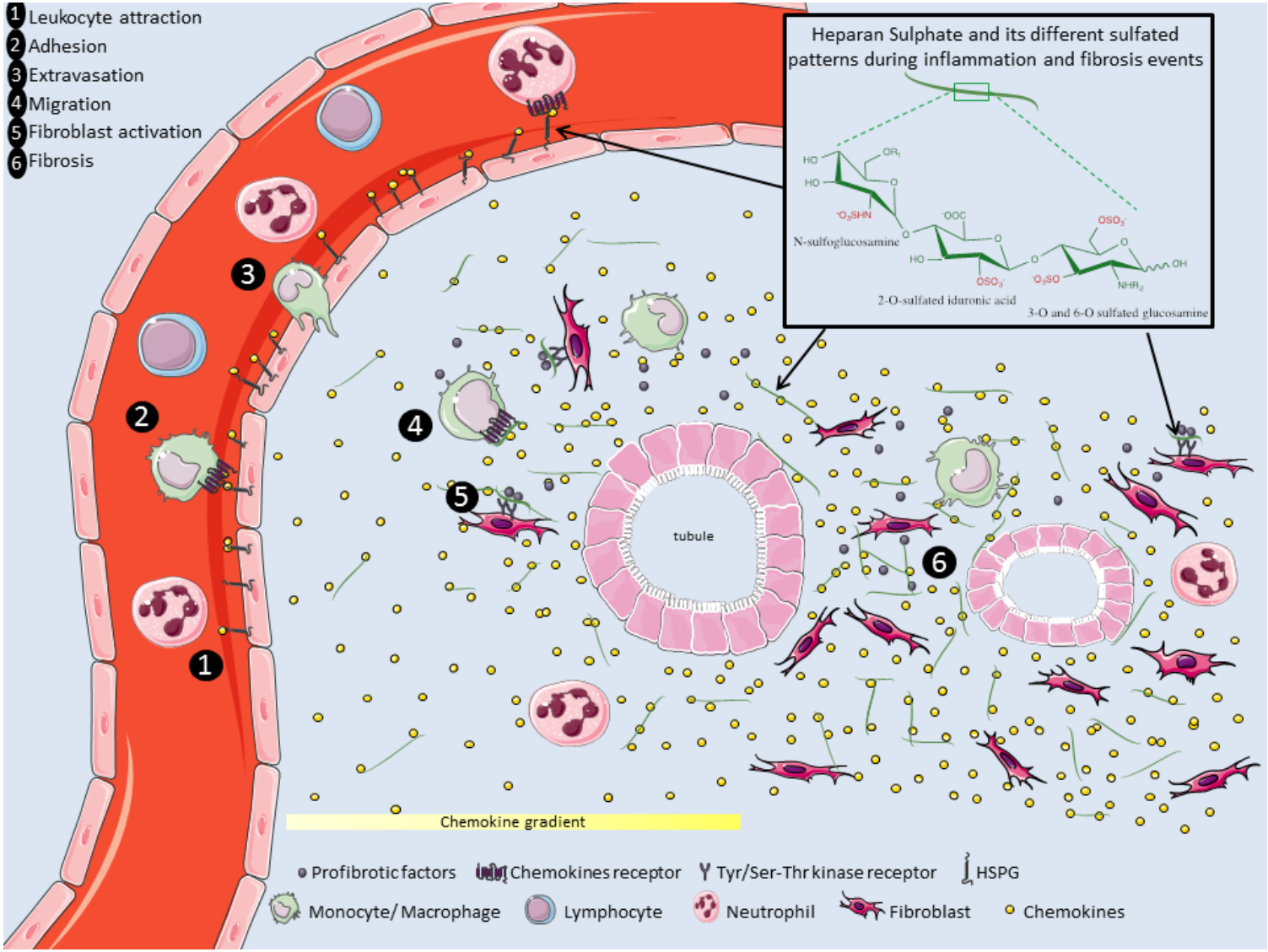

Figure 1-10: Heparan Sulfate in chemotaxis and fibrosis development
From (Ferreras *et al.*, 2015)

1.8.2 HS in fibrosis and pro-fibrotic factor binding

Heparan sulfate proteoglycans are increased in the development of fibrosis with an excess of Collagen XVIII and perlecan. This phenomenon has been observed in kidney isografts and allografts in rats (Rienstra *et al.*, 2010).

The mechanisms leading to fibrosis are complex and many factors are involved. The excess matrix deposition is mainly driven by myofibroblasts but other cells, including glomerular and tubular epithelial cells, can produce matrix components such as collagen (Kreisberg and Karnovsky, 1983; Creely *et al.*, 1988).

Fibroblasts are the key mediators of fibrosis. These cells have a characteristic phenotype with an elongated cell body (spindle shape), large Golgi apparatus and rough endoplasmic reticulum due to their intense synthetic activity. In tissue healing, myofibroblasts (activated fibroblasts) invade the injured tissue. They have both fibroblast and smooth muscle characteristics (Sappino *et al.*, 1990). Fibroblast activation is stimulated by mechanical stress and pro-fibrotic cytokines that are secreted by cells and sequestered by the matrix. During inflammation, fibroblasts are receptive to Platelet Derived Growth Factors (PDGF), Interleukin-13 (IL-13), Transforming Growth Factor β1 (TGFβ1) and Fibroblast Growth Factor 2 (FGF2) (Horvath *et al.*, 1996; Leask and Abraham, 2004). Endothelial cells, and macrophages secrete PDGF which triggers fibroblast proliferation, differentiation, and ECM production (Scotton and Chambers, 2007). T cells secrete IL-13 which stimulates myofibroblast differentiation, collagen production and matrix metalloproteinase expression (Fuschiotti, 2011; Fuschiotti *et al.*, 2013). Neutrophils and macrophages secrete TGF-β1 a factor that plays key roles in fibrosis progression by stimulating inflammatory cytokine production and inducing ECM synthesis by fibroblasts (Leask and Abraham, 2004). Transforming Growth Factor TGFβ1 is modulated by HS (Lyon *et al.*, 1997).

Macrophages and endothelial cells secrete FGF2 that stimulates fibroblasts proliferation. Additionally, FGF2 effect on renal fibroblast proliferation requires HSPG expression on the cell surface (Clayton *et al.*, 2001; Kalluri and Zeisberg, 2006). Because FGF2 binding requires HS, this interaction is an attractive target when studying HS in fibrosis.

1.8.2.1 HS and FGF2

There are more than 20 members in the FGF family involved in cell growth and development (Basilico and Moscatelli, 1992). FGF signalling requires the interaction between FGF, HS and a cell-surface tyrosine kinase receptor (Guimond and Turnbull, 1999). To date, four FGF receptors families have been identified (FGFR1, FGFR2, FGFR3 and FGFR4).

FGF2 was first isolated from pituitary extracts and named basic fibroblast growth factor for its basic and mitotic properties (Armelin, 1973; Gospodarowicz and Moran, 1975). FGF2 is implicated in proliferation, migration, differentiation and angiogenesis (Murphy *et al.*, 1990; Holland and Varmus, 1998; Javerzat *et al.*, 2002). *In vivo* and crystallography studies showed that HS sulfation is essential for FGF2 signalling. HS 2-O sulfation is important for binding to FGF2 (Maccarana *et al.*, 1993), while 6-O-sulfation plays a role in FGFR1 binding (Pye *et al.*, 1998; Schlessinger *et al.*, 2000; Sugaya *et al.*, 2008). This was further confirmed by using mouse embryonic fibroblasts HS6ST1 and HS6ST2 -/- which demonstrated decreased FGF2 signalling (Sugaya *et al.*, 2008).

FGF signalling cascades have been well documented. The tyrosines present in the intracellular domain of FGF receptors are phosphorylated and can activate four different pathways, PI3/Akt pathway, PLCγ the Janus kinase/signal transducer and activator of transcription (Jak/Stat) and ERK pathways (Lanner and Rossant, 2010).

The increase in HS 2-O and 6-O-sulfation seen in chronic rejection could be associated with the increase in FGF2 activity associated with fibrosis (Alhasan *et al.*, 2014). Hence, targeting FGF2 binding to HS is an interesting avenue for preventing fibroblast activation and therefore limiting fibrosis.

1.8.2.2 HS and HB-EGF

Heparin Binding Epidermal growth factor like (HB-EGF) is a member of the EGF family with mitogenic activity (Higashiyama *et al.*, 1991). It was first isolated in 1990 from culture media of macrophages by heparin Sepharose affinity chromatography (Besner *et al.*, 1990). HB-EGF has two forms, it is first synthesised as a transmembrane protein (proHB-EGF) which can be cleaved into a soluble growth factor. HB-EGF expression is triggered by hypoxia in neuronal cells (Jin *et*

al., 2002) and in burn injury (Cribbs *et al.*, 2002). HB-EGF can signal through EGF receptors to activate Jak/Stat, ERK, PI3K-Akt and PLCγ pathways (Knudsen *et al.*, 2014). To date, the specific sequence binding of HB-EGF to HS is yet to be determined.

Following intestinal ischemia reperfusion, HB-EGF -/- mice showed increased injury (El-Assal *et al.*, 2008) suggesting a protective role for HB-EGF. Additional studies from the same group showed that HB-EGF administration following ischemia reperfusion accelerated intestinal recovery (El-Assal and Besner, 2005). In the kidney, HB-EGF has been identified to be important for tubular cells repair (Sakai *et al.*, 1997). In fibrosis, HB-EGF was found to be protective in liver fibrosis (Huang *et al.*, 2012; Takemura *et al.*, 2013). Furthermore, renal transplants show a strong staining for HB-EGF (Celie *et al.*, 2012; Talsma *et al.*, 2017) making it an attractive growth factor to study for preventing fibrosis.

1.8.3 HS and therapeutics

The current knowledge on HS and proteins interaction enables the development of therapeutic opportunities to treat inflammation and fibrosis. Research have shown that heparin was beneficial in different *in vivo* models of kidney diseases. For instance, daily injection of low molecular weight heparin (LMWH) decreased collagen, fibronectin, TGFβ and macrophage infiltration in a rat model of renal fibrosis (Pecly *et al.*, 2006). In line with these results, Braun et al. showed that LMWH was beneficial in chronic renal rejection with a decrease in proteinuria and reduced leukocytes infiltration in treated rats (Braun *et al.*, 2001).

Furthermore, considering the side effects of the use of heparin, derivatives of anticoagulant heparin were developed and showed promising results. One of the first study to demonstrate the beneficial effect of non-anticoagulant heparin was Diamond et al. in a rat model of glomerulosclerosis (Diamond and Karnovsky, 1986). The authors showed a decrease in proteinuria, and normal glomerular filtration rate in rats treated with nonanticoagulant heparin. Later, Purkerson et al demonstrated that N-desulfated-acetylated heparin and heparin provided similar protection in rat subtotal nephrectomy (Purkerson *et al.*, 1988). In puromycin-induced glomerulosclerosis, non-anticoagulant heparin injection induced a better renal function and limited macrophages infiltration (Ceol *et al.*, 2003). Furthermore, after transplantation, glomerular infiltration and TGFβ expression decreased in rat kidneys treated with a hypersulfated derivative of heparin (Gottmann *et al.*, 2007).

Interestingly, small HS mimetics which are heparin derivatives can be generated not only to study specific protein bindings (Freeman *et al.*, 2005) but also to modulate protein activities (Sheng *et al.*, 2013). HS mimetics have a wide range of action including reducing CCL5 chemotactic activities (Sheng *et al.*, 2013), decreasing FGF2 activation of ERK signalling in muscle satellite cells (Ghadiali et *al.*, 2017) and reducing heparanase expression *in vivo* (Hammond *et al.*, 2013). HS mimetics have been assessed in clinical trial for cancer treatment (Liu *et al.*, 2009).

Another approach to target HS binding to proteins is to synthesise HS based antagonist chemokine or peptides that can interfere with binding. Hence, the modified proteins or peptides can compete with the WT protein and decrease its activity. These methods are described section 5.1.

1.9 Questions raised by this study

HSPGs main functions are regulated by the negative charge carried by their GAGs. Some of them can carry HS 3-O-sulfation, a rare but functionally important modification. To date, no study has documented the changes in HS 3-O-sulfation in renal fibrosis. Is this modification important in fibrosis? Does it increase or rather decrease following injury?

Additionally, whether HS 3-O-sulfation increases or decreases, little is known about the growth factors affected by these changes. Do growth factors modulate HS3ST expression during renal fibrosis? Are growth factor binding and signalling events changed by HS 3-O-sulfation?

Finally, with our knowledge of HS in fibrosis, is it possible to alter FGF2 binding by generating HS binding peptides? Can FGF2 binding to renal epithelial cells be altered by positively charged peptides?

1.10 Aims

This project had the ambition to:

1. Determine if HS sulfation and HS modifying enzymes change during the development of renal fibrosis
2. Understand how HS3STs expression is regulated and identify growth factors modulated by HS 3-O-sulfation
3. Generate heparin binding peptides that could compete with FGF2 binding to HSPGs

2 General material and methods

2.1 Cell Culture

All experiments handling tissue culture were performed in a containment class II cabinet. Cells were maintained at 37°C under 5% CO_2 in a humidified incubator. Control Of Substances Hazardous to Health (COSHH) and BIOCOSHH risk assessments were in placed before doing any experiment.

2.1.1 Cell lines and media

In this project, two models of human immortalised renal epithelial cells and one immortalised rat renal fibroblasts cells were studied. From the American Tissue Culture Collection, HK2 cells are cortex/proximal tubular epithelial cells isolated from a normal adult kidney and immortalised with the human papillomavirus 16. HK2 doubling time is not clearly known with studies showing time between 34.1 to 96h (Iwata and Zager, 1996; Keshari *et al.*, 2013; Belmonte *et al.*, 2016).

HKC8 are cortex/proximal tubular cells isolated and immortalised by a hybrid virus, adenovirus 12-SV40. They were isolated from the healthy pole of a renal cell carcinoma nephrectomy. HKC8 doubling time is 20h.

HK2 and HKC8 (Figure 2-1) have the feature of differentiated proximal tubule cells (Ryan *et al.*, 1994; Racusen *et al.*, 1997). However, they display different features at the brush border. HK2 cells have higher alpha-methyl-glucopyranoside uptake, gamma-glutamyl transpeptidase activity and NaK ATPase activity than HKC8. They have similar alkaline phosphatase and Glutathione-S-transferase activity. HKC8 have no Glucose-6-phosphatase activity but have higher lysosomal and mitochondrial activity than HK2 (cathepsin B, succinate dehydrogenase, N-acetyl-beta-D-Glucosaminidase (Racusen *et al.*, 1997)).

NRK-49F are rat renal fibroblasts from the American Tissue Culture Collection and have fusiform shape.

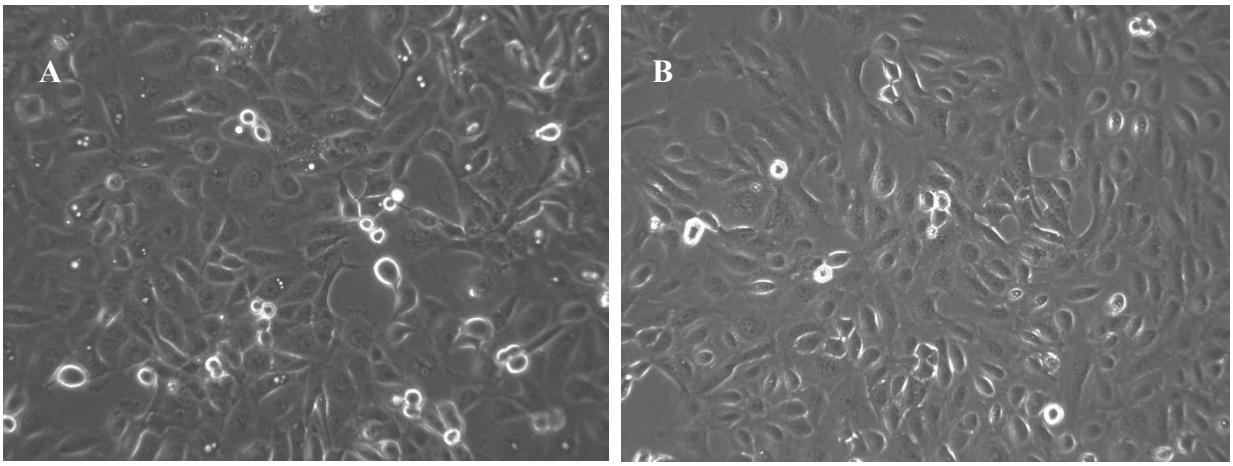

Figure 2-1: HK2 and HKC8 in culture
HK2 (A) and HKC8 cells (B) are human renal epithelial cells. Both cell lines display a typical epithelial cuboidal shape. Magnification 200x.

All media were supplemented with 2mM L-Glutamine, 100U/mL Penicillin, 100µg/mL (Sigma). HK2 were grown in Dulbecco's Modified Eagle Medium (DMEM, Sigma, D5671) supplemented with 10% heat inactivated Fetal Bovine Serum (FBS). HKC8 were cultured in DMEM-F12 (Sigma, D6421) supplemented with 5% FBS. NRK-49F were cultured in DMEM supplemented with 5% FBS.

2.1.2 General handling

Cells were grown in T75 flasks and trypsinised with Trypsin-EDTA solution (Sigma) when confluent. Trypsin detaches the cells by cleaving peptide chains mainly at positively charged Lysine and Arginine on carboxyl side. EDTA prevents the inhibition of trypsin by chelating Ca^{2+} and Mg^{2-} ions that are required for cell adhesion (e. g. integrin adhesion). Cells were washed with phosphate buffer solution (PBS, sigma) prior to trysinisation to remove any left-over medium that could inhibit the protease. Flasks were incubated at 37˚C to allow trypsin activity at the optimum temperature. Cells were collected by using medium with FBS that neutralises trypsin and then centrifuged 5 minutes at 300g. For cell counting, pellets were collected and suspended in 1mL PBS. A volume of 50µL was collected, diluted 20 times in trypan blue solution (0.4%), a dye that enters all cells but is actively excreted by living cells and counted with a Neubauer haemocytometer.

For cells cryopreservation, cell pellets from T75 flasks with a confluency of more than 90% were

suspended in a solution of 90% FBS, 10% Dimethyl sulfoxide (DMSO), a compound that prevents crystal formation during freezing and split in three 1mL cryovials. Vials were frozen at -80˚C in a freezing container (Thermo Scientific) filled with isopropanol that slows down the freezing process. Stocks were stored in a -80°C freezer for short-term storage or in liquid nitrogen for long term storage.

For thawing cells, cryovials were defrosted at 37°C in a water bath, suspended in 3mL of complete medium and seeded into a T75 flasks containing 20mL of complete medium. Media were changed after 16h to remove DMSO.

Cells were screened for mycoplasma once a month with the MycoAlert kit from Lonza. Mycoplasma are small self-replicating bacteria with no cell wall. They can interfere with protein, RNA, DNA production, cell cycle, cell signalling, cell membrane integrity (Drexler and Uphoff, 2002). A volume of 200µL of supernatant from cells cultured more than 24h were collected and centrifuged for 5 minutes at 300g and mycoplasma detection was carried out according to the manufacturer's protocol. The MycoAlert kit allows the detection of mycoplasma by lysing them and sensing the ability of a mycoplasma specific enzyme to transform ADP to ATP. The ATP produced was detected by bioluminescence. Mycoplasma positive cells were treated with MycoZap^{TM}, elimination reagent, Lonza.

2.2 Molecular Biology

The University safety policy was followed for all experiments in accordance with COSHH regulations and approved GM project (03/31 a2).

2.2.1 RNA extraction

Reverse-Transcriptase and quantitative Polymerase Chain Reaction have been developed to study genes expression. Because of the instability and sensitivity of RNAs to RNAse, caution was taken during the procedure. RNAses can be found in the environment, as it is a way of protecting ourselves against pathogens. Furthermore, equipment and the experimenter are a source of DNA contamination. Therefore, filter tips, clean benches, pipettes and gloves were used at all time.

Initially this method starts with the extraction of RNAs from a sample. In this study, two methods

of RNAs extractions were used. A column based one with the Qiagen RNeasy Plus Mini Kit for cell culture RNAs extraction and a Trizol/Chloroform method for mice tissue RNA extraction. The Trizol/chloroform technique is an effective method that includes three main steps: cell lysis; a phase separation to isolate RNAs from proteins, fatty acids, carbohydrates and DNA and finally RNAs precipitation and wash. The Qiagen RNeasy Plus Mini Kits is based on the same principles without the need to have a phase separation. Instead it uses a silica membrane, buffers containing guanidine thiocyanate (denaturing proteins), alcoholic buffers (to wash RNAs) to isolate RNA.

Prior to use the Qiagen RNeasy Plus Mini Kits, cells coated on 6-well plates were washed with PBS, trypsinised, centrifuged 5 minutes at 300g and suspended in 1mL of PBS before a last centrifugation at 300g 5 minutes. Depending on their size, final pellets were vortexed in 350 to 600µL of RLT plus buffer, a buffer that helps genomic DNA to bind to the gDNA eliminator spin column. This is to avoid any genomic DNA contamination. RLT buffer was supplemented with β-mercaptoethanol to denature RNase. Samples were deposed onto a gDNA eliminator spin column and centrifuged 1 min soft mode at 10 000g. Columns were discarded and 1 volume of 70% ethanol was mixed by pipetting to the flow-through which was then deposed onto a RNeasy spin column and centrifuged 15 seconds at 10 000g. Flow-through was discarded and 700µL of RW1 buffer (containing guanidine salt and ethanol) was added to the column to wash it from carbohydrates, proteins, fatty acids that do not bind to the silica membrane of the column and centrifuged 15 seconds at 10 000g. Once again, flow-through was discarded and 500µL of RPE buffer (a mild washing buffer with confidential composition) was added and tubes were centrifuged 15 seconds at 10 000g. This operation was repeated with a longer centrifugation (2 minutes). Finally, the columns were placed in a 1.5mL tubes, 30 to 40µL of Rnase free water was added onto it and tubes were centrifuged 2 minutes soft mode 10 000g.

For tissue extraction, RNAs extraction was performed with a Trizol/ chloroform technique. Small pieces of tissue were lysed and homogenised in 200 µL of TRI reagent (Ambion) using the Tissue Lyser II by Qiagen. An additional volume of 500µL of TRI reagent was added and mixed by inversion. The RNA was isolated from the protein by adding 200µL of chloroform (AnalaR) and mixed by inversion. The samples were centrifuged at 14 000g for 15 minutes at 4ºC. Each aqueous phase containing soluble RNAs was collected and mixed by inversion with 500µL of isopropanol. The tubes were left at room temperature for 10 minutes and spinned down at 14 000g for 10 minutes at 4ºC. The precipitated RNAs formed a pellet that was suspended in 1mL of 70% ethanol and

centrifuged at 14000g for 10 minutes at 4ºC. Lastly pellets were air dried and suspended in 30µL of RNAse free water (Ambion). To avoid gDNA contamination 1 µg of sample was treated with RQ1 DNAse (Promega) for 30 minutes at 37°C. Next, samples were treated with DNase stop solution (Promega) 10 minutes 65°C to inactivate any DNAse before starting the reverse transcription.

RNAs are composed of aromatic nucleobases that absorb 260nm wavelength light. Therefore, after extraction, all RNA concentrations were determined using a Nanodrop analysing density optic at 260nm. Proteins contaminations were determined by measuring the samples absorbance at 280nm. Phenol and guanidine thiocyanate contaminations were determined by measuring the samples absorbance at 230nm. Samples with both ratios above 1.8 were considered as of good quality.

2.2.2 Reverse Transcription and real time Polymerase Chain Reaction

Complementary DNA (cDNA) was generated using Tetro cDNA synthesis kit (Bioline) containing the Moloney Murine Leukemia Virus Reverse Transcriptase. Briefly up to 5µg of RNA from cells extraction or up to 1µg from tissue extraction were incubating with Oligo dT primers, a deoxyNucleotides TriPhosphates mix, RT buffer, a ribosafe inhibitor and the transcriptase and RNAse treated water for a final volume of 20µL. Samples were incubated 30 minutes at 45°C, a temperature where the reverse transcriptase is active. Finally, samples were incubated 5 minutes at 85°C to inactivate the reverse transcriptase. RNA were stored at -20°C for short-term storage and -80°C for long term.

Real Time Quantitative Polymerase Chain reaction is a powerful technique for assessing the difference in genes expression between two samples. In this study, TaqMan probes (Thermofisher) were used to amplify cDNA (Table 2-1).

The Probes carry a FAM fluorophore at their 5’ end and a quencher at their 3’end. When the fluorophore and the quencher are next to each other, no fluorescence can be detected. When the target gene is present, the probe binds to it and during elongation, the activity of Taq polymerase cleaves the probe, releasing the fluorophore and enabling fluorescent activity. This method allows DNA amplification and quantification to happen at the same time. The probe system was chosen, as it is specific to the gene of interest, Taqman probes being mostly designed between 2 exons.

Technically, RT samples were added to a blend of 10µL of 2x Sensifast Probe Hi-ROX mix (Bioline), 1µL of 10mM Probes (life technologies) and adequate volume of RNAse free H_2O for a final volume of 20µL. Triplicates were added in a 96-well plates and amplified using StepOnePlus real time PCR thermal cycler (Applied Biosystems). The PCR cycling conditions included an initial polymerase activation at 95°C for 5 minutes followed by 40 cycles of denaturation at 95°C for 10 seconds and annealing/extension at 60°C for 20 seconds.

HPRT was defined as housekeeping gene to normalise CT values. DNA and water contaminations were assessed. Samples were analysed using the comparative ΔΔCT method.

Species	Gene name	Gene Symbol	Reference
Human	Heparan sulfate-glucosamine 3-O-sulfotransferase 3B1	HS3ST3B1	Hs01391447_m1
Human	Heparan sulfate-glucosamine 3-O-sulfotransferase 1	HS3ST1	Hs00245421_s1
Human	N-deacetylase and N-sulfotransferase 1	NDST1	Hs00925444_mH
Human	heparan sulfate-glucosamine 3-sulfotransferase 5	HS3ST5	Hs00999394_m1
Human	Heparan sulfate-glucosamine 3-O-sulfotransferase 3A1	HS3ST3A	Hs00925624_s1
Human	Hypoxanthine guanine phosphoribosyl transferase	HPRT1	Hs02800695_m1
Human	Heparan sulfate-glucosamine 3-O-sulfotransferase 1	HS3ST1 (for plasmid)	Hs01099196_m1
Mouse	Heparan sulfate 6-O-sulfotransferase 1	HS6ST1	Mm01229698_s1
Mouse	Heparan sulfate (glucosamine) 3-O-sulfotransferase 6	HS3ST6	Mm01299930_m1
Mouse	Heparan sulfate (glucosamine) 3-O-sulfotransferase 1	HS3ST1	Mm01964038_s1
Mouse	Heparan sulfate (glucosamine) 3-O-sulfotransferase 3B1	HS3ST3B1	Mm03052977_s1
Mouse	Hypoxanthine guanine phosphoribosyl transferase	HPRT	Mm03024075_m1
Mouse	Sulfatase 1	SULF1	Mm00552283_m1
Mouse	Sulfatase 2	SULF2	Mm01248029_m1

Table 2-1: Taqman Probes

Gene expression was determined by using TaqMan probes from ThermoFisher. Genes' names, symbols and manufacturer references are displayed in the table below. Hs: Homo sapiens, Mm: Mus musculus. Suffix m indicates probes that are designed between two exons whereas s defines probes that bind within a single exon.

2.2.3 Bacterial transformation

Plasmid EX-TO223-M13 containing HS3ST1 enzyme sequence was purchased from GeneCopoeia (Figure 2-2). The plasmid was amplified by bacterial transformation as pictured Figure 2-3. Transformation of *E.coli DH5α* (Invitrogen) competent cells was performed by heat shock (45 minutes on ice, 40 seconds at 42°C followed by 2 minutes on ice). The change in temperature changes the fluidity of the bacterial membrane, allowing the plasmid to penetrate the host. Varying concentrations of plasmid (4, 8, or 10ng) were added to 50µL of competent cells. After transformation, bacteria were incubated for 1 hour at 37°C in 1mL LB medium (Lysogeny Broth Invitrogen Ref 12780.052) under agitation. Bacterial suspensions were then streaked at 37°C for growth overnight onto LB Agar plates supplemented with 100µg/mL Ampicillin (AMP), the antibiotic plasmid selection. After 15 hours of incubation, a single colony from each plate was selected and incubated overnight in 10mL of LB medium complemented with AMP.

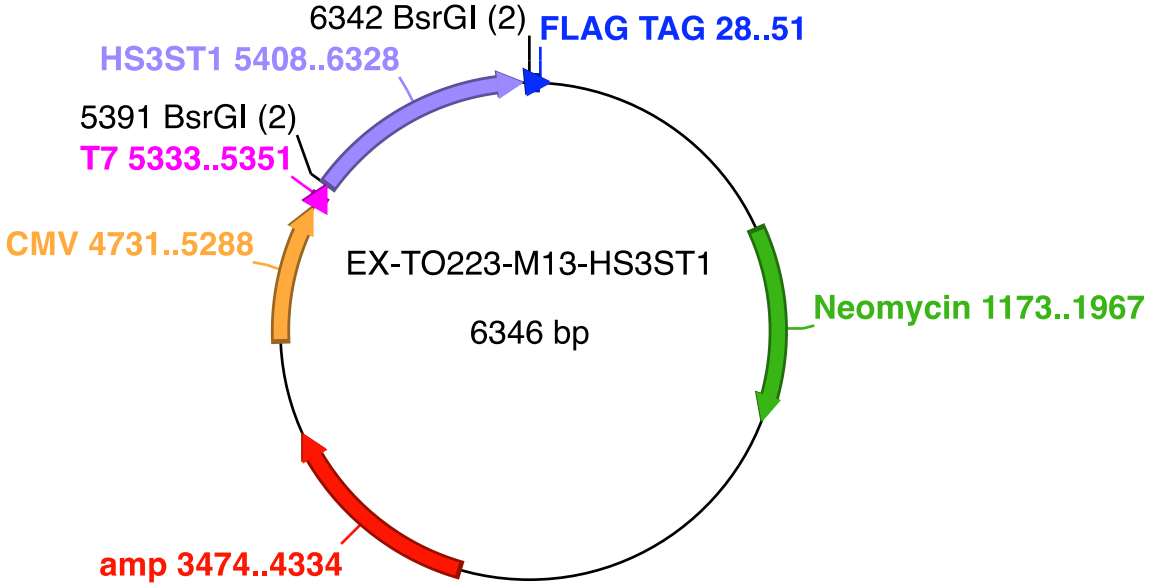

Figure 2-2: EX-TO223-M13 HS3ST1
To initiate gene expression T7 (bacterial promoter) and Cytomegalovirus (CMV, eukaryote promoter) were upstream of HS3ST1. A Flag Tag sequence was added at the C-term of HS3ST1 to label the generated protein. BsrGI restriction endonuclease cleavage sites are used for plasmid digestion and removal of the HS3ST1 sequence. The coding sequence for the resistance to Ampicillin (AMP) was used for bacterial selection and Neomycin for eukaryote cells selection.

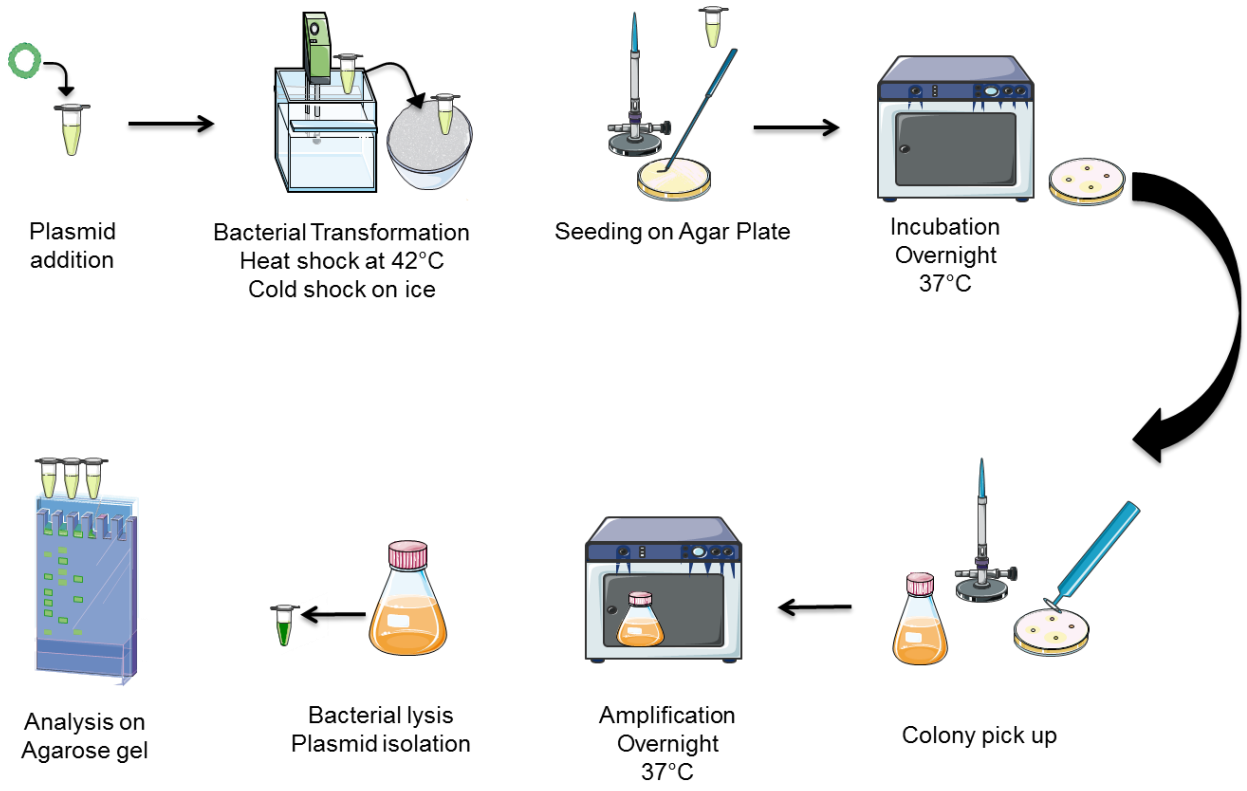

Figure 2-3 Plasmid amplification protocol
Competent bacteria were transformed by heat shock and seeded on agar plate overnight at 37°C. A single colony was amplified in LB medium overnight under agitation at 37°C and the plasmid was isolated and analysed the following day.

2.2.4 Plasmid purification and analysis

Bacterial cells lysis and plasmid purification were performed using Plasmid Mini Kits (Qiagen). Bacterial pellets from 3mL culture were collected by centrifugation (15 minutes 6000g at 4°C) and suspended in 0.3mL of suspension buffer (50 mM Tris·Cl pH 8.0, 10 mM EDTA, 100 µg/ml RNase A) and lysed with 0.3mL of an alkaline solution (200mM NaOH, 1% Sodium Dodecyl Sulfate (SDS) (w/v)) at room temperature. SDS is a detergent that releases bacterial contents by solubilising phospholipids and denaturing proteins present in the membrane, NaOH gives alkaline condition that denatures DNA. Lysates were neutralised with 0.3ml of a cold solution of 3M potassium acetate pH 5.5 and centrifuged 10 minutes at 15 000g. Under these conditions only plasmid DNA will acquire its correct conformation and therefore be in solution. Supernatants were added onto an equilibrated anion exchange column where under low salt conditions DNAs bind. Two salt washing steps with a solution of 1.0M NaCl, 50 mM MOPS, pH 7.0, 15% isopropanol (v/v) removed remaining metabolites, protein and RNAs from the column. DNA was eluted by

adding 1.25M NaCl, 50mM Tris·Cl pH 8.5 15% isopropanol (v/v) onto the column. Plasmid DNA was precipitated with isopropanol and centrifuged 30 minutes at 15 000g. The remaining pellet was washed with 1mL of 70% ethanol and centrifuged 10 minutes 15 000g. Dried pellets were suspended in 40µL of Tris EDTA Buffer.

Nucleic acid concentrations of the samples were calculated from their UV absorbance at 260nm with a nanodrop. To verify the plasmid integrity, samples isolated from the plasmid purification underwent restriction enzymes digests with the enzyme *SalI* that cleaves 2 sites of the plasmid. Following enzymatic digestion, all samples were loaded with 6X blue dye (promega) on a 0.8% agarose gel with 0.5-1µg/mL ethidium bromide and subjected to electrophoresis in Tris Acetate EDTA 1X buffer at 90V for 1-1h15. Fragments were visualised using AlphaImager. Plasmid sequencing was carried out by Source Bioscience.

To generate an empty plasmid (plasmid without HS3ST1 sequence), 3µg of plasmid were digested with 30U of BsrGI (Bsp 1407I, ThermoFisher) in 1X Tango buffer for 3h at 37°C in a final volume of 40µL. The whole digestion was run into a 0.8% agore gel for 1h15 at 90V. The digested plasmid was quickly cut out of the gel under a U.V light and extracted using QIAquick Gel Extraction Kit Plasmid extraction. The final plasmid was ligated 3h at room temperature using T4 DNA ligase.

2.2.5 Proteins extraction

Cells proteins were extracted using CelLytic M (Sigma) complemented with anti-protease (Complete Mini Protease Inhibitor Cocktail, Roche) and for Phospho STAT3 analysis with anti-phosphatase (Roche). At the time of extraction, 6-well plates were quickly placed on ice, washed twice with cold PBS and up to 200µL of lysis buffer was added into each well. The plates were placed on ice on a rotor for 15 minutes then scrapped. Lysates were collected in 2mL tubes and centrifuged 15 000g for 15 minutes at 4°C.

Supernatants protein concentration was estimated with a Pierce^{TM} BCA Protein Assay Kit from ThermoFisher. This kit is based on the ability of bicinchoninic acid (BCA) to form a violet compound when 2 BCA bound to Cu^{1+}. In alkaline condition, proteins will transform Cu^{2+} into Cu^{1+}. The more concentrated the samples the more Cu^{1+}which lead to the formation of a purple compound that absorbs light at 562nm. A standard curve with purified amounts of bovine serum albumin was used to determine the unknown samples concentration (Figure 2-4).

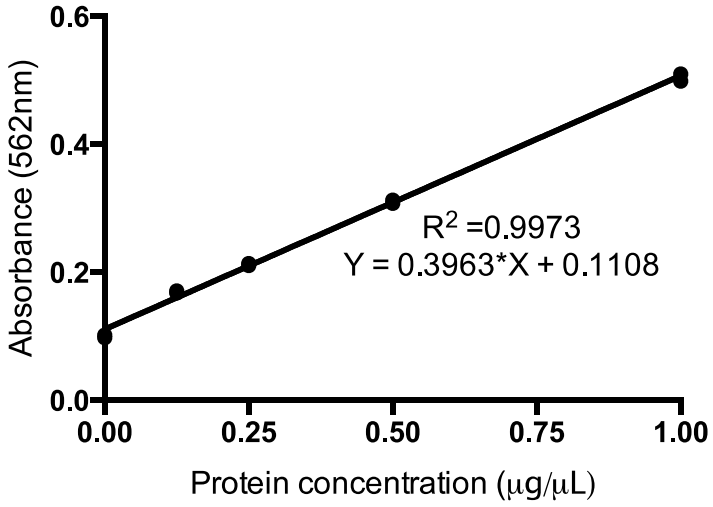

Figure 2-4: Protein concentration standard curve
For protein quantification, a standard curve was generated using a serial dilution of known Bovine Serum Albumin concentration. The concentration was correlated to the absorbance at 562 with a linear function y (absorbance) = A x (protein concentration) + B. The coefficient of determination (R^2) indicates how the equation fits the data with 1 being a perfect fit.

2.2.6 Western Blot

A list of antibodies used for Western Blot can be found Table 2-4. Between 10 to 50μg of protein extracts samples were denatured 10 minutes at 95°C in Laemmli buffer (BioRad) with β-mercaptoethanol (5mM). Samples were electrophoretically separated by SDS Polyacrylamide gel with a 5% acrylamide stacking gel and a 10% acrylamide resolving gel (see composition Table 2-2).

The acryl-bisacrylamide creates a network for the proteins to go through. SDS is an anionic detergent that will denature proteins and charge them. TEMED and ammonium persulfate were added lastly to the mix as they catalyse the polymerisation. To determine protein sizes, samples were loaded together with a protein ladder (Page Ruler, Thermo Scientific) and transferred by semi dry transfer (BioRad) to a nitrocellulose membrane (BioRad). The main buffers used for Western Blot can be found in Table 2-3.

Stacking gel (5%)	Resolving gel (10%)
4.1mL H_2O	4mL H_2O
1mL 30% acryl-bisacrylamide mix	3.3mL 30% acryl-bisacrylamide
0.75mL 0.5M Tris pH 6.8	2.5mL 1.5M Tris pH 8.8
60µL SDS 10%	0.1mL SDS 10%
60µL ammonium persulfate 10%	0.1mL ammonium persulfate 10%
6µL TEMED	4µL TEMED

Table 2-2: SDS-Page gel composition

Membranes were blocked for 1hour at room temperature in 0.1% Tween Tris-buffered saline (TBS) with 5% fat free milk or 5% Bovine Serum Albumin (BSA) when looking at phosphorylated proteins and probed overnight at 4°C using the following primary antibodies diluted in blocking buffer (Table 2-4).

Electrophoresis Buffer 5X	TBS 10X
250mM Tris base (30.3g)	152mM Tris-HCL (24g)
250mM MOPS (52.3g)	46mM Tris base (5.6g)
17mM SDS (5g)	1.5M NaCl (88g)
5mM EDTA (1.5g)	H_2O for final volume of 1L
H_2O for final volume of 1L	pH 7.6

Table 2-3: Western Blot buffer composition

Following overnight incubation, membranes were washed in TBS 0.1% Tween 3 times for 5 minutes. Membranes were incubated with the corresponding secondary antibodies conjugated with Horse Radish Peroxidase (R&D) (Table 2-4) for 1h at room temperature under agitation. Membranes were washed 3 times for 5 minutes with TBS 0.1% Tween and finally immunopositive bands were visualised by enhanced chemiluminescence using Supersignal West Pico, Chemiluminescent, Thermo Scientific Reagents. The membrane was then exposed to X-ray films.

	Type	Target	Reference	Manufacturer	Dilution
I	Rabbit monoclonal	Stat3 Y705	ab76315	Abcam	1:20 000
I	Rabbit polyclonal	Flag tag DYKDDDDK	2368	Cell signalling	1:3000
I	Mouse monoclonal	alpha Tubulin	T6074	Sigma	1:4000
I	Rabbit monoclonal	Phospho-Erk p44/42	4370	Cell signalling	1:1000
I	Mouse monoclonal	Pan ERK	610124	BD Transduction laboratories	1:1000
II	Goat polyclonal-HRP conjugated	Mouse IgG	HAF007	R&D	1:1000
II	Goat polyclonal-HRP conjugated	Rabbit IgG	HAF008	R&D	1:1000

Table 2-4: List of antibodies for Western Blot. I=primary antibody, II= secondary antibodies

2.3 Immunofluorescence

2.3.1 Antibodies

	Type	Target	Reference	Manufacturer	Dilution
I	Rabbit polyclonal	Flag tag DYKDDDDK	2368	Cell signalling	1:800
I	Mouse polyclonal	GM130	ab 169276	Abcam	1:70
I	Rabbit polyclonal	HB EGF	ab 192545	Abcam	1:200
I	Phage display VSV	HS-3-0-sulfation	HS4C3	Prof van Kuppevelt	1:5
I	Rabbit polyclonal	Fibronectin	sc-8422	Santa Cruz	1:100
I	Mouse monoclonal	E-cadherin	610181	BD Biosciences	1:100
I	Mouse monoclonal	smooth muscle α-Actin	sc-32251	Santa Cruz	1:100
II	Mouse monoclonal Cy3	VSV glycoprotein	C7706	Sigma	1:200
II	Goat Polyclonal Alexa fluor 488	Mouse IgG	A11001	Thermo Fisher	1:100
II	Goat Polyclonal Dylight 550	Rabbit IgG	GtxRb-003-D550NHSX	Immunoreagents	1:100

Table 2-5: List of antibodies used for immunofluorescent staining
I=primary antibody, II= secondary antibodies

Techniques of immunofluorescence are a great asset for tissue imaging and to localise and track molecules within the matrix, the basal membrane and within the cell. Images were taken with Leica LCM microscope, Zeiss Axioimager, Nicon A1R confocal microscope. For tissue culture images, pictures were taken by Carl Zeiss 40CFL microscope. Immunofluorescent images were analysed using Fiji and Zen softwares.

2.3.2 Chamber slides staining

All antibodies references and dilutions can be found Table 2-5.

For protein staining:

HK2 and HKC8 cell lines were cultured in complete media into 8-well chamber slides (Falcon, corning). Cells were 60-80% confluent when starting the staining in order to have some space between the cells and therefore a better staining. Cells were fixed in ice-cold methanol for 5 minutes at -20°C and gradually rehydrated with PBS. To avoid unspecific binding, 5% BSA in PBS was added into each well at room temperature for 2h. Albumin binds widely to the proteins on the cells. Primary antibodies were diluted in PBS (see Table 2-5) and incubated overnight at 4°C to allow a slow, specific and high binding of the primary in a humidified chamber to prevent the slides from drying. The next day, slides were washed 3 times for 5 minutes with PBS and incubated 2h at room temperature with the corresponding secondary antibody in the dark to avoid photo bleaching. Finally, slides were washed 3 times for 5 minutes in PBS and mounted with liquid mounting medium containing DAPI (Vectashield) and stored in the dark at 4°C until imaging.

2.3.3 Paraffin embedded staining

Mouse kidneys were dissected and fixed in 4% formalin solution and embedded in paraffin by the Royal Victoria Infirmary pathology services. Serial tissue sections of 4µm thickness were cut and mounted onto slides. Sections were dewaxed for 5 minutes in xylene and gradually rehydrated with incubation in decreasing alcohol concentration solution of 99%, 95%, 75% and finally tap water. Peptide retrieval was performed by microwaving the slides in 200 mL of EDTA buffer two times 5 minutes on high power then cool down for 20 minutes. Sections were blocked 10 minutes with 2% fetal bovine serum in PBS to block non-specific binding sites at room temperature. Sections

were incubated overnight in the dark at 4°C with primary antibodies. The next day sections were washed 3 times 5 minutes with PBS then incubated with secondary antibody diluted in PBS for 1-2h at room temperature. Sections were then washed 3 times 5minutes in PBS, incubated with Sudan Black for 20minutes in the dark at room temperature and finally washed 3 times in PBS before mounting with VECTA shield DAPI liquid mounting medium. Sudan black was used to remove any background of fluorescence.

2.4 Flow cytometry

2.4.1 Principles

Flow cytometry is a powerful tool for analysing single cells. It can distinguish different cell population by examining how a cell scatters a known wavelength light. Cell's size is determined by a Forward Scatter Channel (FSC) that collects light scattered in the forward direction. Internal structure and granulosity are determined by a Side Scatter Channel (SSC) that collects light scattered at 90°. Additionally, cells can be fluorescently labelled to quantify extracellular and intracellular molecules. A laser beam stimulates the fluorophore and a detector collects the emitted fluorescence. All measurements collected by a detector correspond to a parameter. For this study Fluorescein isothiocyanate (FITC) was used with an excitation wavelength of 488nm and a fluorescence emission detectable by a 530/30 filter. An example of excitation-emission spectra can be found Figure 2-5.

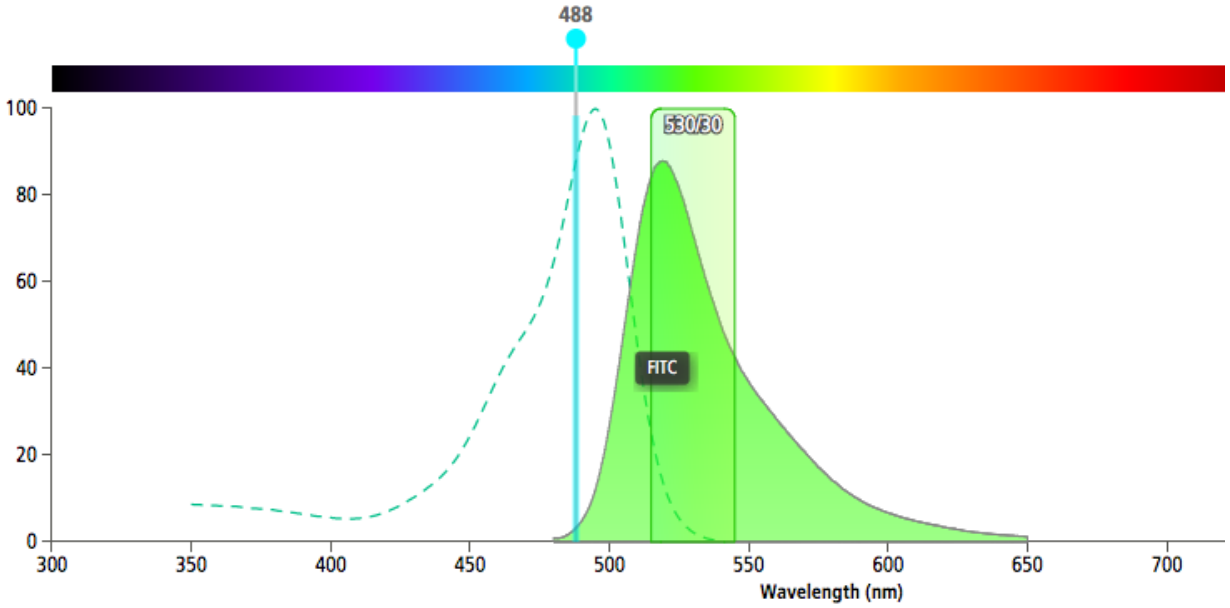

Figure 2-5: FITC laser excitation and emission spectra
Using the FACS Canto II, FITC is excited at 488nm. Fluorescence is detected with a 530/30 filter. Source: BD-biosciences.

2.4.2 FGF2 binding

FGF2 binding was studied with the Human FGF basic biotinylated Fluorokine Flow Cytometry kit (R&D). The use of a biotinylated FGF2 allowed a very strong binding with the associated Avidin-FITC that enables an amplified signal. Cells cultured in T75 flasks were detached with Accutase (Biolegend) or cell dissociation solution (Sigma). Trypsin could not be used as it alters the heparan sulfate proteoglycan present on cell surfaces. Cells suspension was washed twice with PBS and resuspended in PBS containing 2% BSA at a concentration of $4x10^6$ cells/mL. In 2mL tubes, 25µL of the cell suspension (100 000 cells) was incubated with 10µL of 1mg/mL of biotinylated FGF2 or with a biotinylated negative control (a soybean trypsin inhibitor that does not bind to cells) for 1h at 4°C. In the same tube, 10µL of Avidin-FITC conjugated secondary were added for 30 minutes in the dark at 4°C. The cells were washed twice with 2mL of 1X RDF1 (a buffered saline-protein solution specifically designed to minimise background staining and stabilise specific binding) to remove unbound avidin-FITC. Finally, cells were suspended in 0.2mL of 1X RDF1 for flow cytometry analysis with FACS Canto II.

For peptides and peptoids treatments, time of incubation and concentration are specified in the specific method sections.

2.5 Software and statistics

Graphs were created using Microsoft Excel and GraphPad Prism 6.0. Diagrams were generated using Microsoft PowerPoint and Servier Medical Art images (http://servier.com/Powerpoint-image-bank). Chemical compounds were drawn with ChemDraw. Plasmids were designed using ApE (Universal).

Results are expressed as mean±SD. Statistical evaluations were performed using GraphPad Prism 6.0. Significant results were considered when $P<0.05$ (*), $P<0.01$ (**) and $P<0.001$ (***). Unless specified, P values were calculated using one way ANOVA with Bonferonni's correction and two tailed unpaired student's t-test with Welch's correction for *in vitro* treatments and two tailed unpaired student's t-test with Welch's correction for the *in vivo* work.

3 Heparan sulfate modulation *in vivo*

3.1 Introduction

3.1.1 Heparan sulfate in human kidney diseases

The study of HS and its modifications is more complex than studying proteins for which antibodies can be generated and used. Fortunately, in the 1990s, HS antibodies were created to study the number of HS chains attached to a core protein (antibody 3G10), the amount of HS (antibody 10E4) (David *et al.*, 1992), and the different degree of sulfation (phage display antibodies, (van Kuppevelt *et al.*, 1998)). Furthermore, the synthesis of HS disaccharide standards have allowed the development of HS sequencing techniques by high performance liquid chromatography and mass spectrometry (Hart and Varki, 2015).

Because these tools have been newly developed and used, only recent research has examined HS in renal diseases. HS has previously been studied by indirect immunofluorescence in patients with lupus nephritis, membranous glomerulonephritis, minimal change disease and diabetic nephropathy where glomerular staining was decreased (Van Den Born *et al.*, 1993). In the same study, renal biopsies from Alports syndrome and IgA nephropathy showed similar staining to control kidneys. However, when analysing not only HS but HS sulfation, patients with proliferative lupus nephritis had a significant increase of HS N, 2 and 6-O-sulfation in their glomeruli (Rops *et al.*, 2007). Furthermore, human renal allograft biopsies showed an increase in HS 2-O and 6-O-sulfation staining compared to normal human kidney (Alhasan *et al.*, 2014). In contrast, disaccharide analysis of the glomerular basement membrane of diabetic patients revealed a decrease in 3-O-sulfation (Edge and Spiro, 2000).

Another way to study HS sulfation is to analyse HS modifying enzyme expression. To date very little research has analysed the expression of HS sulfotransferases in human kidney diseases. Recent studies have looked at HS3ST1 expression in transplanted patients. One study found HS3ST1 expression increased in the blood of tolerant patients (Sagoo *et al.*, 2010) while another one found it increased in the kidneys of failing grafts (Einecke *et al.*, 2010). Additionally, HS3ST1 expression was found negatively correlated with glomerular filtration rate (Bunnag *et al.*, 2009). No mechanistic explanations were given to determine the significance of HS3ST1 expression for renal function.

Taken together these data indicate that HS sulfation is complex in the way that a decrease in HS does not necessary correlate with a decrease in HS sulfation. Furthermore, depending on the type of disease, HS sulfation can be decreased or increased. Additional studies and *in vivo* models can help elucidate how HS changes during renal fibrosis and what modulates HS with time.

3.1.2 Animal models of renal diseases

The use of animal models is important for understanding the mechanisms of disease development, signalling, testing new drugs and finding biomarkers. There are many different models of renal diseases in rat, pigs and mice. The risk factors for CKD development can be study with the use of genetically modified or selected animals with obesity (ob/ob mice, New Zealand obese Mice, db/db mice, etc), insulin resistance (KK-Ay mouse, Zucker diabetic fatty rat) and also hypertensive animals. However here I will focus on acute injury models that can lead to the development of renal fibrosis.

3.1.2.1 Pre-renal acute injury

Ischemia Reperfusion Injury (IRI) can be studied *in vivo* by clamping a renal artery to generate ischemia and then restoring blood flow to cause reperfusion damage. In this model, a longer ischemic period can induce more damage (Hesketh *et al.*, 2014). The IR procedure can be performed in one or both kidneys. However unilateral ischemia does not allow the study of renal function as the contralateral kidney remains functional. IR can be performed on one kidney and a nephrectomy on the non-ischemic kidney to allow functional measurement. IRI can vary with body temperature, animal strain, age and sex (Wei and Dong, 2012). Various anesthetics can be used but volatile agents such as isoflurane have been found to be protective (Erturk, 2014). This model generates cell death, mitochondrial and ER stress, inflammation and fibrosis. The IRI model is a good tool to understand what happens during organ transplantation as the organ is subjected to IRI and can be used to test drugs to prevent injury. HSPGs such as syndecan-1 can sometimes protect from fibrosis development with Syndecan-1 -/- mice showing increased tubular injury following bilateral IRI (Celie *et al.*, 2012).

Another model of ischemic injury is induced by creating arterial stenosis with the use of a stent to reduce blood flow. Compared to IR surgery, the arterial stenosis model can be less invasive

(Lerman *et al.*, 1999). However, this model only reduces blood flow and does not stop it. Additionally, invasive procedures using clip on one or both arteries to study arterial stenosis can be done.

3.1.2.2 Intrinsic acute injury

The use of drugs to treat disease can damage kidneys. For example, aminoglycoside antibiotics such as gentamicin can accumulate within tubules and trigger necrosis and generate acute injury. Models can be used to understand the toxicity and develop drugs that reverse the side effects (Li *et al.*, 2009). The injection of Adriamycin, a chemotherapy drug, generates podocyte effacement, glomerular hypertrophy and the development of fibrosis accompanied with protein excretion (Lee and Harris, 2011). Adriamycin was found to increase glomerular heparanase expression and decrease HS (Kramer *et al.*, 2006b), indicating a potential role for HS loss in disease progression. Drugs used in renal transplant patients can be nephrotoxic. Calcineurin inhibitors, which inhibit T cell activation, can disrupt endothelial function (Oflaz *et al.*, 2003). The use of animal models to study nephrotoxic drugs is important for the development of improved molecules with fewer side effects.

Finally, there are models of sepsis that can be used. This includes the intraperitoneal injection of lipopolysaccharides (LPS), the ligation into the ileocecal valve (a muscle that separates the small and the large intestine) and puncture of the caecum (Rittirsch *et al.*, 2009) or the insertion of a stent into the ascending colon to allow bacteria to migrate into the peritoneal cavity (Traeger *et al.*, 2010). In this model, a loss of HSPG on the endothelium together with an increase of heparanase within the glomerulus was observed (Xu *et al.*, 2014). The loss of HS could be linked to disease progression and should be further studied. Once again studying these models can help generate new drugs or biomarkers for sepsis.

3.1.2.3 Postrenal acute injury

As discussed in chapter 2, postrenal injury is due to the obstruction of the urinary tract. To date, only two models have been developed. In rats, kidney stones can be generated by injection of vitamin B6, sodium oxalate, ammonium oxalate, hydroxyl-L-proline, ethylene glycol, glycolic acid

and glyoxalate (Khan, 2010). HSPG are thought to play a role in crystal formation with syndecan-1 expression increasing in rat kidneys with stone formation (Iida *et al.*, 1997).

The other model, which is studied in this chapter, is Unilateral Ureteral Obstruction (UUO). The UUO model can be used to study reversible injury if the obstruction is removed or chronic irreversible injuries when the obstruction is definitive (Chevalier *et al.*, 2009). It induces tubular dilatation, immune cells infiltration and the development of interstitial fibrosis. The contralateral kidney can be used as a control even though some changes can occur in response to the other damaged kidney. In this model, renal function can only be assessed if the UUO is performed together with re-implantation and a nephrectomy of the contralateral kidney. This model can be used to study recovery when the obstruction is removed. The first functional damage can be observed within 24h (Vaughan *et al.*, 2004). The obstructed kidney shows increased staining of interstitial col I, col III, fibronectin and perlecan between 3 to 7 days of UUO (Sharma *et al.*, 1993). This model is adequate for the study of interstitial fibrosis, a disease which is currently irreversible. Hence the importance and the use of UUO for this project.

Taken together, the review of the different models of kidney diseases and the lack of information regarding HS 3-O-sulfation raised interest about the potential changes in sulfation. The aims of this chapter are:

-To identify if the UUO model was suitable for assessing HS sulfation changes during the development of interstitial fibrosis

-To analyse the changes in HS 3-O-sulfation with renal fibrosis

-To identify new HS binding growth factors possibly modulated by HS 3-O-sulfation

3.2 Specific material and methods

3.2.1 Unilateral Ureteral Obstruction experiment

The UUO model was selected to analyse the changes in HS during renal fibrosis. In order to observe the changes with the severity of disease, three different time points were selected. Mice were subjected to UUO for 5, 10 and 15 days. All experiments were carried out under UK Home Office regulations (PPL60/4521) at the Comparative Biology Centre (CBC), Newcastle University. Mice were housed in cages of 6 animals and had free access to food and water throughout the experiment.

C57BL/6 female mice aged 8-10 weeks were anaesthetised (ketamine/medetomidine), shaved around their lower abdomen and injected subcutaneously with the pain killer buprenorphine. To access the left kidney, a laparotomy incision in the lower abdomen was made. Once the ureter was isolated, it was tied from 1cm of the kidney with Mersil 6.0. A second knot was made at approximately 3mm from the first one and the ureter was cut in-between the two knots. The abdomen was then closed with 5.0 vicryl. The right kidney was not manipulated and used as a control. At the end of the surgery, mice were injected with the reversal atipamezole. Eye ointment was applied to all animals to avoid eye dryness.

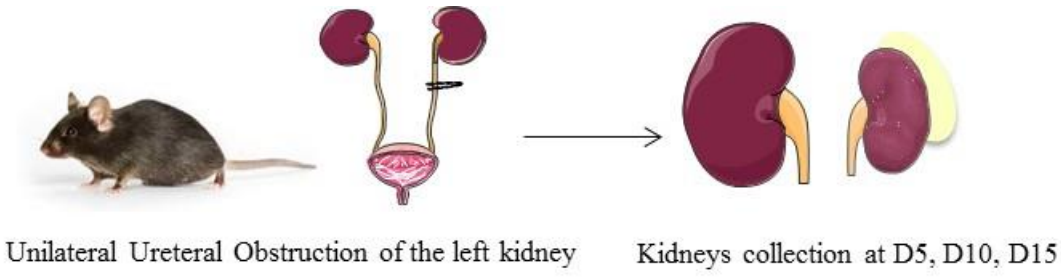

Figure 3-1: UUO plan of experiment

3.2.2 Samples collection

At D5, D10 and D15 after UUO, blood, urine, spleen and kidneys were retrieved. However, urine, blood and spleen samples were not used for this study. Kidneys were dissected into 4 parts. Half of the kidney was directly put into a cassette and placed in 4% formalin for paraffin embedding. The other half was cut into three pieces, one was left in RNAlater for RNA extraction, the two last

pieces were snap frozen for disaccharide analysis and cryosections. The experimental plan is illustrated Figure 3-2.

RNAs extraction and staining on mice kidneys were described in section 2.

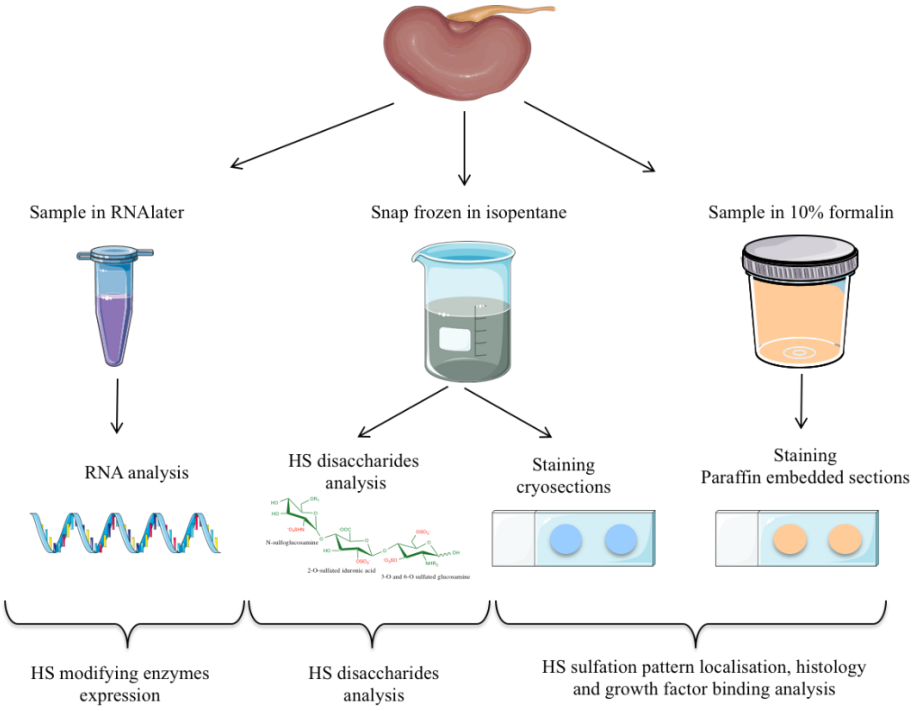

Figure 3-2: Samples collection and analysis following UUO

3.2.3 HS disaccharides analysis from mice kidney

HS disaccharides analysis was performed at the "Institut de Biologie Structurale", Grenoble France by Dr Romain R Vives and the PhD student Rana el Masri as described previously (Hijmans *et al.*, 2017).

3.2.4 Paraffin embedded sections staining

Paraffin embedded kidney tissues were cut at 4µm thickness and mounted onto slides. All staining started with a dewax and rehydration step. Sections were dewaxed 5 minutes in xylene and rehydrated in decreasing concentration of ethanol. First slides were incubated for 10 seconds in 99% ethanol, then 10 seconds in 95% ethanol, 10 seconds in 70% ethanol and finally 1 minute in tap water.

Haematoxylin and Eosin (H&E) staining was performed on paraffin embedded sections. Following dewaxing and rehydration, slides were incubated for 80 seconds in Mayers haematoxylin and washed for 1 minute under tap water. The Mayers haematoxylin solution is composed of hematein (oxydised haematoxylin) complexed to metal ions (usually Al^{+3}) providing an overall positive charge. The complex binds negatively charged molecules such as chromatin and may bind to mucin and proteoglycans. In general, hematein Al^{+3} gives a red/purple nuclear coloration, to turn the nuclear coloration into blue, slides were incubated in Scott's solution 30 seconds and washed in tap water. Slides were incubated 30 seconds in alcoholic eosin and washed briefly in tap water. Eosin is a negatively charged synthetic dye and therefore binds positively charged proteins within the tissue. Red blood cells are colored red and muscle, collagen, cytoplasm pink. Slides were dehydrated by 10 seconds incubation in 70%, 90%, 95% ethanol and finally xylene. Slides were mounted with DPX and imaged using Zeiss Axioimager.

For Sirius red staining, nuclei were stained 8 minutes in Weigert's haematoxylin and washed in tap water. Slides were then incubated for 1 hour in 0.1% solution picro Sirius red and washed twice in acidified water (5mL of glacial acetic acid into 1L of water). Sirius red sulfonic acid groups can bind to basic amino acids and gives a pink/red color. It can stain collagen I and III but also amyloid fibrils. The acidified water removes any excess of staining. Finally, samples were dehydrated in three quick washes of ethanol 100% and mounted. Images were analysed using LeicaQWin analysis software with 10 cortex fields analysed per section for each kidney.

Peptide retrieval was performed by microwaving the slides in EDTA buffer. Sections were blocked 10 minutes with 2% FBS in PBS and incubated overnight at 4°C with primary antibody (HB-EGF ab192545 Abcam 1:200, HS4C3 1:5 given by Toin van Kuppevelt, Radboud University, Netherlands). The next day, sections were washed in PBS, then incubated with secondary antibody (anti VSV C7706 sigma, Dylight 550 Immunoreagent) diluted in PBS for 1-2 hours at room temperature. Sections were then washed in PBS, incubated with Sudan Black for 20 minutes in the dark at room temperature and finally washed in PBS before mounting with VECTA shield DAPI liquid mounting medium.

Immunofluorescence images were analysed using Fiji and Zen softwares.

3.2.5 Cryosection staining

3.2.5.1 Generating fluorescently labelled AT

Fluorescently labelled Antithrombin III (AT) was generated using Alexa fluor 647 labelling kit from ThermoFisher Scientific, A20173. The procedure is shown Figure 3-3. A quantity of 1mg of AT (Calbiochem, 169756) was suspended in PBS and dialysed twice with 6mL of PBS to remove any Tris that could interfere with the labelling as the dye binds to amine residues. Alexa fluor 647 is a succinimidyl ester that reacts best at pH 7.5-8.5. Therefore, a volume of 50µL of 1M bicarbonate was added to 450µL of the dialysed AT to increase the pH. The solution of AT was then incubated for 2h at room temperature with Alexa fluor 647 and gently mixed with a magnetic stirrer. A BioGel P30 column was used to separate the labelled AT from the free dye. Labelled AT was eluted by gradually adding elution buffer (10mM potassium phosphate, 150mM NaCl, pH 7.2, 0.2mM sodium azid). The labelled AT was collected into a final volume of 1.2mL. The final labelled protein was diluted 1 in 5 and absorbance values at A280, A650 were taken to determine the degree of labelling using the formula:

$$\text{Protein concentration (M)} = \frac{(\boldsymbol{A280} - (\boldsymbol{A650} \times \mathbf{0.03})) \times \boldsymbol{dilution\ factor}}{\mathbf{37\ 700}}$$

37 700 $cm^{-1}M^{-1}$ is the molar extinction coefficient of AT.

$$\text{Moles dye per mole protein} = \frac{\boldsymbol{A650} \times \boldsymbol{dilution\ factor}}{\mathbf{239\ 000} \times \boldsymbol{protein\ concentration\ (M)}}$$

239 000 $cm^{-1}M^{-1}$ is the molar extinction coefficient of the Alexa fluor dye.

The degree of labelling was about 25.5 moles of dye per mole of protein. This can be considered as over-labelling. Overlabel can cause aggregation, dye quenching and unspecific staining. Therefore, optimisation and assessment of the staining quality and specificity was required.

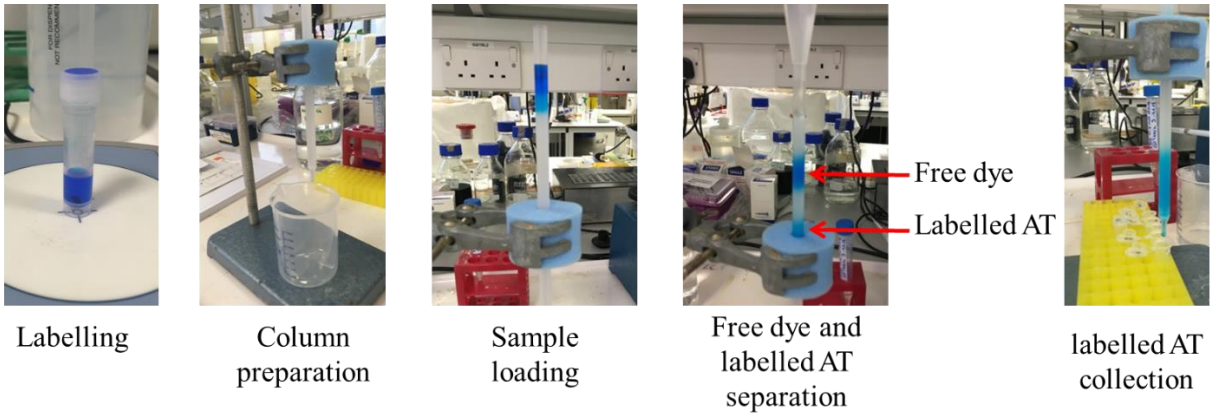

Figure 3-3: Antithrombin III labelling with Alexa fluor 647
AT was purchased from Calbiochem and labelled with Alex fluor 647 (ThermoFisher Scientific).

3.2.5.2 Antithrombin III staining

The use of labelled AT to detect HS 3-O-sufation has been previously described (Girardin *et al.*, 2005) and this method was followed for staining. Cryosections of 7µm thickness were fixed in acetone and hydrated 15 minutes in PBS. Slides were blocked with 1% BSA in PBS for 20 minutes at room temperature and incubated for 1h with 1:5 labelled AT (lb AT) in the dark. Sections were then washed 3 times with blocking buffer and 1 time in PBS. Slides were mounted using Vectashield containing DAPI. As observed Figure 3-4, the staining with lb AT showed positive staining on the tubules basement membrane and blood vessels. Due to the faint DAPI staining, glomerular staining was difficult to assess. Therefore, a second optimisation was performed using a different mounting medium. The second time slides were mounted with Prolong Diamond antifade containing DAPI (ThermoFisher Scientific) mounting medium and were incubated for 24h at room temperature in the dark before imaging. As observed Figure 3-5, the staining was localised at the tubular basement membrane, on vessels and within the glomerular vascular structures. This staining was similar to what was observed before (Girardin *et al.*, 2005). However, to make sure the staining was specific for heparan sulfate, a competition assay was performed with heparin.

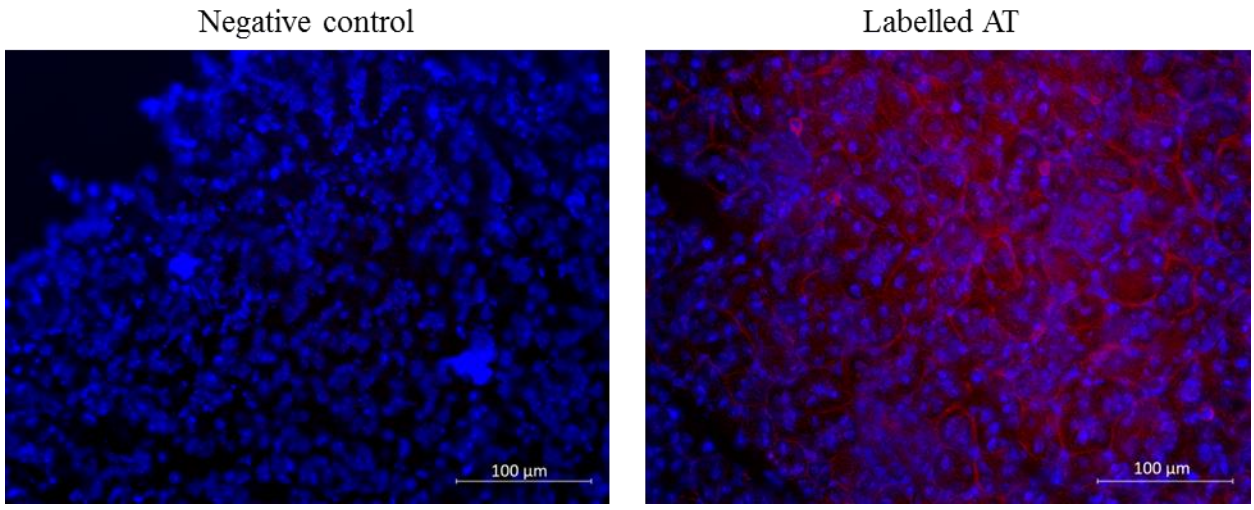

Figure 3-4: First staining with labelled antithrombin III
Representative images of labelled AT staining. Control kidney cryosections were blocked for 20 minutes in 1% BSA and incubated for 1h with 1:5 labelled AT or with blocking buffer (negative control). Slides were mounted with Vectashield containing DAPI. Scale bars represent 100µm.

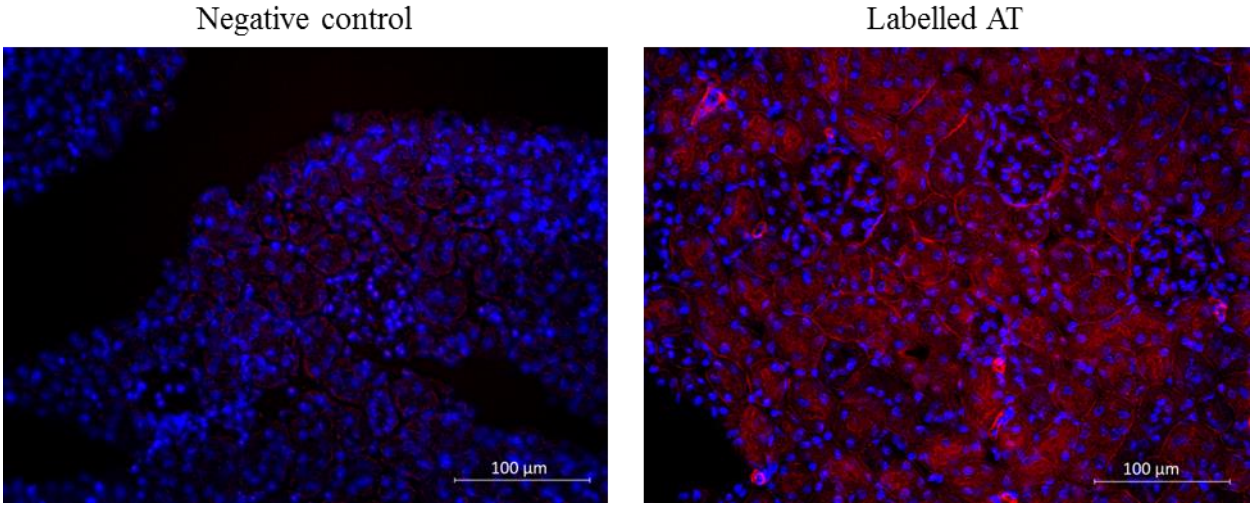

Figure 3-5: Second staining with labelled antithrombin III staining
Representative images of labelled AT staining. Cryosections from control kidney were blocked for 20 minutes in 1% BSA and incubated for 1 hour with 1:5 labelled AT or blocking buffer (negative control). Slides were mounted with prolong diamond antifade containing DAPI and were stored 24h at room temperature before imaging. Scale bars represent 100µm.

3.2.5.3 Testing AT staining specificity

Slides were blocked for 20 minutes at room temperature in 1% BSA in PBS and incubated for 1 hour with 1:5 lb AT ± 20-200µM heparin. Slides were then washed three times with blocking buffer, mounted with prolong diamond antifade with DAPI 24 hours before imaging. As seen

Figure 3-6, the staining was completely abolished with the addition of heparin, confirming specificity of the labelled AT binding.

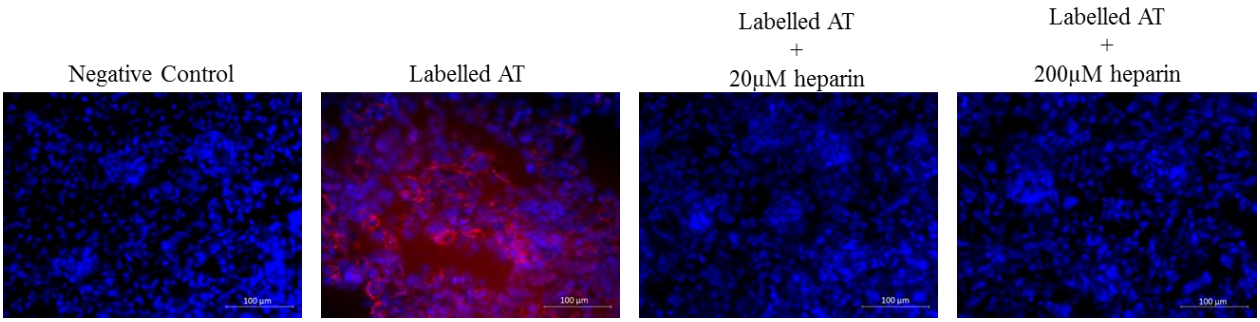

Figure 3-6: Assessing labelled AT staining specificity with heparin competition
Representative images of labelled AT staining. Cryosections from control kidney were blocked for 20 minutes in 1% BSA and incubated for 1 hour with 1:5 labelled AT ± Heparin (20-200µM) or blocking buffer (negative control). Slides were mounted with prolong diamond antifade containing DAPI and were stored 24 hours at room temperature before imaging. Scale bars represent 100µm. N=3

3.3 Results

3.3.1 Anatomical changes during UUO

As seen Figure 3-7, H&E staining of control, D5, D10 and D15 UUO kidney tissues showed morphological changes with the development of fibrosis. The staining was different in ureteral obstructed kidneys compared to control due to the increase in infiltrating cells and the excess deposition of ECM. Additionally, tubular structures were dilated at D5, D10 and predominantly at D15. At D15 UUO, the cortex was very damaged and narrow making it difficult to analyse. Therefore, further experiments focused on D5 and D10 UUO.

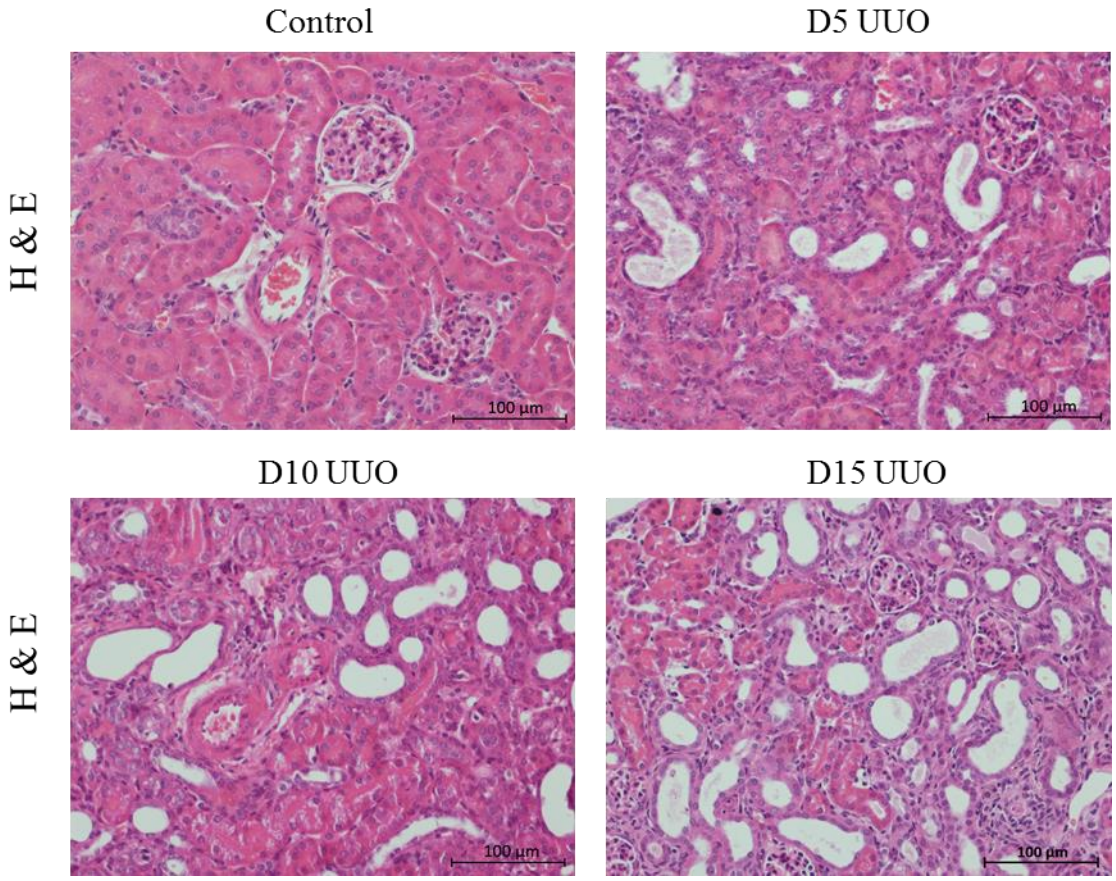

Figure 3-7: Haematoxylin and Eosin staining of control, D5, D10 and D15 UUO
Representative images of Haematoxylin and Eosin staining of cortex from control unobstructed kidney, D5, D10 and D15 UUO. Paraffin embedded sections of 4µm were dewaxed, rehydrated, stained for H&E and mounted with DPX. UUO generates tubular dilatation which was found to be very severe at D15 UUO. Images were taken by Zeiss Axioimager. Scale bars represent 100 µm. N≥5 per group with 3 cortical fields captured per section.

In order to estimate the level of fibrosis, slides were stained with Sirius red, a dye that stains collagen fibers red. In control tissue, glomerular capillaries, vessels and some interstitial tissues displayed a red staining. At D5 and D10 UUO, the staining was different to control with an increase in collagen deposition in the interstitium as seen Figure 3-8. Sirius red quantification showed significantly increased staining at D5 ($p<0.05$) and D10 ($p<0.001$) UUO.

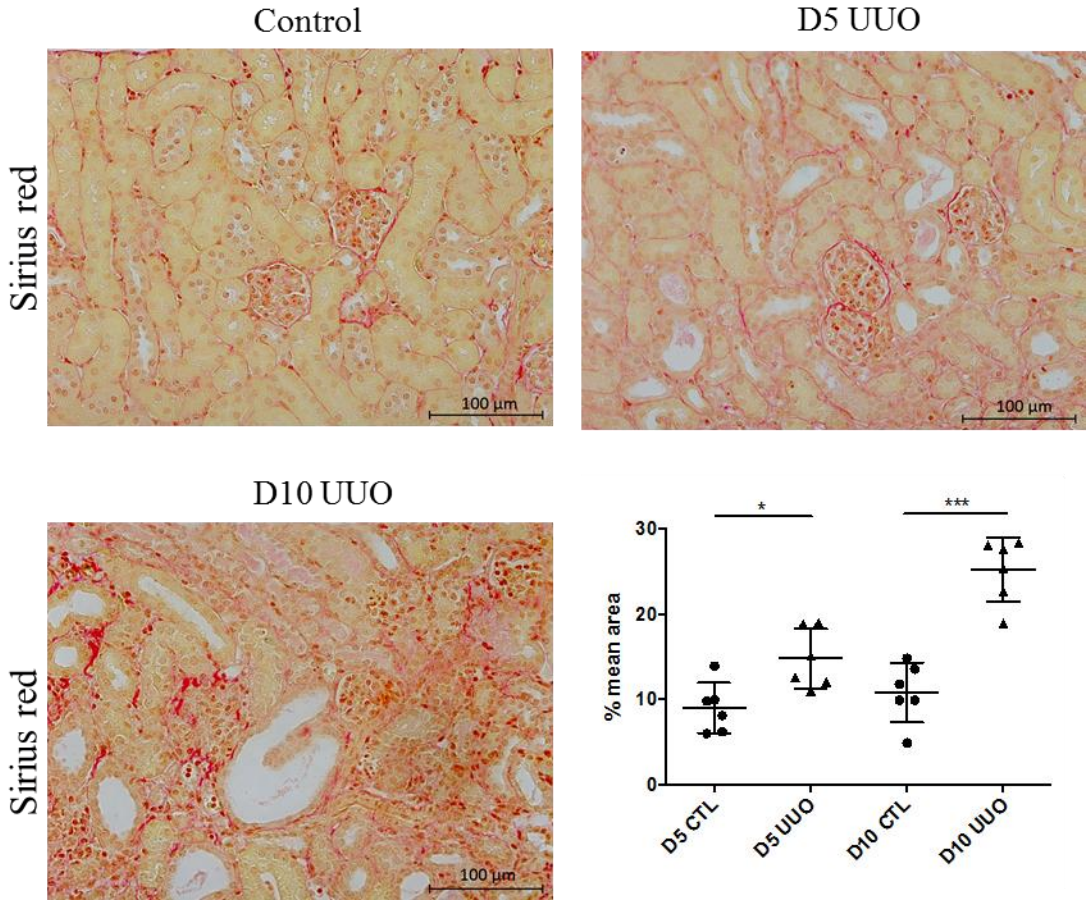

Figure 3-8: Sirius red staining and quantification
Paraffin embedded sections of 4µm were dewaxed, rehydrated, stained with Sirius red and mounted with DPX. Interstitial fibrosis was quantified by Sirius red staining (graph). N=6 per group with 10 cortex fields analysed per section for each kidney. Collagens are stained in red. Images were analysed using LeicaQWin analysis software. Two-tailed unpaired t test, $p<0.05$ (*), $p<0.001$ (***).

3.3.2 Heparan sulfate 2-O and 6-O-sulfation changes in renal fibrosis

The changes in the ECM with the development of fibrosis is well-described in the literature. However, not much is known about HS sulfation changes. To assess if there was an alteration in HS sulfation in the UUO model of fibrosis, HS sulfation and disaccharide sequencing analyses were performed in collaboration with the institute of structural biology in Grenoble.

N-acetylation and N-sulfation were not changed at D5 UUO (Figure 3-9). However, a decrease of 12.6% in N-acetylation together with an increase of 14.4% in N-sulfation was observed at D10 UUO.

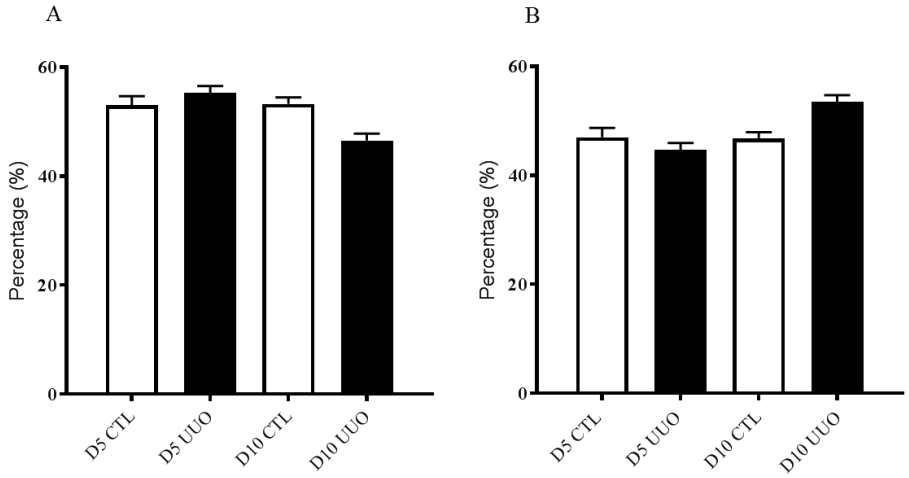

Figure 3-9: Total N-acetylation and N-sulfation in control and D5, D10 UUO
HS sulfation of 6 pooled control unobstructed kidney, D5 UUO and D10 UUO is represented as percentage of total disaccharides with error bars from three technical replicates. A represents N-acetylation and B N-sulfation. Results are represented as mean ±SD.

As observed Figure 3-10, total HS 2-O-sulfation was increased at D5 and D10 UUO by 45.3% and 19.2% respectively compared to control. In contrast, there was a slight decrease in total HS 6-O-sulfation in UUO at D5 (-6.4%) and D10 (-4.4%).

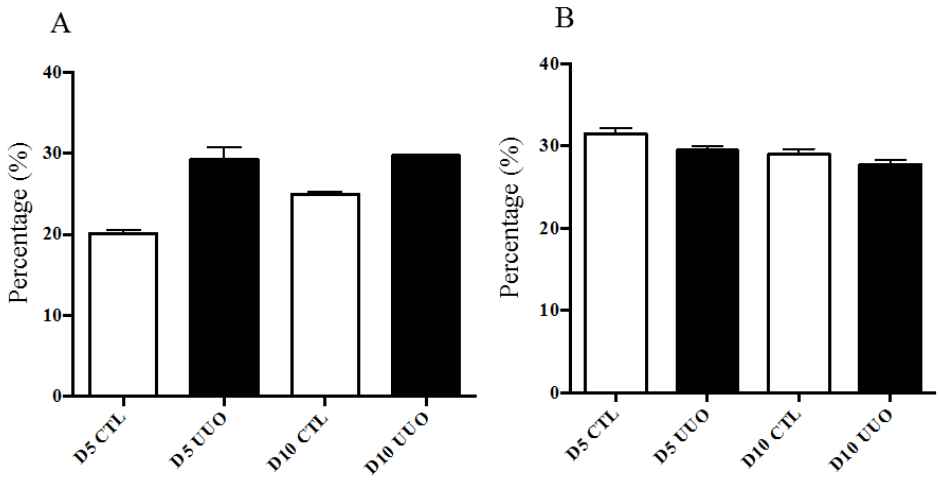

Figure 3-10: Total HS 2-O and 6-O-sulfation in control and D5, D10 UUO
HS sulfation of 6 pooled control unobstructed kidney, D5 UUO and D10 UUO is represented as percentage of total disaccharides with error bars from three technical replicates. A represents HS 2-O-sulfation and B HS 6-O-sulfation. Results are represented as mean ±SD.

For a deeper understanding of disaccharide changes responsible for the changes in total sulfation, HS disaccharide composition was studied. The proportion of monosulfated disaccharides are shown in Figure 3-11. At D5 UUO, N-sulfated and 6-sulfated monosaccharides were decreased by

24% and 11.2% while there was three times more ΔUA2S-GlcNAc compared to control. At D10 UUO, the 6-O monosulfated disaccharides was still decreased by almost 30% compared to control while ΔUA-GlcNS increased by 14.4% and ΔUA2S-GlcNAc decreased by nearly 50%.

Regarding disulfated disaccharide (Figure 3-12), ΔUA2S-GlcNS was increased at both time points with a 43% increase at D5 and 29.5% at D10 UUO compared to control. In contrast, ΔUA-GlcNS6S decreased by 43.5% at D5 and 14.4% at D10.

The unsulfated disaccharide ΔUA-GlcNAc was not changed with UUO. However, the trisulfated disaccharide ΔUA2S-GlcNS6S showed an increase by 23.4% at D5 and 17.4% at D10 UUO (Figure 3-13). Together, these data revealed an increase in HS 2-O-sulfation with a decrease in HS 6-O-sulfation with the UUO model.

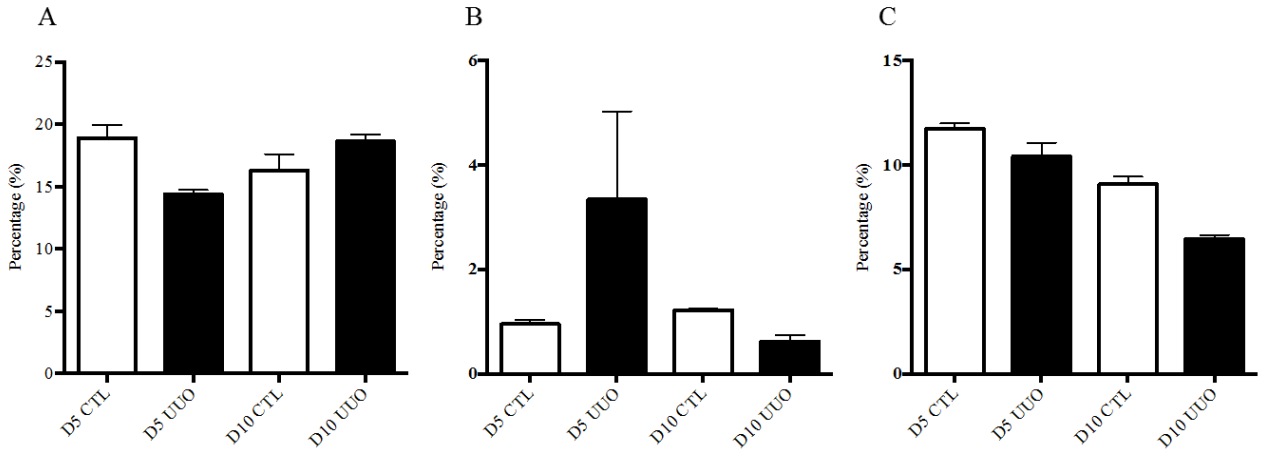

Figure 3-11: Monosulfated disaccharides analysis in control and at D5 and D10 UUO
HS monosulfated disaccharides analysis of 6 pooled control unobstructed kidney, D5 UUO and D10 UUO is represented as percentage of total disaccharides with error bars from three technical replicates. The monosulfated disaccharides ΔUA-GlcNS is represented in A, ΔUA2S-GlcNAc is represented in B and ΔUA-GlcNAc6S in C. Results are represented as mean ±SD.

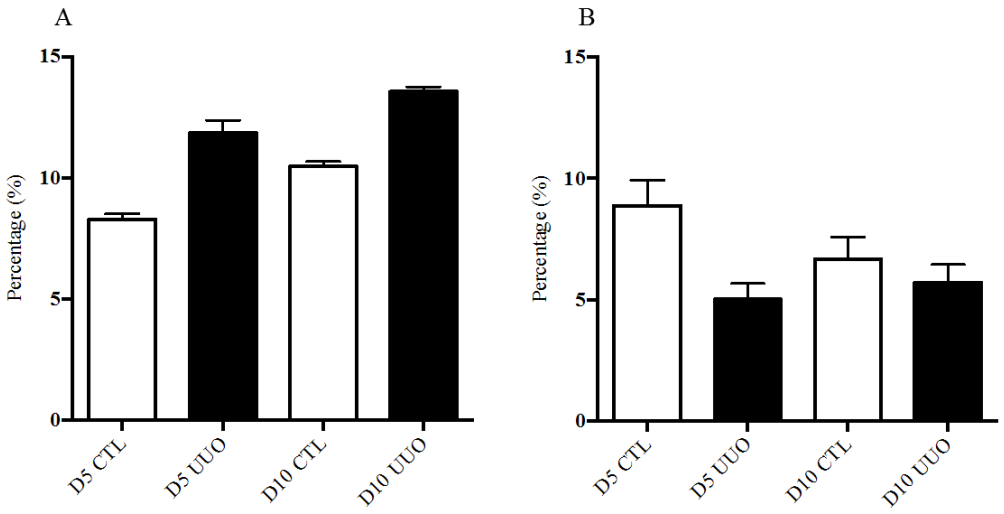

Figure 3-12: Disulfated disaccharides analysis in control and at D5 and D10 UUO
HS disulfated disaccharides analysis of 6 pooled control unobstructed kidney, D5 UUO and D10 UUO is represented as percentage of total disaccharides with error bars from three technical replicates. The disulfated disaccharides ΔUA2S-GlcNS is represented in A and ΔUA-GlcNS6S in B. Results are represented as mean ±SD.

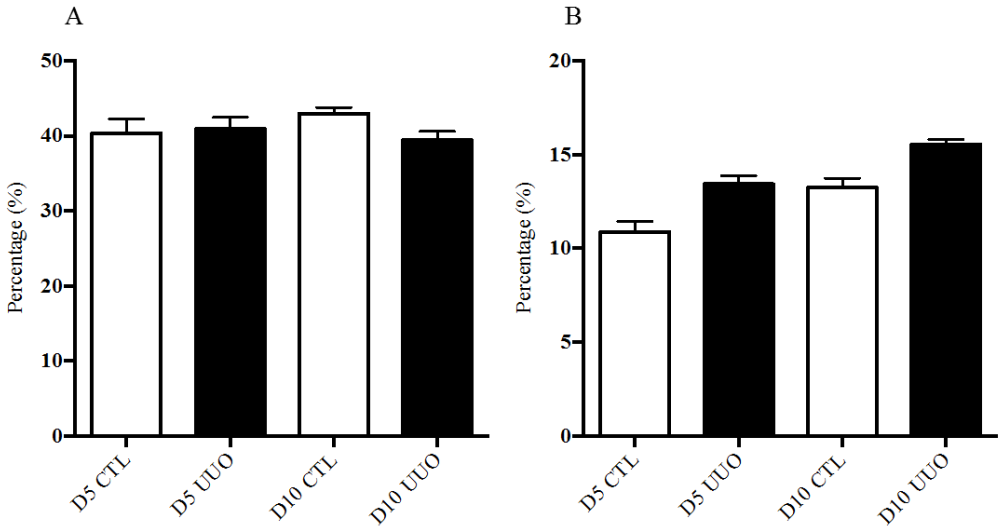

Figure 3-13: Unsulfated and trisulfated disaccharides analysis in control, D5 and D10 UUO
HS disulfated disaccharides analysis of 6 pooled control unobstructed kidney, D5 UUO and D10 UUO is represented as percentage of total disaccharides with error bars from three technical replicates. The unsulfated disaccharides ΔUA-GlcNAc is represented in A and the trisulfated disaccharides ΔUA2S-GlcNS6S in B. Results are represented as mean ±SD.

HS sulfation analysis was also performed in samples from D15 UUO. These data are presented separately as the results were unexpected, with a very high level of trisulfated disaccharides potentially due to an incomplete digestion. However, it is possible that there is an increase in sulfation at D15 but caution should be taken when analysing these data (Figure 3-14).

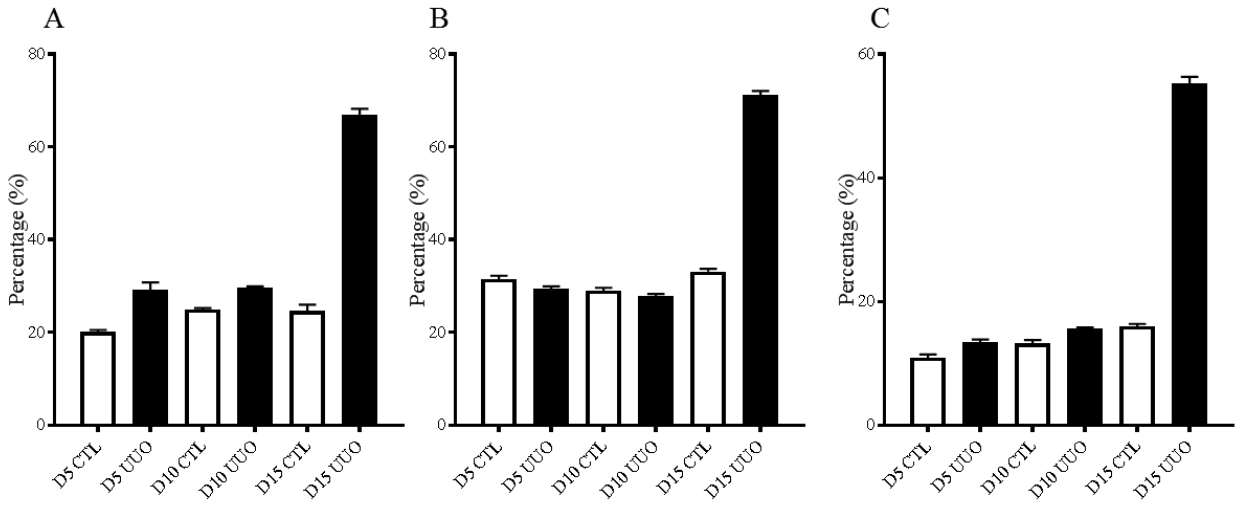

Figure 3-14: HS sulfation increase at D15 UUO
HS disulfated disaccharides analysis of 6 pooled control unobstructed kidney, D5 UUO, D10 UUO and D15 UUO are represented as percentage of total disaccharides with error bars from three technical replicates. A is the total 2-O-sulfation, B 6-O-sulfation and C is the trisulfated disaccharides ΔUA2S-GlcNS6S. Results are represented as mean ±SD.

To assess if HS sulfation was correlated with the expression of HS sulfation modulating enzymes, HS O-sulfotransferases and sulfatase 1 and 2 expression were analysed by RT-qPCR.

First, the HS 2-O-sulfation increase was mirrored by HS2ST1 expression which was significantly increased by 4-fold at D10 UUO ($p<0.01$) (Figure 3-15). HS2ST1 expression correlated significantly ($p<0.001$) to the Sirius red quantification with $r=0.6750$.

Regarding HS6ST1 expression, the level of expression detected by RT-qPCR was not sufficient to be interpreted. As the expression of the 6-O-sulfotransferase could not be detected, the expression of the endosulfatases SULF1 and SULF2 which cleave 6-O-sulfation were analysed. As seen Figure 3-16, SULF1 expression was increased at D5 by 4.4-fold and D10 UUO by 6 fold but only significantly at D5 ($p<0.05$). Additionally, SULF1 expression was significantly correlated to Sirius red quantification ($p<0.01$) with $r=0.5643$. In contrast, SULF2 expression was not changed with UUO and did not correlate with Sirius red staining (Figure 3-17).

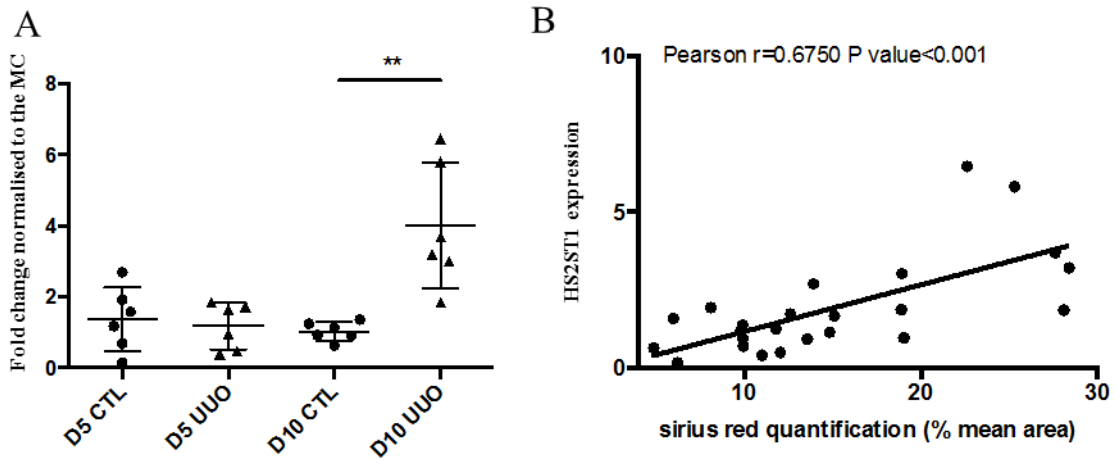

Figure 3-15: HS2ST1 expression and correlation to Sirius red staining
Expression was adjusted to HPRT1 expression and normalised to the mean of controls (MC) N=6. RT-qPCR data are displayed in A and HS2ST1 correlation to Sirius red staining is shown in B. Two-tailed unpaired t test with Welch's correction with $p<0.01$ (**). The Pearson's correlation coefficient was generated with the data from HS2ST1 expression and results from Sirius red staining.

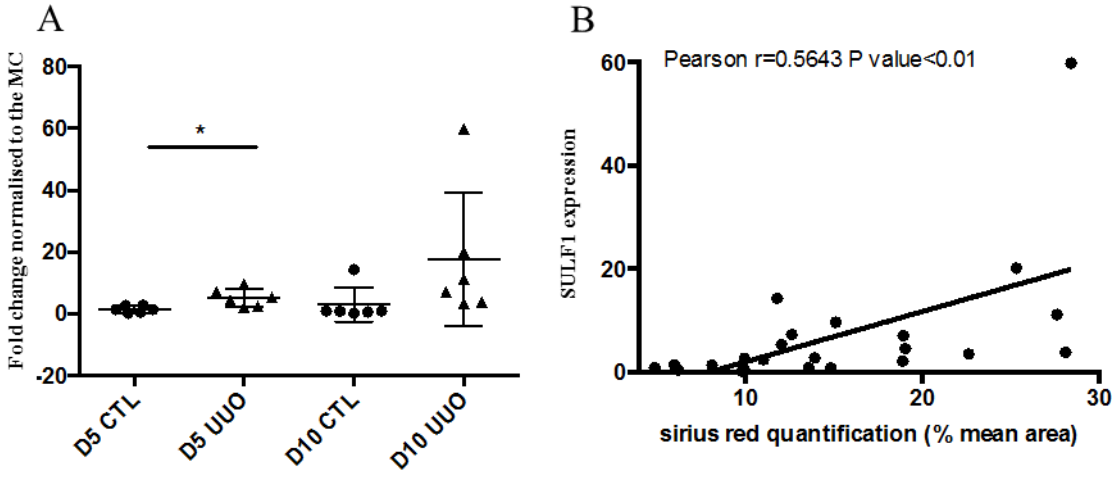

Figure 3-16: SULF1 expression and correlation to Sirius red staining
Expression was adjusted to HPRT1 expression and normalised to the mean of controls (MC) N=6. RT-qPCR data are displayed in A and SULF1 correlation to Sirius red staining is shown in B. Two-tailed unpaired t test with Welch's correction with $p<0.05$. The Pearson's correlation coefficient was generated with the data from SULF1 expression and results from Sirius red staining.

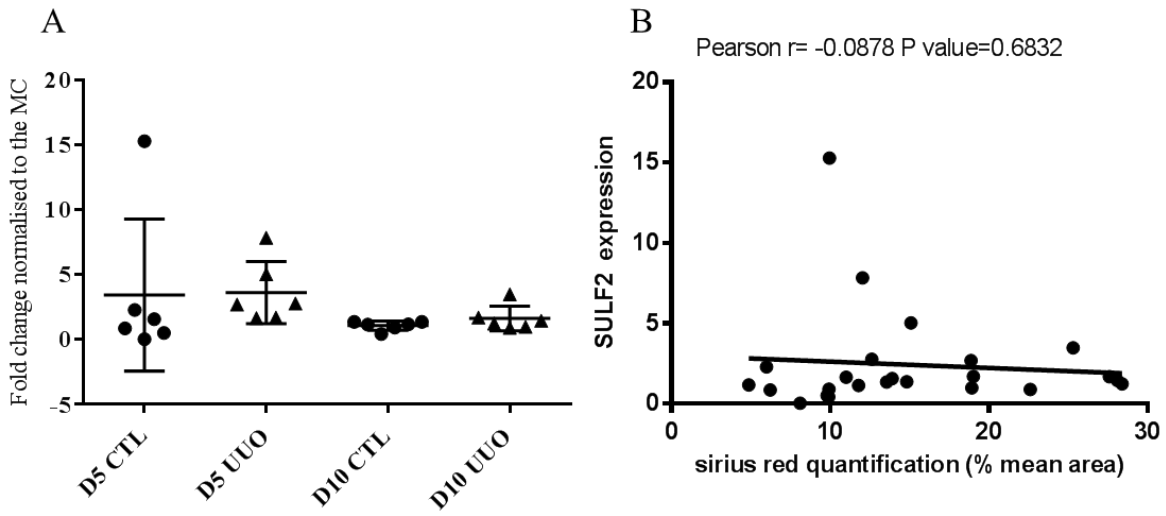

Figure 3-17: SULF2 expression and correlation to Sirius red staining
Expression was adjusted to HPRT1 expression and normalised to the mean of controls (MC) N=6. RT-qPCR data are displayed in A and SULF2 correlation to Sirius red staining is shown in B. Two-tailed unpaired t test with Welch's correction. The Pearson's correlation coefficient was generated with the data from SULF2 expression and results from Sirius red staining.

3.3.3 Heparan sulfate 3-O-sulfation changes in renal fibrosis

The technique used to analyse HS sulfation and disaccharide composition could not provide any data about HS 3-O-sulfation as no standard for this particular pattern of sulfation was available. Therefore, HS 3-O-sulfation was analysed by immunofluorescence. The phage display antibody HS4C3 recognises a highly-sulfated pattern of HS including 3-O-sulfation. Interestingly, HS4C3 staining was found decreased in the tubular basement membrane and glomerular capillaries of all UUO samples (Figure 3-18). Only blood vessels maintained a strong staining within all tissues.

To assess if the decrease in HS 3-O-sulfation was accompanied by a decrease in HS3STs expression, HS3ST3A and HS3ST1 expression in control, D5 and D10 UUO were analysed by RT-qPCR. HS3ST3A was decreased in UUO with a significant drop by 0.6-fold in expression at D5 ($p<0.05$). Additionally, HS3ST3A was significantly correlated with Sirius red staining ($p<0.05$, $r=-0.4429$) (Figure 3-19). In contrast, HS3ST1 was significantly increased at D5 and D10 UUO by 2.7 fold and 4.5 fold respectively ($p<0.001$). Regarding HS3ST1 correlation to Sirius red staining it was the best-correlated enzyme with $r=0.7881$ and $p<0.001$ (Figure 3-20).

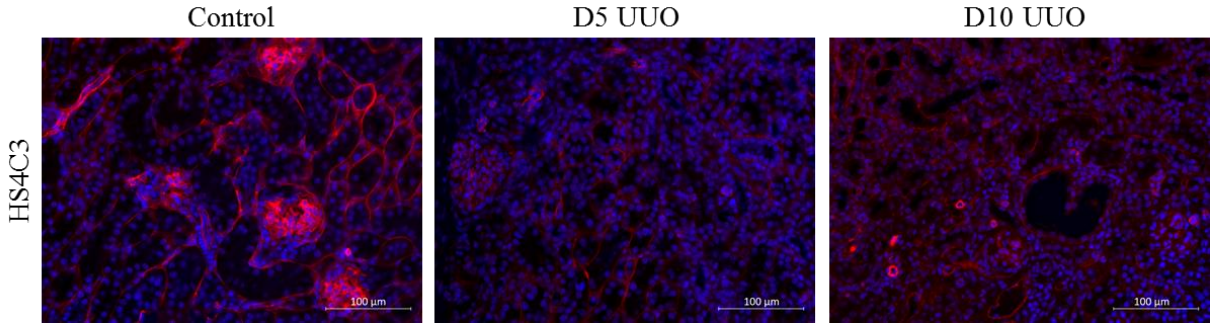

Figure 3-18: Highly sulfated HS staining on control, D5 and D10 UUO kidneys
Representative images of HS4C3 staining on paraffin embedded sections of control tissues, D5 UUO and D10 UUO. Paraffin embedded sections of 4µm were dewaxed, rehydrated. Peptide retrieval was performed by microwaving the slides in EDTA buffer. Sections were blocked for 10 minutes with 2% FBS in PBS and incubated overnight at 4°C with primary antibody HS4C3 1:5 given by Toin van Kuppevelt, Radboud University, Netherlands. The next day, sections were washed in PBS, then incubated with secondary antibody. Sections were then washed in PBS, incubated with Sudan Black for 20 minutes in the dark at room temperature and finally washed in PBS before mounting with VECTA shield DAPI liquid mounting medium. HS4C3 antibody, which stains heavily sulfated HS, showed glomerular, vascular and tubular staining. N=6 with 10 cortex fields analysed per section for each kidney. Scale bars represent 100 µm.

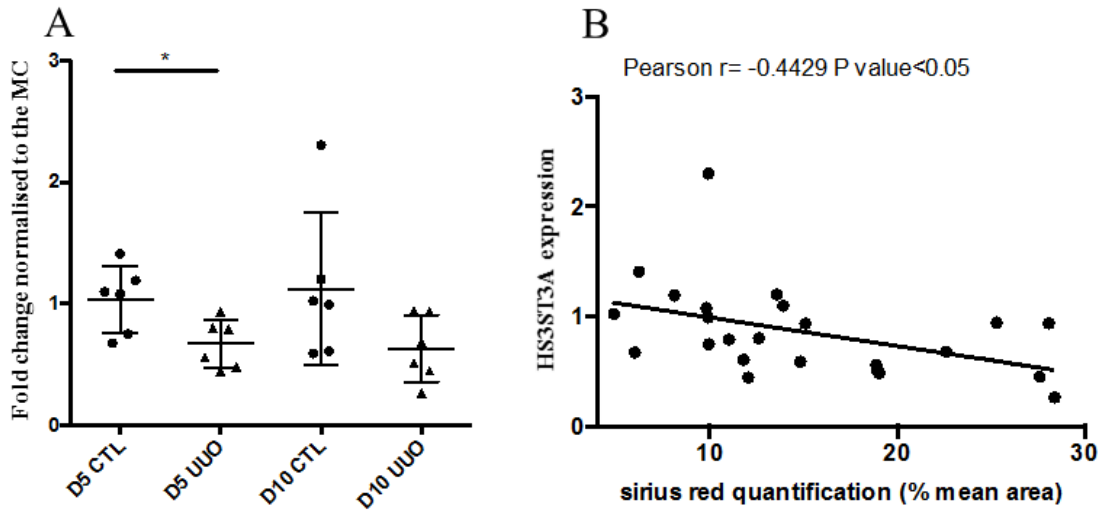

Figure 3-19: HS3ST3A expression and correlation to Sirius red staining
Expression was adjusted to HPRT1 expression and normalised to the mean of controls (MC) N=6. RT-qPCR data are displayed in A and HS3ST3A correlation to Sirius red staining is shown in B. Two-tailed unpaired t test with Welch's correction with $p<0.05$ (*). The Pearson's correlation coefficient was generated with the data from HS3ST3A expression and results from Sirius red staining.

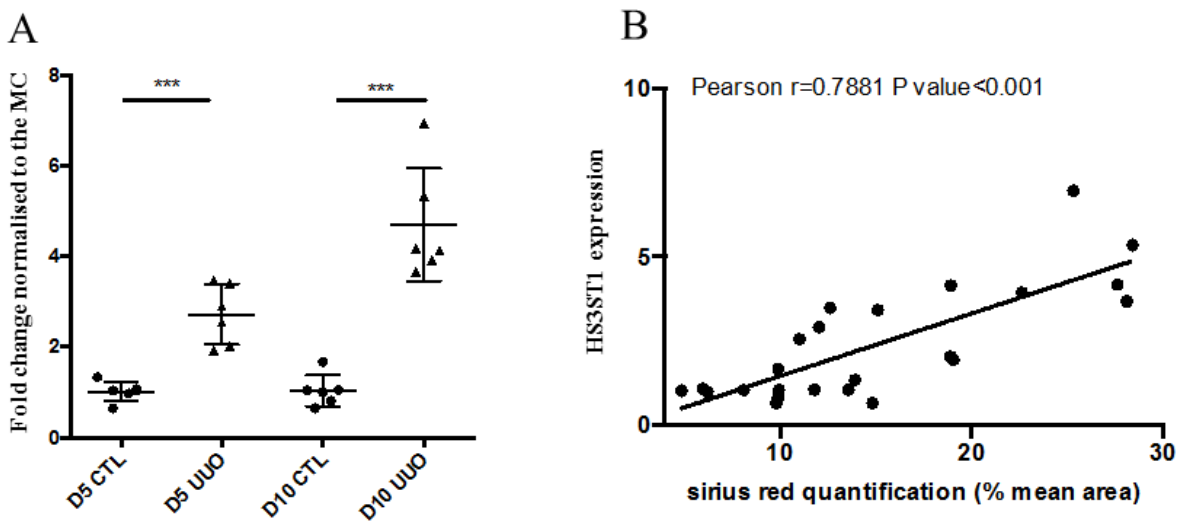

Figure 3-20: HS3ST1 expression and correlation to Sirius red staining
Expression was adjusted to HPRT1 expression and normalised to the mean of controls (MC) N=6. RT-qPCR data are displayed in A and HS3ST1 correlation to Sirius red staining is shown in B. Two-tailed unpaired t test with Welch's correction with $p<0.001$ (***). The Pearson's correlation coefficient was generated with the data from HS3ST1 expression and results from Sirius red staining.

To better understand the impact of H3ST1 in UUO, slides were stained with a fluorescently labelled antithrombin III (lbAT). HS3ST1 and HS3ST5 are known to generate the HS binding site for AT. HS3ST5 has a very low expression in kidney. Therefore, detecting AT binding would give an indication on HS3ST1 activity within the kidney. As seen Figure 3-21, lbAT stained the tubular basement membrane, the vessels, the Bowman's capsule and within the vascular structure of the glomerulus in both control and D5 UUO. Remarkably, lbAT also stained some interstitial tissue in D5 UUO. This staining was not seen in control kidney. Overall tubular lbAT staining decreased in all sections from D5 UUO while vascular structure remained unchanged. Unfortunately, D10 UUO tissues were of poor quality and could not be analysed. The sections were stained and from the experimenter, the staining decreased too at D10 UUO (data not shown).

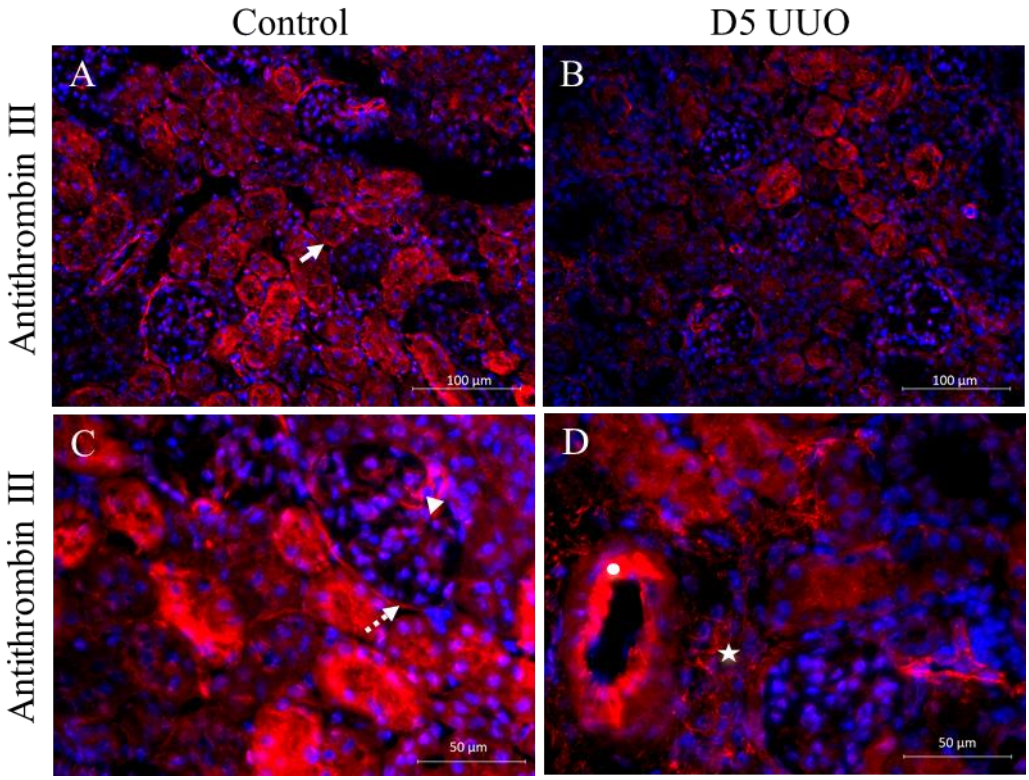

Figure 3-21: Antithrombin III staining in control and D5 UUO cryosections
Representative images of antithrombin III (AT) staining on cryosections from control kidney (A, C) and D5 UUO (B, D). Sections were blocked for 20 minutes in 1% BSA in PBS and incubated for 1h in fluorescently labelled AT. Slides were mounted with prolong diamond antifade with dapi. AT binding was detectable around Bowman's capsule (⇢), on blood vessels (❍), on the tubular basement membrane (→), at the vascular pole of the glomerulus (▵) and in the expanded interstitium at D5 UUO (☆). N=6 with at least 5 cortex fields analysed per section for each kidney. Scale bars represent 100 and 50µm.

3.3.4 Heparin Binding-EGF localisation in renal fibrosis

Heparin Binding Epidermal Growth factor like (HB-EGF) is a protein that binds strongly to heparin and was found overexpressed after ischemia reperfusion in rats (Homma *et al.*, 1995) with a predominant staining in distal tubules (Sakai *et al.*, 1997). Furthermore, HB-EGF staining was found increased in basolateral tubular epithelial cells of renal allograft biopsies with minor histological alteration (Celie *et al.*, 2012). I hypothesised that potentially HB-EGF binding could require HS 3-O-sulfation and therefore studied if HB-EGF staining was changed in fibrosis.

Paraffin embedded sections were stained for HB-EGF and analysed in control, D5 and D10 UUO sections (Figure 3-22). HB-EGF staining was localised mainly on the basolateral pole of tubules.

Surprisingly, not all tubules were stained and the staining was heterogeneous. It is possible that the staining is present on only proximal or distal tubules. The staining decreased at D5 and D10 UUO.

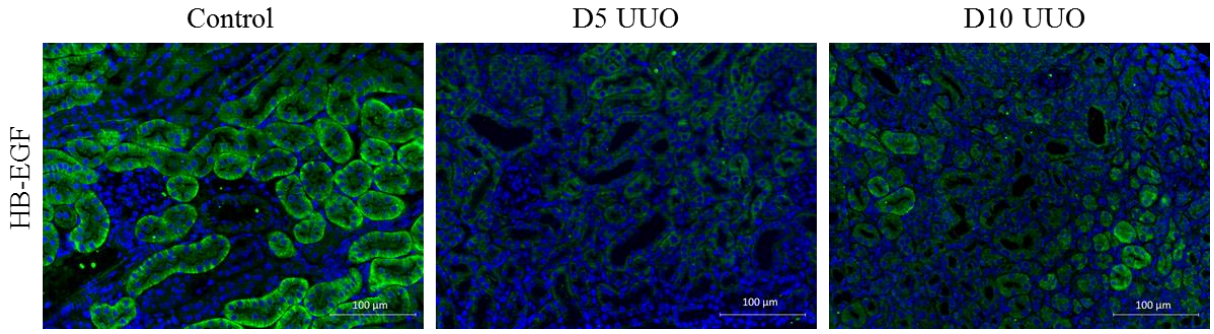

Figure 3-22: HB-EGF staining on control, D5 and D10 UUO kidneys
Representative images of HB-EGF staining on paraffin embedded sections of control tissues, D5 UUO and D10 UUO. Paraffin embedded sections of 4µm were dewaxed and rehydrated. Peptide retrieval was performed by microwaving the slides in EDTA buffer. Sections were blocked for 10 minutes with 2% FBS in PBS and incubated overnight at 4°C with primary antibody. The next day, sections were washed in PBS, then incubated with secondary antibody Dylight 550 PBS for 1-2 hours at room temperature. Sections were then washed in PBS, incubated with Sudan Black for 20 minutes in the dark at room temperature and finally washed in PBS before mounting with VECTA shield DAPI liquid mounting medium. HB-EGF staining was mainly present on the tubular basement membrane. N=6 with 10 cortex fields analysed per section for each kidney. Scale bars represent 100 µm.

3.4 Discussion

To date, renal fibrosis is irreversible. The use of *in vivo* murine models such as UUO has generated in recent years a better understanding of disease development (Stefanska *et al.*, 2016), identified new biomarkers (Yuan *et al.*, 2015) and new promising therapeutics (Fox *et al.*, 2016).

Results presented in this chapter showed that the obstruction of one ureter led to a significant increase in collagen deposition within the cortex. Additionally, tubules were found dilated and the interstitium expanded. These are characteristics of fibrosis and proved that the surgical procedure was successful. The analysis of HS sulfation showed a minor change in N-acetylation/N-sulfation at D10 with an increase in sulfation. These findings are consistent with what was found in idiopathic pulmonary fibrosis, where N-sulfation was also increased (Lu *et al.*, 2014; Westergren-Thorsson *et al.*, 2017). During inflammation and fibrosis, N-sulfated/acetylated/sulfated patterns are important in attracting immune cells as they play a role in HS binding to cytokines such as interferon-γ (Lortat-Jacob *et al.*, 1995) and Interleukin 8 (Spillmann *et al.*, 1998). Therefore, the changes in N-acetylation and N-sulfation observed in UUO could either enhance or decrease pro-

inflammatory cytokines binding. Additionally, N-sulfation is essential for the activity of other sulfotransferases. Therefore, another explanation of the increase in N-sulfation is the drive to increase the general sulfation status of the cell surface and ECM. Increasing N-sulfation, is permissive to sulfotransferase and sulfatase activity (Rong *et al.*, 2001; Sheng *et al.*, 2011) changing the whole GAGs sulfation pattern.

The N-sulfation was not the only sulfation increased with UUO. Indeed, the most noticeable changes in the disaccharides analysis was an increase in the monosulfated disaccharide ΔUA2S-GlcNAc and an increase in the disulfated disaccharide ΔUA2S-GlcNS. These results are consistent with the increase in trisulfated disaccharides ΔUA2S-GlcNS6S seen in lung fibrosis (Lu *et al.*, 2014). The increase in HS 2-O-sulfation mirrored by HS2ST1 overexpression in D10 UUO suggests the importance of this pattern in fibrosis. In fact, 2-O-sulfation plays an important role in the pro-fibrotic FGF family binding to HS (Turnbull *et al.*, 1992; Ashikari-Hada *et al.*, 2004). FGF7 was increased in UUO (Girshovich *et al.*, 2012) and FGF2 staining was increased in chronic rejection (Alhasan *et al.*, 2014). Consequently, the change in 2-O-sulfation could trigger more FGF binding and signalling during the development of fibrosis.

No increase was observed in the level of 6-O-sulfation in UUO. It has been previously published that HS 6-O-sulfation increased in idiopathic fibrosis (Lu *et al.*, 2014; Westergren-Thorsson *et al.*, 2017) and HS staining with antibodies recognising 6-O-sufation increased in UUO (Alhasan *et al.*, 2014). One can suggest that HS sequencing is more accurate than staining, therefore the increase previously seen in UUO can be related to an increase in total HS. Second, lungs and kidneys are two different organs and the 6-O-sulfation seems to be important for lung development, with HS6ST1-/- mice showing abnormal lung development with an increased intra alveolar space whilst kidney development is normal (Habuchi *et al.*, 2007). The decrease in 6-O-sulfation could have been attributed to the overexpression of SULF1 in the fibrotic kidneys, an endosulfatase that cleaves 6-O residues. However, the preferential substrate of SULF1 is the trisulfated disaccharides ΔUA2S-GlcNS6S, which was actually increased. One explanation could be that the increase in the trisulfated disaccharides is being regulated by the cells to prevent an oversulfation of the cell surface and ECM. The fact that disulfated ΔUA2S-GlcNS, a product of the SULF1 activity, increased suggests that this could be the case.

The change in HS modulating enzymes was remarkable, with most enzymes being significantly correlated to the Sirius red staining and therefore to the degree of fibrosis. This is not the first time that HS modifying enzymes are found modulated during the development of fibrosis. In idiopathic pulmonary fibrosis HS3ST1 and HS6STs were overexpressed (Lu *et al.*, 2014; DePianto *et al.*, 2015) and in liver fibrosis, heparanase, SULF1, SULF2 and HS3ST1 were overexpressed in fibrotic tissue compared to non-fibrotic liver (Tátrai *et al.*, 2010). The increase in SULF1 in fibrotic kidneys is potentially due to the presence of TGFβ1, a pro-fibrotic factors that stimulate SULF1 expression (Yue *et al.*, 2008).

In fibrotic liver, amongst all HS modulating enzymes studied, HS3ST1 showed the highest fold change increase (Tátrai *et al.*, 2010). These results, together with the finding that HS3ST1 correlated with glomerular filtration rate and graft survival (Bunnag *et al.*, 2009; Einecke *et al.*, 2010; Sagoo *et al.*, 2010), suggest the potential of HS3ST1 as a biomarker of disease progression. It was not possible to identify any changes in 3-O sulfated disaccharides due to the lack of standard for 3-O-sulfated residues. Because of the promising results obtained with the enzyme expression, immunofluorescence staining for total 3-O-sulfation (HS4C3 staining) and 3-O sulfation specific of HS3ST1/5 (AT) was performed.

HS 3-O-sulfation was mainly found on blood vessels, Bowman's capsule, glomerular vasculature and tubular basement membrane as observed in previous studies (Girardin *et al.*, 2005). Unexpectedly, the increase in HS3ST1 expression did not lead to an increase in HS 3-O-sulfation in D5 and D10 UUO. HS 2-O residues are known to inhibit the activity of HS3ST1. Therefore HS 3-O-sulfation decrease could be explained by a lack of HS precursor. The decrease of staining was mainly observed on the tubular basement membrane. There was no change in the blood vessels staining. It is possible that the increase in HS3ST1 expression is mainly found in endothelial cells, which are known to produce HS with 3-O-sulfation (Marcum *et al.*, 1986). Additionally, infiltrating cells could express HS3ST1 as macrophages do express high levels of expression (Martinez *et al.*, 2015). While the increase in 2-O-sulfation could be a pro-inflammatory mechanism to increase pro-fibrotic factors binding, HS3ST1 could be a defensive mechanism. Smits *et al.* found that HS3ST1 -/- mice are more susceptible to death following acute septic shock (Smits *et al.*, 2017). Hence HS3ST1 may be involved in tissue recovery. All changes in HS N-acetylation, sulfation and modifying enzymes expression with UUO are summarised Table 3-1.

	D5 UUO	D10 UUO
N-acetylation	-	↓
N-sulfation	-	↑
2-O-sulfation	↑	↑
6-O-sulfation	↓	↓
3-O-sulfation	↓	↓
HS2ST1	-	↑
SULF1	↑	↑
SULF2	-	-
HS3ST3A	↓	↓
HS3ST1	↑	↑

Table 3-1: HS modification and modifying enzymes expression at D5 and D10 UUO
An increase is represented by "↑"and a decrease by "↓"no change by "–".

The changes in HS sulfation observed in the UUO model can lead to a change in growth factor binding. The analysis of HB-EGF staining revealed a decrease in all fibrotic tissues. In previous studies, HB-EGF signalling was decreased by SULF1 expression (Lai *et al.*, 2003). Therefore, the drop in HB-EGF staining can be explained by the increase in SULF1 activity. Additionally, the decrease in 3-O-sulfation could be related to the decrease in HB-EGF binding but this would need further experiments. HB-EGF was found expressed following acute injury in an ischemia reperfusion model. The authors suggested that it was a protective mechanism of distal tubules to stimulate regeneration (Sakai *et al.*, 1997). Additionally, in a recent study, HB-EGF staining was increased in basolateral tubular epithelial cells of renal allograft biopsies with minimal histological alteration while IFTA biopsies showed similar staining score to control tissues (Celie *et al.*, 2012). Therefore, HB-EGF could be secreted in the initial events of tissue damage as an homeostatic regulation to resolve minimal damage. Conversely, the decrease in staining in chronic stages could be due to the changes in HS sulfation not allowing the growth factor to bind to the cells. In the intestine, HB-EGF has shown to have protective capacities by protecting pericytes, decreasing level of cytokines and decreasing cell death (Yang *et al.*, 2014). Hence, there might be a potential link between HB-EGF, HS 3-O-sulfation and renal healing that should be further explored.

In conclusion, unilateral ureteral obstruction in mice is an excellent model to study HS sulfation changes during the development of interstitial fibrosis with major changes in 2-O and 3-O-sulfation. Additionally, HS sulfotransferases have a great potential to be used as biomarkers with HS3ST1 being the most promising. Hence these results raised a lot of questions and curiosity regarding what can modulate HS3STs enzymes within the kidney and during fibrosis and what role they play in binding pro-fibrotic growth factors. These questions will be discussed in-depth in the next section of this thesis.

4 Heparan sulfate 3-O-sulfotransferases expression: modulation and effect on growth factors signalling

4.1 Introduction

4.1.1 Control of HS3ST expression

In the last decade, several studies have described factors that modulate the expression of HS3ST enzymes. Remarkably, HS3STs modulation differs between cell types and origin. In epithelial cells, it was found that IL-4 and IL-13 treatment increased HS3ST1 expression in intestinal epithelial cells (Takeda *et al.*, 2010). Moreover, FGF10 treatment of salivary gland epithelia increased HS3ST1 and HS3ST6 expression at 4 hours and HS3ST3A and HS3ST3B at 2 and 4 hours (Patel *et al.*, 2014).

Additionally, HS3STs expression in endothelial cells is of big interest as HS integrity and sulfation on the surface of the vascular system is important for inflammation. A preliminary study from Krenn *et al.*, showed that 20 hours treatment of TNFα downregulated HS3ST1 and HS3ST4 and upregulated HS3ST3B in human microvascular endothelial cells (Krenn *et al.*, 2008). In the same study, LPS treatment for 4h decreased HS3ST1, 2,3B and HS3ST4. Furthermore, the authors observed a decrease in HS4C3 staining on the cells treated with TNFα. Unfortunately, this study did not do any statistical tests on these results and therefore caution should be taken when interpreting these data. Especially as the study from Takeda *et al.* showed no difference in HS3ST1 expression after 24h treatment with TNFα and LPS treatment on intestinal epithelial cells (Takeda *et al.*, 2010). The difference in results could also be explained by the difference in treatment concentration and cell types.

Because of the role of HS3STs in cancer development, HS3STs modulation in immune cells has recently been studied. LPS treatment increased HS3ST1, HS3ST3A, and HS3ST3B in human primary monocytes and only HS3ST3A-B in human monocytic leukemia cells. Furthermore TNFα, IL6, IL4, IFNγ, PGN all increased HS3ST3B expression in the human leukemia cells together with an increase in HS4C3 staining (Sikora *et al.*, 2016). HS3STs expression have also been studied in

activated macrophages. While HS3ST1, HS3ST2 are expressed at higher levels in M2 macrophages, HS3ST3B is more highly expressed in M1 (Martinez *et al.*, 2015).

4.1.2 HS 3-O-sulfation binding proteins

There are very few proteins known to require HS 3-O-sulfation for binding to HS.
The most studied is antithrombin (AT). Its binding motif is created by the activity of HS3ST1 and HS3ST5. AT inhibits thrombin, factor IXa and factor Xa and its binding to heparin enhances its catalytic activity (Rosenberg and Damus, 1973). For this reason, low molecular weight heparin (LMWH) is used in clinics to prevent clot formation. Initially, anticoagulant HSPG (aHSPG) were first studied on endothelial cells (Marcum *et al.*, 1986; De Agostini *et al.*, 1990; HajMohammadi *et al.*, 2003) but were also found in many other structures such as the genital tract within the uterus e.g. the oviduct, follicular fluid (De Agostini, 2006); in fibroblasts (Marcum and Rosenberg, 1984) and epithelial cells (Pejler *et al.*, 1987; Berry *et al.*, 1991). Additionally, within the kidney aHSPG can be found on vessels, glomerular basement membrane and tubules (Girardin *et al.*, 2005).

HS3ST activity also generates a binding sequence for Herpes Simplex virus type 1 (HSV-1). In order to be able to enter the host cells, the viral glycoprotein of HSV-1, glycoprotein D has to bind to HS 3-O sulfation of the cell surface. Chinese Hamster Ovarian-K1 (CHO-K1) cells that do not have HS 3-O-sulfation are protected against HSV-1 infection but become infected when expressing HS3ST2 (O'Donnell *et al.*, 2006), 3A, 3B (Shukla *et al.*, 1999), 4 (Tiwari *et al.*, 2005), 5 (Xia *et al.*, 2002) and 6 (Xu *et al.*, 2005).

The implication of HS 3-O-sulfation in the binding of FGF family members to their receptors has also been well studied. FGF7 was protected from proteases by decasaccharides and tetrasaccharides containing 3-O-sulfation (Ye *et al.*, 2001) and AT binding fraction of heparin can bind strongly to FGF2 receptor 1 (McKeehan *et al.*, 1999). Additionally, Li *et al.* studied the interaction between FGF-2 and multiple HS disaccharides (Li *et al.*, 2014). They found that the disaccharide with N-, 3-O-sulfated GlcN and 2-O-sulfated IdoA had the highest affinity (KD= 1.73±0.31μM), showing that the 3-O sulfation might be implicated in the interaction between FGF2 and HS. However, a recent study on HS isolated from CHO cells transfected with HS3ST1 or HS3ST2 did not find any difference in FGF2 binding with HS 3-O-sulfation (Thacker *et al.*, 2016b). This same study found

Neuropillin 1 binding to HS to be increased with 3-O-sulfation, a growth factor implicated in axonal growth and angiogenesis.

Another protein of interest, cyclophilin B, which has chemotactic properties and is important for leukocytes recruitment to injured sites might require HS 3-O-sulfation. It was shown *in vitro* that the knock down of HS3ST3B in Jurkat T cells led to a decrease in cyclophilin B binding and P-ERK signalling (Vanpouille *et al.*, 2007).

Finally, the clearance of heparin in the liver by stabilin is increased by its 3-O-sulfation. *In vitro* data showed that heparin endocytosis by Flp-In-293 cells (transformed human embryonic kidney cells) overexpressing stabilin receptors was at the highest rate when HS polysaccharides were 3-O sulfated. *In vivo* the retention of heparan sulfate in the liver of mice was decreased when 3-O-desulfated (Pempe *et al.*, 2012).

Taken together, this literature shows how very little is known about HS 3-O-sulfation. The lack of information on the factors influencing HS3ST expression in renal cells prevents us from understanding what modulates HS 3-O-sulfation in kidney fibrosis.

The aims of this chapter are:

-To discover new regulators of HS3ST expression in renal epithelial cells and fibroblasts.

-To identify the impact of HS 3-O-sulfation on growth factors binding in renal epithelial cells by generating an *in vitro* model of renal epithelial cells overexpressing one isoform of HS3STs.

4.2 Specific material and methods

4.2.1 Cells starvation and treatments

All cytokines were from PeproTech unless specified. FGF2 (SRP4037) and HB-EGF (E4643) were from Sigma. As seen Figure 4-1, cells were seeded with complete medium and starved when reaching 80% confluence with medium supplemented with only 0.5% FBS. Starvations were

treatment dependent (between 16 to 24h) and are specified in the results sections. Cells were treated with either 5ng/mL TGFβ1, 10ng/mL TGFβ2 + 10ng/mL IL1β, 10ng/mL FGF2 or 10ng/mL HB-EGF. RNAs extractions were performed at different time points after treatment. The UG student Imogen L Wilson supervised by Laura Ferreras contributed in part to the work assessing HS3ST expression.

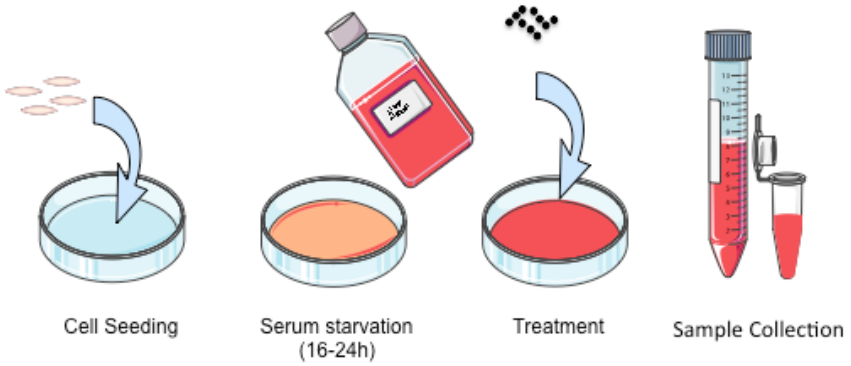

Figure 4-1: Treatments experimental design
Cells were seeded on the first day, incubated with 0.5% FBS between 16 to 24h when 80% confluent and treated with different factors (time and concentration are specified in results sections).

4.2.2 Transfection: G418 killing curve

Cells were transfected with a plasmid coding for neomycin gene which confers resistance to geneticin (G418), a prokaryote and eukaryote antibiotic. G418 (Invitrogen) is an aminoglycoside antibiotic toxic for both prokaryotes and eukaryotes cells as it blocks polypeptide synthesis. In eukaryotic cells peptide synthesis is disrupted by irreversible binding to the 80S ribosomes. Therefore, stably transfected cell lines were selected and maintained in media supplemented with G418. Prior to transfection, the concentration used was determined with a killing curve titration to determine the conditions of cell selection.

HKC8 cells were seeded in 24-well plates with $2.5x10^4$ cells per well. When cells reached 60% confluence they were treated in duplicate with different concentrations of G418 (0, 50, 100, 200, 300, 400, 500, 600, 700, 800, 900 and 1000 µg/ml) in complete media. Antibiotic supplemented media was changed every two days and cell confluency was assessed every day for a week. The lowest concentration at which all cells died was used for selection.

As seen Figure 4-2, HKC8 cells were treated with different concentration of antibiotics ranging from 0 to 300µg/mL. The concentration of 300 µg/mL and 200µg/mL successfully killed the cells. The lowest of the two, 200µg/mL was chosen for further experiments.

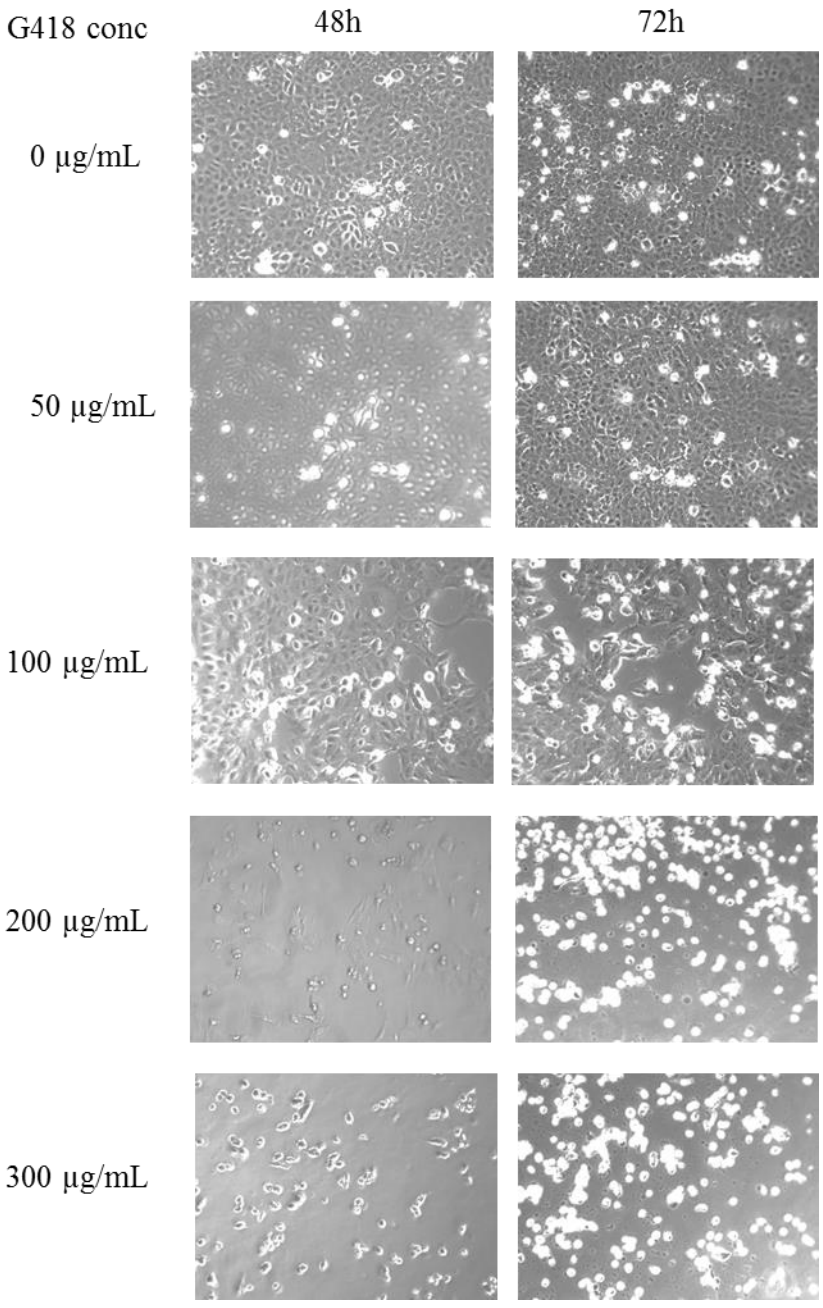

Figure 4-2: Killing curve for HKC8 cells with G418
HKC8 cells were seeded at $2.5x10^4$ cells per well in 24-well plate and treated with G418 concentration ranging from 0 to 300 µg/mL when 60% confluence was reached. Cells were imaged at 48 hours and 72 hours respectively after transfection with a Carl Zeiss 40CFL microscope, magnification x100.

4.2.3 Transfection: optimising transfection method

Cells transfection can affect cells integrity and generate damage. Furthermore, the ratio DNA to Effectene is important to provide a general positive charge complex to allow binding to negatively charged cell surface glycoproteins. Therefore, different transfection conditions were assessed. HKC8 cells were seeded at different cell densities and transfected with a 1:10 or 1:25 ratio of effectene complexed with 400ng of plasmid DNA. As observed in Figure 4-3, cell death and cell fragmentation could be observed at low seeding density with high concentration of effectene while cells remained healthy at the lower dose and with a seeding of $3x10^5$cells per well in a 6-well plate. Therefore, cells had to be 80 to 90% confluent to allow the cells to remain healthy after transfection.

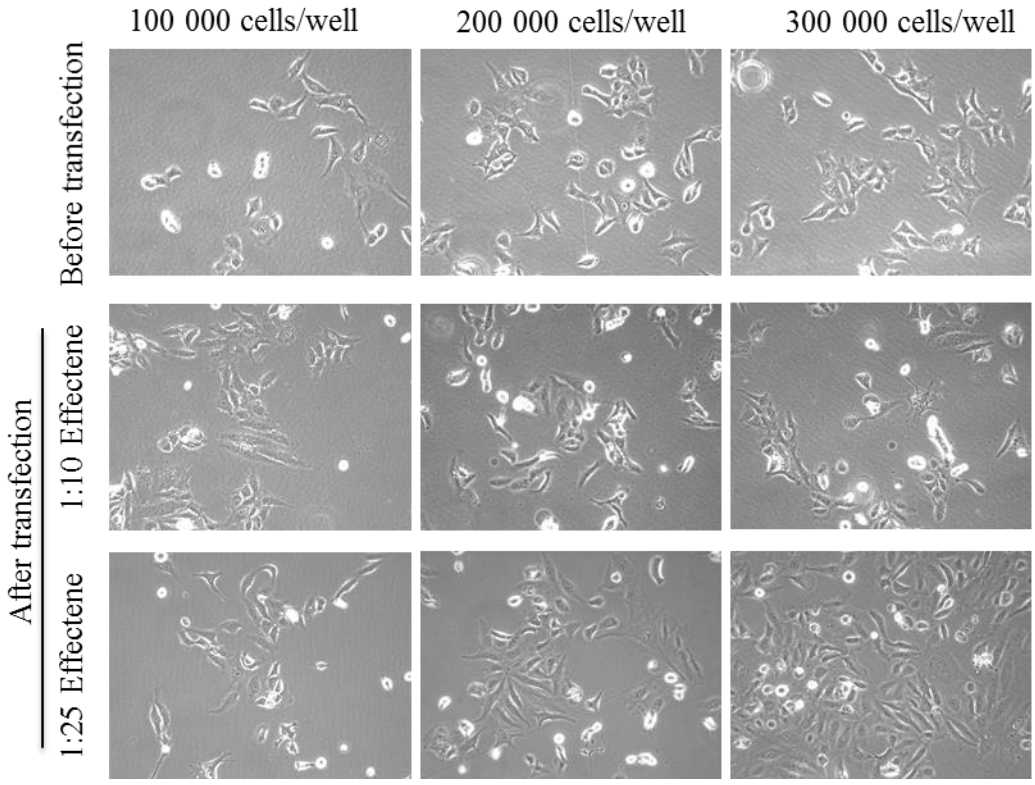

Figure 4-3: Transfection optimisation
HKC8 cells were seeded in 6-well plate at concentrations ranging from 10^5 to $3x10^5$ and transfected with 400ng of DNA mixed with enhancer and with 1:10 or 1:25 of effectene. Cells were imaged before transfection and 24h after transfection with a Carl Zeiss 40CFL microscope, magnification x200.

4.2.4 Transfection: generating stable cell line

Cells were seeded in 10cm petri dishes and grown until 80-90% confluent. First 2µg plasmid DNA was condensed by interaction with the Enhancer (16 µL) in 279µL of buffer. The condensed plasmid solution was then vortexed for 1 second and left 3 minutes at room temperature. A volume of 60 µL of Effectene Reagent was then added to the condensed DNA to produce condensed Effectene–DNA complexes. The complex was vortexed for 10 seconds and left for 7 minutes at room temperature. While incubating, media was removed from the 10cm dish, cells were washed with PBS and 7mL of complete media added. The Effectene–DNA complexes were finally mixed with 3mL of complete medium and directly added to the cells in a drop wise manner. The plasmid-effectene complex is taken up by endocytosis and reaches the cytoplasm and for some cells integrates in the genome. The antibiotic selection selects stable transfectants. The following day, fresh media containing 200µg/mL of G418 was added to the transfected cells. Two to three days after transfection, cells were split in 1:5 in media complemented with 200µg/mL of G418. Colonies were isolated by using cloning cylinders where 200µl of pre-warmed trypsin was added to detach the cells. Cells were then cultured in 24-well plates, one well corresponding to an individual colony. Once confluent cells were grown in 6-well plates, T25 and finally T75 flasks. Gene expression for each colony was assessed by RT-qPCR.

4.2.5 GAG sequencing

The isolation of radiolabelled Heparan Sulfate from cultured cells is a sensitive method that should be carried out with extra care. Bergen University policies were followed for handling radioactivity substances. Experiments with dangerous goods and gas were carried out in a fume hood. Figure 4-4 shows a simplified plan of experiment for disaccharides isolation.

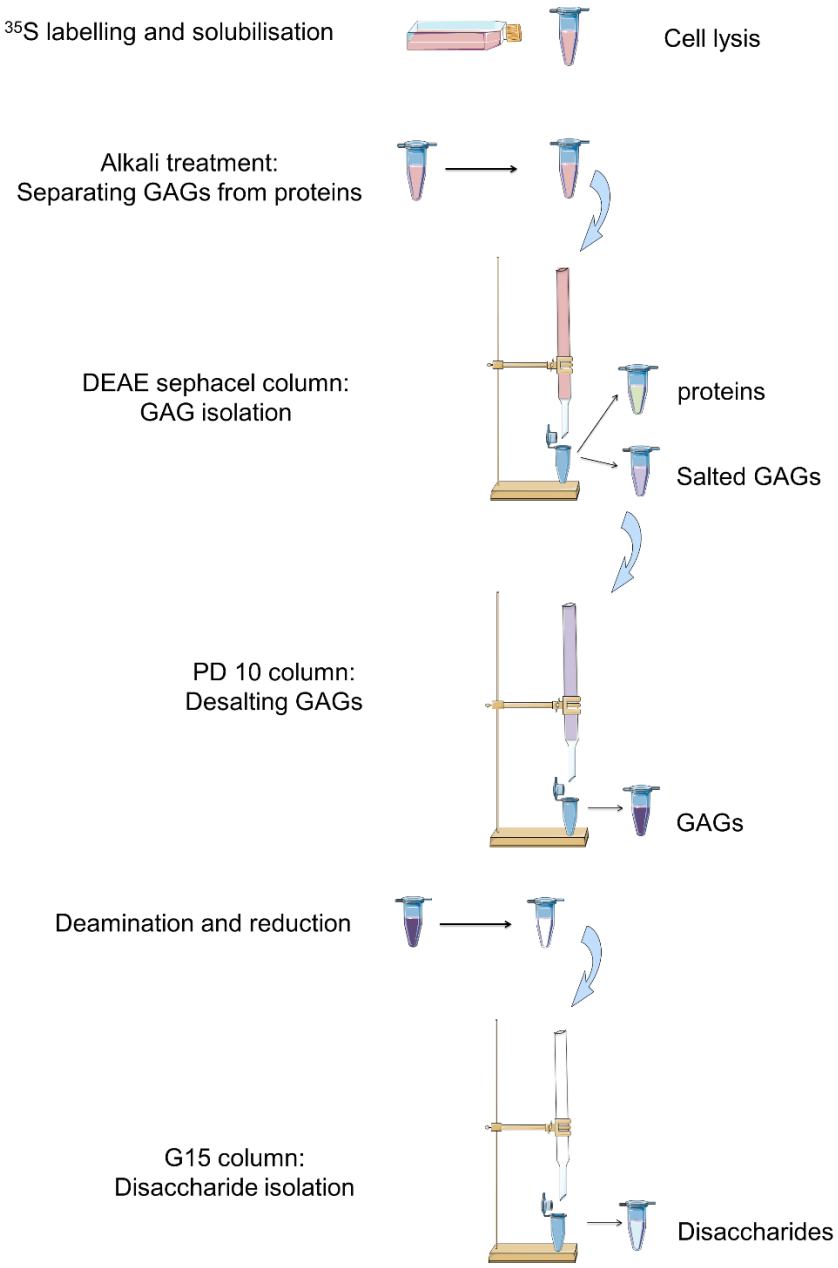

Figure 4-4: Disaccharide isolation
GAGs were radiolabeled with ^{35}S and isolated from proteins by alkali treatment. Different column-based isolation and acidic treatments were required to isolate disaccharides from the initial cell lysate.

4.2.5.1 Cell labelling and proteoglycans isolation

In a T75 flask, 80% confluent cells were labelled with 200 µCi/ml $Na_2{}^{35}SO_4$ (Perkin Elmer) diluted in fresh medium at 37°C for 24 hours. Cells were incubated for a day to allow them to generate

new HS with labelled sulfate. The media contained labelled GAGs on proteoglycans released to the medium (secreted or shredded). Cells were carefully washed 2 times with PBS and incubated on a rotating platform for 1 hour at 4°C with 3mL of solubilisation buffer (1% Triton TX-100, 50mM Tris/HCl pH (7.4), 0,15M NaCl). This solution lyses the cells but also preserves the integrity of the proteoglycans and their GAG chains. Cells were then scraped, collected in labelled tubes and centrifuged at 2000rpm for 15 minutes. The pellet contains cells debris and the supernatant proteins and GAGs. A volume of 100µL of this supernatant was kept for determining protein concentration.

4.2.5.2 Isolating the GAGs chains from the core protein

HS and CS chains are coupled to a core protein. Alkali treatment releases the GAG chains from the proteins. The final supernatant (minus 100µL) volume was measured and 4M NaOH was added to it to obtain a final concentration of 0.5M.

The samples were then left at 4ºC overnight for the alkali treatment to be effective. The next day, 10M HCl was used to adjust the pH to 8. This was required before applying to a DEAE-Sephacel column equilibrated at pH 8. DEAE Sephacel is a weak anion exchanger based on beaded cellulose (ion exchange group is diethylaminoethyl) which was used to isolate GAGs from any proteins or other compounds in the supernatants. Samples were diluted to a final concentration of 0.15M Cl^- (same concentration of the equilibration buffer for the column) with 0.02M Tris/HCl pH8. Initially samples were estimated to contain 0.5M NaCl.

DEAE columns were brought at room temperature and 500µL of DEAE sephacel was added on top of the column and equilibrated with 0.05M Tris/HCl pH8; 0.15M NaCl; 0.1% TX-100. Samples were added on top of the column followed by washes with 500µL of equilibration buffer. The flow through was kept in a 15mL tube in case the sample does not bind properly to the column.

To elute the proteins, 5mL (in 500µL aliquots) of 0.05M Acetate pH4, 0.15M NaCl, 0.1% TX-100 was added on top of the column. The drop in pH releases most proteins from the column. Each time 500µL was added, the elute was collected in a new Eppendorf tube. To increase pH and wash away Triton, ten times 500µL of 0.05M Tris/HCl pH 7.4, 0.15M NaCl was applied to the column.

Finally, GAG elution was performed by adding ten aliquots of 500µL of 1.5M NaCl. Five µL of each fraction was collected and added to 1mL of scintillation fluid to assess the level of radioactivity in each fraction. The fractions with the most radioactivity were pooled and checked for radioactivity level.

4.2.5.3 Desalting step.

Because the elution was performed with 1.5M NaCl it was required to remove the salt from the isolated GAGs. Samples volumes were adjusted to a final volume of 2.5mL with water and twelve 1.5 mL Eppendorf labelled. A PD 10 column eluted with H_2O was used for desalting, 1mg of heparin was added followed by another 50mL wash. Samples were applied to the column and eluted 12 times with 500µL water. Each elute was collected in a fresh tube and analysed by beta counting. Salt-free fractions with the most radioactivity were pooled and freeze-dried.

4.2.5.4 Deamination and reduction

The procedure was carried out in a fume hood as strong acids and bases were used. The samples were dissolved in 20µL of H_2O and the deamination was performed with HNO_2 at pH1.5. Deamination removes N-S groups leading to breaking of glycosidic bond. The reaction was stopped by adding 40µL of 2M Na_2CO_3, pH was checked and adjusted to 7-9 (8.5 ideally).

Following deamination, the samples were reduced with 50µL of $NaBH_4$ (solution 20mg/mL 10mM NaOH) for 3h at room temperature. To neutralise borohydride, samples were incubated with 60µL of 4M HAc for 10 minutes at room temperature. H_2 gas will be released during the reaction.

4.2.5.5 Disaccharides isolation and analysis

The disaccharides were desalted and isolated by gel chromatography on a long G15 column in 0.5M NH_4HCO_3, 0.5mL/min/fraction with 60 fractions. Radioactivity was assessed for each fraction and the ones containing the disaccharides were pooled, freeze-dried and diluted in water for compositional analysis. The disaccharide analysis was performed by strong anion exchange HPLC (SAX-HPLC). All buffers were degassed prior to use. In principle, the disaccharides bind

to the column. The elution occurs with aqueous KH_2PO_4 by stepwise increasing concentration at a rate of 1 ml/min therefore the retention time is proportional to the number and orientation of sulfate groups. Finally, fractions were collected and analysed for radioactivity. The disaccharide composition of the samples and more specifically the amount of sulfate group was assessed by analysing the amount of radioactivity for each fraction.

4.2.6 Cell proliferation and wound healing

Cell proliferation was measured with WST-1 test (Roche) following manufacturer's instructions. WST-1 test is dependent of the quantity of NADPH produced by the cells and is therefore correlated with the metabolic activity of the cells.

The capacity of the cells to migrate was assessed by a wound-healing assay. In this assay the cells are grown in an insert that generates an empty space within the cell layer. Ibidi inserts are silicone made with two gaps to allow cell growth and the generation of a well-defined scratch once removed (Figure 4-5). The cell velocity is determined by analysing the distance traveled by the cells at different intervals. In each well of a 12-well plate, cells were suspended at 21 000 cells/reservoir of Ibidi insert in complete media or with 0.5% FBS media for FGF2 stimulation studies. The next day, inserts were removed with sterile tweezers, washed with complete media or 0.5% FBS media supplemented with 10ng/mL FGF2 and a final volume of 2mL was added before starting imaging. Images for cell migration was acquired every hour in a Nikon Biostation.

Cell velocity was determined during the linear growth when the speed of closure is constant.

Cell velocity= (area of the wound/height of the picture/2 (two cell front))/ time B-time A

With time A= starting time of linear growth, time B= ending time of linear growth.

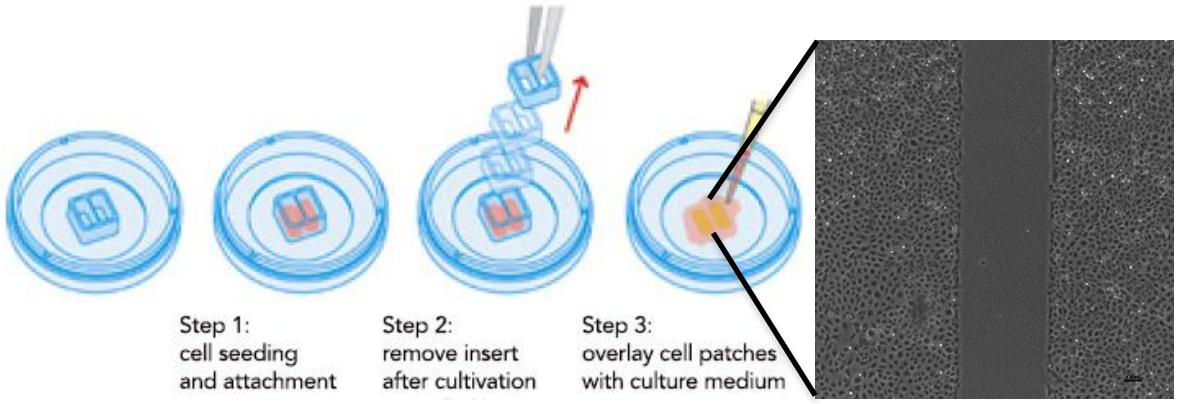

Figure 4-5: Wound healing assay
Cells were seeded at $3x10^5$cells/mL with 70µL per Ibidi insert in 12-well plate. The next day, inserts were removed with sterile tweezers and complete media or 0.5% FBS media ± 10ng/mL was added to the cells. Images were acquired by Nikon Biostation every hour. Image adapted from http://animalab.eu/products/culture-insert-2-well.

4.3 Results

4.3.1 Cell characterisation

In order to characterise the cell lines and making sure of their authenticity, the cells studied in this chapter were stained for different markers such as a cell surface marker E-cadherin, a cytoskeleton fiber marker α-Smooth Muscle Actin (α-SMA) and the ECM protein, fibronectin. As seen Figure 4-6, HK2 and HKC8 cells which are epithelial cells showed a positive staining of extracellular fibronectin. Fibronectin staining was seen as a well-defined network around the cells. E-cadherin expression was found to be heterogeneous. Not all HK2 and HKC8 cells expressed E-cadherin and fibronectin seemed to be more expressed in these cells. In contrast, the NRK-49F cells which are rat renal fibroblasts did not express E-cadherin and showed low expression of fibronectin. NRK-49F cells were further stained with α-Smooth Muscle Actin (α-SMA) which is a marker of activated fibroblasts. Less than 5% of the cells were positive but those cells that were positive displayed a very strong staining with α-SMA located on contractile fibers.

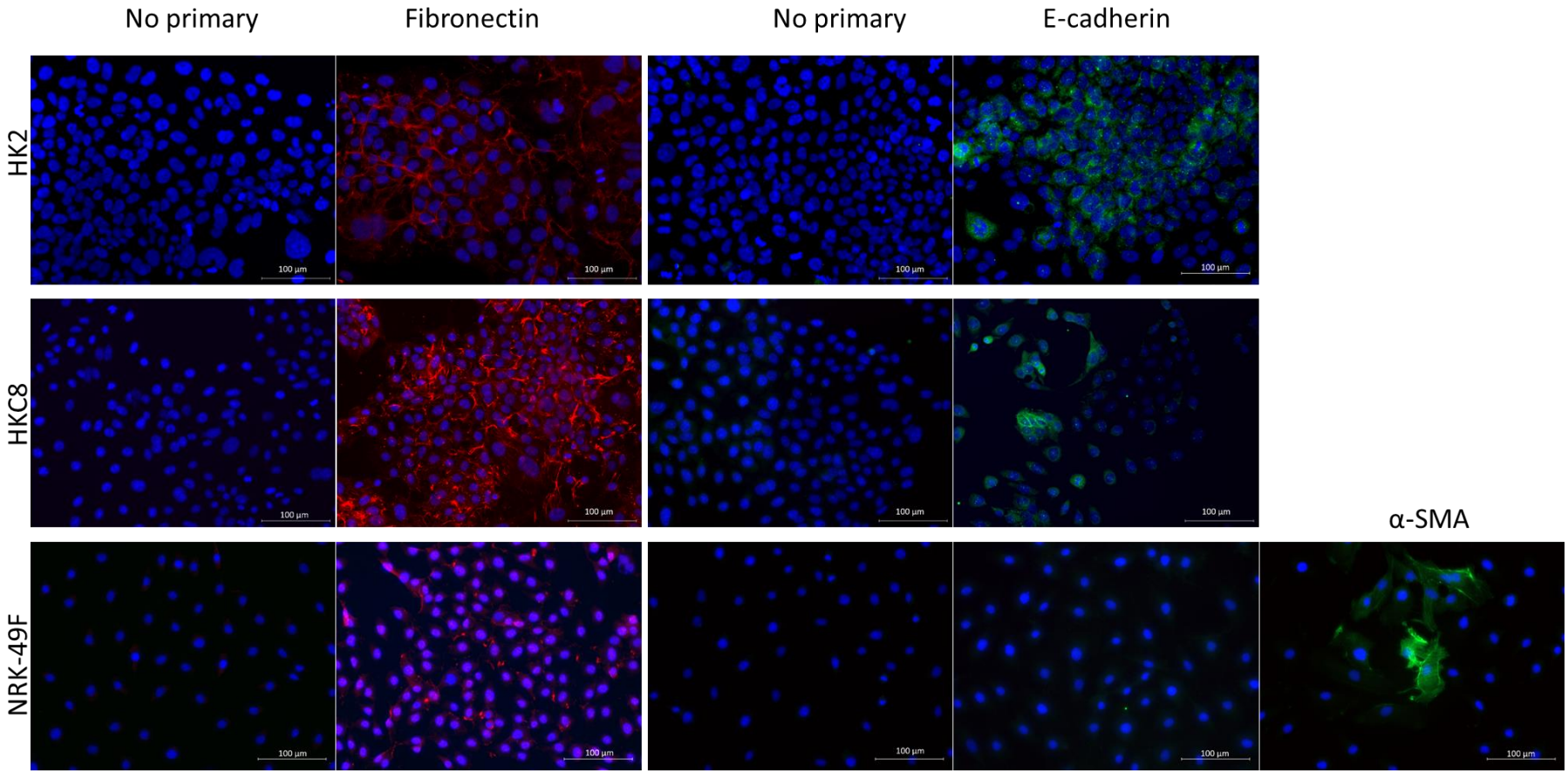

Figure 4-6: Cells characterisation

HK2, HKC8 and NRK-49F cells were seeded in 8 well-chamber slides and grown until 60-80% confluent. Cells were fixed for 10 minutes in ice cold methanol at -20°C and incubated for 1 hour at room temperature in 1% BSA to avoid unspecific binding. Slides were incubated with the primary antibodies overnight at 4°C. The next day slides were washed with PBS and incubated for 2h at room temperature with the corresponding secondary antibody. Slides were mounted in Vectashield with DAPI. Cells incubated with only secondary (no primary) were used as negative control. Scale bar represents 100µm. N≥2. UG student Imogen L Wilson and MRes student Hanna Lane contributed to the staining under supervision of Laura Ferreras.

Very little is known about the HS3STs in kidney tissue and in view of the results observed *in vivo* with HS3ST1 expression in fibrosis, this project studied what growth factors could modulate their expression. The three different cell types described above, and two pro-fibrotic treatments were used.

4.3.2 The effect of TGFβ1 on HS3STs expression in renal epithelial cells

As described in section 1, TGFβ1 is one of the most studied pro-fibrotic factors. However, to the best of our knowledge, its role in HS3ST expression has never been described before. Therefore, HK2 and HKC8 cells were treated with 5ng/mL TGFβ1 for different time periods to identify a potential action of TGFβ1 on renal epithelial cells HS3ST expression.

4.3.2.1 HS3ST in HK2 cells

HK2 cells were seeded in 6-well plates with $2x10^5$cells per well. After 24h incubation in 0.5% FBS media, cells were treated with TGFβ1 (5ng/mL) for 3, 6, 24, 48 hours. HS3ST1 and HS3ST3B expression was analysed by RT-qPCR. HS3ST1 was decreased but only significantly at 6 hours and 48 hours after treatment ($p<0.05$) (Figure 4-7). In contrast, HS3ST3B expression was increased after TGFβ1 treatment. The upregulation of HS3ST3B was time dependent and significant at 24 hours ($p<0.01$) and 48 hours ($p<0.01$) (Figure 4-8).

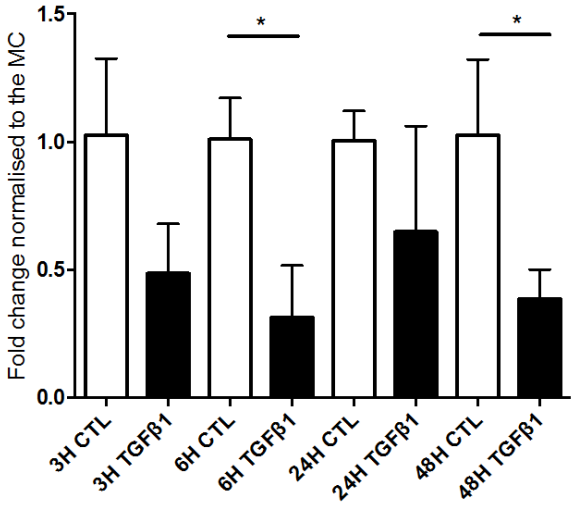

Figure 4-7: HS3ST1 expression in HK2 cells treated with TGFβ1 (5ng/mL)
HK2 cells were seeded in 6-well plates with $2x10^5$cells per well. Cells were incubated with 0.5% FBS medium 24 hours before being treated with 5ng/mL TGFβ1 or only buffer (CTL) for 3, 6, 24, 48 hours. Results are expressed as mean ± SD. Results were normalised to the house keeping gene HPRT1 and compared to the average of the mean of controls (MC). Two-tailed unpaired t test with Welch's correction, $p<0.05$ (*) N=3.

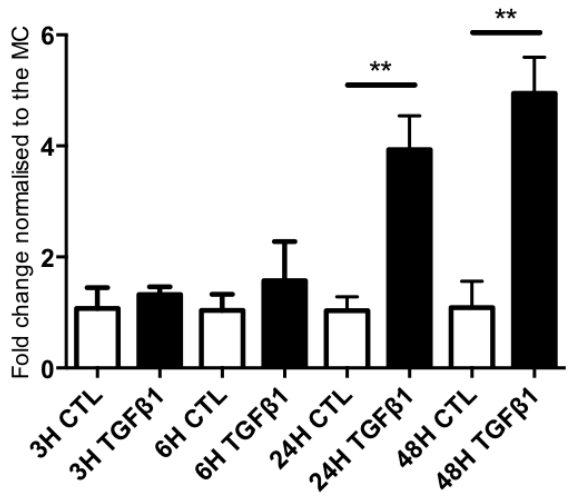

Figure 4-8: HS3ST3B expression in HK2 cells treated with TGFβ1 (5ng/mL)
HK2 cells were seeded in 6-well plates with $2x10^5$cells per well. Cells were incubated in 0.5% FBS medium for 24 hours and treated with 5ng/mL TGFβ1 or only buffer (CTL) for 3, 6, 24, 48 hours. Results are expressed as mean ± SD. Results were normalised to the house keeping gene HPRT1 and compared to the average of the mean of controls (MC). Two-tailed unpaired t test with Welch's correction, $p<0.01$ (**) N≥3.

Two other isoforms of HS3STs, HS3ST3A and HS3ST6 were analysed at 24h and 48h treatment with 5ng/mL TGFβ1 but no significant changes were observed (Figure 4-9). HS3ST2, 4 and 5 were not analysed considering their low or non-existent expression in kidney tissue (Shworak *et al.*, 1999; Mochizuki *et al.*, 2008).

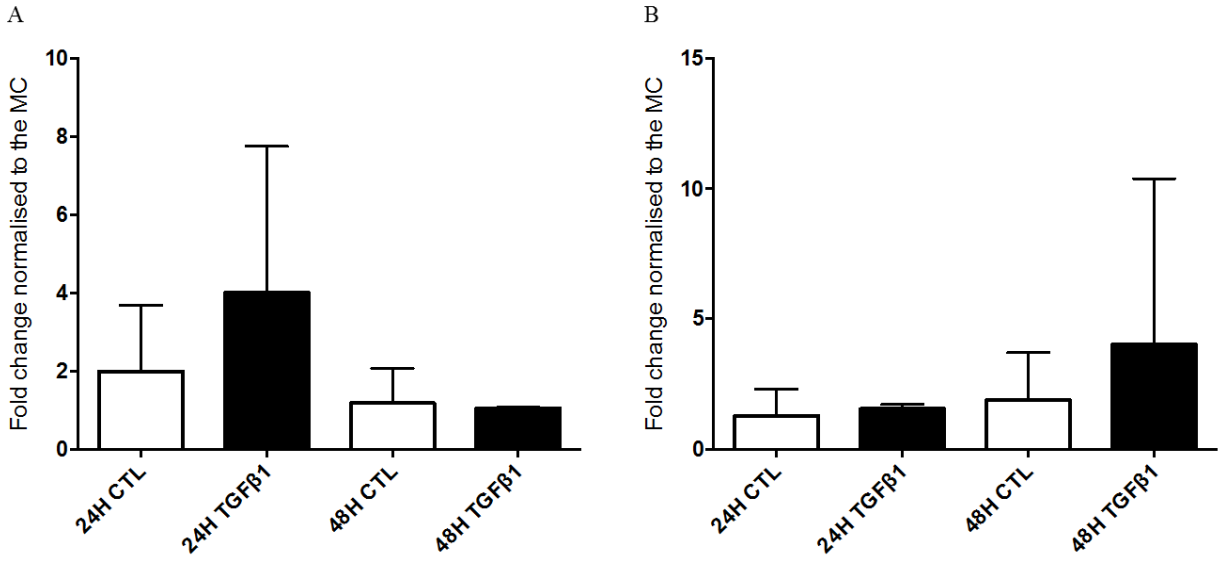

Figure 4-9: HS3ST3A and HS3ST6 expression in HK2 cells treated with TGFβ1 (5ng/mL)
HK2 cells were seeded in 6-well plates with $2x10^5$cells per well. Cells were incubated in 0.5% FBS medium for 24 hours and treated with 5ng/mL TGFβ1 or only buffer (CTL) for 24 and 48 hours. HS3ST3A expression is displayed in A, HS3ST6 expression is displayed in B. Results are expressed as mean ± SD. Results were normalised to the house keeping gene HPRT1 and compared to the average of the mean of controls (MC). N≥2.

4.3.2.2 HS3STs in HKC8 cells

HKC8 cells were seeded in 6-well plates with $2.4x10^5$cells per well and incubated in 0.5%FBS for 24 hours media prior to treatment with 5ng/mL TGFβ1 for 3, 6, 24, 48 hours. HS3STs expressions were analysed by RT-qPCR. HS3ST1 expression was very low in HKC8 cells and therefore this isoform expression was not studied in these cells (CT values between 36 and undetermined). Overall, TGFβ1 (5ng/mL) treatment did not induce any significant change in HS3STs expression as seen in Figure 4-10 and Figure 4-11.

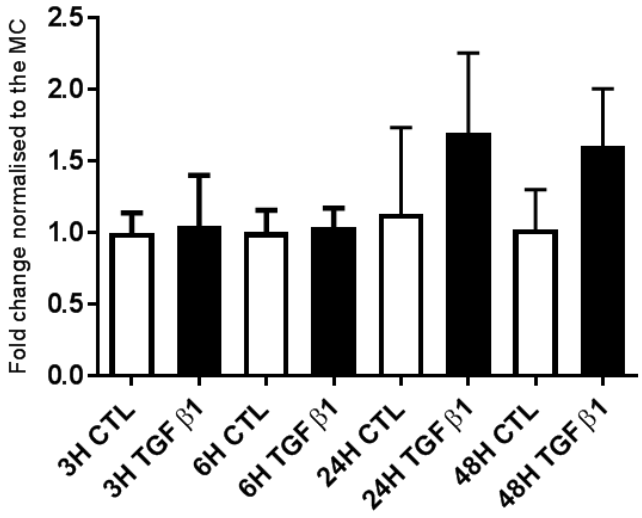

Figure 4-10: HS3ST3B expression in HKC8 cells treated with TGFβ1 (5ng/mL)
HKC8 cells were seeded in 6-well plates with 2.4x10^{5}cells per well. Cells were incubated in 0.5% FBS medium for 24 hours and treated with 5ng/mL TGFβ1 or only buffer (CTL) for 3, 6, 24, 48 hours. Results are expressed as mean ± SD. Results were normalised to the house keeping gene HPRT1 and compared to the average of the mean of controls (MC). N≥2.

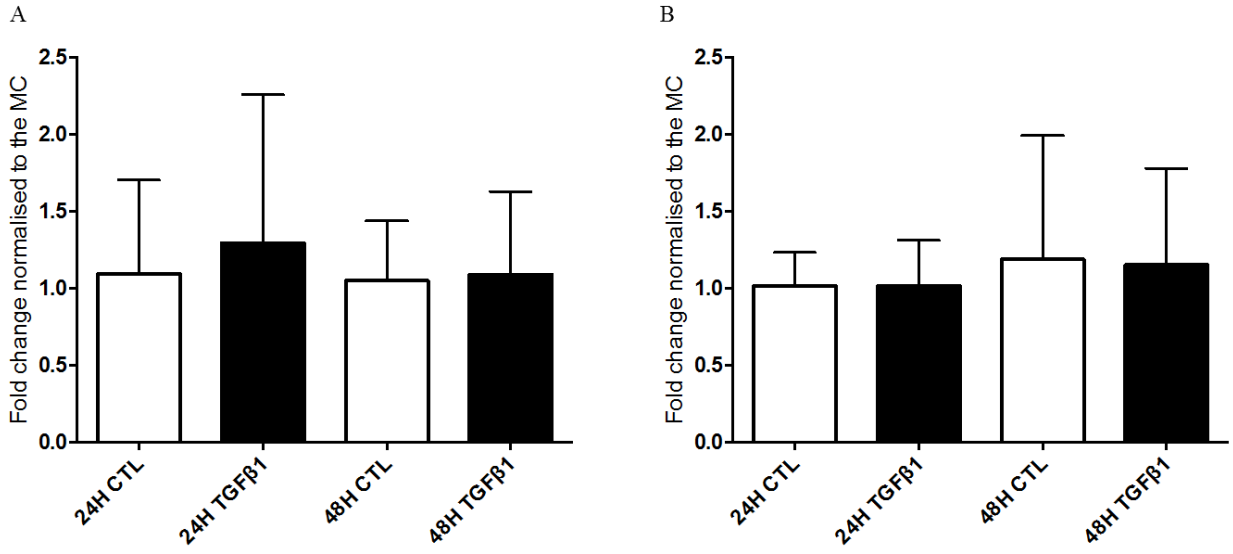

Figure 4-11: HS3ST3A and HS3ST6 expression in HKC8 cells treated with TGFβ1 (5ng/mL)
HKC8 cells were seeded in 6-well plates with 2.4x10^{5}cells per well. Cells were incubated in 0.5% FBS medium for 24 hours and treated with 5ng/mL TGFβ1 or only buffer (CTL) for 24 and 48 hours. HS3ST3A expression is displayed in A, HS3ST6 expression is displayed in B. Results are expressed as mean ± SD. Results were normalised to the house keeping gene HPRT1 and compared to the average of the mean of controls (MC) N≥2.

4.3.3 HS3STs modulation by TGFβ2 and IL1β in renal epithelial cells

The combination of treatment of TGFβ2 and IL1β has been shown to promote endothelial to mesenchymal transition and this study addressed if the treatment could have an effect on renal epithelial cells. The same seeding condition as in TGFβ1 treatment was used for these experiments.

4.3.3.1 HK2 cells

After 24h incubation in 0.5% FBS followed by TGFβ2 and IL1β treatment (10ng/mL) for 3, 6, 24, 48h, HS3ST1 expression decreased in HK2 cells. This decrease was only significant at 6 hours and 24 hours after treatment with TGFβ2 and IL1β ($p<0.05$, $p<0.01$ respectively) (Figure 4-12). In contrast, HS3ST3B was increased after TGFβ2 and IL1β treatment. The upregulation of HS3ST3B was time dependent and significant at 24 hours ($p<0.001$) and 48 hours ($p<0.01$) as seen Figure 4-13. The expression of HS3ST3A and HS3ST6 after TGFβ2 and IL1β treatment of HK2 cells was variable and no clear changes in expression as observed Figure 4-14.

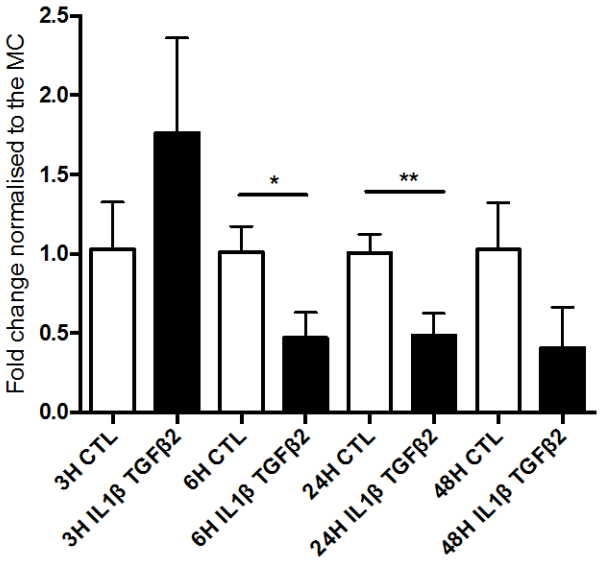

Figure 4-12: HS3ST1 expression in HK2 cells treated with TGFβ2 and IL1β (10ng/mL)
HK2 cells were seeded in 6-well plates with $2x10^5$cells per well. Cells were incubated in 0.5% FBS medium for 24 hours and treated with 10ng/mL TGFβ2 and IL1β or only buffer (CTL) for 3, 6, 24, 48 hours. Results are expressed as mean ± SD. Results were normalised to the house keeping gene HPRT1 and compared to the average of the mean of controls (MC). Two-tailed unpaired t test with Welch's correction, $p<0.05$ (*) and $p<0.01$ (**) N=3.

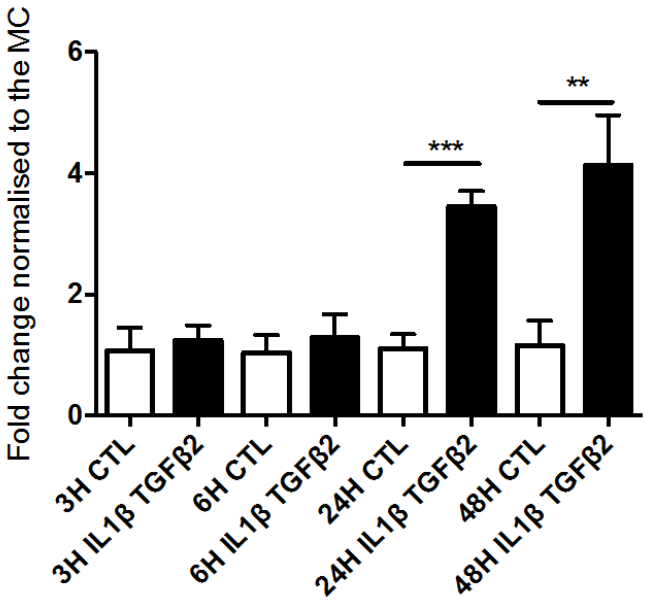

Figure 4-13: HS3ST3B expression in HK2 cells treated with TGFβ2 and IL1β (10ng/mL)
HK2 cells were seeded in 6-well plates with $2x10^5$cells per well. Cells were incubated in 0.5% FBS medium for 24 hours and treated with 10ng/mL TGFβ2 and IL1β or only buffer (CTL) for 3, 6, 24, 48 hours. Results are expressed as mean ± SD. Results were normalised to the house keeping gene HPRT1 and compared to the average of the mean of controls (MC). Two-tailed unpaired t test with Welch's correction, $p<0.01$ (**) and $p<0.001$ (***) $N\geq3$.

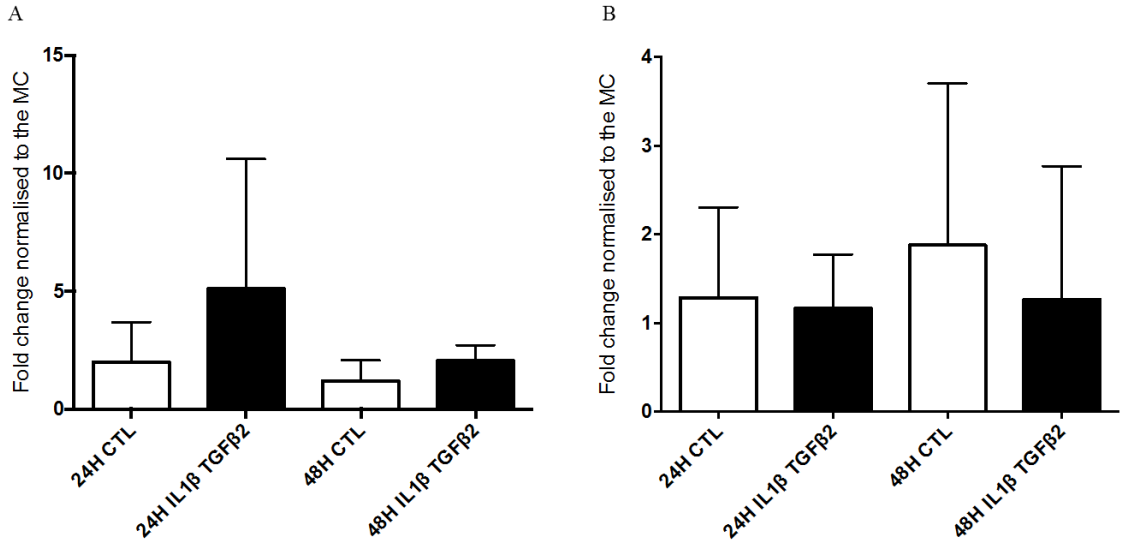

Figure 4-14: HS3ST3A and HS3ST6 expression in HK2 cells treated with TGFβ2 and IL1β (10ng/mL)
HK2 cells were seeded in 6-well plates with $2x10^5$cells per well. Cells were incubated in 0.5% FBS medium for 24 hours and treated with 10ng/mL TGFβ2 and IL1β or only buffer (CTL) for 24 and 48 hours. HS3ST3A expression is displayed in A, HS3ST6 expression is displayed in B. Results are expressed as mean ± SD. Results were normalised to the house keeping gene HPRT1 and compared to the average of the mean of controls (MC). $N\geq2$.

4.3.3.2 HKC8 cells

HKC8 showed the same response as HK2 cells to TGFβ2 and IL1β with an increase in HS3ST3B expression. However, this increase was not significant (Figure 4-15). Additionally, HS3ST3A was increased at 24 hours and 48 hours but not significantly and HS3ST6 expression was not affected by TGFβ2 and IL1β treatment (Figure 4-16).

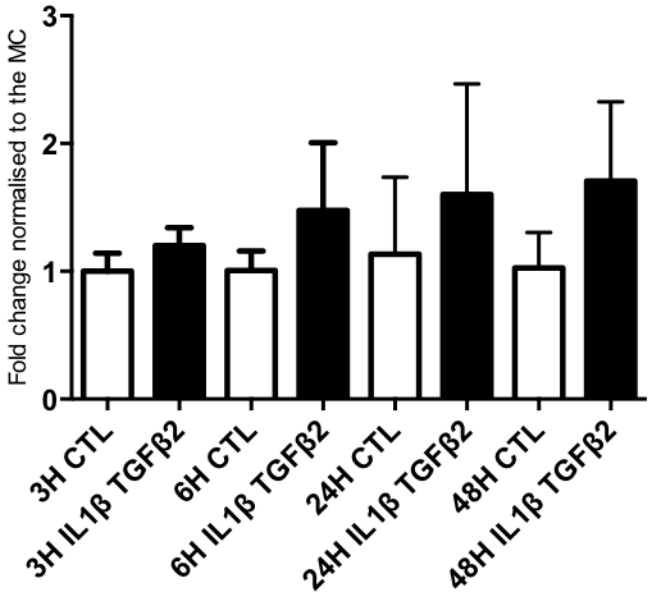

Figure 4-15: HS3ST3B expression in HKC8 cells treated with TGFβ2 and IL1β (10ng/mL)
HKC8 cells were seeded in 6-well plates with $2.4x10^5$cells per well. Cells were incubated in 0.5% FBS medium for 24 hours and treated with 10ng/mL TGFβ2 and IL1β or only buffer (CTL) for 3, 6, 24, 48 hours. Results are expressed as mean ± SD. Results were normalised to the house keeping gene HPRT1 and compared to the average of the mean of controls (MC). Two-tailed unpaired t test with Welch's correction, N=3.

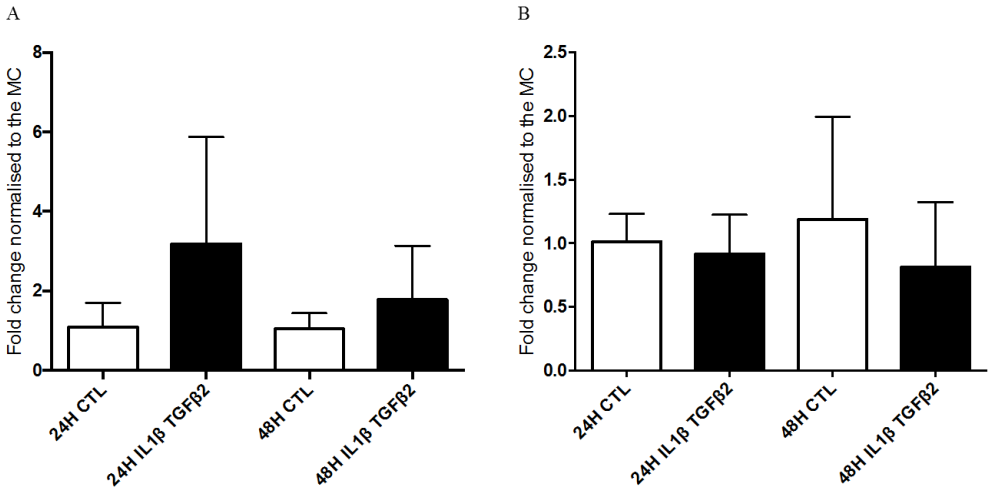

Figure 4-16: HS3ST3A HS3ST6 expression in HKC8 cells treated with TGFβ2 and IL1β (10ng/mL)
HKC8 cells were seeded in 6-well plates with 2.4x10^{5}cells per well. Cells were incubated in 0.5% FBS medium for 24 hours and treated with 10ng/mL TGFβ2 and IL1β or only buffer (CTL) for 24 and 48 hours. HS3ST3A expression is displayed in A, HS3ST6 expression is displayed in B. Results are expressed as mean ± SD. Results were normalised to the house keeping gene HPRT1 and compared to the average of the mean of controls (MC). N≥2.

4.3.4 HS3ST1 expression in renal fibroblast

The study further addressed if the changes seen in HS3ST1 expression in the HK2 cells could be seen in other cell types such as NRK-49F a rat renal fibroblast line. Cells were gown and treated in T75 flasks to allow a sufficient quantity and quality RNA to be collected. NRK-49F were very sensitive to TGFβ1 (5ng/mL) and TGFβ2 and IL1β (10ng/mL) and showed a change in morphology after 24h. As observed Figure 4-17 they were elongated, and the cells had a needle myofibroblast like shape.

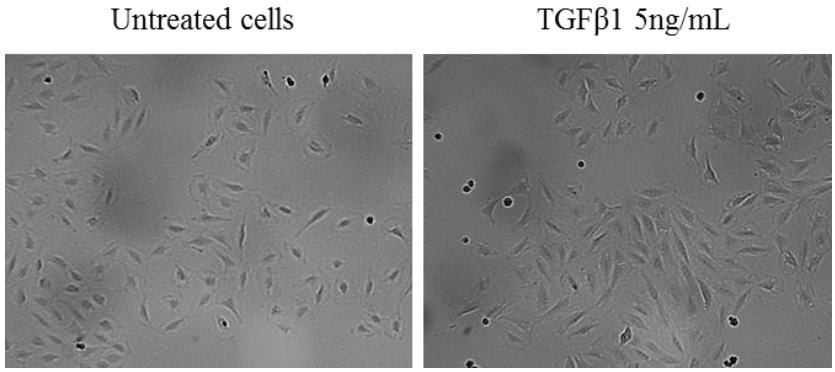

Figure 4-17: NRK-49F cells morphology after TGFβ1 treatment
NRK-49F cells were seeded in T75 flasks until 60-80% confluent. Cells were starved with 0.5% FBS media for 24h and were then treated with 5ng/mL of TGFβ1 for 24h. Magnification x200.

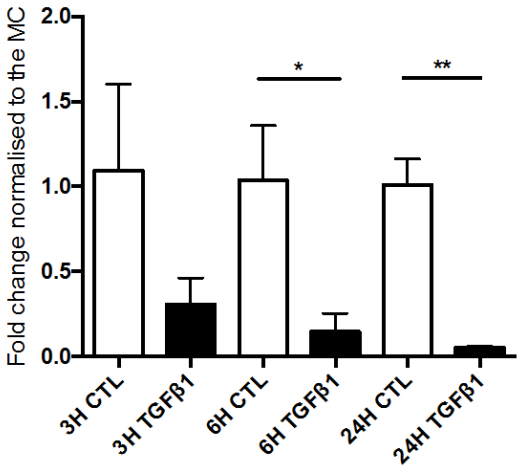

Figure 4-18: HS3ST1 expression in NRK-49F cells treated with TGFβ1
NRK-49F cells were seeded in T75 flasks and were incubated in 0.5% FBS medium for 24 hours once they reached 60% confluence. Cells were incubated in 0.5% FBS medium for 24 hours and treated with 5ng/mL TGFβ1 or only buffer (CTL) for 3, 6, 24 hours. Results are expressed as mean ± SD. Results were normalised to the house keeping gene HPRT1 and compared to the average of the mean of controls (MC). Two-tailed unpaired t test with Welch's correction, $p<0.05$ (*) N=3.

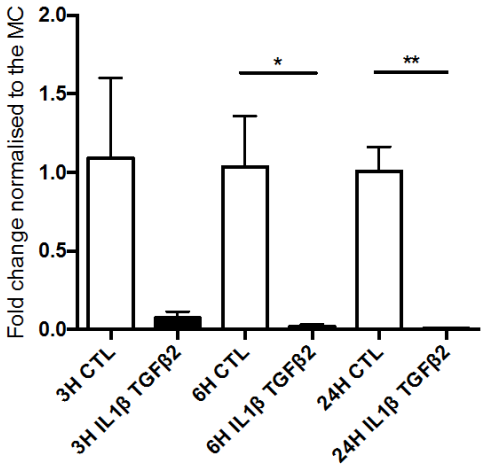

Figure 4-19: HS3ST1 expression in NRK-49F cells treated with TGFβ2 IL1β (10ng/mL)
NRK-49F cells were seeded in T75 flasks and were incubated in 0.5% FBS medium for 24 hours once they reached 60% confluence. Cells were treated with 10ng/mL TGFβ2 IL1β or only buffer (CTL) for 3, 6, 24 hours. Results are expressed as mean ± SD. Results were normalised to the house keeping gene HPRT1 and compared to the average of the mean of controls (MC). Two-tailed unpaired t test with Welch's correction, $p<0.05$ (*) and $p<0.01$ (**) N=3.

4.3.5 Generating HKC8-HS3ST1 and HKC8-CTL stable transfectants

In addition to the strong correlation between HS3ST1 and fibrosis *in vivo*, the modulation of HS3ST1 in HK2 and NRK-49F by pro-fibrotic factors *in vitro* increased interest regarding the role

of HS3ST1. As HS3ST1 expression was barely detectable in HKC8 cells, it was a suitable model for generating HS3ST1 overexpressing cells.

4.3.5.1 HS3ST1 and empty plasmid amplification

HS3ST1 plasmid (genecopoeia) was amplified in *E. coli DH5α*. Plasmid concentration, size and quality were assessed (Figure 4-20). Plasmid extraction resulted in a concentrated solution of 466.2ng/µL. To analyse the plasmid, 1µg of isolated DNA was digested by *SalI* and 50ng, 100ng, 250ng of the digested plasmid together with 200ng of the whole plasmid were analysed by agarose gel electrophoresis. HS3ST1 plasmid is 6346bp long and *SalI* cleaves at 2280bp and 4468bp and therefore produced two bands, one at 4158bp and one at 2188bp. Plasmid digestion showed 2 bands, one around 2kb and one around 4kb as seen Figure 4-20. This result highlighted that the plasmid sequence correlated with what was expected. The plasmid was then sent for sequencing.

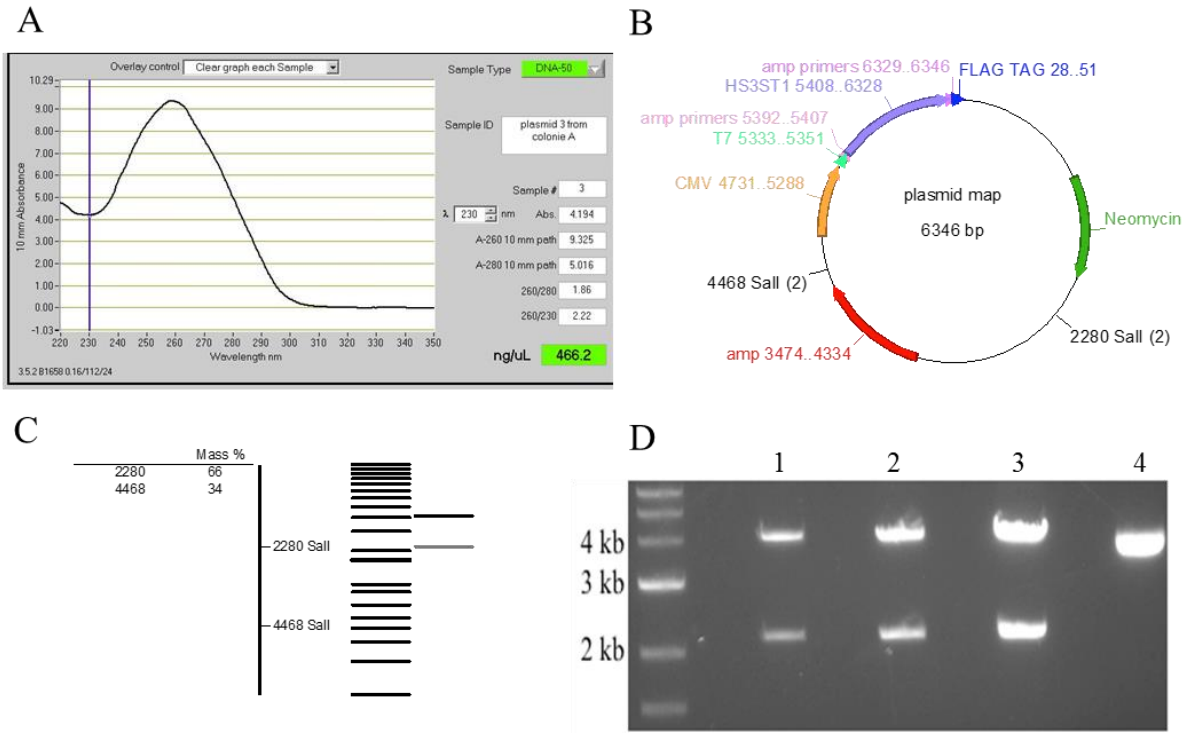

Figure 4-20: HS3ST1 plasmid amplification and analysis

Plasmid concentration following transformed bacteria lysis and purification (Qiagen mini-prep) was analysed by nanodrop DNA measurement (A). *SalI* restriction enzymes cleaves the plasmid in two sites, 2280bp and 4468bp (B) and generates two fractions, a 2188bp and 4158bp fragment (C). The digested and undigested plasmids were run into a 0.8% agarose gel together with a 1kb ladder and analysed under UV light (D). Digested plasmid lines (1= 50ng, 2=100ng, 3=250ng) showed the two expected band (4.158 kb and 2.188 kb). The fourth line is 200ng of undigested plasmid.

Plasmid sequencing by Source Bioscience showed 97% homology with the HS3ST1 sequence of the plasmid. The 3% difference was due to the analysing software being unable to identify some bases in the plasmid (N) (Figure 4-21).

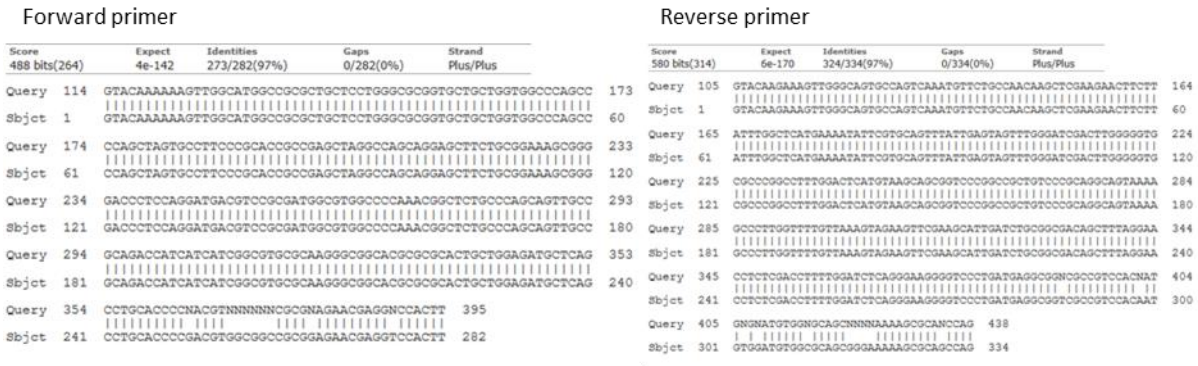

Figure 4-21: Blast alignment of the sequencing from the generated plasmid and HS3ST1 sequence

The generation of an empty plasmid was required to generate Mock cells in parallel with HS3ST1 overexpressing cells for control purposes. The empty plasmid was generated by *BsrGI* digestion, a restrictive enzyme which cleaves at the extremity of HS3ST1 gene sequence. After the successful digestion of HS3ST1 plasmid for 3h at 37ºC, the empty linear plasmid and HS3ST1 sequence were observed by agarose gel as seen Figure 4-22.

The empty plasmid was extracted from the gel and was ligated with T4 ligase 3 hours at room temperature. The empty circular plasmid was then transfected to competent bacteria *E.coli DH5α*. Out of five colonies, three were selected. Plasmid integrity and sequence were analysed by multiple restriction enzymes digestions. First to confirm that HS3ST1 sequence was not within the plasmid, the newly ligated plasmid was digested by *KpnI,* an enzyme cleaving exclusively within HS3ST1 sequence. As seen Figure 4-23 C, digestion with *KpnI* linearised HS3ST1 plasmid but not the empty one as expected. Hence the presence of more than one band after digestion, representing nicked, linear and supercoiled forms of plasmids. Second, when digested with *BsrGI*, HS3ST1 sequence could only be seen in the HS3ST1 plasmid and only linearised the empty one with the expected size of around 6Kb.

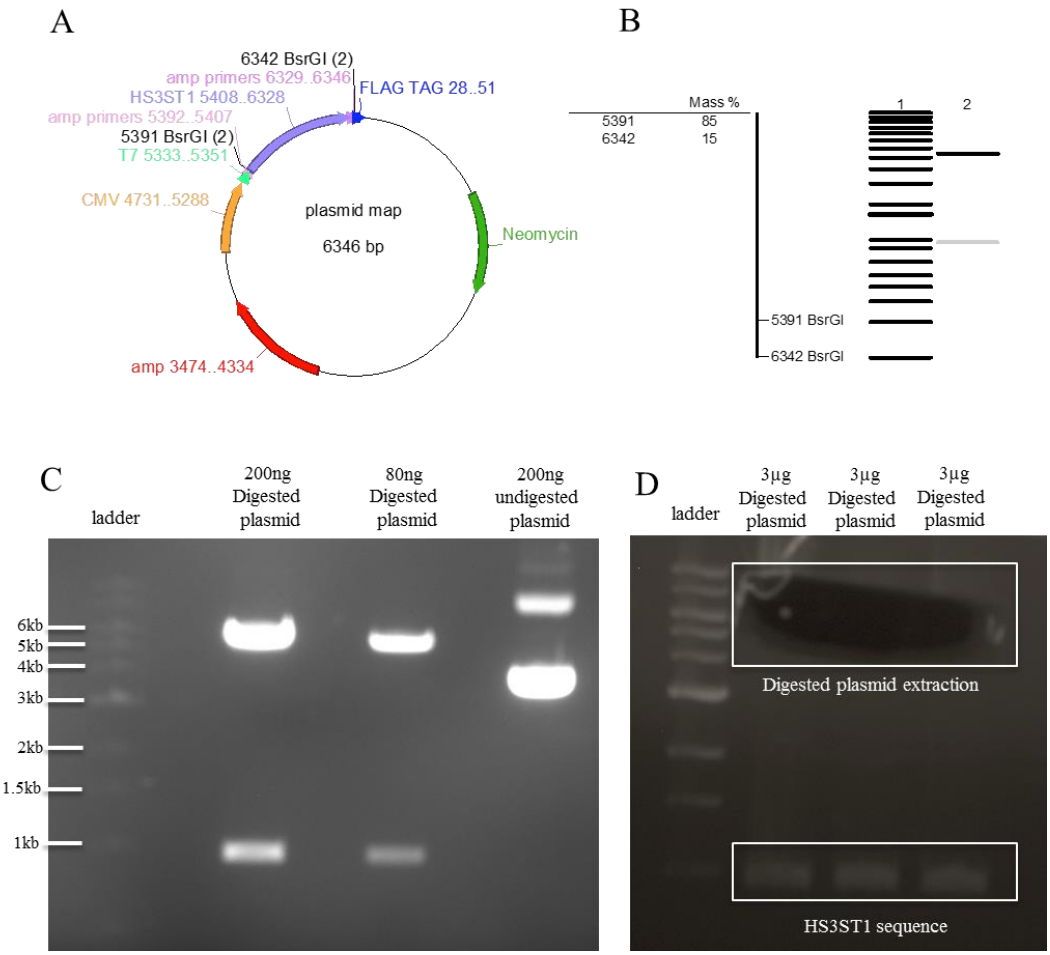

Figure 4-22: Generating empty plasmid by restrictive enzyme *BsrGI* digestion.
BsrGI cleaves at the extremity of HS3ST1 sequence at 6342bp and 5391bp (A) and is expected to generate the empty plasmid of 5395bp (85% of the mass) and HS3ST sequence 951bp (15% of the mass) (B). *BsrGI* digestion of HS3ST1 plasmid was run into a 0.8% agarose gel together with a 1kb ladder and analysed under UV showing the expected two bands in 200ng and 80ng of digested plasmid (C). The undigested product showed the nicked, linear and supercoiled forms of plasmids. The empty plasmid was excised from the gel using a sterile blade under UV light (D).

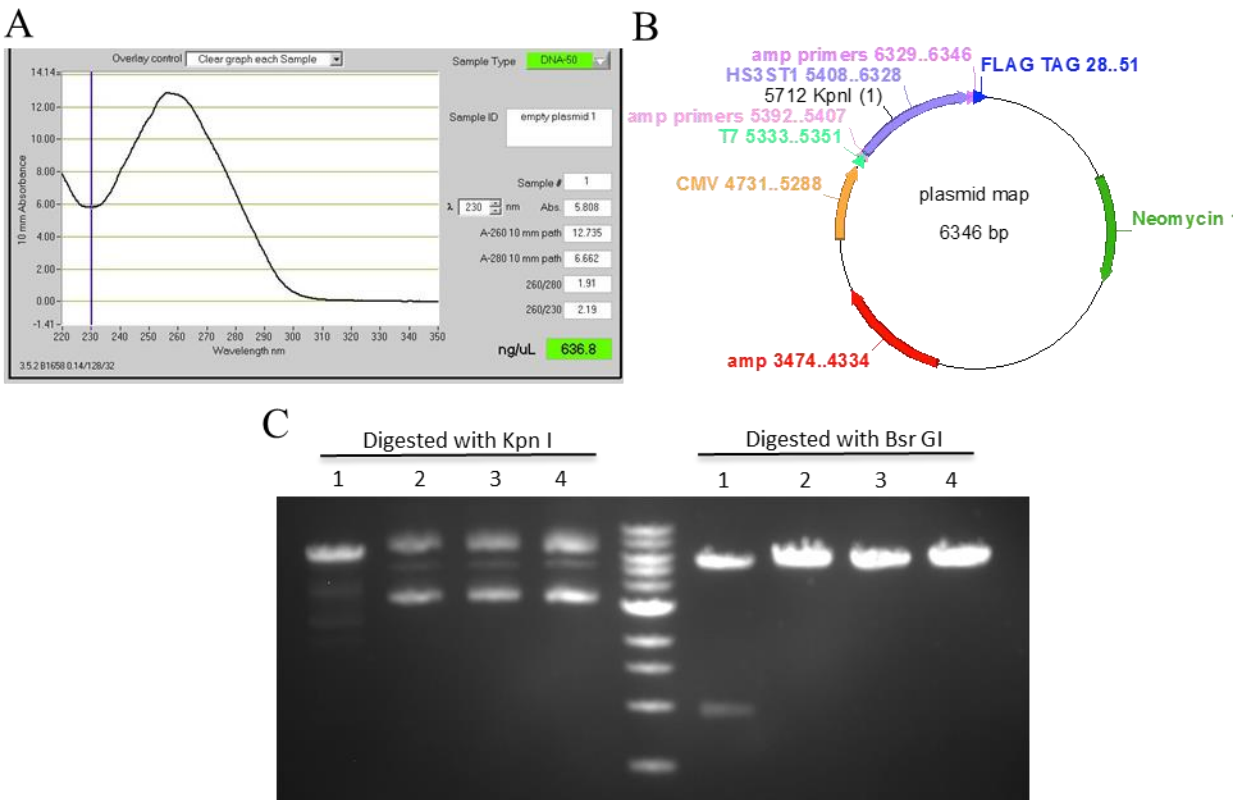

Figure 4-23: Assessing empty plasmid sequence
Empty plasmid and HS3ST1 plasmid were digested with either *KpnI* or *BsrGI* restrictive enzymes 3h at 37ºC. The digested plasmids were run into a 0.8% agarose gel together with a 1kb ladder and analysed under UV light. *KpnI* cleaves HS3ST1 plasmid within HS3ST1 gene sequence while *BsrGI* cleaves at the extremity of it. Line 1 is HS3ST1 plasmid (800ng) lines 2-4 are the empty plasmid from three different colonies (1µg). The empty plasmid was not digested by *KpnI* and therefore line 2-4 *KpnI* showed the nicked, linear and supercoiled forms of plasmids.

4.3.5.2 Generating HKC8-HS3ST1 and HKC8-CTL

HKC8 cells were grown in 10 cm petri dish until 90% confluent and were transfected with 2µg of linearised HS3ST1 plasmid. Forty-eight hours after transfection, cells were split 1:5 and grown in media supplemented with G418 to select stably transfected cells. Thirty-five clones (HKC8-HS3ST1) were selected and cultured for several days. HS3ST1 expression in the 35 HKC8-HS3ST1 clones was assessed by RT-qPCR. As seen Figure 4-24, all clones had different levels of expression and clone 3, 9, 10, 12 and 33 were selected to assess protein expression.

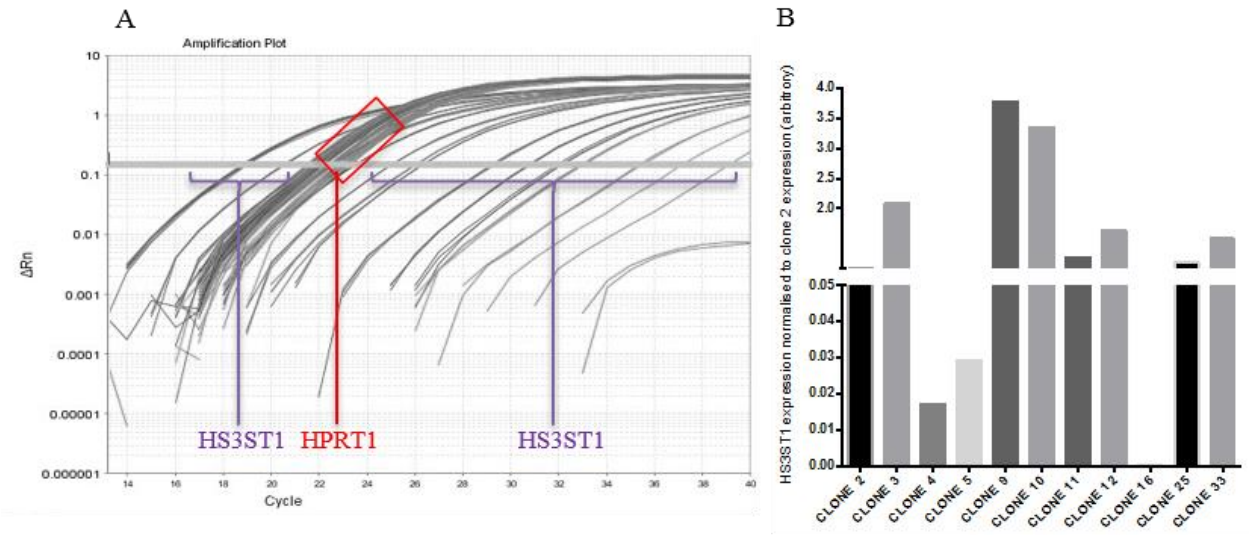

Figure 4-24: HS3ST1 expression in isolated clones
Wild type HKC8 cells were transfected in 10cm petri dish with 2µg of HS3ST1 plasmid and effectene. Two days after transfection, cells were split 1:5 and grown in media supplemented with 200µg/mL G418. Thirty-five clones were isolated by cloning ring and expanded. The clones' HS3ST1 expression was analysed by qPCR. The amplification plot (A) shows heterogeneity in HS3ST1 expression between the different clones which is highlighted when compared arbitrary to clone 2 (B).

HS3ST1 expression in the 5 selected clones was mirrored by their protein levels as seen Figure 4-25. Clone 9 had the highest expression and protein level of HS3ST1 and was selected for future experiments. Additionally, clone 12 which had a lower expression was also selected to allow the study of two different clones. The HS3ST1 plasmid contains the HS3ST1 sequence with a flag tag at the C-term. Because most antibodies for HS3ST1 are unsuccessful or not trust worthy, the flag tag was used to allow western blot and immunofluorescence detection of the protein. The flag tag had to be added at the C-terminal of the protein due to the presence of a signal peptide at the N-terminal.

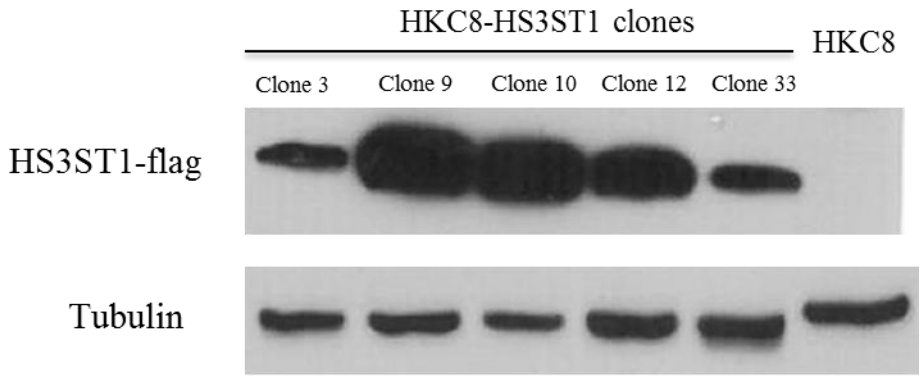

Figure 4-25: HKC8-HS3ST1 clones protein levels
Five HKC8-HS3ST1 clones were selected and their protein levels analysed by Western Blot. A quantity of 20µg of protein lysates were run into a 10% acrylamide gel for 1h30 at 110V and transferred onto a nitrocellulose cell membrane. The membrane was blocked 1h in 5% milk 0.1% TBST and incubated overnight at 4°C with flag tag antibody. The next day the membrane was washed with 0.1%TBST and incubated with secondary anti-rabbit antibody before detection. After a mild stripping and a blocking step, the membrane was probed for tubulin as a loading control. N=2

Because generating stably transfected cells can have non-specific effects in cells, HKC8 control (HKC8-CTL) were generated as controls for future experiments. HKC8 cells were transfected in 10cm petri dish with 2µg of empty plasmid. Three days after transfection, cells were grown in media supplemented with G418 to select stably transfected cells. Two clones were selected and HS3ST1 expression in the newly generated HKC8-CTL was analysed by RT-qPCR (Figure 4-26) and Western blot (Figure 4-27). HKC8-CTL cell HS3ST1 expression remained low.

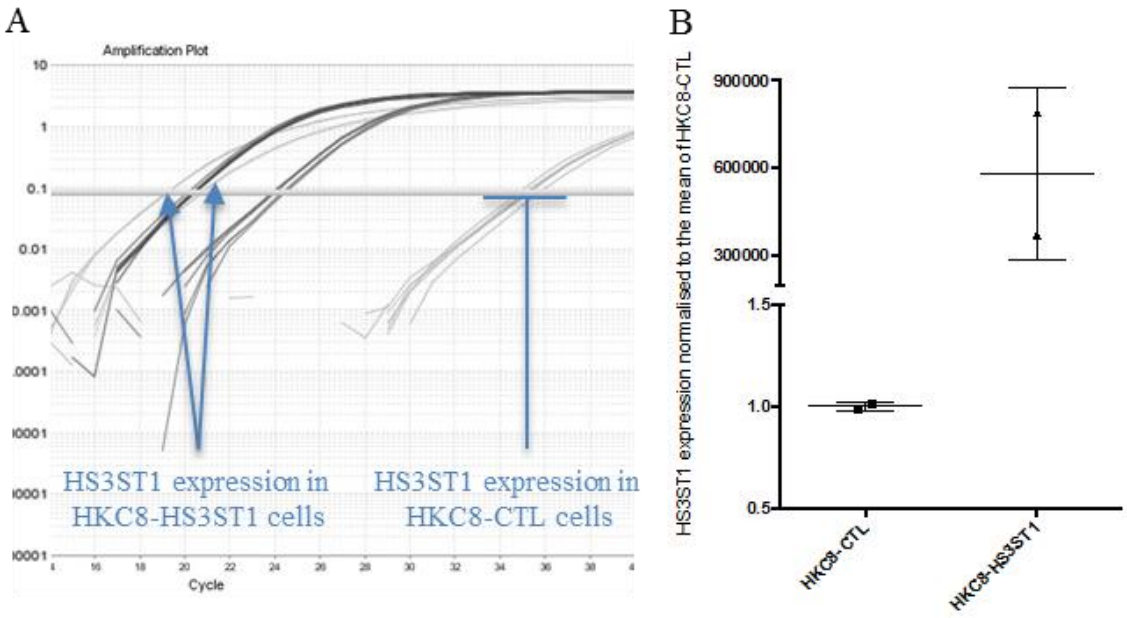

Figure 4-26: HS3ST1 expression in HKC8-CTL and HKC8-HS3ST1
Wild type HKC8 cells were transfected in 10cm petri dish with 2µg of empty plasmid and effectene. Three days after transfection, cells were split 1:5 and grown in media supplemented with 200µg/mL G418. Cells mRNAs were extracted using Qiagen RNAeasy kit. Data were analysed by qPCR with HPRT1 as housekeeping gene. Two mock clones were selected for further studies.

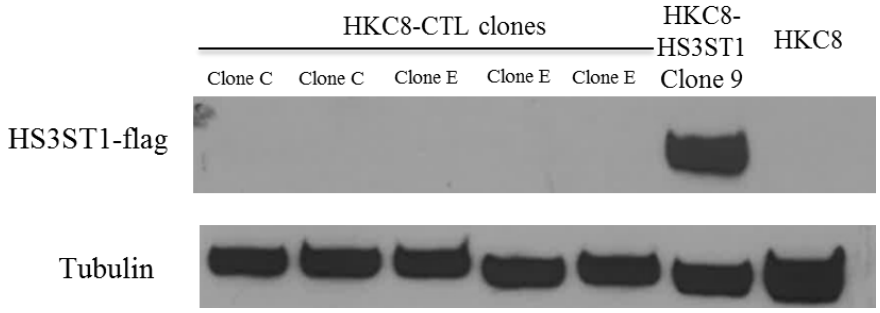

Figure 4-27: HKC8-CTL clones protein levels
Two clones HKC8-CTL (clone C and clone E) were selected and their protein levels analysed by Western Blot. A quantity of 10µg of protein lysates were run into a 10% acrylamide gel for 20 minutes at 180V and transferred onto a nitrocellulose cell membrane. The membrane was blocked 1h in 5% milk 0.1% TBST and incubated overnight at 4°C with flag tag antibody. The next day the membrane was washed with 0.1%TBST and incubated with secondary anti-rabbit antibody before detection. After a mild stripping and a blocking step, the membrane was probed for tubulin as a loading control.

To confirm that HS3ST1 was directed to the Golgi apparatus after synthesis, HKC8-HS3ST1 and HKC8-CTL were stained with a flag Tag antibody and GM130, a cis-Golgi marker (Figure 4-28).

HS3ST1-flag staining could be found colocalised with cis Golgi marker and around the nucleus. No detectable level of Flag tag protein was detected in the HKC8-CTL.

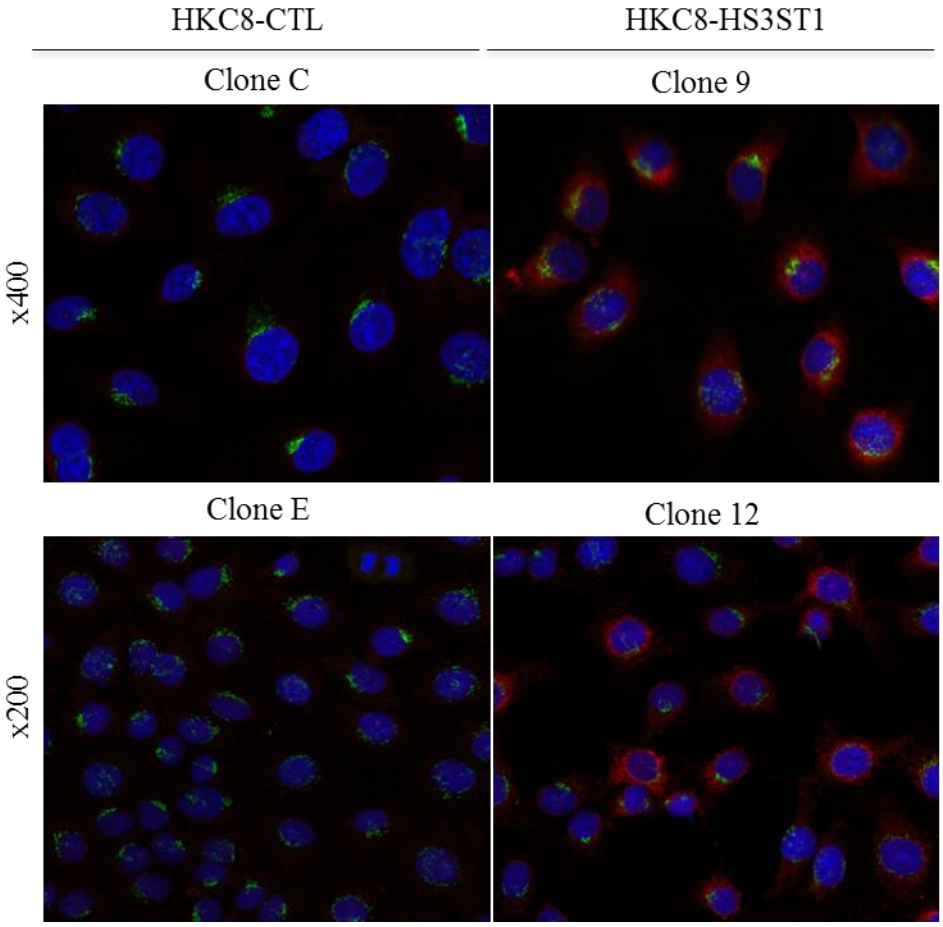

Figure 4-28: immunofluorescence characterisation of HKC8-CTL and HKC8-HS3ST1
HKC8-CTL (clone C and E) and HKC8-HS3ST1 (clone 9 and 12) cells were seeded in 8-well chamber slides and fixed 5-10 minutes in ice cold methanol at -20°C. Cells were incubated 1 hour at room temperature in 5% BSA to avoid unspecific binding and incubated with the primary antibodies overnight at 4°C. The next day slides were washed with PBS and incubated 2h at room temperature with the corresponding secondary antibody. Slides were mounted in Vectashield with DAPI. N≥2

One popular hypothesis regarding HS is that the expression of one modifying enzymes can alter the expression of another (Esko and Selleck, 2002). Therefore HKC8-HS3ST1 and HKC8-CTL were screened for the other HS modifying enzyme expression (Figure 4-29). Firstly, there was no significant change in the other HS3ST expression even though HS3ST6 was downregulated in both clones but not significantly. HS3ST5 was not detectable. Secondly, HS6ST1 and SULF2 were

significantly decreased in HKC8-HS3ST1 compared to HKC8-CTL ($p<0.05$). It might be that the HKC8-HS3ST1 not only have a change in the 3-O-sulfation but also other sulfation patterns.

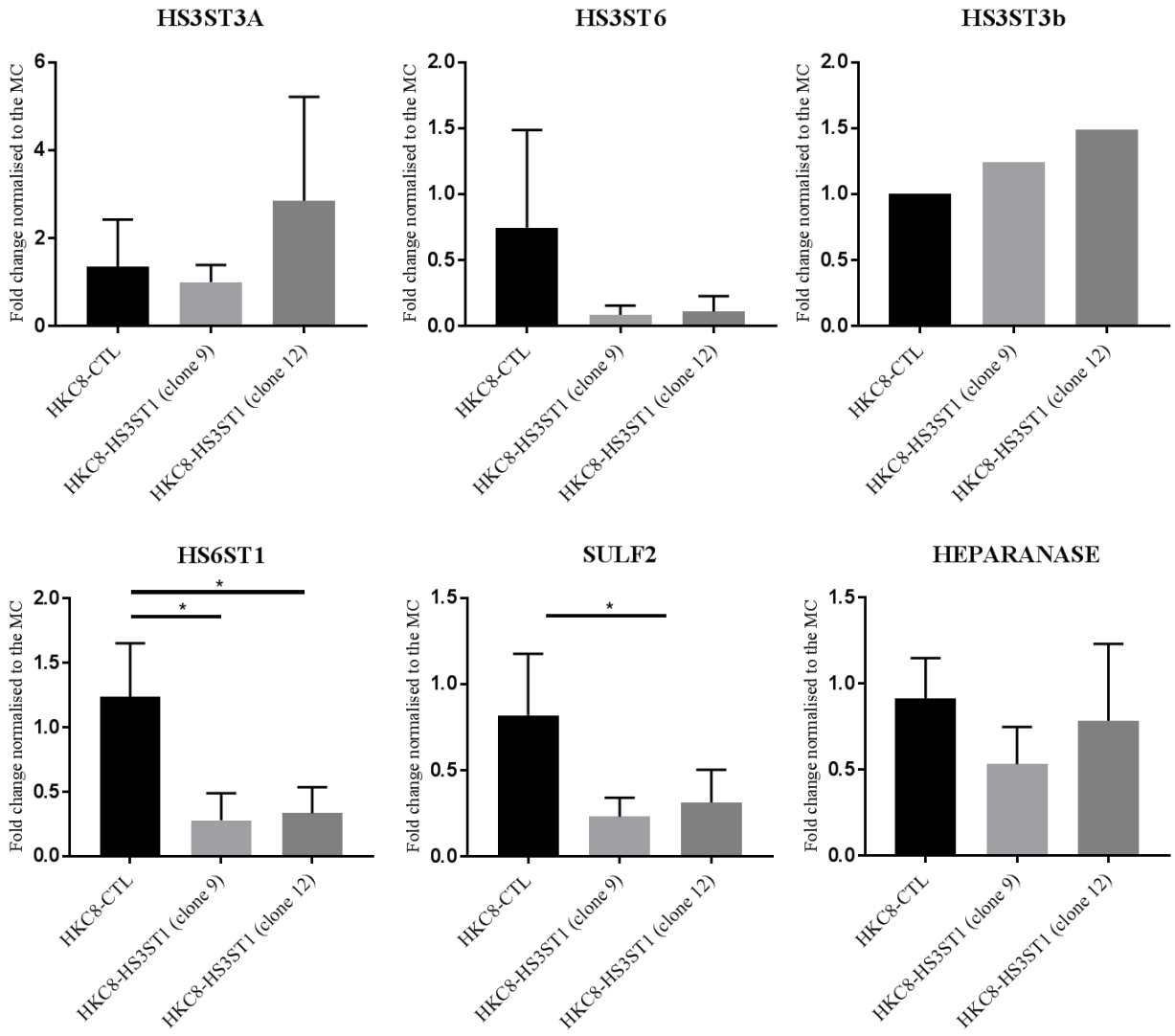

Figure 4-29: HS modifying enzymes expression in HKC8-CTL and HKC8-HS3ST1 cells
RNAs from HKC8-CTL and HKC8-HS3ST1 cells was extracted at different passage and analysed by qPCR with HPRT1 as housekeeping gene. Data were compared to the average of the mean of HKC8-CTL (MC). N=3 except HS3ST3B where N=1. One-way ANOVA, Bonferroni's multiple comparison, $p<0.05$(*).

The presence of HS3ST1 within cells does not provide information regarding enzyme activity. Additionally, the significant changes in expression of other enzymes could alter HS sulfation patterns on the surface of the transfected cells. Therefore, HS sulfation patterns on the cells was analysed to identify if HS3ST1 was active within the cells and if any other sulfation was affected by it.

4.3.6 Cell surface and ECM HS sequencing and imaging

HKC8-CTL and HKC8-HS3ST1 disaccharide analysis showed five different types of sulfated disaccharides (Figure 4-30). GlcA-GlcNS3S6S represents a disaccharide with N, 3-O and 6-O sulfation. Interestingly HKC8-CTL had no detectable 3-O-sulfation even though they expressed other HS3ST isoforms. When analysing the total sulfated HS disaccharides, clone 9 had 1.6% of 3-O-sulfation and clone 12 had 3.7%. These results show that the enzyme was active in the cells. However, it was surprising to observe half the amount of 3-O-sulfation in clone 9 compared to clone 12. The 3-O-sulfation being the last and rarely generated pattern on HS, it requires a specific HS chains structure. Clone 9 might have less 3-O-sulfation due to a lack of targeted sequence on HS. This clone also has a higher percentage of the 2-O sulfated disaccharide IdoA2S-aManR (61% for clone 9 against 36.5% for clone 12 of total sulfated disaccharide), a sulfation pattern known to prevent the activity of HS3ST1.

Moreover, both clones showed less GlcA-GlcNS6S compared to HKC8-CTL. It was 6.5 times lower in clone 9 and 2.1 times lower in clone 12. Additionally, clone 9 displayed less trisulfated disaccharides while clone 12 showed more compared to HKC8-CTL. In contrast, clone 9 had more IdoA2S-GlcNS than clone 12 and HKC8-CTL. It could be possible that the activity of 6-O-sulfatase on the trisulfated disaccharides on clone 9 led to a decrease in IdoA2S-GlcNS6S and an increase in IdoA2S-GlcNS on the cells.

The changes in HS cell surface composition in HKC8-HS3ST1 could potentially lead to a change in growth factors binding, signalling and activity. Therefore, both cell types were screened for cell binding to FGF2 (flow cytometry), cell proliferation (WST-1 test), cell migration (wound healing) and cell signalling (Western blot) following treatment with 10ng/mL FGF2.

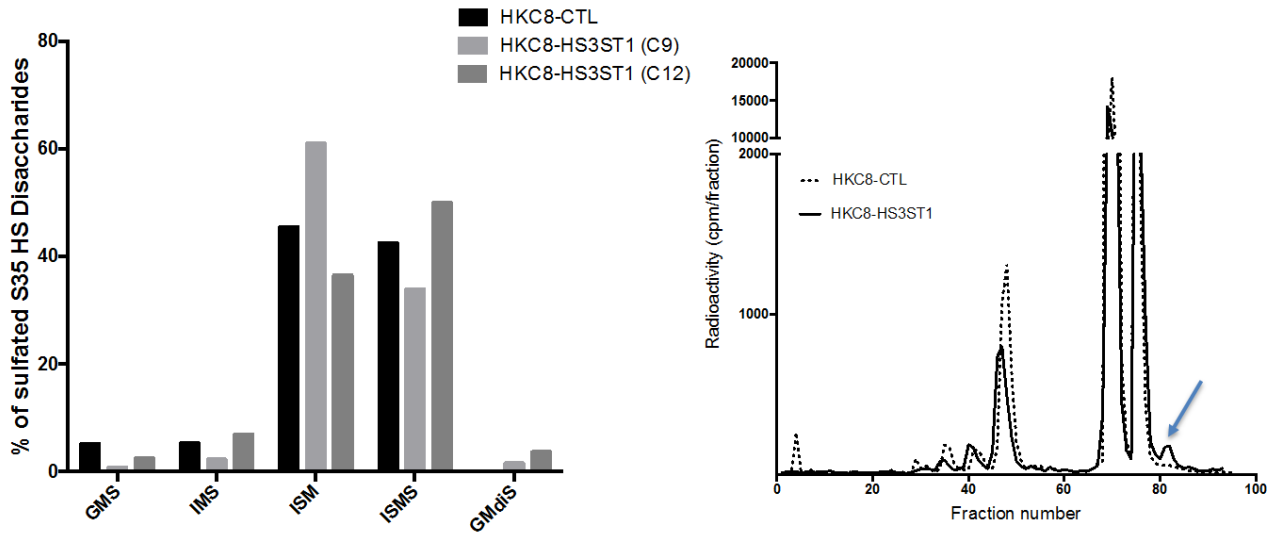

Figure 4-30: HKC8-CTL and HKC8-HS3ST1 HS disaccharides composition
HKC8-CTL and HKC8-HS3ST1 cells were labelled with ^{35}S. Cells were lysed, and GAGs were isolated from protein by alkali treatment. GAGs were isolated by DEAE column and desalted by PD10 column before being eluted with a G15 column. In collaboration with Prof Marion Kusche-Gullberg, Bergen University. GlcA-GlcNS6S (GMS), IdoA-GlcNS6S (IMS), IdoA2S-GlcNS (ISM), IdoA2S-GlcNS6S (ISMS), GlcA-GlcNS3S6S (GMdiS, pointed by blue arrow).

4.3.7 FGF2 and HS 3-O-sulfation

4.3.7.1 FGF2 binding

FGF2 binding to the clones was analysed by flow cytometry (Figure 4-31). The slight shift observed in HKC8-CTL fluorescence with FGF2 was not seen in HKC8-HS3ST1 cells (Figure 4-31 A, B, C). The FGF2 kit to study cells binding comes with a negative control, a soya protein that should not bind to the cells. However, the negative control bound more to HKC8-HS3ST1 than HKC8-CTL (Figure 4-31, D, E). The reason for this was not known. Therefore, only the MFI values of single cells was analysed and as seen in Figure 4-31, there was no significant change in FGF2 binding between clones. Nevertheless, these data were not conclusive considering the slight shift in fluorescence observed even with the CTL cells. The kit might have had some dysfunction in our experiment. Therefore, to further investigate the potential action of HS 3-O-sulfation in FGF2 binding with its receptor, we decided to compare FGF2 signalling in HKC8-CTL and HKC8-HS3ST1.

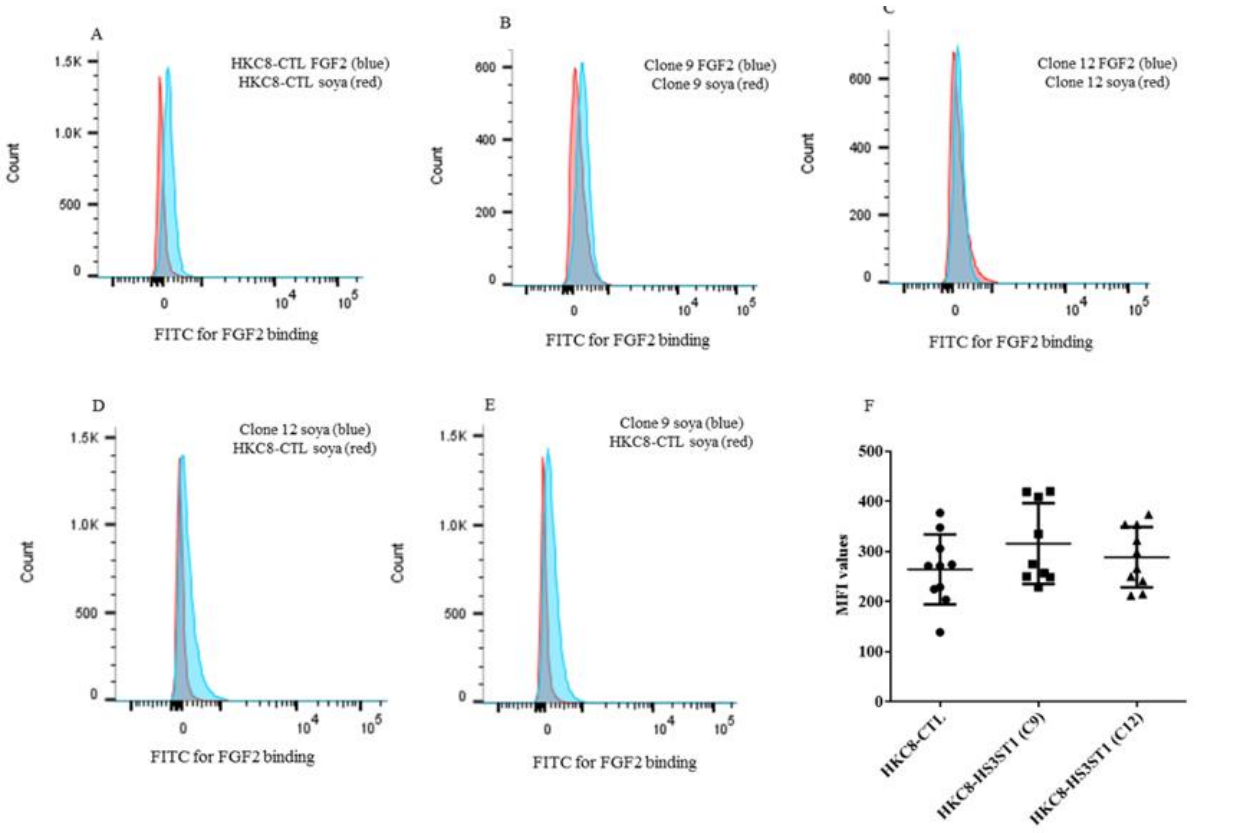

Figure 4-31: FGF2 binding to transfected cells
HKC8-CTL (clone E) and HKC8-HS3ST1 (clone 9 and 12), $4x10^6$cells/mL were incubated with biotinylated FGF2 or biotinylated soya protein control for 1h at 4°C and Avidin-FITC for 30 minutes at 4°C. Cells fluorescence was analysed using Facs CantoII flow cytometer. Data were analysed by FlowJo. A-C clones binding to soya protein (red) or FGF2 (blue). D-E: Clone E binding to soya protein (red) compared to clone 12 (D) and clone 9 (E). F: Mean Fluorescence Intensity (MFI) of HKC8-CTL and HKC8-HS3ST1 binding to FGF2, each dot square and triangle represent one independent experiment.

4.3.7.2 FGF2 signalling

To determine if FGF2 signalling was modified with HS3ST1 overexpression, the phosphorylation of ERK pathway was assessed in the transfected cells. HKC8-CTL displayed a strong signalling 10 minutes after FGF2 treatment (10ng/mL). HKC8-HS3ST1 showed a similar signalling in both clones with an increase in ERK phosphorylation 10 minutes after stimulation （Figure 4-32）. In conclusion, the phosphorylation of ERK following FGF2 treatment was not affected by HS3ST1 overexpression.

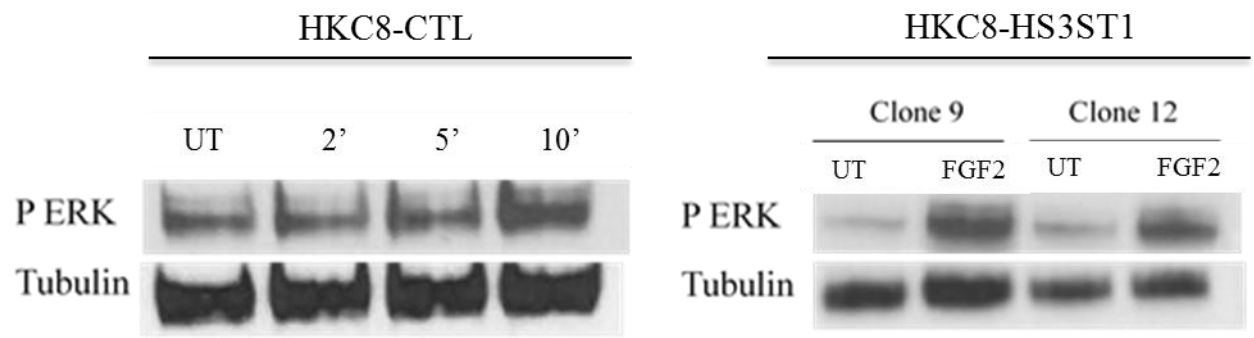

Figure 4-32: FGF2 signalling in HKC8-CTL and HKC8-HS3ST1
Representative images of FGF2 signalling studied by western blot. HKC8-CTL were incubated in 0.5%FBS media for 24 hours and were then treated 2, 5 or 10 minutes at 37°C with 10ng/mL of FGF2 or buffer (untreated UT) (left panel). HKC8-HS3ST1 were incubated in 0.5% FBS media for 24 hours and were then treated 10 minutes at 37°C with 10ng/mL of FGF2 or buffer (untreated UT) (right panel). A quantity of 10-20µg of protein lysates were run into a 10% acrylamide gel and transferred onto a nitrocellulose cell membrane. The membrane was blocked 1h in 5% BSA 0.1% TBST and incubated overnight at 4°C with P-ERK antibody. The next day the membrane was washed with 0.1%TBST and incubated with secondary anti-rabbit antibody before revelation. After a mild stripping and a blocking step, the membrane was probed for tubulin as a loading control. N=3

These data suggest that HS 3-O-sulfation is not implicated in FGF2 binding and signalling. However, it does not give any indication about other pathways activated by FGF2 and the changes in different biological activities and this could vary between HKC8-HS3ST1 and HKC8-CTL.

4.3.7.3 FGF2, cell proliferation and migration

One of the main action of FGF2 is to stimulate cell growth. HKC8-CTL and HKC8-HS3ST1 proliferation and migration with and without treatment were analysed (Figure 4-33). There was no significant change in cell proliferation in 0.5% FBS media and with FGF2 treatment (10ng/mL). Additionally, cell front velocity with and without FGF2 treatment were assessed by wound healing assay (Figure 4-33). Once again FGF2 treatment did not have a significant effect. However, an increase in cell velocity in HKC8-CTL and HKC8-HS3ST1 (both clone 9 and 12) was observed with FGF2 stimulation.

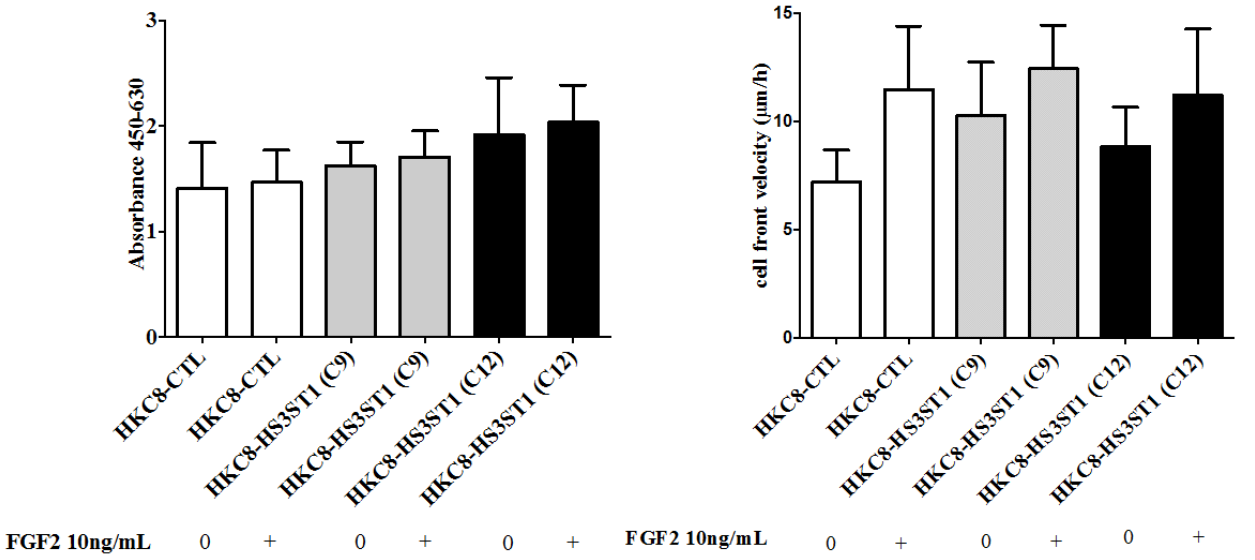

Figure 4-33: HKC8-CTL and HKC8-HS3ST1 cells proliferation and migration after 48h treatment with FGF2

A: HKC8-CTL and HKC8-HS3ST1 cells were seeded in 96-well plate and treated with 10ng/mL FGF2 for 48h. Cells viability was measured with WST-1 test, a tracker of metabolically active cells. Absorbance at 450 and 630 were measured. B: Cells were seeded in Ibidi inserts at $3x10^5$cells/mL. The next day, the inserts were removed, generating a wound within each well of 12-well plates. Cells were incubated with 0.5% FBS media ± 10ng/mL FGF2 and wound closure was imaged every hour by Nikon Biostation. See methods section for cell velocity calculation. N=3 for A and N=4 for B.

Noteworthy HKC8-HS3ST1 clone 12 displayed a significantly higher cell front velocity ($p<0.01$) in complete media（Figure 4-34）. As the increase in cell proliferation was only observed in one clone, more clones were screened for cell migration. Surprisingly the increase in cell migration was only seen in clone 12. When generating these cells, the clone selection might have selected a clone that has a higher capacity for migration. Secondly it is important to report that HS3ST1 is expressed differently in every clone and as mentioned above some clones have less 3-O-sulfation than others (clones 9 has 50% less than clone 12). However, it is possible that the difference observed in cell migration is due to more sulfated HS.

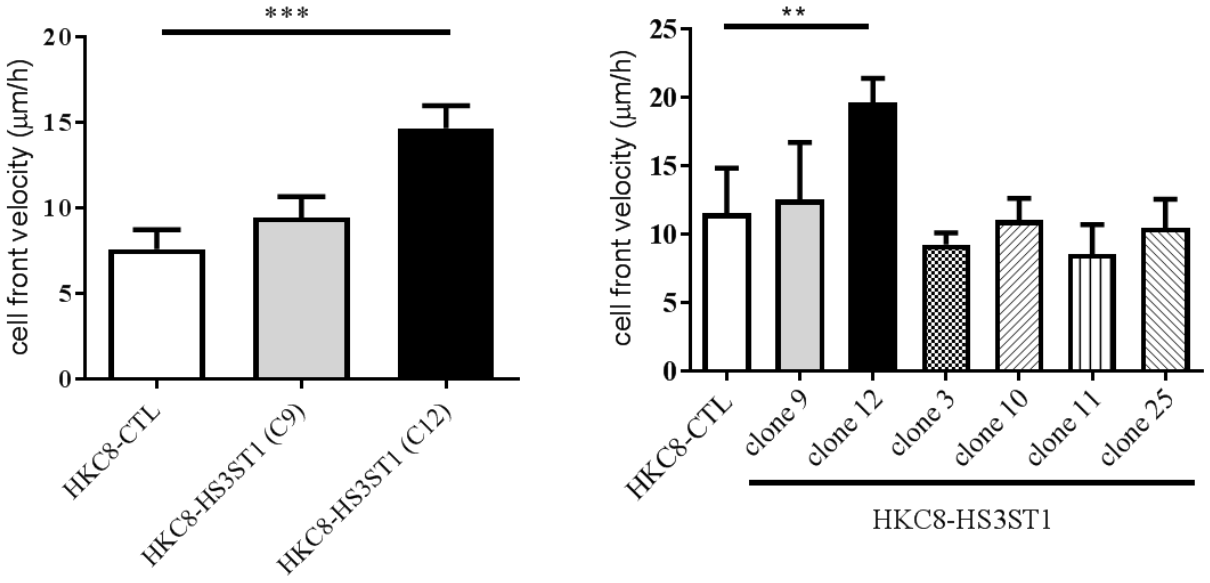

Figure 4-34: Cell velocity in complete media
Cells were seeded in Ibidi inserts at $3x10^5$cells/mL. The next day, the inserts were removed, generating a wound within each well of 12-well plate. Cells were incubated with 5%FBS media and wound closure was imaged every hour by Nikon Biostation. See methods section for cell velocity calculation. N=3. Statistical significance was calculated using a one-way ANOVA with Bonferroni's multiple comparison test $p<0.01$(**), $p<0.001$ (***).

All these data did not show any difference in FGF2 binding and its biological activity between HKC8-CTL and HKC8-HS3ST1. However, the increase in cell velocity with FBS in clone 12 could indicate the presence of other growth factors in the serum that is affected by HS 3-O-sulfation. In the previous chapter, HB-EGF was found decreased together with HS 3-O-sulfation *in vivo*. Therefore, HB-EGF signalling was analysed.

4.3.8 HB-EGF and HS 3-O-sulfation

HB-EGF is involved in cell proliferation and repair. It is also present in the blood circulation and was recently suggested as a potential biomarker of disease such as primary ovarian cancer (Miyata *et al.*, 2017).

HB-EGF signalling can be transient. Therefore, as preliminary data, WT HKC8 cells were serum starved for 16h and treated at different time points (5, 15, 30 minutes and 1 hour) with 1µm HB-EGF to identify at what time STAT3 phosphorylation was detectable. As seen Figure 4-35, STAT3 was phosphorylated at 5 minutes and decreased until coming back to baseline at 1h. To

identify if HB-EGF binding was affected by the overexpression of HS3ST1, HKC8 clones were serum starved for 16 hours and stimulated with 1µm HB-EGF for 5 minutes and 1 hour. STAT3 phosphorylation was studied by Western Blot Figure 4-36.

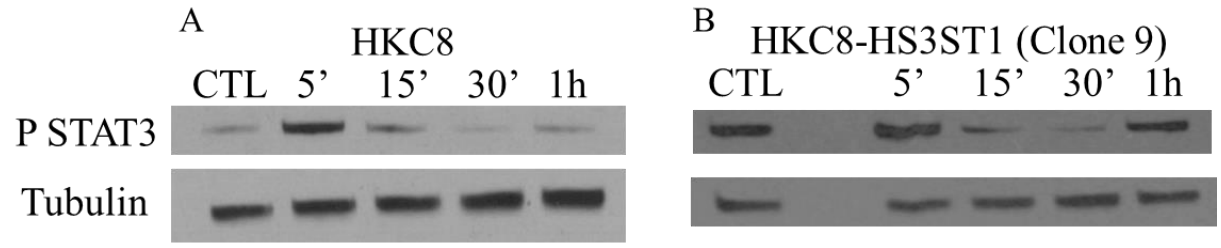

Figure 4-35: Phospho-STAT3 induction by HB-EGF in WT HKC8 and HKC8-HS3ST1
Serum starved Wild Type HKC8 (A) and HKC8-HS3ST1 (B) were treated for 5, 15, 30 minutes and 1 hour at 37°C with 1µM of HB-EGF or buffer (CTL). Protein lysates were run into a 10% acrylamide gel and transferred onto a nitrocellulose cell membrane. The membrane was blocked for 1h in 5% BSA 0.1% TBST and incubated overnight at 4°C with P-STAT3 antibody. The next day the membrane was washed with 0.1% TBST and incubated with secondary anti-rabbit antibody before visualisation. After a wash in 0.1% TBST, the membrane was probed for tubulin as a loading control.

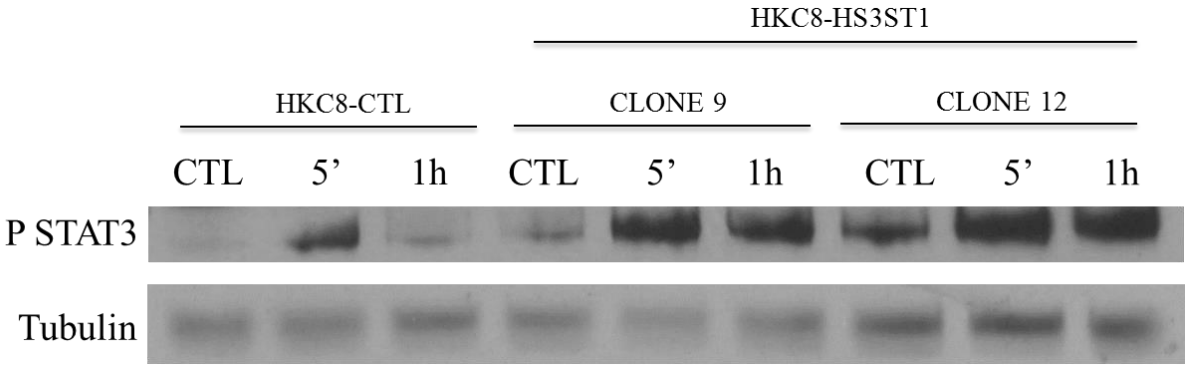

Figure 4-36: HB-EGF signalling in HKC8-CTL and HKC8-HS3ST1
Representative images of HB-EGF signalling studied by western blot. Serum starved cells were treated for 5 minutes and 1hour at 37°C with 1µM of HB-EGF or buffer (CTL). A quantity of 10-20µg of protein lysates were run into a 10% acrylamide gel and transferred onto a nitrocellulose cell membrane. The membrane was blocked for 1h in 5% BSA 0.1% TBST and incubated overnight at 4°C with P-STAT3 antibody. The next day the membrane was washed with 0.1% TBST and incubated with secondary anti-rabbit antibody before development. After a wash in 0.1% TBST, the membrane was probed for tubulin as a loading control.

The signalling pattern of HB-EGF in HKC8-CTL showed a strong signalling at 5 minutes that returned to baseline at 1 hour. However, HKC8-HS3ST1 showed a strong signalling at 5 minutes that comes back after 1 hour treatment as seen Figure 4-35. The activation of STAT3 at 1h was observed in both clones of HKC8-HS3ST1 (Figure 4-36).

4.4 Discussion

Three different cell lines were used for the first part of this work. Two human renal epithelial cells HK2, HKC8 and one rat renal fibroblasts NRK-49F. As expected HK2 and HKC8 cells were positive for E-cadherin, an epithelial marker while NRK-49F cells were negative. The heterogeneous staining observed in HK2 and HKC8 cells can be explained by the low confluency of the cells at the time of staining. Furthermore, proximal tubule cells do not express high level of E-cadherin compared to other renal cells such as distal tubule cells (Baer *et al.*, 2006) or collecting duct (Nouwen *et al.*, 1993; Prozialeck *et al.*, 2004). Cytokeratin 18 could have been a better marker for these cells but was not available at the time of experiment.

The second marker studied was fibronectin which is commonly known to be a marker of mesenchymal cells, but human tubular cells secrete fibronectin into their ECM (Burton *et al.*, 1996) and is a positive marker of HK2 cells according to the ATCC. Therefore, the low level of staining of E-cadherin and strong staining of fibronectin in HK2 and HKC8 were good indications of the cells origin.

The absence of E-cadherin staining and the positive staining of fibronectin were good indicators of the fibroblast characteristics of the NRK-49F cells. Surprisingly the α-SMA was weaker than expected, potentially because it is a marker of activated fibroblasts and the medium where the cells were grown did not stress or activate them enough to trigger expression of α-SMA.

After characterising the cells, this work aimed to discover what growth factors regulate HS3STs expression. First TGFβ1 was used as it is a well-known pro-fibrotic factor (Leask and Abraham, 2004). The data suggests that TGFβ1 is an important modulating factor of HS3ST3B and HS3ST1 expression in renal epithelial and fibroblast cells. It upregulates HS3ST3B and downregulates HS3ST1. This correlates with previous studies showing a change in HS modifying enzymes following TGFβ1 treatment. *In vitro*, 24h treatment with TGFβ1 (0.05-5ng/mL) induced significant increase of SULF1 expression and a significant decrease in SULF2 at 1 and 5ng/mL in primary normal human lung fibroblasts (Yue *et al.*, 2008). *In vivo* mice treated with adenovirus encoding active TGFβ1 via oropharyngeal aspiration showed an increase in pulmonary expression of SULF1 and SULF2. Furthermore, TGFβ1 treated astrocytes (10ng/mL) showed an increase in HS2ST1 (Properzi *et al.*, 2008).

HS3ST3A and HS3ST6 expression did not vary with the treatment. However, the heterogeneity between samples might have hidden a possible effect of the treatment. Additional repeats could clarify this.

Second, the combination of TGFβ2 and IL1β which has a role in fibrosis by promoting endothelial to mesenchymal transition (Maleszewska *et al.*, 2013) was analysed in renal epithelial and fibroblast cells. The results were similar to what was found with TGFβ1 alone. There was a progressive decreased in HS3ST1 expression and an increase in HS3ST3B with no change in HS3ST3A and HS3ST6.

Together these data show that TGFβ1, 2 and IL1β differentially regulate HS3STs in potentially an attempt to modify HS sulfation on the cell surface and ECM. Further disaccharides analysis of treated cells would enable us to assess if the change in RNAs expression is mirrored by a change in sulfation. However, due to time restriction and the lack of HS 3-O-sulfation standard, this could not be performed.

The most dramatic change in HS3ST1 expression was seen in the NRK-49F which also showed a severe change in morphology. TGFβ1 and TGFβ2 were both shown to be pro fibrotic in the NRK-49F cells (Yu *et al.*, 2003) highlighting a possible role of HS3ST1 downregulation during fibroblast activation.

These *in vitro* data identified growth factors that downregulate HS3ST1 expression. It is potentially these growth factors that triggered the decrease in HS 3-O-sulfation observed in the tubules of fibrotic kidneys in chapter 3. However, no treatment was found to upregulate HS3ST1 *in vitro* and therefore failed to explain the increase observed in total renal tissue seen *in vivo*. Fibrosis is triggered by more than two growth factors and it is highly possible that still unidentified growth factors or cytokines increase HS3ST1 expression in renal epithelial cells and fibroblasts. We could have potentially used IL-4 , IL-13 and FGF10 as they increased HS3ST1 in different cell lines (Takeda *et al.*, 2010; Patel *et al.*, 2014). Furthermore, the use of only two different cell types does not reflect exactly what is happening *in vivo.* Pro inflammatory factors can modulate HS3STs expression in endothelial cells and increase HS3ST1 expression in immune cells (Krenn *et al.*, 2008; Sikora *et al.*, 2016). Macrophages can be found during the development of fibrosis and could be the origin of the increased expression.

The second part of this chapter was to analyse which growth factors would be affected by HS 3-O-sulfation. Due to the very low expression of HS3ST1 in HKC8 cells, they were an excellent model to study the impact of HS3ST1 expression on growth factors binding, signalling and activity.

To study HS3ST1 expression, both mock and HS3ST1 stable transfectants were successfully generated. No other HS3STs isoforms were altered in the stable cell lines. Surprisingly it did lead to a decrease in HS6ST1 expression in both clones of HKC8-HS3ST1 and a decrease in SULF2 expression in clone 9 suggesting a potential decrease in HS 6-O-sulfation. Remarkably, the decrease in HS6ST1 was mirrored by a decrease in GlcA-GlcNS6S (GMS) in HKC8-HS3ST1 compared to HKC8-CTL (6.5 times lower in clone 9 and 2.1 times lower in clone 12). The reason behind the differences between both clones could be the level of HS3ST1 expressed in the cells. Clone 9 has more HS3ST1 than clone 12 at both RNA and protein levels and even though SULF2 only decreased significantly in clone 9, its expression decreases in clone 12 too but with p=0.08. Thus, HS3ST1 might decrease HS6ST1 expression and activity but more effectively in clone 9 than clone 12. When looking at 3-O-sulfated disaccharides, the overexpression of HS3ST1 led to an increase in HS 3-O-sulfation between 1.6% (clone 9) and 3.7% (clone 12). This level of sulfation is similar to what was found in Chinese Hamster Ovarian cells transfected with HS3ST1 which displayed about 4% of HS with an AT binding site (Datta *et al.*, 2013). Endothelial cells have 1% of HS-3-O sulfation (Marcum *et al.*, 1986). Thus our *in vitro* data was in agreement with what was observed *in vivo* and in other *in vitro* studies of HS3ST1 activity. The lower amount of 3-O-sulfation in clone 9 could be surprising considering that it was the clone with the most HS3ST1 expression. However, as mentioned previously, this clone might have less substrate than clone 12.

To summarise, the overexpression of HS3ST1 in HKC8 cells generates effectively more 3-O-sulfation. Interestingly, it also changes other HS modifying enzymes expression. The cell might have a very well controlled system within the Golgi apparatus to balance the overexpression of one enzyme and prevent any damaging alteration of HS sulfation on the cell surface.

In the last part of this chapter, the implication of FGF2 and HB-EGF with HS 3-O-sulfation were studied. FGF2 has been widely studied and its binding with HS 2-O, 6-O sulfation and HS-FGFR complex are well described (Pye *et al.*, 1998). Because there have been conflicting results regarding the role of HS 3-O-sulfation and its implication in FGF2 binding we analysed its binding, signalling and biological activity on the transfected cells. There was no noticeable change between HKC8-

HS3ST1 and HKC8-CTL. These results are in line with what Thacker *et al.* showed with CHO cells overexpressing HS3ST1 having no difference in FGF2 binding (Thacker *et al.*, 2016a). We can conclude that HS 3-O-sulfation does not play a significant role in FGF2 activity in renal epithelial cells. The increase of HS3ST1 expression seen *in vivo* might then not be related to increasing FGF2 activity.

HB-EGF is a less studied growth factor and its structural binding to HS not very well documented. The increase in STAT3 phosphorylation at 5 minutes and 1h in HKC8-HS3ST1 cells showed a biphasic response of the cells to the treatment. This second signalling was not observed in HKC8-CTL nor WT HKC8. The first explanation could be a retention of HB-EGF on the ECM of the cells which signals again when the EGF receptors are recycled at the cell surface. The second explanation could be a second messenger. In fact the biphasic signal observed in the HKC8-HS3ST1 has been previously seen in vascular smooth muscle cells treated with HB-EGF (Lee *et al.*, 2007). In this study, they identified the second signalling as interleukin 6 (IL-6) dependent. Treated cells showed an increase in IL-6 expression at 30 and 45 minutes after HB-EGF treatment (10ng/mL) and an increase in IL-6 secretion in the media at 60 minutes compared to untreated cells. The phosphorylation of STAT3 at 1h was decreased when using IL-6 neutralising antibody. Additional studies showed that the biphasic phosphorylation of STAT3 was caused by IL-6 related cytokines in cardiomycoytes after angiotensin II treatment (Sano *et al.*, 2000) and in mouse cardiac fibroblast after isoproterenol treatment (Yin *et al.*, 2003). IL-6 can bind heparin and heparan sulfate which confers protection to degradation by endoproteinase Lys-C. Furthermore, this binding did not seem to require 2-O-sulfation, a sulfation that prevent HS3ST1 action (Mummery and Rider, 2004). An ELISA assay using conditioned media from the treated/untreated HKC8-CTL and HKC8-HS3ST1 cells could answer whether or not IL6 is secreted in response to HB-EGF in our model.

In conclusion, this chapter showed that the TGFβ growth factors together with IL1β are regulators of HS3STs enzymes. HS3ST1 overexpression is capable of generating HS 3-O-sulfation in renal epithelial cells but induced a decrease in HS6ST1 and SULF2 expression. This highlights a possible intra cellular regulation of HS modifying enzymes by the cell itself. Finally, HB-EGF signalling was identified as being potentially enhanced by HS 3-O-sulfation.

5 Synthesis of potential inhibitors of FGF2 binding to heparan sulfate

5.1 Introduction

The current knowledge on HS interaction with growth factors, cytokines and their receptors make it an excellent target for drug development. X-ray crystallography, isothermal titration calorimetry (ITC) and sequencing, to just name a few techniques have allowed us to identify the specific motifs/ functional groups within a molecule that binds to HS. In fact, crystallography can identify the atomic details of protein-ligand interaction, ITC gives more precision about the type of binding (exothermic, endothermic), the strength of the binding (Kd) and sequencing gives the amino acid sequence of the protein. Therefore, recent technology has enabled the synthesis of recombinant and mutated protein to increase binding to HS, to receptors or to decrease affinity. All approaches are excellent tools to understand the role of HS in scavenging, binding, protecting or enhancing protein activity.

For example, chemokines and HS interaction can be targeted by preparing mutant chemokine lacking HS binding which can compete for receptor binding and inhibit chemotactic gradient formation and cell migration (Cripps *et al.*, 2005; Anders *et al.*, 2006; O'Boyle *et al.*, 2009). A mutant form of the chemokine CXCL12, where three basic residues at sequence positions 24, 25, and 27, were replaced by serine, showed inhibition of peripheral blood mononuclear cells transendothelial migration *in vitro* and decreased leukocyte recruitment *in vivo* (O'Boyle *et al.*, 2009). Similar results were found with a mutant CCL7 where two lysine (position 44, 46) and one arginine (position 49) were changed to alanine residues. The mutant inhibited leukocyte infiltration in a mouse isograft skin transplant model (Ali *et al.*, 2010). Occasionally, targeting HS binding sequence does not significantly inhibit cell migration *in vitro* but does *in vivo* as seen in CXCL11 mutants (Severin *et al.*, 2010). This highlights the complexity of HS and protein interactions.

Generating HS based antagonist chemokine can also be beneficial. Basic amino acid residues (termed "B" e.g. lysine and arginine) are important due to their positive charges interaction with HS negative charges. For example, the motif BBXB has been found important for binding CCL5 to HS (Proudfoot *et al.*, 2001), hence mutant chemokines with more basic residues increase binding (Brandner *et al.*, 2009). A CXCL8 mutant with a higher affinity for HS and a lower affinity for the

G protein-coupled receptor (GPCR) showed no neutrophil chemotactic activity *in vitro*. This dominant negative mutant had additional lysine residues and lacked the ELR motif (glutamic acid-leucine-arginine), important for GPCR binding. *In vivo*, after ischemia reperfusion injury in rat kidneys, the administration of mutant CXCL8 diminished tubulointerstitial damage and granulocyte infiltration (Bedke *et al.*, 2010). Furthermore, in a model of acute rejection, the daily injection of the mutant CXCL8 decreased inflammation, tubulitis, the number of ED1 positive cells (equivalent to the CD68 human monocyte marker) and CD8 (T-cells) cells in glomerular cross sections (Bedke *et al.*, 2010). This mutant CXCL8 was found beneficial in other diseases such as cystic fibrosis (McElvaney *et al.*, 2015) and in murine models of pulmonary fibrosis and urinary tract infection (Gschwandtner *et al.*, 2017).

Further work showed that small compounds based on the HS binding sequence can modify inflammatory responses. Peptides from the C-term sequence of CXCL9 (74-103) with high affinity to HS decreased CXCL8-induced neutrophil extravasation (Vanheule *et al.*, 2015). IFNγ C-terminal sequence, hypothesised to be HS binding sequence, was used to generate a synthetic octapeptide (MC-2, LRKRLRSR). When used in a rat allograft skin transplant model, the peptide demonstrated delayed graft rejection (Fernandez-Botran *et al.*, 1999, 2002) The same peptide was found to decrease liver injury in mice following hemorrhagic shock (Matheson *et al.*, 2016).

Synthetic peptides based on FGF2 sequence have previously been used to inhibit FGF2 mediated vascular endothelial cell proliferation (Yayon *et al.*, 1993). Inhibiting FGF2-HS interaction might reduce fibroblast proliferation and ECM deposit and therefore limit fibrosis. Li *et al.* studied the interaction between FGF-2 and multiple disaccharides that HS can be theoretically composed of (Li *et al.*, 2014). They found two main sites essential for the binding, the Asn27 and an electropositive pocket formed by residues 119-135. Depending on the sulfation pattern, the affinity of the disaccharide for FGF-2 changes. A disaccharide, GlcNS3S, IdoA2S with N-, 3-O and 2-O-sulfation had the highest affinity (Kd= 1.73±0.31μM). This finding shows that the 3-O-sulfation might be implicated in the binding process. However, we previously showed that HS 3-O-sulfation did not alter FGF2 signalling. One possible explanation could be that FGF2 can bind to HS 3-O-sulfation but does not require it for its biological activity. In this chapter, FGF2 was studied for the competition work assay as its structure and binding sequence are well characterised and documented.

The aims of this chapter are:

-To identify a peptide that could compete with FGF2 binding to HS. The electropositive pocket described previously was used to inform the first peptide sequence synthesised "KRTGQYKLGSKTGPGQKAI".

-To show the importance of positively charged amino acids on HS binding by synthesising a modified peptide KRTGQYALGSKTGPGQKAI.

5.2 Specific material and methods

Peptides synthesis and characterisation were carried out in collaboration with Durham University under the supervision of Dr Steven Cobb and Dr Ehmke Pohl.

5.2.1 Solid Phase Peptide Synthesis

The use of Solid Phase Peptide Synthesis (SPPS) was preferable to liquid phase as it uses a larger excess of reagents at high concentration, which allows completion of coupling reactions. Furthermore, filtration and washings can be performed in the same vessel. This also provides a faster method for peptide synthesis (Amblard *et al.*, 2006).

In principle, with the strategy used, the first N-protected-side chain protected-C terminal amino acid is bound via its carboxyl group to a resin (in my case an amino resin: amine-linked peptide). The peptide sequence is linked from C to N terminus. Consequently, for the FGF2 peptide KRTGQYKLGSKTGPGQKAI, the synthesis starts with isoleucine and alanine. It starts with a N-term deprotection followed by a coupling reaction that is repeated n times. During the synthesis, side chains of the amino acid are always protected with a protecting group to prevent mislinking. The amino group is temporarily protected and is unprotected before coupling. The procedure is illustrated Figure 5-1.

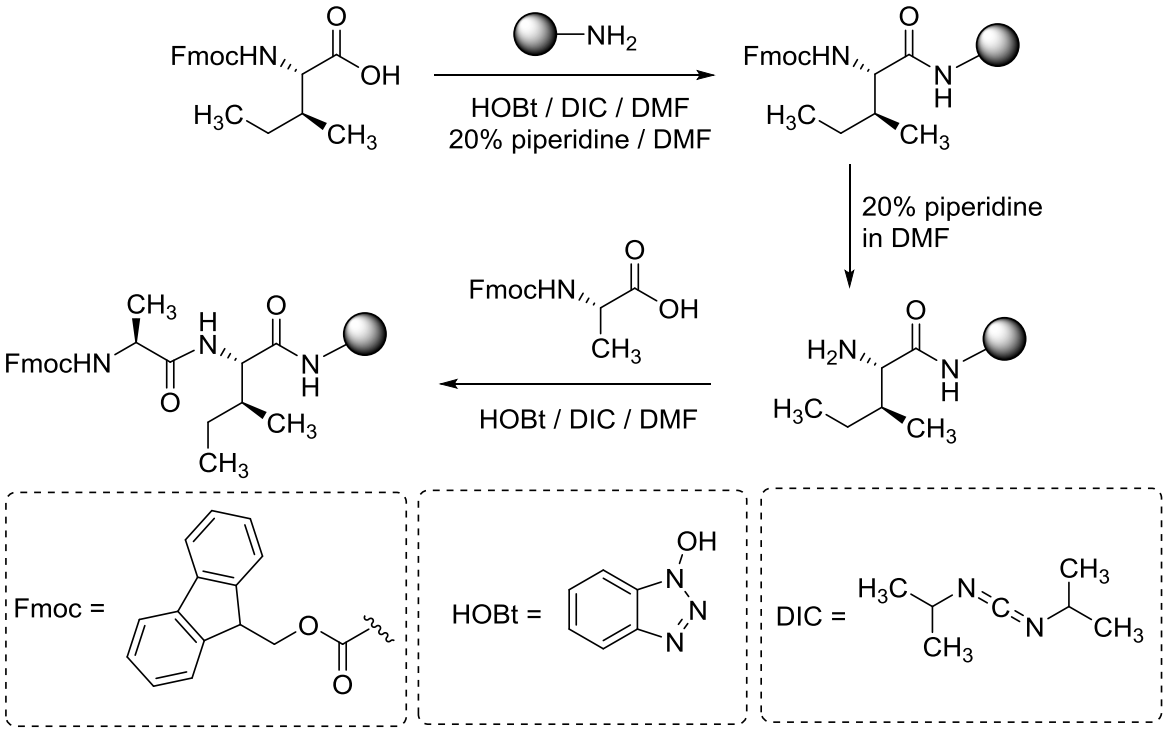

Figure 5-1: First steps of FGF2 peptide synthesis
The Fmoc-Ile-OH amino acid was anchored to Rink amide resin. Elongation was performed with Nterm deprotection and next amino acid activation Fmoc-Ala-OH. DIC: Diisopropylcarbodiimide, HOBt: 1-hydroxybenzotriazole, DMF; Dimethylformamide.

5.2.1.1 Experimental details

The synthesis was carried out using a 30 mL polytetrafluoroethylene (PTFE) reaction vessel. 0.1 mmol of rink resin was incubated for 1h with Dimethylformamide (DMF) to permit its swelling. A 5-fold excess of Fmoc-protected amino acid, piperidine (20% in DMF), 0.8 M of DIC in DMSO and 0.5 M of 1-hydroxybenzotriazole (HOBt) in DMF were used. Coupling was generated with a 60 minutes room temperature following by 10 minutes microwave couplings at 0.10mmol scale, the temperature was set at 75 °C and power at 25W. Fmoc groups were removed at room temperature by treatment with 20% piperidine in DMF.

Reagents used were from Sigma-Aldrich unless specified. The Rink amide resin was purchased from Novabiochem. DMF was purchased from AGTC Bioproducts (Hessle, UK). DMF is an organic solvent that facilitates the amino acid coupling reaction as it swells the resin. As 99% of coupling sites are situated inside the resin beads, the swelling allows an optimal permeation of activated amino acids. DMF will turn the resin from a shrunken state to a swollen state, it is the

reaction solvent. Amino acid derivatives were purchased from CEM, Novabiochem (Merck) or AGTC.

Side chains of the different amino used were protected as follow:

Fmoc-Arg(Pbf)-OH, Fmoc-Gln(Trt)-OH, Fmoc-Glu(tBu)-OH, Fmoc-Lys(Boc)-OH, Fmoc-Ser(tBu)-OH, Fmoc-Thr(tBu)-OH and Fmoc-Tyr(tBu)-OH.

To resume, each amino acid will have a base-labile N-Fmoc group on the alpha amino function, an acid-labile protecting group on side chains if necessary, and an acid labile linker on the C terminus.

The Boc/Bzl protection was not chosen as it implicates the use of the highly toxic hydrofluoric acid and strong acidic conditions can be deleterious for structural integrity of the peptide. The Fmoc strategy permits a mild acidic condition for both peptide deprotection and cleavage from the resin. A base, piperidine was used to expose the amino acid in order to react with the next activated amino acid. This is the Fmoc deprotection step and was carried out using a 20% (v/v) solution of piperidine in DMF. Diisopropylcarbodiimide (DIC) and HOBt were used to activate peptide bond formation. DIC activates the carboxyl function. HOBt prevents racemisation to occur. They are activators for coupling.

5.2.1.2 Acetylation and cleavage

Following the 30 hour-synthesis, the peptide-resin was washed with DMF. The peptide needed to be acetylated to prevent any undesired reaction with the N-terminus of the last amino acid. Briefly, the peptide-resin was incubated twice with a 25% solution of acetic anhydride in DMF for 20 minutes under agitation. It was then drained and washed 5 times with DMF and 2 times with diethylether (Et_2O). The last wash removed the DMF and thus allow a better cleavage reaction. Peptide cleavage was carried out with a solution of 95:5:5 (v/v/v) Trifluoroacetic acid, Triisopropylsilane (TIPS) and water for 3 hours under agitation. Water and TIPS scavenge the protecting groups. The peptide resin mixture was filtered in order to collect the peptide. The filtrate was then concentrated with a rotary evaporator followed by ether wash. The solid peptide was dissolved in deionised water and acetonitrile (acetonitrile helps hydrophobic molecules to dissolve in solution). The crude peptide was analysed by mass spectrometry and lyophilised overnight for storage.

5.2.2 Peptoid synthesis

Peptoid structure differs from peptides as the side chains are on nitrogen atoms. Their backbones are achiral (Figure 5-2). Peptoids were synthesised by Hannah Bolt (Cobb research group Durham University) using an Aapptec Apex 396 synthesiser as described before (Bolt, Williams, *et al.*, 2017). All experiments were done at room temperature unless specified. Briefly, about 0.1mmol of Fmoc-protected Rink Amide resin was swollen in 2 mL of DMF during 2 min shaking at 475 rpm. The resin was deprotected with 1 mL of 20% 4-methylpiperidine solution in DMF for 1 min, 475 rpm and then with 2 ml of solution for 12 min, 475 rpm. The acylation step was done by treating the resin with 1 mL of a 0.6 M haloacetic acid solution (either bromo- or chloroacetic acid diluted in DMF) for 20 min at 475 rpm. Five washing steps using 2 mL of DMF for 1 min at 475 rpm were carried out before adding the amine sub-monomer. This was performed by incubating 1 mL of 1.5M amine sub monomer in DMF for 60 mins with shaking at 475 rpm. The 5 washing steps were done once again following by acetylation and amine displacement steps until the sequence was complete. The crude peptoid was shrunk in diethyl ether and peptoid cleavage was carried out with 4 mL of a 95:5:5 (v/v/v) mixture of TFA:TIPS:water for 30 min on an orbital shaker at 250 rpm. The cleavage mixture was filtered and evaporated *in vacuuo*. The resulting residue was precipitated in about 20mL of diethyl ether. The crude peptoid was obtained via centrifugation (15 mins, 4,000 rpm, 5 ˚C) and the ether layer decanted to yield the crude product as a white/yellow powder.

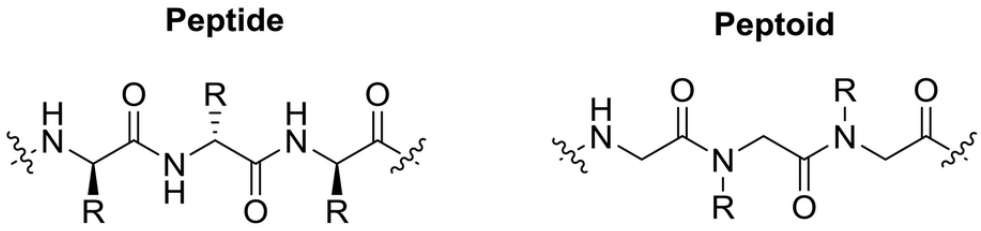

Figure 5-2: Structure of an α-Peptide and α-Peptoid structure
Adapted from (Bolt, Eggimann, *et al.*, 2017)

5.2.3 Compounds used in the study

This study aimed to synthesise a peptide that could compete with FGF2 binding, as this growth factor is implicated in fibrosis (WT peptide). The sequence of interest was designed considering the FGF2 residues involved in Heparan Sulfate binding (Li *et al.*, 2014). The importance of a lysine

residue in binding sulfation patterns was studied by synthesising a modified peptide (MD peptide) where the lysine was substituted by an alanine. The peptides have 19 amino acid residues as it is representative of the electropositive pocket of FGF2 (Li *et al.*, 2014), a longer peptide could have been designed but the longer the peptide the harder the synthesis. Two peptides were synthesised by Fmoc-SPPS and four peptoids were kindly given by Hannah Bolt. Peptoids were first used as positive control for the ITC experiment as it has been shown that peptoids can have high binding affinity with HS (Ford *et al.*, 2013). One peptoid used was based on earlier publication (HLB03-50) and Dr Steven Cobb helped in designing 3 others peptoids that are positively charged (HLB03-39, HLB03-41, HLB04-01). Characteristics and structures of the six compounds are summarised Figure 5-3.

WT Peptide

KRTGQYKLGSKTGPGQKAI, $C_{90}H_{155}N_{29}O_{26}$, 2058 g/mol

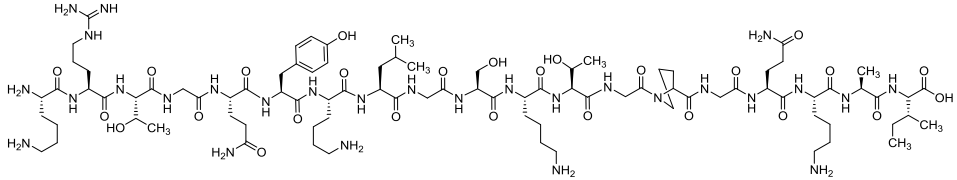

MD Peptide

KRTGQYALGSKTGPGQKAI, $C_{87}H_{148}N_{28}O_{26}$, 2001 g/mol

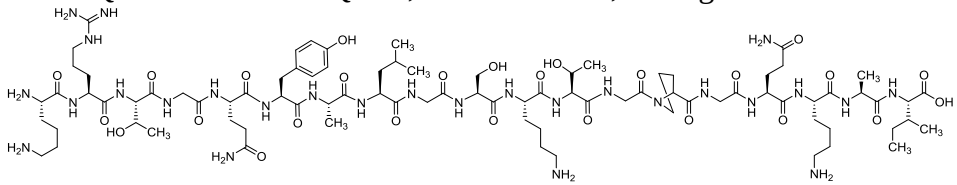

HLB03-50

$(NLysNbutNspe)_4$, $C_{88}H_{139}N_{17}O_{12}$, 1626 g/mol

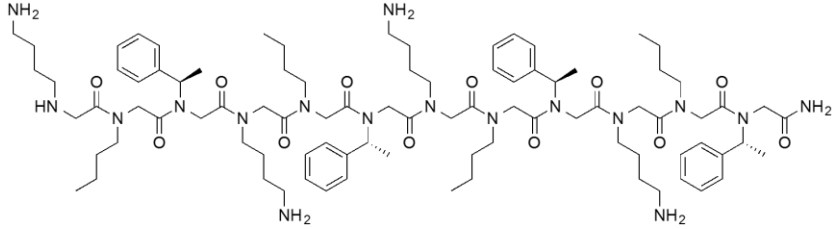

HLB03-39

$(NLysNLysNspe)_4$, $C_{88}H_{143}N_{21}O_{12}$, 1686 g/mol

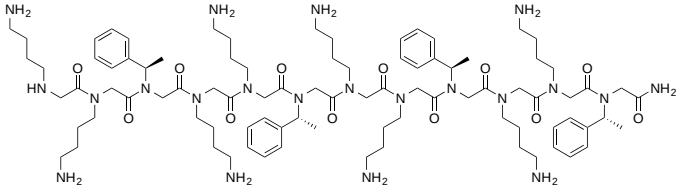

HLB03-41

$(NaeNaeNspe)_4$, $C_{88}H_{143}N_{21}O_{12}$, 1463 g/mol

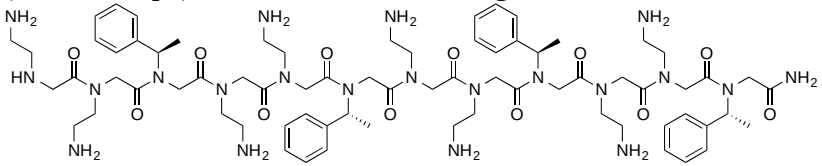

HLB04-01

$(NaeNbutNspe)_4$, $C_{80}H_{123}N_{17}O_{12}$, 1515 g/mol

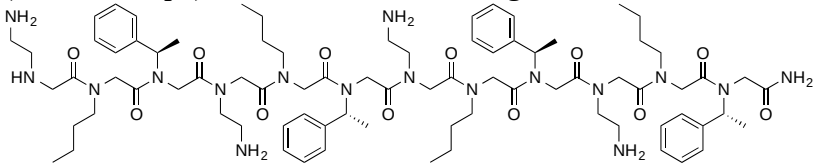

Figure 5-3: Peptides and Peptoids characteristics

Sequences, Molecular composition and weight are given for each compound. Abbreviations used: NSpe, N-((S)-1-phenylethyl) glycine; NLys, N-(4-aminobutyl)glycine); Nbut, N-butylglycine

5.2.4 Mass spectrometry analyses

Mass spectrometry (MS) is a very common technique to analyse both crude and purified peptides. Each peptide was dissolved in a mixture of deionised water and MeCN to a concentration of approximately 1mg/mL. The Matrix-Assisted laser desorption/ionization (MALDI) service in Durham performed all experiments using an Autoflex II ToF/ToF mass spectrometer (Bruker Daltonik GmBH). In principle, the matrix is composed of the sample and molecules α-cyano-4-hydroxy-cinnamic acid (50 mg/mL) in a ratio of 1:9. A 337nm nitrogen laser is directed onto the matrix where energy is absorbed, and the matrix is ionised. The ionisation protects the samples from the laser and ionises them. Then samples are submitted to an electrical field, where all molecules are separated, and a detector analyses their time of flight. The speed at which the compound reaches the detector gives information about its weight. Results are therefore given as mass/charges written m/z.

5.2.5 Purification and analytical HPLC

High performance Liquid Chromatography was carried out using an Acquity HPLC system (Waters Ltd, UK) equipped with a 200 LC pump, and Waters 486 UV tunable absorbance detector, set to 280 nm for peptides and 250 nm for peptoids. Chromatography purifies compounds according to their hydrophobic properties. Samples are injected onto a column where they interact with the hydrophobic ligands coated onto the column. The running buffer gradually changes from water to a non-polar organic solvent that weakens the interaction and therefore free the previously bound compound. A UV detector records absorbance and samples are collected based on their time of elution which correlates with the solvent concentration at point when the interaction with hydrophobic ligand is reversed. In this work, 1-2mL of samples were injected onto an SB Analytical C8 column and the running buffer was from 95% H_2O, 5%MeCN, and 0.1% TFA to 95%MeCN, 5%H2O, and 0.1% TFA. Each fraction was collected and lyophilised.

5.2.6 Circular Dichroism spectra

Dichroism reflects light absorption differences depending on direction. Plane polarised light is composed of a right and left circularly polarised lights. Plane polarised light can become circulatory when passing through a birefringent surface. Circular Dichroism is based on the effect of circular

polarised light on a molecule. Left and right handed circularly polarised light are absorbed differently when directed onto the compound. CD spectropolarimeter measures the far UV absorbance of left and right handed light. It measures the difference in absorption between the right and left-handed light components. This difference in absorption leads to an ellipticity. The angle of polarisation defined by the eclipse is measured in degrees (deg). This angle gives information about the secondary structure of a molecule. All samples were analysed with a Jasco J-810 spectropolarimeter.

5.2.7 Isothermal Titration Calorimetry (ITC)

ITC measures the heat released or absorbed upon the binding of two components. As seen in Figure 5-4 two cells are used for this purpose. One reference cell containing the buffer only and one cell where one of the compounds of interest is added. A power unit maintains the same temperature in the two cells. A syringe is inserted on top of the sample cell and filled with a solution containing the second compound of interest diluted in the same buffer as compound 1. Gradually the syringe injects small volumes of compound 2 into the sample cells leading to an interaction between the two molecules (Figure 5-4). The power unit detects the temperature variations due to this interaction and provides the power needed to keep isothermal conditions. The calibrated power units between the reference cell and the sample cell are recorded. As an example, an exothermic reaction will release heat and therefore gives a negative differential power and inversely for endothermic reaction (Figure 5-5). The final graph gives a curve where affinity, stoichiometry and enthalpy of the binding can be determined (Figure 5-5).

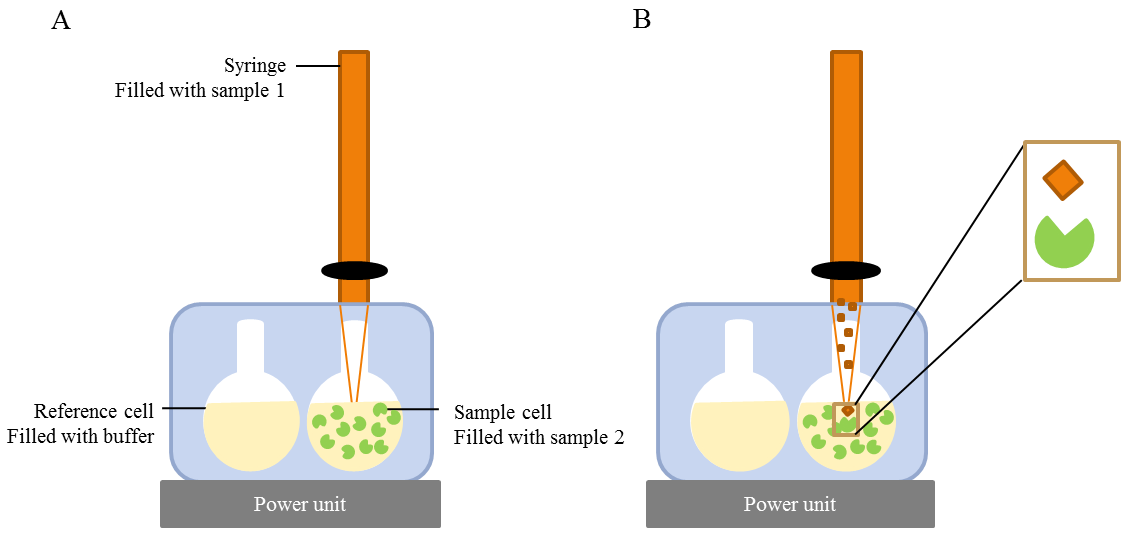

Figure 5-4: Isothermal Titration Calorimetry apparatus
ITC apparatus (A) is composed of a power unit, a reference cell, a sample cell and a syringe. To study the binding of two compounds, the syringe is filled with one compound and the sample cell with the other one. The syringe injects the compound of interest into the sample cell (B).

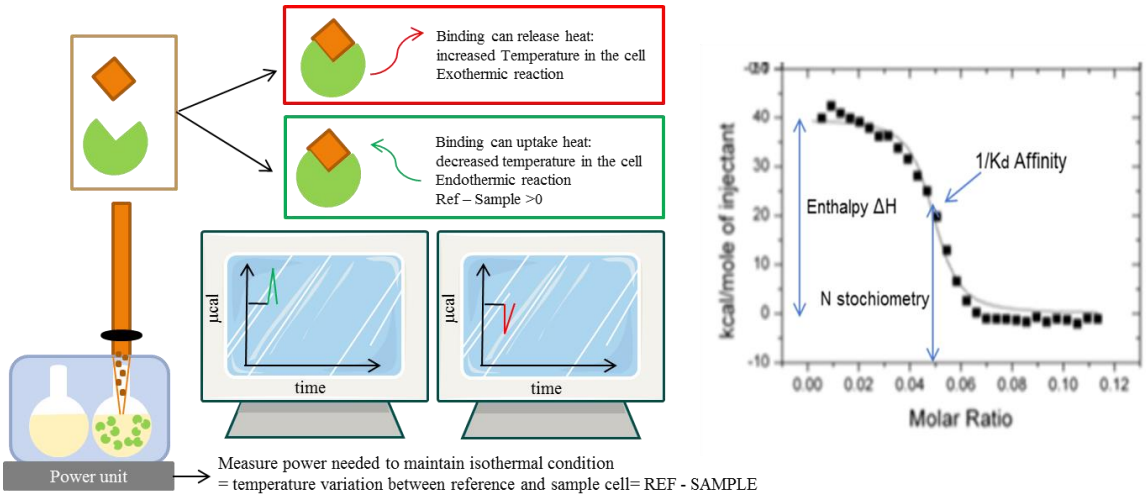

Figure 5-5: Isothermal Titration Calorimetry principles
The syringe injects the compound of interest into the sample cell and the change in temperature following the binding of the 2 compounds inside the sample cell is detected by the power unit (left panel). An endothermic reaction will decrease the temperature in the sample cell leading to a positive difference between the reference cell temperature and the sample one (REF-SAMPLE). This will be display on the screen as a peak (green graph). On the contrary, an exothermic reaction within the sample cell will increase the temperature generating a negative REF-SAMPLE temperature and therefore a drop on the analytical graph (red graph). Plotting all experimental data (right panel) allows the calculation of affinity, enthalpy and stoichiometry characteristics of the binding.

5.2.7.1 Samples preparation

All samples were diluted in 50mM sodium phosphate buffer pH 7.4, filtered with 0.22µm filter and degassed prior to each experiment. For heparin solution, 5mL of 1mM Heparin was dialysed overnight with magnetic stirring at 4°C using a Maxi Geba Flextube Dialysis Kit MWCO 8kDa against 800 mL of the sodium phosphate buffer. Final heparin concentration used for peptoids experiments was 0.11mM and 0.1mM for peptides. Peptoids solutions were at a concentration around 0.1mM (it was not possible to use UV technique to control concentration precisely). Peptides solutions were at a concentration between 0.1-0.3mM and concentrations were checked using a nanodrop before each experiment.

5.2.7.2 Instrument and experiment settings

ITC measurements were carried out using a VP-ITC isothermal titration calorimeter (MicroCal, Inc). Reference power was set at 15 µcal/sec, initial delay 60 seconds and the stirring speed at 307rpm. Cells temperature was set at 25°C. A volume of 1.8mL of peptide/peptoid was loaded to the sample cell when 300µL of heparin was charged into the syringe (see specific concentrations below).

For peptoids experiments, 30 injections of 6µL of 0.11mM heparin solution were titrated into a 0.1mM peptoid solution. Each injection lasted 60 seconds with a spacing time of 300 seconds and a filter period of 2 seconds.

For peptides experiments, 19 injections of 15µL of 0.1mM heparin solution were titrated into a 0.1-0.3mM peptide solution. Each injection lasted 60 seconds with a spacing time of 300 seconds and a filter period of 2 seconds.

5.2.8 Data analysis

Dilution effect was corrected by subtracting samples data for control experiment (i.e. heparin titration into phosphate buffer). Once corrected, titration data were integrated and analysed using Origin 7.0 software (MicroCal Inc). Results were fit with the one-set-of-sites model with Ligand in syringe parameters. Dissociation constant (Kd), binding stoichiometry (N), enthalpy, energy

change (ΔH) and change in entropy (ΔS) were determined by ITC software. The free energy (ΔG) was calculated with the formula:

$$\Delta S = \frac{\Delta H - \Delta G}{T}.$$

5.3 Results

First, the two peptides sequences from FGF2 were synthesised by SPPS. After synthesis, each compound was subjected to HPLC and MALDI-TOF. Evaluation of crude peptides by MALDI shows whether the peptide is present in the crude preparation or not. Other unwanted peptides can be detected at higher and lower *m/z* value. For some figures, a table with the main *m/z* value and their meaning was created.

5.3.1 WT peptide synthesis: run 1

As seen in Figure 5-3, the expected molecular weight of WT peptide was 2058.17 g/mol. MALDI spectrum from crude peptide in Figure 5-6 had a peak at 2060 *m/z* which was the target peptide ($M+H^+$). The peak at 1926 *m/z* was the peptide minus Arginine (Arg or R) (+Na). The peak at 2312 *m/z* is likely to be the target peptide plus a Pbf protecting group (Pbf = 2, 2, 4, 6, 7-pentamethyldihydrobenzofuran-5-sulfonyl), on the Arg side chain.

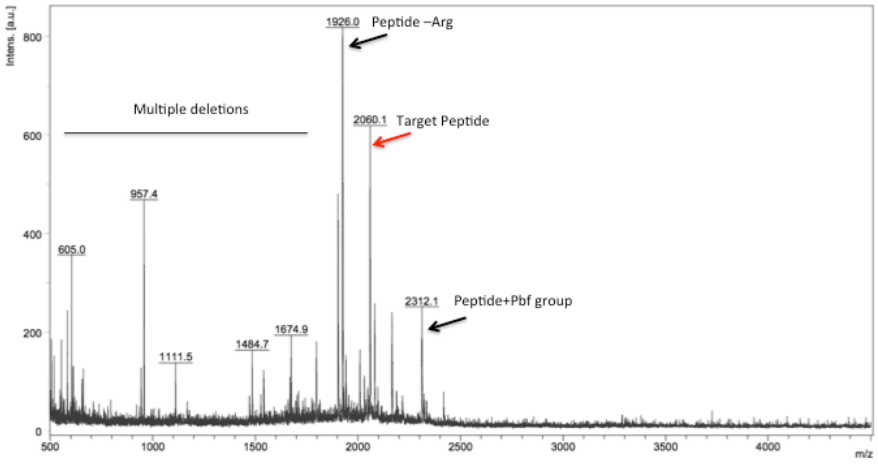

Figure 5-6: MALDI Mass Spectrum from first crude WT peptide
The target peptide was 2060 *m/z* (red arrow). Peaks that are on the right side of the target peptide show unwanted peptide with additional amino acid/ protecting group. Peaks that are on the left side are unwanted peptides with one or several amino acid deletions.

A second cleavage was done to try to remove the Pbf group and therefore increase the yield of the target peptide. Results are shown Figure 5-7. The additional cleavage did not cleave all the arginine protecting groups as the 2312 *m/z* peak was still present.

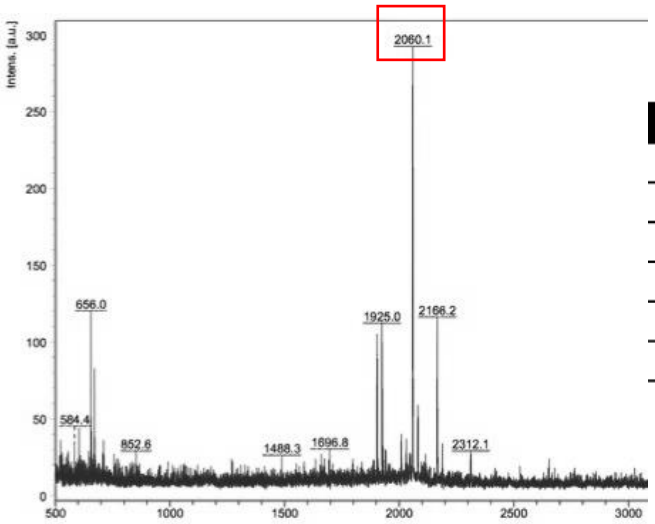

Peak (*m/z*)	Deletion (s)	Adduct (s)
1674	K, R, T	
	Q, R, T	
1926.1	R	Na+
2060	-	-
2166	A, P	Na+, Pbf
2312		Pbf

Figure 5-7: MALDI Mass Spectrum after an additional cleavage
The WT peptide was 2060 *m/z* (in red). The peptide+ Pbf group was still present (2312 *m/z* peak). Table： *m/z* values from first FGF2 peptide synthesis and their respective interpretation.

In order to purify our peptide, samples were purified by Reverse Phase High Performance Liquid Chromatography (RP-HPLC). The RP-HPLC trace is displayed Figure 5-8. Six main peaks were observed. After an overnight lyophilisation, samples from fractions 1 and 6 were found empty. They might have been only buffer. Samples 2, 3, 4 and 5 were analysed by MALDI.

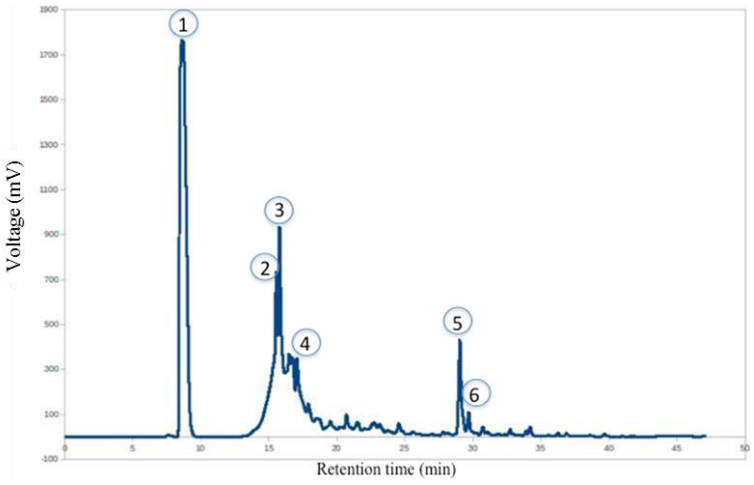

Figure 5-8: RP-HPLC trace of first WT peptide
HPLC gradient: 0-100% B over 45min (A=5:95:0.1 Acetonitrile/H_2O/TFA; B=95:5:0.1). Absorbance was recorded at 280nm. Fractions 1-6 were collected and lyophilised overnight.

Surprisingly the MALDI spectra from RP-HPLC fractions were similar to the crude one (Figure 5-9). The separation was not successful. However, fraction 2 contained the most WT peptide. All fractions contained the peptide minus arginine. The 2166 *m/z* peak was only seen in fraction 4 and 5. The peak 2060 *m/z* of the FGF2 peptide was weakly seen in fraction 4 analysis.

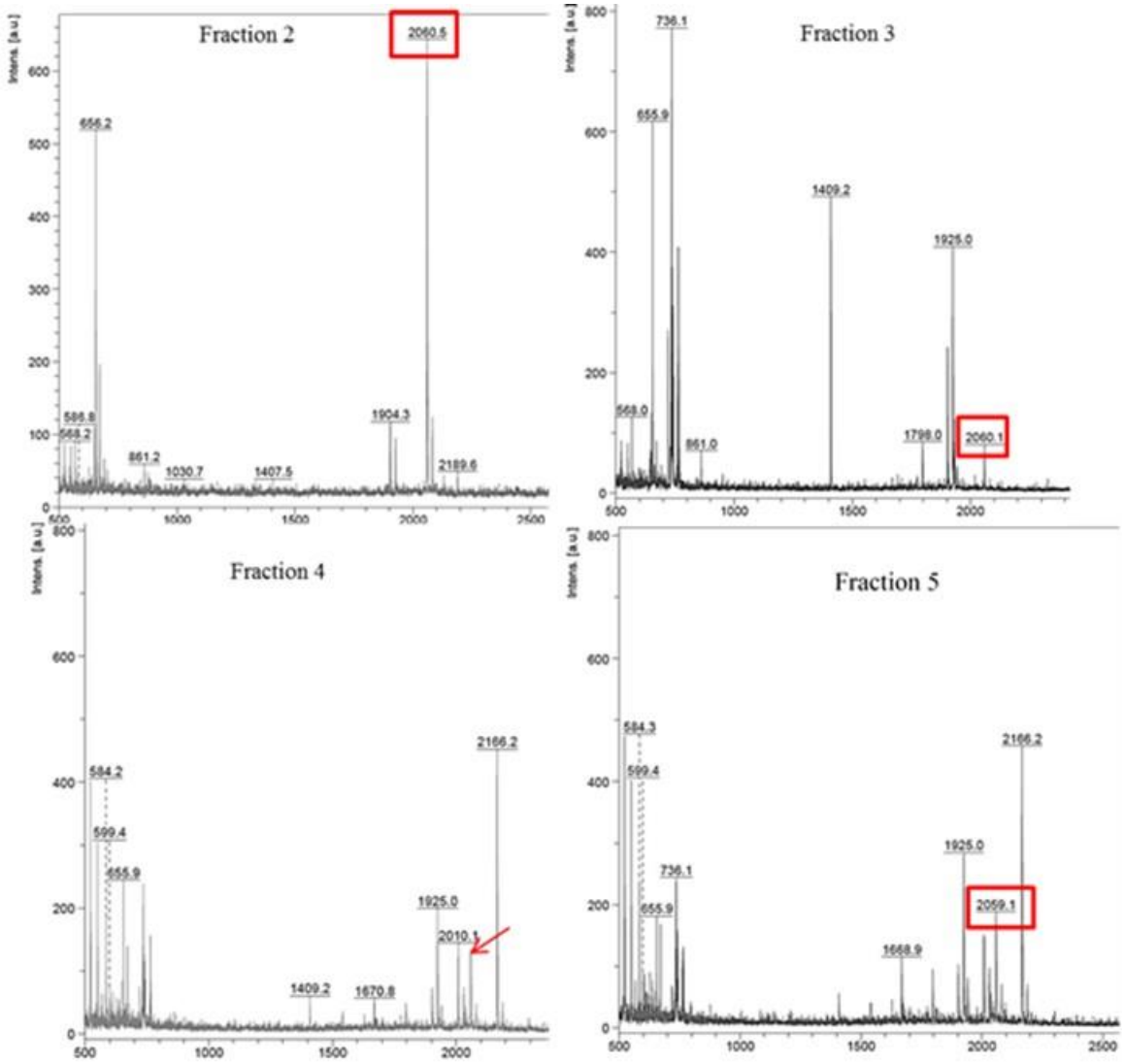

Figure 5-9: MALDI mass spectrum after RP-HPLC
Fraction 2 is shown on top left, fraction 3 on top right, fraction 4 on left bottom and fraction 5 on right bottom. Fraction 2 had one major peak of *m/z*= 2060.5= WT peptide. In the 3 other fractions, there was a peptides mixture. FGF2 peptide *m/z* peak is indicated by red square or red arrow.

5.3.2 WT peptide synthesis: run 2

Because the first synthesis did not lead to a fully purified peptide, a second synthesis was performed. The procedure used was the same as explained previously except that a double coupling

was used for Arginine (2 x 60 mins) and a longer TFA cleavage time was used (5h) to help avoid Arginine deletions and to ensure full deprotection of all Pbf groups. The MALDI of the crude peptide from the second synthesis is shown Figure 5-10. The WT peptide (2060.1m/z) was present but again so were the target peptide –Arginine (1904m/z) and the target peptide + a Pbf group (2312m/z).

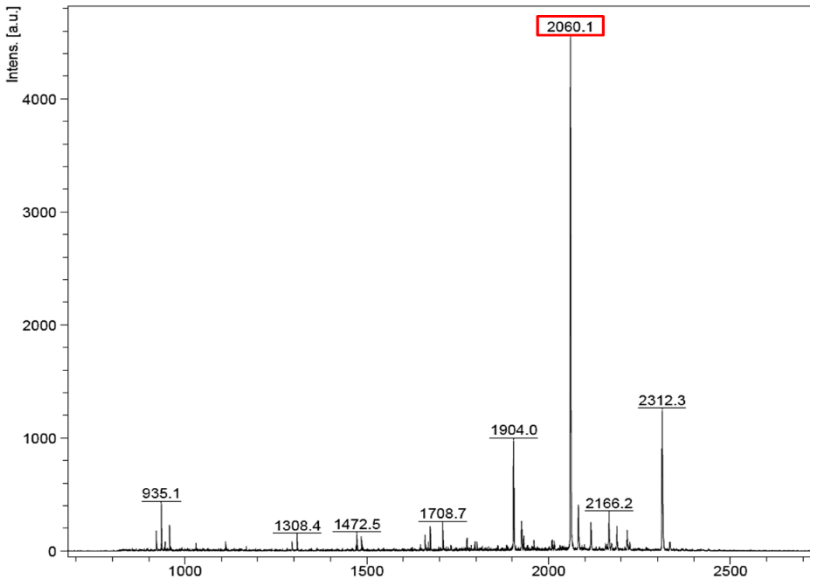

Figure 5-10: MALDI Mass Spectrum of the second WT peptide synthesis
In red is the target peptide. The crude also had the peptide minus an Arginine (1904 *m/z*) and with Pbf group (2312 *m/z*).

The crude peptide was subjected to RP-HPLC where 3 fractions were collected (see Figure 5-11). Fraction 1 mainly had the WT peptide (see Figure 5-12) compared to other fractions (data not shown).

The second synthesis and RT-HPLC provided a clearer HPLC graph, showing a successful synthesis. Fraction 1 was chosen for ITC experiments. From 130mg of crude peptide, approximately 15mg was purified. The yield was around 11.5%, which is low but better than the first synthesis where all fractions had arginine deletions. The low yield was mainly due to the fact that a lot of fractions contained the peptide with arginine deletion.

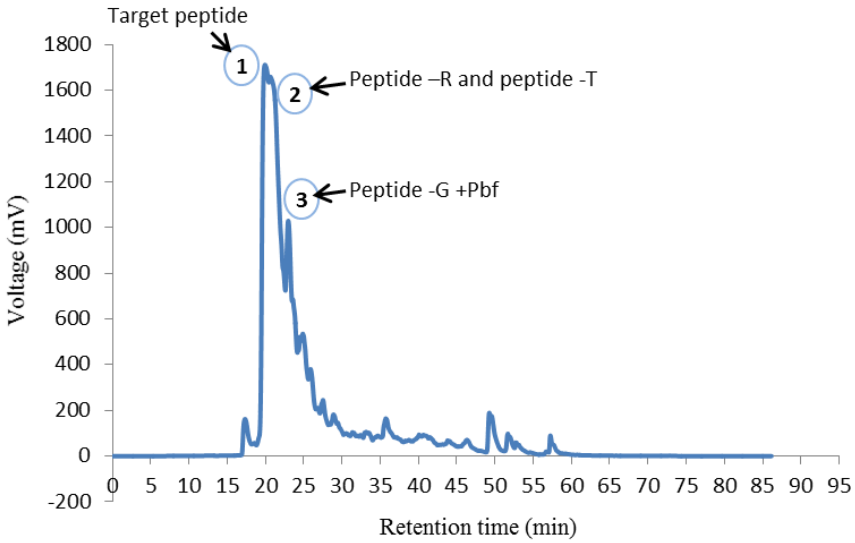

Figure 5-11: RP-HPLC trace of second WT peptide
HPLC gradient: 0-100% B over 45min (A=5:95:0.1 Acetonitrile/H_2O/TFA; B=95:5:0.1). Absorbance was recorded at 280nm. Fractions 1-3 were collected and lyophilised overnight. R: Arginine, T: Threonine, G: Glycine.

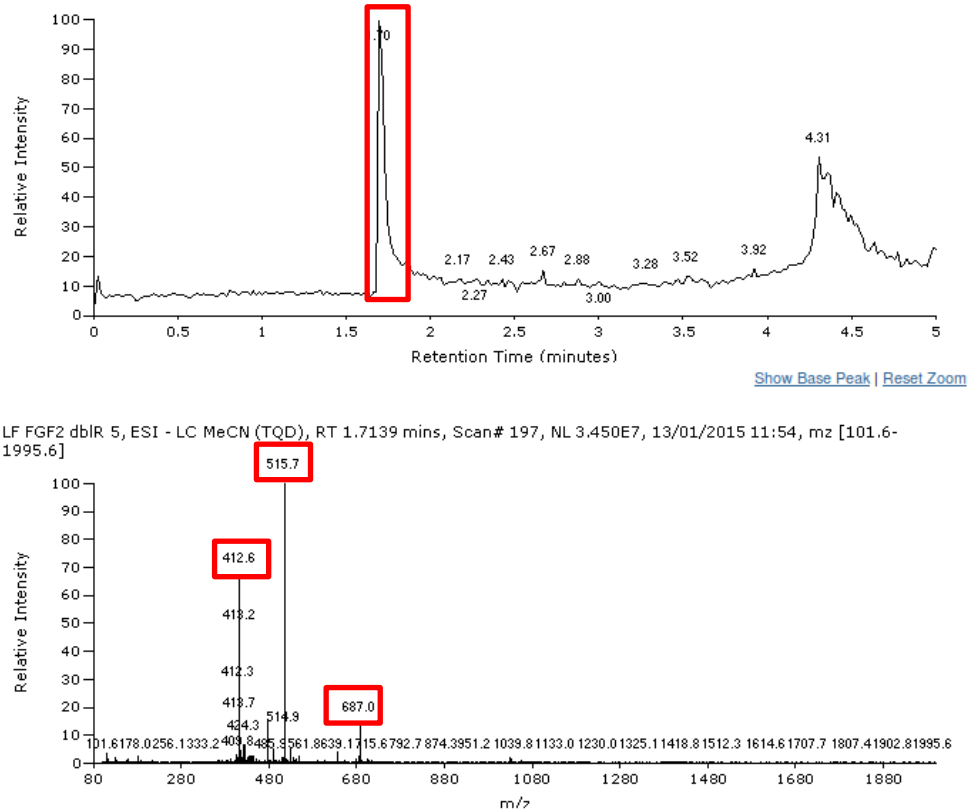

Figure 5-12: LC-MS of fraction 1-second WT peptide
Major peak in LC (1.7 min) had masses at 687, 515 and 412 that correspond to the desired product (M+3H, M+4H, M+5H). *M/z* values of the target peptide are highlighted in red.

5.3.3 Modified peptide synthesis

In the modified peptide as seen Figure 5-3, the 7th amino acid from WT peptide (lysine) was substituted by an alanine. As observed Figure 5-3, the expected molecular weight of modified peptide (MD pep) was 2001 g/mol. In Figure 5-13, the peak at 2003 *m/z* was the target peptide ($M+H^+$). The peak at 1847 was the peptide minus Arginine (+Na) and the peak at 2255 could be the peptide plus a Pbf group, the Arginine side chain protecting group.

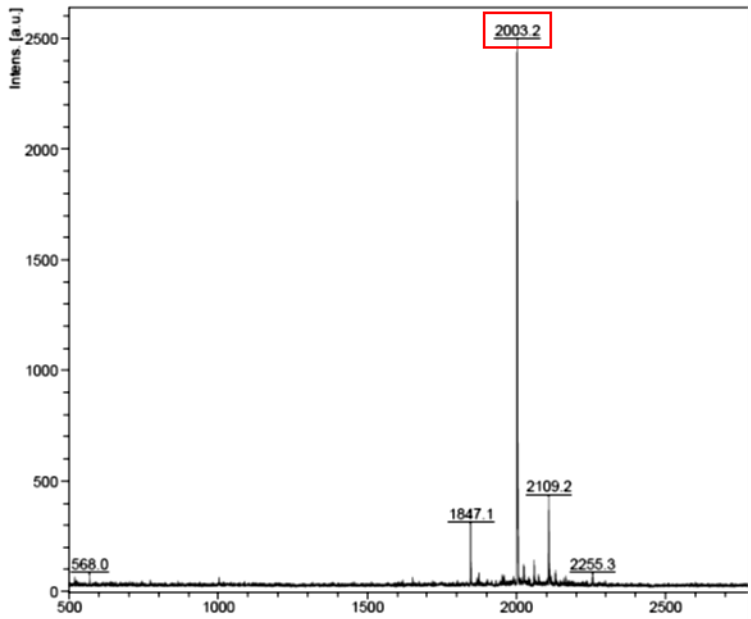

Peak	Deletion	Adduct
1847	R	
2003	-	-
2109	A, P	Na+, Pbf
2255		Pbf

Figure 5-13: MALDI Mass Spectrum of modified peptide
The target peptide is 2003 *m/z* (in red). The crude has the peptide, peptide + Pbf group (2255*m/z* peak), peptide-Arginine (1847*m/z*) and peptide with multiple deletions and additions (2109 *m/z*). Table: *m/z* values from MALDI crude modified peptide synthesis spectrum and their respective interpretation.

RP-HPLC trace following synthesis is represented Figure 5-14. The purification was successful, all MALDI data are not displayed, only the one from the fraction with the highest purification. Fraction 1 was selected for ITC experiments. From 120 mg of crude peptide, approximately 36 mg has been purified (yield=30%).

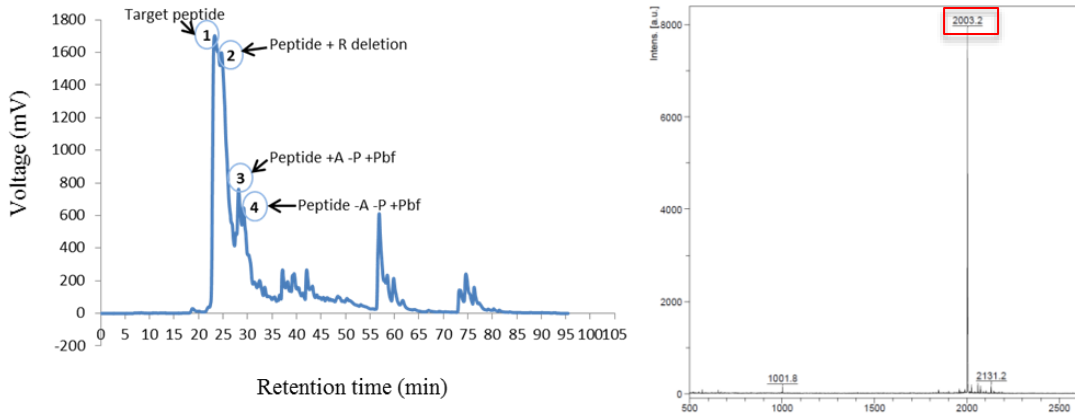

Figure 5-14: RP-HPLC trace of modified peptide and fraction 1 mass spectrometry analysis HPLC gradient: 0-100% B over 45min (A=5:95:0.1 Acetonitrile/H2O/ TFA; B=95:5:0.1). Absorbance was recorded at 280nm (left image). Fractions 1-4 were collected and lyophilised overnight. MALDI analyses of all fractions showed that fraction 1 was the most purified fraction for the target peptide (right figure). R: Arginine, A: Alanine, P: Proline.

5.3.4 Peptoid purification

The four peptoids were synthesised by Hannah Bolt and purified in Durham. RP-HPLC traces and MALDI spectra from the best fractions are represented Figure 5-15. The purification of the four peptoids did not give high yield (see Table 5-1). This might be explained by a poor synthesis. Only HLB03-50 and HLB04-01 peptoids had a final mass above 5mg. These two peptoids were later used for CD analysis and ITC experiments.

	Initial mass (mg) crude peptoid	Final mass (mg) purified peptoid	Yield
HLB 03-39	195	<2mg	around 1%
HLB 03-41	90	<2mg	around 2%
HLB 03-50	80	12	15%
HLB 04-01	80	6	7.5%

Table 5-1: Peptoids yield and purified mass

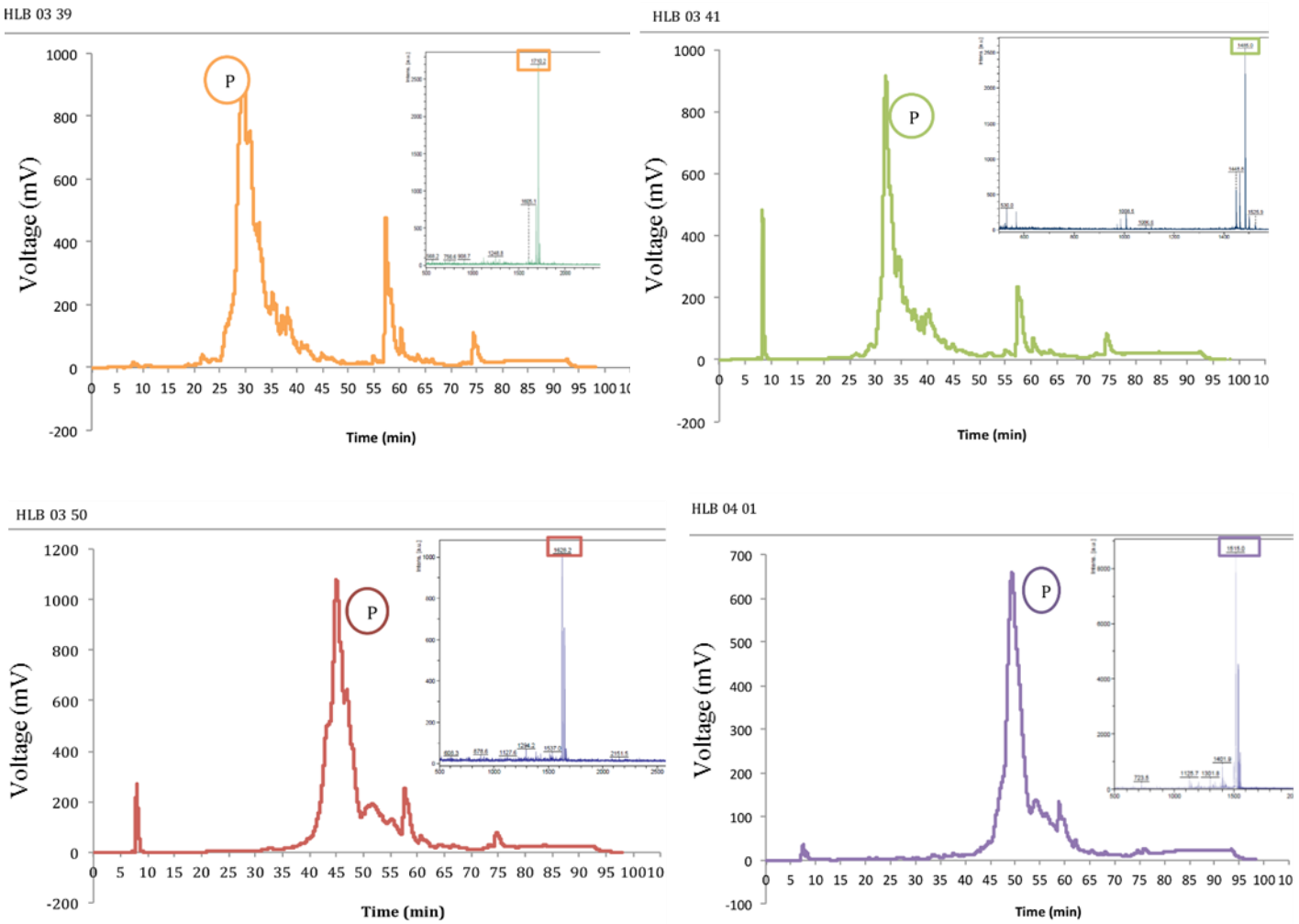

Figure 5-15: RP-HPLC traces of the four peptoids
HPLC gradient: 0-60% B over 60min (A=5:95:0.1 Acetonitrile/H_2O/TFA; B=95:5:0.1). Absorbance was recorded at 250nm. All fractions were collected, lyophilised overnight and analysed with mass spectrometry the next day. (P) represents the fraction were most purified peptoids were collected. Highlighted *m/z* peaks represent the target peptoid peak.

5.3.5 Analytical HPLC

All compounds used for ITC experiments were subjected to analytical HPLC (Figure 5-16). WT peptide had a purity around 90%, MD peptide 95%, HLB04-01 around 86% and HLB03-50 around 96%. These levels of purity were satisfactory and no more HPLC was necessary for these compounds.

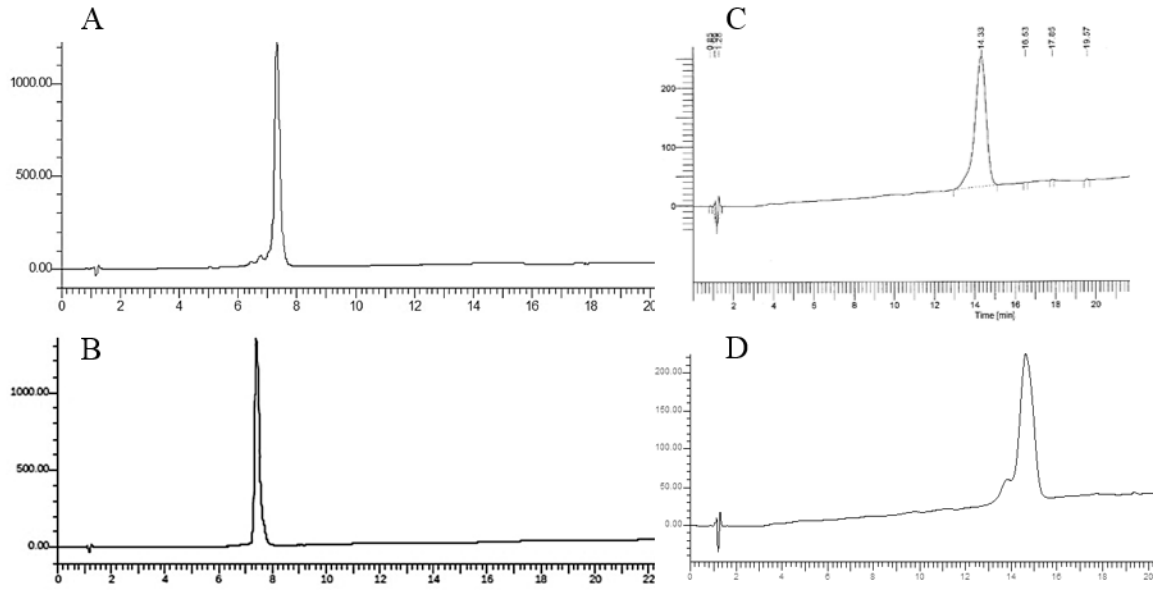

Figure 5-16: Analytical HPLC graphs
Purified WT Peptide (A) and modified peptide (B) and peptoid HLB03-50 (C) and HLB04-01 (D).

5.3.6 Circular Dichroism analyses

CD provides secondary structure for peptides and peptoids of interest. Helical structures are characterised by negative bands at 222 and 208 nm and with a positive band at 193nm. β-sheets are characterised by a negative band at 218nm and positive at 195 nm while unfolded molecules have low ellipticity over 210nm and negative trace around 195 nm (Figure 5-17) (Greenfield, 2006). Peptides showed a random coil while peptoid displayed a helical structure with two negatives bands between 227 and 197nm and a last positive band around 195nm. Only WT peptide and HLB03-50 graphs are represented, MD peptide was similar to WT peptide and HLB04-01 to HLB03-50 (data not shown).

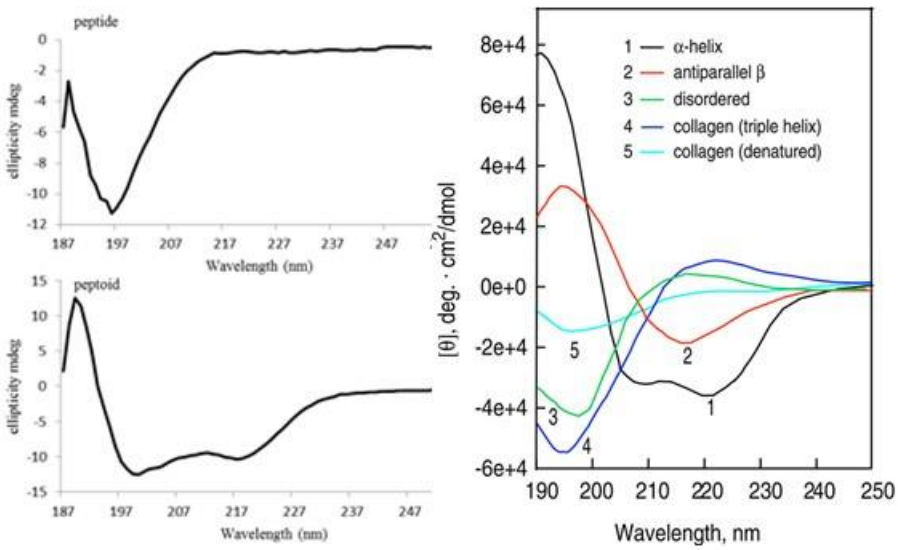

Figure 5-17: CD spectra analyses
Samples were diluted in PBS 10µM peptide and 100µM peptoid and analysed at 20°C with wavelength ranging from 180nm to 260nm. WT peptide (top left image) showed a curve typical of random coil structure. HLB03-50 (bottom left image) displayed an alpha helix structure. Right image from (Greenfield, 2006).

5.3.7 Isothermal titration calorimetry experiments

Isothermal titration calorimetry (ITC) was performed for all four compounds described before. All data are summed up in Table 5-2 and Figure 5-18, Figure 5-19. Surprisingly the peptides did not bind strongly to Heparin with a Kd between 100 and 1 000µM for WT peptide and MD peptide respectively. The lack of secondary structure as seen in Figure 5-17 might explain this. The dissociation constant of HLB03-50 peptoid was considerably lower than both peptides and had more binding sites, once again the helicoidal structure of the peptoid might favour stronger binding. However, the WT peptide bound with a Kd almost ten times lower than MD but with less binding sites (N=7 for WT vs N=17 for MD). This result confirmed that positively charged amino acids influence peptide binding to HS but the difference was not significant. It is noticeable that peptoid and peptides did not bind heparin the same way (Figure 5-18), while peptide titration indicated an exothermic binding ($\Delta H<0$), peptoid binding displayed an endothermic reaction ($\Delta H>0$).

HLB03-50	Kd (µM)	Kd SD (µM)	N	ΔH (cal/mole)	ΔH SD	ΔS (cal/mole/deg)	ΔG (cal/mole)
exp 1	1.19	0.33	23	1906	43.31	33.5	1068.5
exp 2	1.07	0.26	21	1905	37.33	33.7	1062.5
exp 3	1.29	0.28	23	1574	28.67	32.2	769
Average	1.18		22	1795		33.1	966.7
WT peptide	Kd (µM)	Kd SD (µM)	N	ΔH	ΔH SD	ΔS	ΔG
exp 1	120	10	9	-720.5	4.66	15.5	-1108
exp 2	130	10	6	-912.3	6.89	14.7	-1279.8
exp 3	140	10	7	-834.2	5.27	14.9	-1206.7
Average	130		7	-822.33		15	-1198.2
MD peptide	Kd (µM)	Kd SD (µM)	N	ΔH	ΔH SD	ΔS	ΔG
exp 1	1450	750	24	-577.9	14.97	11.1	-855.4
exp 2	550	150	8	-586.2	18.59	12.9	-908.7
exp 3	420	40	15	-579.5	4.96	13.5	-917
exp 4	1300	1170	21	-607.2	28.93	11.2	-887.2
Average	930		17	-587.7		12.2	-892.1

Table 5-2: ITC data for HLB03-50, WT peptide and MD peptide
Dissociation constant (Kd), binding stoichiometry (N), enthalpy, energy change (ΔH) and change in entropy (ΔS) were determined by ITC software. The free energy (ΔG) was calculated with the formula $\boldsymbol{\Delta G = \Delta H - T\Delta S}$. Exp= experiment. N was given as integer and without SD considering that a binding site cannot be less than 1.

As seen Figure 5-19, HLB04-01 did not fit to a one binding site model but to a model with two binding sites. The first two experiments displayed two binding sites. The third time, all instruments, syringes, cells were cleaned and new buffer, new heparin prepared but once again, the binding of HLB04-01 to heparin displayed two binding sites. Another fraction from a different RT-HPLC (data not shown) was used and again two binding sites appeared. It could be that the purification of the peptoid was not good and that two different molecules were in the cells. However, the analytical HPLC did not indicate impurity. No data can be given for the two binding sites constants as the software could not analyse a two binding site model when ligand is in the syringe.

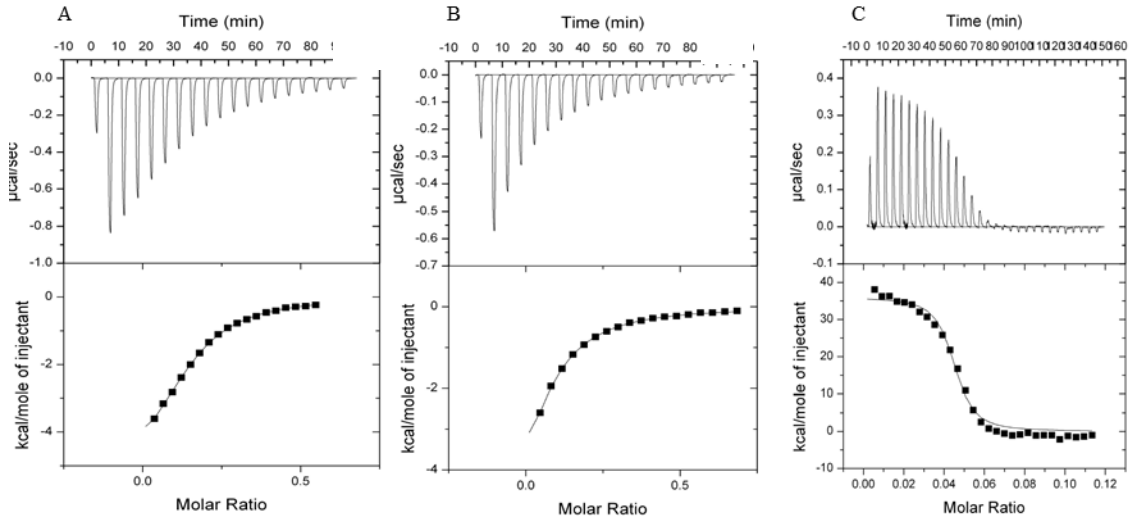

Figure 5-18: Representative ITC titrations of WT peptide, MD peptide and HLB03-50
Samples were diluted in 50mM sodium phosphate buffer pH 7.4, filtered with 0.22µm filter and degassed prior to each experiment. Peptides and peptoids concentrations were checked using a nanodrop before each experiment. ITC measurements were carried out using a VP-ITC isothermal titration calorimeter (MicroCal, Inc). Reference power was set at 15 µcal/sec, initial delay 60 seconds and the stirring speed at 307rpm. Cells temperatures were set at 25°C. A volume of 1.8mL of peptide/peptoid was loaded to the sample cell when 300µL of heparin was charged into the syringe. For peptoids experiments, 30 injections of 6µL of 0.11mM overnight dialysed heparin solution were titrated into a 0.1mM peptoid solution. Each injection lasted 60 seconds with a spacing time of 300 seconds and a filter period of 2 seconds. For peptides experiments, 19 injections of 15µL of 0.1mM heparin solution were titrated into a 0.1-0.3mM peptide solution. Each injection lasted 60 seconds with a spacing time of 300 seconds and a filter period of 2 seconds. Dilution effect was corrected by subtracting samples data for control experiment (i.e. heparin titration into phosphate buffer). Once corrected, titration data were integrated and analysed using Origin 7.0 software (MicroCal Inc). Results were fit with the one-set-of-sites model with Ligand in syringe parameters. A: WT peptide (N=3), B: MD peptide (N=4), C: HLB03-50 (N=3)

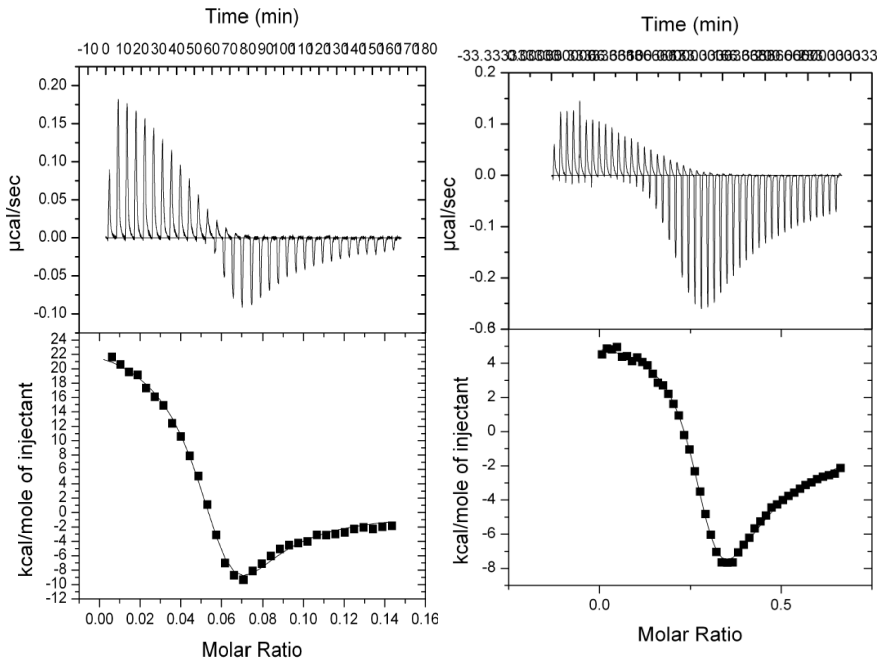

Figure 5-19: Representative ITC titrations of HLB04-01
Samples were diluted in 50mM sodium phosphate buffer pH 7.4, filtered with 0.22µm filter and degassed prior to each experiment. Peptoid concentration were checked using a nanodrop before each experiment. ITC measurements were carried out using a VP-ITC isothermal titration calorimeter (MicroCal, Inc). Reference power was set at 15 µcal/sec, initial delay 60 seconds and the stirring speed at 307rpm. Cells temperatures were set at 25°C. A volume of 1.8mL of peptoid was loaded to the sample cell when 300µL of heparin was charged into the syringe. For each experiment, 30 injections of 6µL of 0.11mM overnight dialysed Heparin solution were titrated into a 0.1mM peptoid solution. Each injection lasted 60 seconds with a spacing time of 300 seconds and a filter period of 2 seconds. Dilution effect was corrected by subtracting samples data for control experiment (i.e. heparin titration into phosphate buffer). Once corrected, titration data were integrated and analysed using Origin 7.0 software (MicroCal Inc). Results were fit with the one-set-of-sites model with Ligand in syringe parameters. Left image: HLB04-01 (N=3). Right image: HLB04-01 from a new fraction (N=1).

To investigate the potential use of the peptides and peptoids to prevent renal fibrosis, their ability to inhibit FGF2 binding to renal epithelial cells was analysed by flow cytometry.

5.3.8 FGF2 binding to renal epithelial cells by flow cytometry

The first experiment was to verify the functionality of the FGF2 binding kit and its detection by flow cytometry. HKC8 cells were incubated with biotinylated FGF2 for 1h at 4°C or in buffer followed by 30 minutes incubation with Avidin-FITC at 4°C. FGF2 binding was analysed by flow cytometry with Facs Canto II excitation at 488nm and emission 530nm. Cells incubated only with FGF2 and buffer showed the same profile while cells incubated with FGF2 and Avidin-FITC

showed an increase in FITC fluorescence and therefore a binding of FGF2 and Avidin-FITC to the cells (Figure 5-20 B). As a negative control, cells were incubated with heparin which inhibited FGF2 binding to the cells (Figure 5-20 C). Overall, the binding of FGF2 was successful in all conditions with heparin inhibiting FGF2 interaction with the cell surface (Figure 5-20 D）

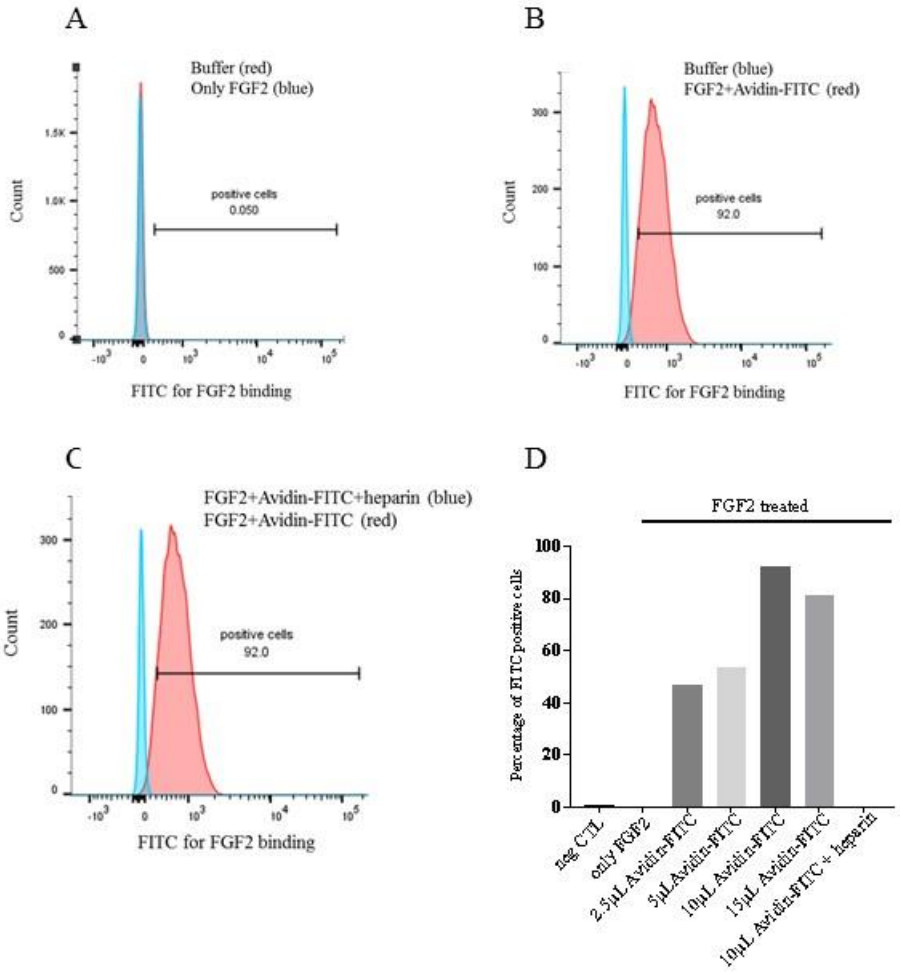

Figure 5-20: FGF2 binding to HKC8 cells

HKC8 cells grown in T75 flask were detached with warm accutase at 37°C and were suspended in 3.2% BSA in PBS. FGF2 binding to cells was carried out with R&D kit NFFB0 following manufacturer's instructions. About 100 000 cells were incubated with biotinylated FGF2 or biotinylated Soya protein (negative CTL) or buffer for 1h at 4°C. As a negative control, cells were incubated with 10µL of 500µg/mL of heparin with biotinylated FGF2 for 1h at 4°C. Then cells were incubated with Avidin conjugated FITC or buffer for 30 minutes at 4°C. Cells were washed two times and resuspended in wash buffer before analysis with FACS Canto II recording 10 000 events with excitation at 488nm and emission at 530nm. The binding of FGF2 is associated with an increase in the cells fluorescence intensity and therefore a shift to the right of the population. N=1

In order to test the competition activity of the peptoids with FGF2 binding, three different concentrations of peptoids were used and cells were incubated 30 minutes at 4°C with each compound prior to FGF2 treatment. As observed in Figure 5-21 both HLB03-50 and HLB04-01 inhibited FGF2 binding in a dose dependent manner with the concentration of 370µM showing an MFI value similar to the negative control.

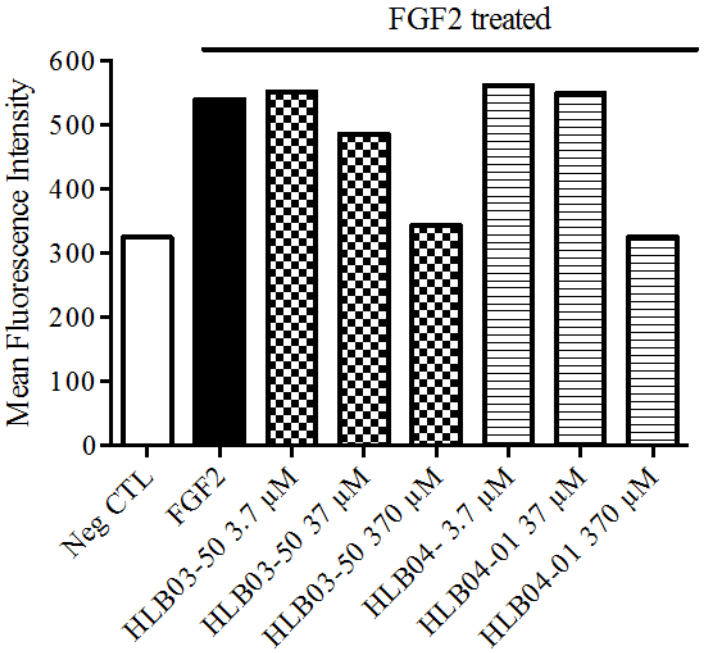

Figure 5-21: Increased concentration of peptoids treatment decrease FGF2 binding
HKC8 cells grown in T75 flask were detached with warm accutase at 37°C and were suspended in 3.2% BSA in PBS. FGF2 binding to cells was carried out with R&D kit NFFB0 following manufacturer's instructions. About 100 000 cells were incubated with PBS or peptoid treatment with HLB03-50 (3.7µm, 37µM, 370µM) or HLB04-01 (3.7µm, 37µM, 370µM) for 30 minutes at 4°C. Cells were then incubated 1h with biotinylated FGF2 or biotinylated soya protein (negative CTL) for 1h at 4°C. Then cells were incubated with Avidin conjugated FITC or H_2O for 30 minutes at 4°C. Cells were washed two times and resuspended in wash buffer before analysis with FACS Canto II recording 10 000 events with excitation at 488nm and emission at 530nm. N=1

However, when recording the cells fluorescence by flow cytometry, a new population of cells was observed when treated with peptoid concentrations of 37µM and 370 µM (Figure 5-22). Peptoids are known for permeabilising membranes. The compounds used might have been be toxic for the cells at high concentration. Therefore, cell death was analysed in HKC8 cells with peptoid treatments. The nuclear dye DAPI was used to detect cells integrity in treated cells (Figure 5-23).

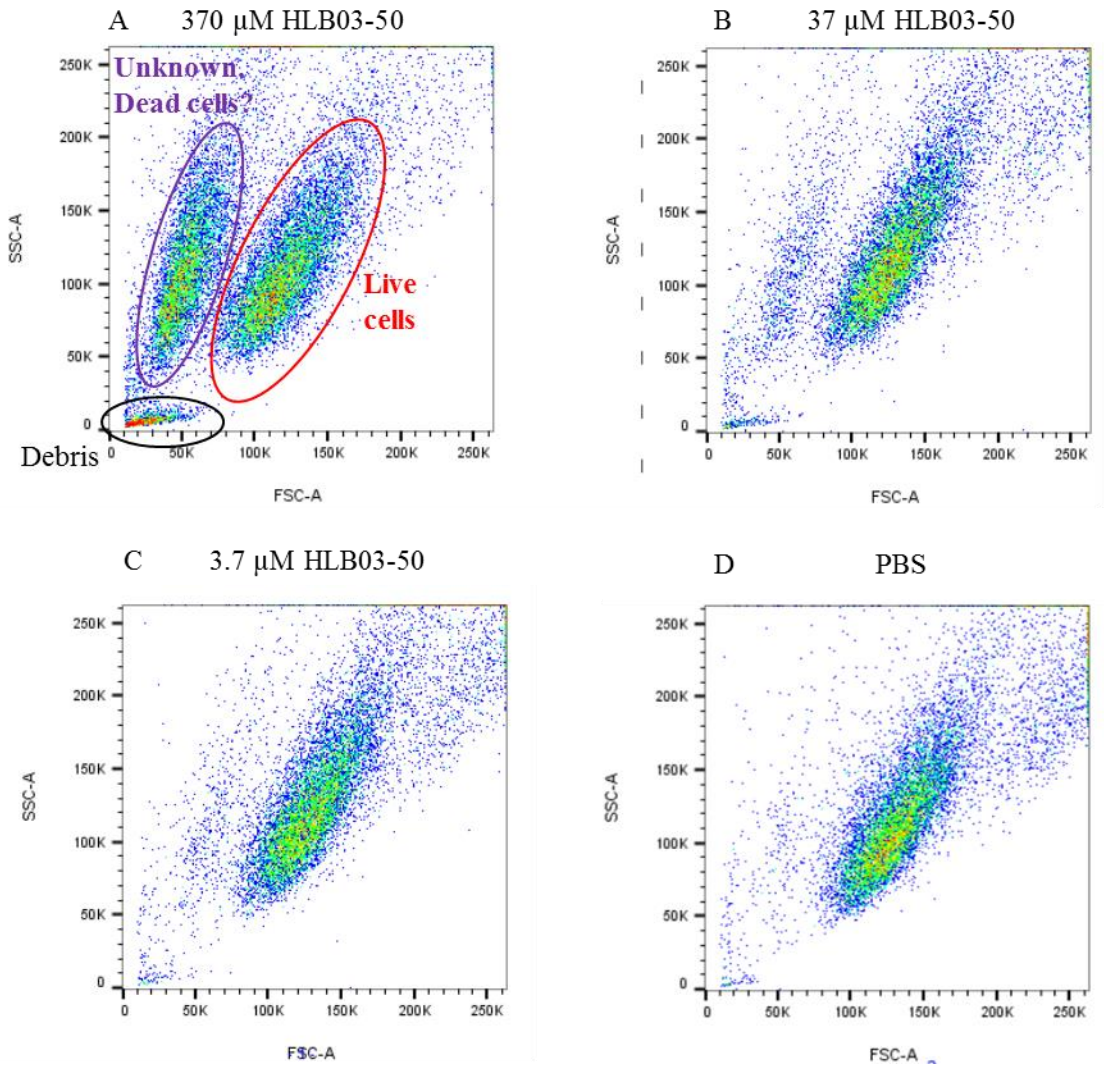

Figure 5-22: Example of the switch in cell morphology with FGF2 treatment and peptoid HLB03-50

HKC8 cells grown in T75 flask were detached with warm accutase at 37°C and were suspended in 3.2% BSA in PBS. FGF2 binding to cells was carried out with R&D kit NFFB0 following manufacturer's instructions. About 100 000 cells were incubated with PBS (D) or peptoid treatment with HLB03-50 (370µM, 37µM, 3.7µm) for 30 minutes at 4°C (A-C respectively). Cells were then incubated 1h with biotinylated FGF2 or PBS for 1h at 4°C. Then cells were incubated with Avidin conjugated FITC or PBS for 30 minutes at 4°C. Cells were washed two times and resuspended in wash buffer before analysis with FACS Canto II recording 10 000 events with excitation at 488nm and emission at 530nm. Live cells are circled in red while debris are seen in black. N=1

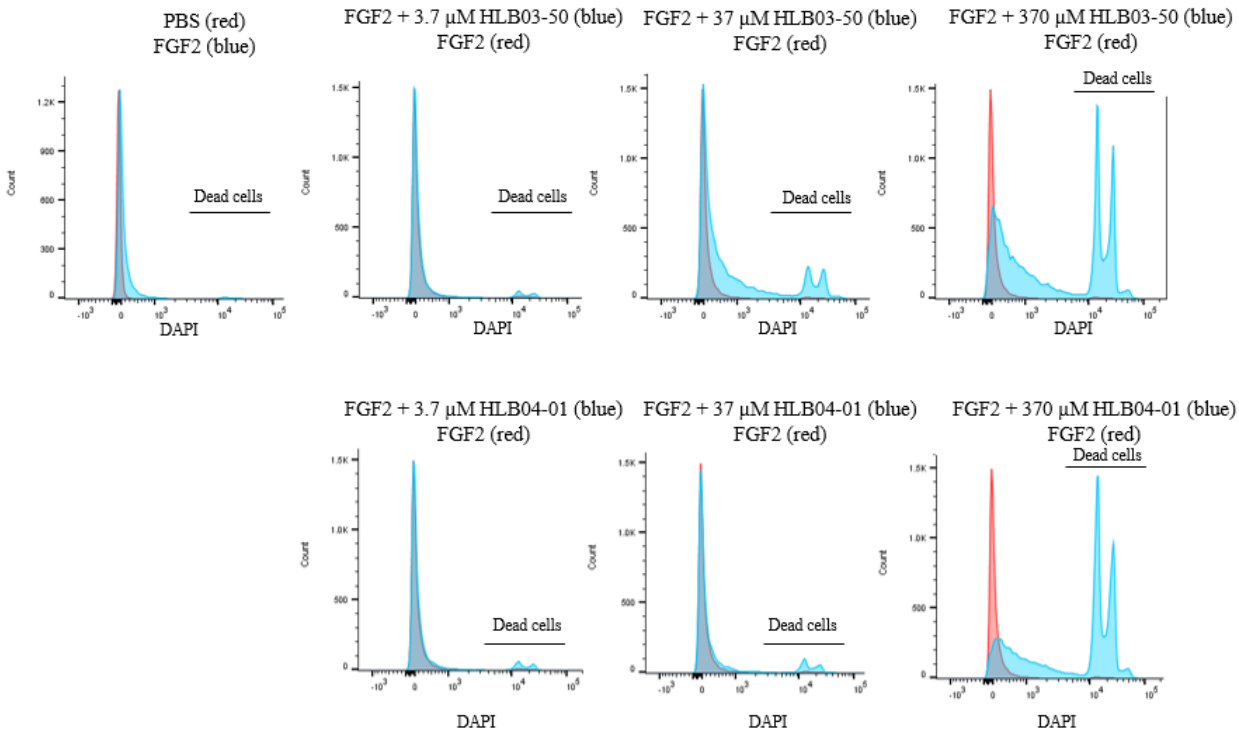

Figure 5-23: DAPI staining with peptoids treatment
HKC8 cells grown in T75 flask were detached with warm accutase at 37°C and were suspended in 3.2% BSA in PBS. FGF2 binding to cells was carried out with R&D kit NFFB0 following manufacturer's instructions. About 100 000 cells were incubated with PBS or peptoid treatment with 03-50 and peptoid HLB 04-01 (370µM, 3.7µm, 37µM) for 30 minutes at 4°C. Cells were then incubated 1h with biotinylated FGF2 or PBS for 1h at 4°C. Then cells were incubated with Avidin conjugated FITC or PBS for 30 minutes at 4°C. Cells were washed two times and resuspended in wash buffer containing DAPI before analysis with FACS Canto II recording 10 000 events with excitation at 488nm and emission at 530nm. DAPI positive cells represent dead cells with a shift of the cell population to the right of the graph.

As observed Figure 5-23, the peptoids treatments increased cell death especially at 370µM. For this reason only a low dose of 4µM was used for the study. Peptides treatment did not show any cell death and therefore the highest dose of 370µM was used in all experiments.

Unfortunately, both peptides and peptoids did not show inhibition of FGF2 binding as seen Figure 5-24. Even though the WT peptide caused a reduction in FGF2 binding, the decrease was not significant. The strong binding of FGF2 to HS with a Kd of about 10^{-9}M could explain the difficulties to compete with binding.

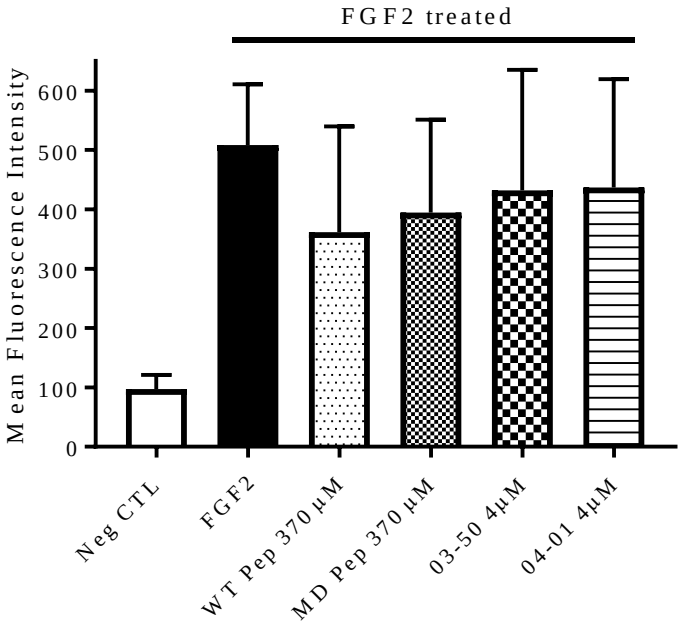

Figure 5-24: FGF2 binding with peptides and peptoids treatment
HKC8 cells grown in T75 flask were detached with warm accutase at 37°C and were suspended in 3.2% BSA in PBS. FGF2 binding to cells was carried out with R&D kit NFFB0 following manufacturer's instructions. About 100 000 cells were incubated with PBS or peptide treatment (370µM) and peptoid treatment (4 µM) for 30 minutes at 4°C. Cells were then incubated 1h with biotinylated FGF2 or soya protein (negative CTL) for 1h at 4°C. Then cells were incubated with Avidin conjugated FITC or PBS for 30 minutes at 4°C. Cells were washed two times and resuspended in wash buffer before analysis with FACS Canto II recording 10 000 events with excitation at 405nm and emission at 450nm. FGF2 binding to the cells resulted in an increase in the Mean Fluorescence Intensity. All peptides and peptoids treatment did not successfully inhibit FGF2 binding. N≥3.

5.4 Discussion

Peptides based therapies are very attractive. Compared to larger molecules, they are less immunogenic, often more active, quicker to generate and cheaper. However, it does have challenges. Their degradation and clearance can be fast (sometimes within minutes), they often have a poor solubility and therefore often need to be delivered intravenously (Vlieghe *et al.*, 2010). However, in cancer research, FGF2 based peptides had already been developed in order to inhibit proliferation (Terada *et al.*, 2006; Fan *et al.*, 2015). Peptides binding to HS have been shown to inhibit herpes virus entry *in vitro* (Dogra *et al.*, 2015) and for amyloid deposit *in vitro* and *in vivo* (Wall *et al.*, 2011; Martin *et al.*, 2013). This highlights the potential of synthesising a peptide with high affinity to HS. Additionally, studying peptoids gives a lot of advantages as they are resistant to proteases, not immunogenic and have a better cell permeability compared to peptides (Simon *et*

al., 1992; Kwon and Kodadek, 2007; Astle *et al.*, 2008). Their helical structure is an advantage for HS binding as the positive charges are displayed in a different manner than linear peptides.

It was somewhat surprising to observe dissociation constants above 100µM for both synthesised peptides. These results are likely to be related to their unfolded structure as a strong relationship between spatial arrangement of positive charge and a peptide's ability to bind HS has been reported in the literature (Rullo and Nitz, 2010). A 3-10 helix was expected for the peptides as the sequence chosen generates this pattern within FGF2. The unfolded structure could be explained by a lack of hydrogen bonding on the peptides. The α-chiral side chain on every third residue of the peptoid generates the helical secondary structure and was expected (Ford *et al.*, 2013). In fact, peptoid HLB03-50 displayed a helicoidal repartition of the positive charges and had a stronger binding, almost ten times higher than the peptide and a higher binding stoichiometry. Peptide binding to heparin showed an exothermic reaction while peptoid was endothermic. Furthermore, this study did not find a significant difference between MD peptide and WT peptide. The replacement of only one positively charged amino acid could explain this. Additionally, it is possible that if both peptides were helical, the difference in binding would be increased.

The body already has some molecules that modulate FGF2 availability and bioactivity. In future studies, a peptide sequence based on known proteins that compete or inhibit FGF2 binding should be used. For example, thrombospondin 1 was shown to reduce the binding of FGF2 to the endothelium (Margosio *et al.*, 2003). *In vitro*, the anti-proliferative activity of endostatin has been hypothesised to be due to its binding to HS FGF2 binding patterns (Ricard-Blum *et al.*, 2004). The pentraxin-related protein PTX3 naturally inhibits FGF2 stimulated angiogenesis and specific peptides from the binding pattern of PTX3 were successful at showing similar effects (Leali *et al.*, 2010). Within the circulation, the plasma protein α2-macroglobulin can bind to FGF2 and diminish fetal bovine heart endothelial proliferation *in vitro* (Asplin *et al.*, 2001). Furthermore, FGF2 activity can be diminished by Platelet factor 4 which supposedly inhibit FGF2 dimerisation and therefore binding to the receptor (Perollet *et al.*, 1998). Platelet derived growth factor abolished bovine aorta endothelial cells proliferation and migration in response to FGF2 (de Marchis *et al.*, 2002). CXCL13 can display FGF2 from cells and decreased FGF2 induced proliferation of HUVEC (Spinetti *et al.*, 2001). This shows that there are other possible peptides that could be more effective in competing FGF2 binding.

Another strategy to target growth factor binding to HS would be the use of HS mimetics which are chemically modified heparin derivatives. These compounds have shown promising results in muscle satellite cells where FGF2 activation of ERK signalling was decreased with treatment (Ghadiali *et al.*, 2017). Our laboratory has just started a collaboration with the University of Liverpool and the first results of HS mimetics treatment with renal epithelial cells HKC8 showed a decrease in FGF2 biological activity as seen Figure 5-25.

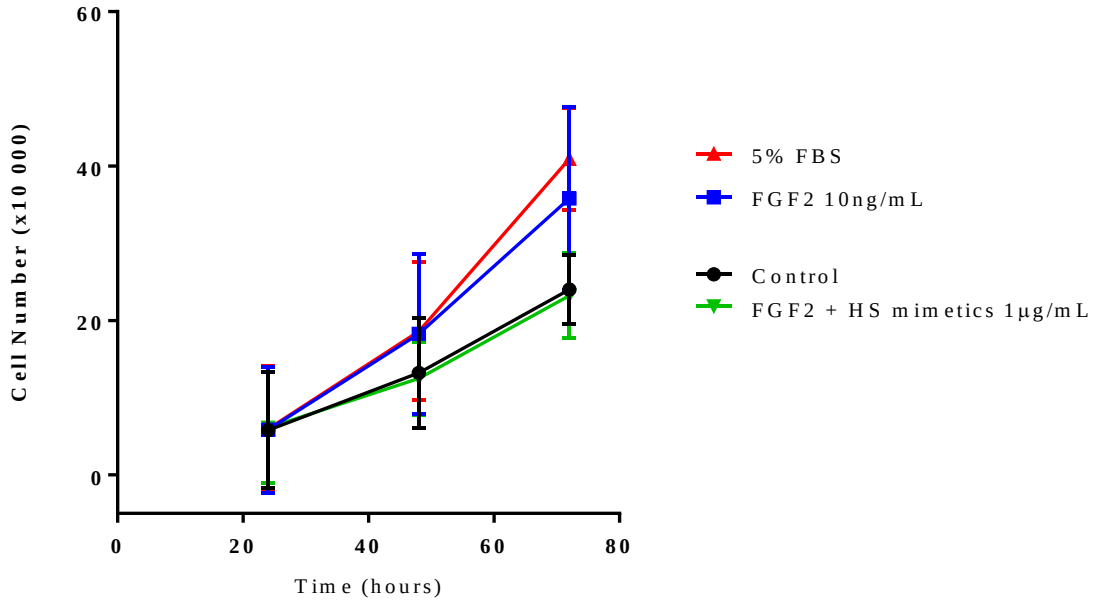

Figure 5-25: HS mimetic on HKC8 proliferation
HS mimetics were kindly given by Prof. Jeremy Turnbull the University of Liverpool. HKC8 cells were seeded in 24 well plate and counted at 24h, 48h and 72h with a haemocytometer. Control cells were incubated with 0.5%FBS media supplemented with dilution buffer only. Treated cells were incubated with 0.5%FBS media supplemented with FGF2 10ng/mL ± HS mimetic 1µg/mL. A positive control with 5%FBS media was used to assess maximum growth rate. These data were generated by MRes student Hanna Lane supervised by Laura Ferreras.

HKC8 growth was increased with FGF2 treatment and the addition of HS mimetic reduced the growth to basal level as seen with starvation media only. HS mimetics can be specifically desulfated. The one used in Figure 5-25 is specifically 6-O-desulfated but does have N and 2-O-sulfation, the latter being important for HS binding to FGF2. Therefore, it could be hypothesised that this HS mimetic binds to FGF2 but does not allow the growth factor to bind its receptor due to the lack of 6-O-sulfation and therefore inhibit its biological activity. The use of HS mimetic is very promising and will further be explored in our laboratory.

In conclusion, results presented in this chapter showed that positive charge organisation on a molecule can affect HS binding, with a helicoidal molecule having a stronger affinity. Additionally, peptide and peptoids synthesised did not significantly change FGF2 binding to renal epithelial cells. The use of peptoids at high concentration was found to be toxic for the cells and therefore could not be developed further. New peptide sequences inspired by competitive protein for FGF2 binding should be further explored together with HS mimetics.

6 General discussion

Heparan Sulfate plays a central role in development, homeostasis and disease progression as it is present on the cells membrane and ECM. HS sulfation is essential for HS function. The sulfated patterns regulate HS interaction with proteins including cytokines and growth factors, hence, modulating cell signalling and behaviour. To date, there is very little literature about HS and renal diseases even though some HS modifying enzymes are overexpressed during fibrosis and therefore promising biomarkers (Einecke *et al.*, 2010; Tátrai *et al.*, 2010; Yue *et al.*, 2013; Lu *et al.*, 2014; DePianto *et al.*, 2015). Renal fibrosis is incurable, and every avenue should be explored to understand and develop new therapeutics. This project had the ambition to analyse the modulation of HS during fibrosis, understand the biological significance of it and finally to develop potential inhibitors of HS growth factors binding.

6.1 Findings arising from this study

6.1.1 HS modulation *in vivo*: results and implications

The first aim of this work was to determine if HS sulfation and HS modifying enzymes changed during the development of renal fibrosis.

In chapter 3, HS sulfation was analysed in an *in vivo* model of renal fibrosis. GAGs sequencing showed an increase in HS N- and 2-O-sulfation together with a decrease in 6-O-sulfation at D5 and D10 of unilateral ureteral obstruction (UUO). Total HS 3-O-sulfation staining was decreased at D5 and D10 UUO. Specific staining of HS3ST1 generating HS 3-O-sulfation showed similar results.

These results showed that renal fibrosis progression triggered HS N- and 2-O-sulfation increase and HS 3-O and 6-O-sulfation diminution. It can be speculated that this change in cells and matrices surfaces modulates growth factors binding. Potentially these alterations are promoting fibrosis. In accordance with the present results, previous studies have demonstrated that N-sulfation was increased in pulmonary fibrosis (Lu *et al.*, 2014; Westergren-Thorsson *et al.*, 2017) and N-sulfated/acetylated/sulfated patterns were important in attracting immune cells by modulating cytokines presented by the cells (Lortat-Jacob *et al.*, 1995; Spillmann *et al.*, 1998). Hence

decreasing N-sulfation can be a promising target for limiting pro fibrotic growth factors activities. However, as N-sulfation is often required for other sulfated pattern, the inhibition of HS 2-O-sulfation might be more specific for targeting renal fibrosis. The somehow surprising decrease in HS 6-O-sulfation was conflicting with the increase observed in lung fibrosis (Lu *et al.*, 2014; Westergren-Thorsson *et al.*, 2017). However, this result supports evidence from previous observations from Tatrai *et al.* who showed a decrease in 6-O-sulfation with liver fibrosis (Tátrai *et al.*, 2010). The modulation of HS 6-O-sulfation might be organ specific. In fact, HS 2-O-sulfation seems more important than 6-O-sulfation in kidneys as HS2ST1 -/- mice but not HS6STs -/- mice developed renal agenesis (Bullock *et al.*, 1998; Habuchi *et al.*, 2007; Habuchi and Kimata, 2010). Therefore, HS 2-O-sulfation in kidney should be further studied as it has good potential as a marker of renal function. Another therapeutic approach would be to increase the amount of HS 3-O-sulfation. The decrease in HS 3-O-sulfation seen in our model was also observed in liver fibrosis (Tátrai *et al.*, 2010). Restoring HS 3-O-sulfation could enhance binding and signalling of potent cytoprotective growth factors including HB-EGF.

Additionally, HS modifying enzymes expression were detected by RT-qPCR. HS2ST1, SULF1 and HS3ST1 were increased and significantly correlated to collagen deposition. In contrast, HS3ST3A was decreased but also significantly correlated to collagen deposition. These results are in line with those of previous studies. HS6STs and HS3ST1 were overexpressed in pulmonary fibrosis (Lu *et al.*, 2014; DePianto *et al.*, 2015) and heparanase, SULF1, SULF2, HS3ST1 were overexpressed in liver fibrosis (Tátrai *et al.*, 2010).

These findings highlight the potential of HS modifying enzymes as biomarkers. Remarkably, HS3ST1 enzymes stands out by having the best correlation in our and other studies (Tátrai *et al.*, 2010). Additionally, HS3ST1 correlates with glomerular filtration rate and graft survival (Bunnag *et al.*, 2009; Einecke *et al.*, 2010; Sagoo *et al.*, 2010).

There are several explanations for the inconsistency between HS3ST1 increase and HS 3-O-sulfation decrease. First, the increase in expression can originate from endothelial cells considering that blood vessels staining were not decreased with the days of UUO. Second, infiltrating cells could have an increased expression of HS3ST1 as interstitial staining was observed at D5 UUO. In fact, activated macrophages M2 have high level of HS3ST1 mRNA level (Martinez *et al.*, 2015). Another potential explanation could be the lack of HS precursor for HS3ST1 activity. Finally, HS

3-O-sulfation was analysed by immunofluorescence and there is a possibility that the sulfation pattern is masked by proteins bound to it. Further work is required to confirm these findings and hypothesis.

6.1.2 Modulation of Heparan sulfate 3-O-sulfotransferases expression: results and implication

The first aim of chapter 4 was to investigate what modulates HS3STs expression. TGFβ1 is one of the most studied pro-fibrotic growth factors. Additionally, research has shown that TGFβ1 increased SULF1 expression *in vitro* and *in vivo* (Properzi *et al.*, 2008; Yue *et al.*, 2008). However, the impact of TGFβ1 on HS3STs expression has never been explored before. This study showed for the first time that TGFβ1 is involved in regulating HS3STs expression in renal epithelial cells and fibroblasts. In renal epithelial cells, while HS3ST1 was generally decreased, HS3ST3B was increased with treatment. Furthermore, renal fibroblasts showed the highest decrease in HS3ST1 expression accompanied with a change in cells morphology.

IL1β is a cytokine involved in inflammation and tissue repair. Additionally, the combination of TGFβ2 and IL1β has pro-fibrotic properties by promoting endothelial to mesenchymal transition (Maleszewska *et al.*, 2013). This treatment showed similar results to TGFβ1. HS3ST1 was decreased in renal epithelial cells and fibroblasts while HS3ST3B was increased in renal epithelial cells.

Together these results provide important insights into HS3STs regulation by TGFβs and IL1β stimulation. Considering the results seen *in vivo* in chapter 3, it can be suggested that these factors are contributing to the decrease in HS 3-O-sulfation observed on the tubules basement membrane of UUO samples. However, none of the treatments used increased HS3ST1 expression as seen *in vivo*. This increase could potential come from endothelial cells or macrophages which express high levels of HS3ST1 (Martinez *et al.*, 2015). To develop a full picture of HS3ST1 expression in renal fibrosis, additional studies will be needed that analyse different cell lines and different growth factors.

The generation of HS3ST1 overexpressing tubular epithelial cells led to the decrease of HS6ST1 expression. This observation may support the hypothesis of a GAGosome within the cells where

HS modifying enzymes interact with each other. It can thus be suggested that the increase in HS3ST1 within the Golgi inhibits HS6ST1 expression by a yet to be determined mechanism. The decrease in HS6ST1 was mirrored by a decrease in the disulfated disaccharide GlcA-GlcNS6S. The same disaccharide was found decreased *in vivo*. Therefore, these data suggest that the decrease in HS 6-O-sulfation and the increase in HS3ST1 expression could be correlated.

HKC8-HS3ST1 cells binding and signalling of FGF2 was similar to HKC8-CTL. The 3-O-sulfation does not seem to be involved in FGF2 binding. These data correlate with previous studies on HS3ST1 transfected CHO cells which showed no difference in FGF2 binding compared to control (Thacker *et al.,* 2016b). However, HKC8-HS3ST1 showed a biphasic response to HB-EGF treatment seen by a phosphorylation of STAT3 at 5 minutes and 1 hour. Whether this second signalling is from HB-EGF potentially retained in the ECM or a second messenger is to be determined. The association of HS3ST1 expression and HB-EGF signalling could explain the decrease observed in both HS 3-O-sulfation and HB-EGF staining *in vivo*. Hence, it could conceivably be hypothesised that HB-EGF requires HS 3-O-sulfation to bind to tubular epithelial cells.

HB-EGF has both protective and healing properties. Following intestinal ischemia reperfusion, HB-EGF -/- mice are more susceptible to intestinal ischemia reperfusion injuries (El-Assal *et al.*, 2008) and HB-EGF administration accelerated intestinal recovery after ischemia reperfusion (El-Assal and Besner, 2005). Furthermore, HB-EGF is important for tubular cells repair (Sakai *et al.*, 1997) and protective in liver fibrosis (Huang *et al.,* 2012; Takemura *et al.*, 2013). Therefore, the modulation of HS 3-O-sulfation and to some extend HB-EGF binding should be further explored to potentially create new therapeutics.

A summary of chapter 3 and chapter 4 findings on HS3STs and HS 3-O-sulfation modulation in fibroblasts and epithelial tubular cells/ tubular staining is displayed Figure 6-1.

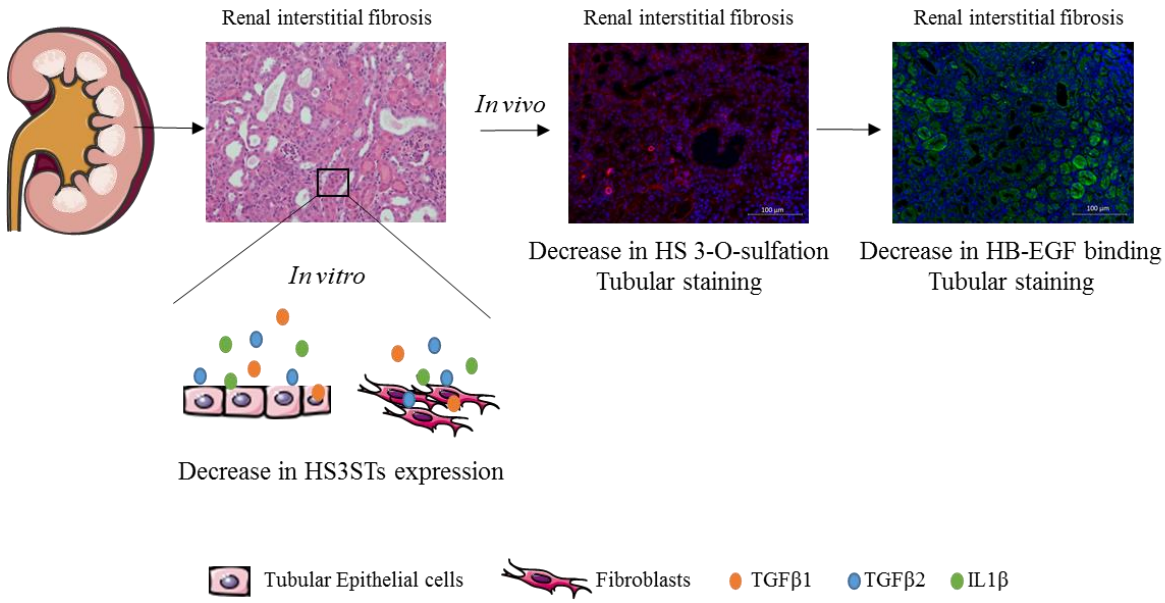

Figure 6-1: Summary of HS 3-O-sulfation modulation by growth factors *in vitro* and by interstitial fibrosis progression *in vivo*

6.1.3 Synthesis of potential inhibitors of FGF2 binding to heparan sulfate: results and implication

Peptides and peptoids synthesis offer a large range of new compounds and potential drugs. HS, FGF2 and FGFR have been crystalised and FGF2 binding to HS extensively studied. The aim of section 5 was to assess the binding of peptides and peptoids to heparin and investigate their potential binding competition with FGF2 to renal tubular epithelial cells. The peptides were designed based on FGF2 binding region with HS.

The WT peptide with more positive charged displayed a stronger binding than the MD peptide. However, peptoids had the best constant binding dissociation compared to peptides. These results provide two indications on HS binding to protein. First that positive charge is important for binding and second, that their structural organisation has a significant impact on the binding strength. Interestingly, FGF2 WT and MD peptides did not significantly decrease FGF2 binding to the cells at high concentration. Peptoids at high concentration showed a promising inhibition of binding. However, due to the toxicity of the peptoids, they could not be used at high concentration and low dose were not as effective.

FGF2 peptides have been generated previously and successfully decreased proliferation and migration in endothelial cells stimulated with FGF2 *in vitro* and angiogenesis *in vivo* (Facchiano *et al.*, 2003). However, in this study, the sequence used DPHIKLQLQAE is predicted to be required for FGF2 dimerisation. Hence, the authors targeted FGF2 dimerisation and not its interaction with HS. The strong binding between HS and FGF2 (Kd= 32nM) could explain the incapacity of the compounds to inhibit or displace FGF2 to HS (Ibrahimi *et al.*, 2004).

The dosage of peptoids is important due to their potential toxicity. However they are very promising and are nowadays being developed and used *in vivo* as antimicrobial agents (Czyzewski *et al.*, 2016).

6.2 Limitations and future work

There are several questions that remain unanswered from the *in vivo* results. First, the cells overexpressing HS3ST1 during fibrosis have not been identified. The isolation of different cell types from fibrotic kidneys would provide insights into what cells trigger the change in HS3ST1 expression. Furthermore, the staining of renal tissue with the labelled AT generated in our laboratory should give thought-provoking questions regarding the clinical relevance of what was found *in vivo*.

The analyses of HS 3-O-sulfation for the *in vivo* work was only assessed by fluorescence staining due to the lack of standard for the HPLC. Fluorescence is a great tool for localising molecule but is not the best technique for quantification. Staining techniques have several limitations with technical and interpretation bias including fixation technique, peptide retrieval, types and clones of antibodies and the observer accuracy (Matos *et al.*, 2010). GAGs composition can be analysed by mass spectrometry (Staples and Zaia, 2011), a technique that could have been better. Only few groups are capable of doing it and my collaborators could not do it.

Additionally, only one model of renal interstitial fibrosis was used. An ischemia reperfusion injury model could have been used to reinforce the data on the correlation between HS modifying enzymes and the development of fibrosis.

HS modifying enzymes expression was only analysed on a gene level. In the current market, the antibodies generated for these enzymes are of poor quality and not very specific. I did try to use an antibody for HS3ST1 by using the HKC8-HS3ST1 cells as positive control, but it was unsuccessful.

Regarding the *in vitro* work, only two cell types, renal epithelial cells and fibroblasts were used. It would have been interesting to use endothelial cells and leukocytes with the different treatments used in my study. This could potential specify which cells were responsible for the increase of HS3ST1 in the kidney. Additionally, the cell lines were immortalised cells and primary cells could have further validated our *in vitro* data.

The two treatments of TGFβ1, TGFβ2 IL1β were used as they were widely used in my laboratory. The treatments concentration had been optimised by previous students. However, other growth factors and cytokines such as TNFα, LPS could have been used to screen their effect on renal epithelial and fibroblast cells.

The generation of overexpressing cells can influence the cell activity, behaviour and response to treatment. However, I tried to avoid any bias by generating mock cells and by using different clones. Additionally, the use of HS3ST1-/- mice would have been ideal to study. However, considering the time frame of my project it was not feasible. The interaction between HS 3-O-sulfation and HB-EGF has only been studied by cell signalling. Further studies looking at HB-EGF binding to HS should be required to determine the exact sequence essential for binding and signalling.

The use of peptides and peptoids in only one cell type can explain the lack of competition observed. FGF2 being important for fibroblast, it would have been interesting to screen the peptides and peptoids inhibition on them. However, the NRK-49F cells only became available during the last months of my project.

Initially, the peptoids were used as positive control for ITC but due to their strong binding to heparin, were further studied. However, they were only used for FGF2 binding competition assay. As they are not specific to FGF2, it would have been interesting to use these compounds in other models with different growth factors.

6.3 New avenues

This work highlighted for the first time the significance of several HS modifying enzymes correlation to renal fibrosis. The panel of these enzymes should be further studied in human renal fibrosis as they could potentially be biomarkers of disease progression. Furthermore, as seen in Figure 6-2, the changes in HS modifying enzymes do not seem to be only specific to renal fibrosis and a wider study on multiple fibrotic tissues could investigate if HS sulfotransferase and sulfates expression have a specific signature during fibrosis.

In line with the data on HS3ST1 expression, Einecke *et al.* found that HS3ST1 was overexpressed in rejected renal graft (Einecke *et al.*, 2010).Therefore, it would be interesting to see if HS3ST1 is correlated with renal allograft pathologies. Furthermore, HS3ST1 is found overexpressed in renal, liver and lung fibrosis (Figure 6-2). There is a huge potential in HS3ST1 studies to discover a potential biomarker or target for treating fibrosis.

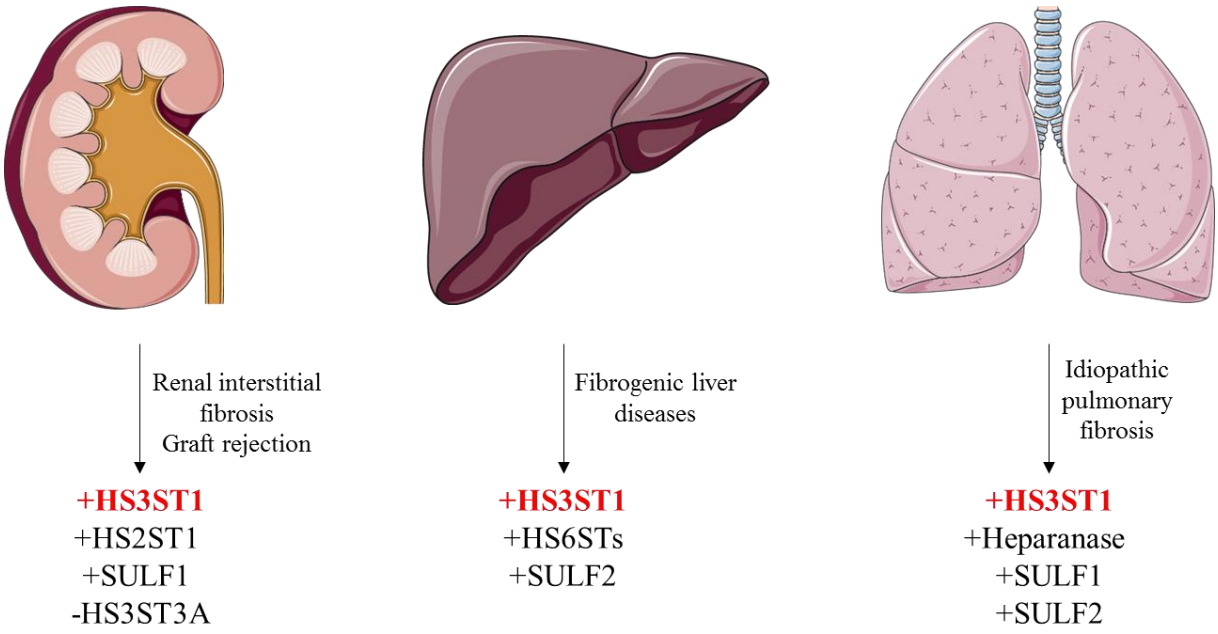

Figure 6-2: HS modifying enzymes in fibrosis
Summary of several research on HS in fibrotic diseases. A "+" means an increase of mRNA level in the tissue and a "-"a decrease. (Einecke *et al.*, 2010; Tátrai *et al.*, 2010; Yue *et al.*, 2013; Lu *et al.*, 2014; DePianto *et al.*, 2015).

To further explore the potential of HS as biomarker, recent studies have measured HS in urine samples of patients with septic shock by mass spectrometry. The authors found that HS was elevated in patients with sepsis and was correlated with renal dysfunction. Furthermore, the amount of HS was predictive of patients mortality (Schmidt *et al.*, 2016). Even though the analysis of HS levels and HS sulfation are attractive predictive tools, the use of mass spectrometry is costly. Therefore, there is a need to develop further the techniques currently used for GAGs analysis to make them easier and cheaper.

Most studies about HS sulfation in diseases have not studied HS 3-O-sulfation. This is mainly due to its rare prevalence and because it is technically difficult to analyse. However, the work presented in this thesis emphasises the need to explore the relevance of HS 3-O-sulfation in disease progression and the necessity to develop HS 3-O-sulfated standards for HPLC analysis.

In conclusion, this project demonstrated that HS 3-O-sulfotransferases expression is modulated by pro-inflammatory and pro-fibrotic growth factors and are correlated with the development of fibrosis. These may affect HS pattern on the cell surface and ECM to enhance or diminish the binding of growth factors. Furthermore, HS 3-O-sulfation is implicated in HB-EGF signalling in a potentially protective mechanism. Finally, the generation of peptides and peptoids to inhibit HS binding to growth factors should have specific secondary structure to allow strong binding. The use of peptoids is promising but more optimisation on their toxicity vs efficacy dose should be performed.

A better understanding of the role of HS3STs in growth factor signalling and fibrosis will allow the development of novel biomarkers and potential therapeutics that could prevent fibrosis and organ loss.

7 References

De Agostini, A. I. (2006) ‘An unexpected role for anticoagulant heparan sulfate proteoglycans in reproduction’, *Swiss Medical Weekly*, 136(37–38), pp. 583–590.

De Agostini, A. I., Dong, J. C., Arrighi, C. D. V., Ramus, M. A., Dentand-Quadri, I., Thalmann, S., Ventura, P., Ibecheole, V., Monge, F., Fischer, A. M., Hajmohammadi, S., Shworak, N. W., Zhang, L., Zhang, Z. and Linhardt, R. J. (2008) ‘Human follicular fluid heparan sulfate contains abundant 3-O-sulfated chains with anticoagulant activity’, *Journal of Biological Chemistry*, 283(42), pp. 28115–28124.

De Agostini, A. I., Watkins, S. C., Slayter, H. S., Youssoufian, H. and Rosenberg, R. D. (1990) ‘Localization of anticoagulantly active heparan sulfate proteoglycans in vascular endothelium: Antithrombin binding on cultured endothelial cells and perfused rat aorta’, *Journal of Cell Biology*, 111(3), pp. 1293–1304.

Aikawa, J. and Esko, J. D. (1999) ‘Molecular cloning and expression of a third member of the heparan sulfate/heparin GlcNAc N-deacetylase/ N-sulfotransferase family.’, *The Journal of biological chemistry*, 274(5), pp. 2690–5.

Alhasan, A. A., Spielhofer, J., Kusche-Gullberg, M., Kirby, J. A. and Ali, S. (2014) ‘Role of 6-O-sulfated heparan sulfate in chronic renal fibrosis.’, *The Journal of biological chemistry*, 289(29), pp. 20295–306.

Ali, M. M., Karasneh, G. A., Jarding, M. J., Tiwari, V. and Shukla, D. (2012) ‘A 3-O-sulfated heparan sulfate binding peptide preferentially targets herpes simplex virus 2-infected cells.’, *Journal of virology*, 86(12), pp. 6434–43.

Ali, S., O’Boyle, G., Hepplewhite, P., Tyler, J. R., Robertson, H. and Kirby, J. A. (2010) ‘Therapy with nonglycosaminoglycan-binding mutant CCL7: a novel strategy to limit allograft inflammation.’, *American Journal of Transplantation*, 10(1), pp. 47–58.

Altrock, E., Sens, C., Wuerfel, C., Vasel, M., Kawelke, N., Dooley, S., Sottile, J. and Nakchbandi, I. A. (2015) ‘Inhibition of fibronectin deposition improves experimental liver fibrosis’, *Journal of Hepatology*, 62(3), pp. 625–633.

Amblard, M., Fehrentz, J.-A., Martinez, J. and Subra, G. (2006) ‘Methods and Protocols of Modern Solid Phase Peptide Synthesis’, *Molecular Biotechnology*, 33(3), pp. 239–254.

Anders, H.-J., Ninichuk, V. and Schlöndorff, D. (2006) ‘Progression of kidney disease: blocking leukocyte recruitment with chemokine receptor CCR1 antagonists.’, *Kidney international*, 69(1), pp. 29–32.

Armelin, H. A. (1973) ‘Pituitary extracts and steroid hormones in the control of 3T3 cell growth.’, *Proceedings of the National Academy of Sciences of the United States of America*, 70(9), pp. 2702–6.

Ashikari-Hada, S., Habuchi, H., Kariya, Y., Itoh, N., Reddi, A. H. and Kimata, K. (2004) ‘Characterization of Growth Factor-binding Structures in Heparin/Heparan Sulfate Using an Octasaccharide Library’, *Journal of Biological Chemistry*, 279(13), pp. 12346–12354.

Asplin, I. R., Wu, S. M., Mathew, S., Bhattacharjee, G. and Pizzo, S. V (2001) ‘Differential regulation of the fibroblast growth factor (FGF) family by alpha(2)-macroglobulin: evidence for selective modulation of FGF-2-induced angiogenesis.’, *Blood*, 97(11), pp. 3450–7.

Astle, J. M., Udugamasooriya, D. G., Smallshaw, J. E. and Kodadek, T. (2008) ‘A VEGFR2 Antagonist and Other Peptoids Evade Immune Recognition’, *International Journal of Peptide Research and Therapeutics*, 14(3), pp. 223–227.

Axelsson, J., Xu, D., Kang, B. N., Nussbacher, J. K., Handel, T. M., Ley, K., Sriramarao, P. and Esko, J. D. (2012) ‘Inactivation of heparan sulfate 2-O-sulfotransferase accentuates neutrophil infiltration during acute inflammation in mice.’, *Blood*, 120(8), pp. 1742–51.

Babelova, A., Moreth, K., Tsalastra-Greul, W., Zeng-Brouwers, J., Eickelberg, O., Young, M. F., Bruckner, P., Pfeilschifter, J., Schaefer, R. M., Gröne, H.-J. and Schaefer, L. (2009) ‘Biglycan, a danger signal that activates the NLRP3 inflammasome via toll-like and P2X receptors.’, *The Journal of biological chemistry*, 284(36), pp. 24035–48.

Baer, P. C., Bereiter-Hahn, J., Schubert, R. and Geiger, H. (2006) ‘Differentiation status of human renal proximal and distal tubular epithelial cells in vitro: Differential expression of characteristic markers’, *Cells Tissues Organs*, 184(1), pp. 16–22.

Baker, M. E. (1998) ‘Albumin’s role in steroid hormone action and the origins of vertebrates: Is albumin an essential protein?’, *FEBS Letters*, 439(1–2), pp. 9–12.

Balazs, E. A., Laurent, T. C. and Jeanloz, R. W. (1986) ‘Nomenclature of hyaluronic acid.’, *The Biochemical journal*, 235(3), p. 903.

Basile, D., Anderson, M. and Sutton, T. (2012) ‘Pathophysiology of Acute Kidney Injury’, *Comprehensive Physiology*, 2(2), pp. 1303–1353.

Basilico, C. and Moscatelli, D. (1992) ‘The FGF family of growth factors and oncogenes.’, *Advances in cancer research*, 59, pp. 115–65.

Bedke, J., Nelson, P. J., Kiss, E., Muenchmeier, N., Rek, A., Behnes, C.-L., Gretz, N., Kungl, A. J. and Gröne, H.-J. (2010) ‘A novel CXCL8 protein-based antagonist in acute experimental renal allograft damage.’, *Molecular immunology*, 47(5), pp. 1047–57.

Bello, A. K., Alrukhaimi, M., Ashuntantang, G. E., Basnet, S., Rotter, R. C., Douthat, W. G., Kazancioglu, R., Köttgen, A., Nangaku, M., Powe, N. R., White, S. L., Wheeler, D. C. and Moe, O. (2017) ‘Complications of chronic kidney disease: current state, knowledge gaps, and strategy for action’, *Kidney International Supplements*, 7(2), pp. 122–129.

Belmonte, J. M., Clendenon, S. G., Oliveira, G. M., Swat, M. H., Greene, E. V, Jeyaraman, S., Glazier, J. A. and Bacallao, R. L. (2016) ‘Virtual-tissue computer simulations define the roles of cell adhesion and proliferation in the onset of kidney cystic disease’, *Molecular Biology of the Cell*, 27(22), pp. 3673–3685.

Berry, L., Andrew, M., Post, M., Ofosu, F. and O’Brodovich, H. (1991) ‘A549 Lung Epithelial Cells Synthesize Anticoagulant Molecules on the Cell Surface and Matrix and in Conditioned Media’, *American Journal of Respiratory Cell and Molecular Biology*, 4(4), pp. 338–346.

Bertram, J. F., Douglas-Denton, R. N., Diouf, B., Hughson, M. D. and Hoy, W. E. (2011) ‘Human nephron number: Implications for health and disease’, *Pediatric Nephrology*, 26(9), pp. 1529–1533.

Besner, G., Higashiyama, S. and Klagsbrun, M. (1990) ‘Isolation and characterization of a macrophage-derived heparin-binding growth factor.’, *Cell regulation*, 1(11), pp. 811–9.

Biroccio, A., Cherfils-Vicini, J., Augereau, A., Pinte, S., Bauwens, S., Ye, J., Simonet, T., Horard, B., Jamet, K., Cervera, L., Mendez-Bermudez, A., Poncet, D., Grataroli, R., de Rodenbeeke, C. T., Salvati, E., Rizzo, A., Zizza, P., Ricoul, M., Cognet, C., Kuilman, T., Duret, H., Lépinasse, F., Marvel, J., Verhoeyen, E., Cosset, F.-L., Peeper, D., Smyth, M. J., Londoño-Vallejo, A., Sabatier, L., Picco, V., Pages, G., Scoazec, J.-Y., Stoppacciaro, A., Leonetti, C., Vivier, E. and Gilson, E. (2013) 'TRF2 inhibits a cell-extrinsic pathway through which natural killer cells eliminate cancer cells', *Nature Cell Biology*, 15(7), pp. 818–828.

Bobik, A. (2004) 'Hypertension, transforming growth factor-beta, angiotensin II and kidney disease', *J Hypertens*, 22(7), pp. 1265–1267.

Bolt, H. L., Eggimann, G. A., Jahoda, C. A. B., Zuckermann, R. N., Sharples, G. J. and Cobb, S. L. (2017) 'Exploring the links between peptoid antibacterial activity and toxicity', *MedChemComm*, 8(5), pp. 886–896.

Bolt, H. L., Williams, C. E. J., Brooks, R. V., Zuckermann, R. N., Cobb, S. L. and Bromley, E. H. C. (2017) 'Log D versus HPLC derived hydrophobicity: The development of predictive tools to aid in the rational design of bioactive peptoids', *Biopolymers*, 108(4), p. e23014.

Border, W. A., Noble, N. A., Yamamoto, T., Harper, J. R., Yamaguchi, Y., Pierschbacher, M. D. and Ruoslahti, E. (1992) 'Natural inhibitor of transforming growth factor-β protects against scarring in experimental kidney disease', *Nature*, 360(6402), pp. 361–364.

Van Den Born, J., Van Den Heuvel, L. P. W. J., Bakker, M. A., Veerkamp, J. H., Assmann, K. J., Weening, J. J. and Berden, J. H. (1993) 'Distribution of GBM heparan sulfate proteoglycan core protein and side chains in human glomerular diseases', *Kidney International*, 43(2), pp. 454–463.

Borza, D. B. (2016) 'Alternative pathway dysregulation and the conundrum of complement activation by IgG4 immune complexes in membranous nephropathy', *Frontiers in Immunology*, 7(ART157), pp. 1–8.

Borza, D. B. (2017) 'Glomerular basement membrane heparan sulfate in health and disease: A regulator of local complement activation', *Matrix Biology*, 57–58, pp. 299–310.

Brandner, B., Rek, A., Diedrichs-Möhring, M., Wildner, G. and Kungl, A. J. (2009) 'Engineering the glycosaminoglycan-binding affinity, kinetics and oligomerization behavior of RANTES: a tool

for generating chemokine-based glycosaminoglycan antagonists.', *Protein engineering, design & selection : PEDS*, 22(6), pp. 367–73.

Braun, C., Schultz, M., Fang, L., Schaub, M., Back, W. E., Herr, D., Laux, V., Rohmeiss, P., Schnuelle, P. and van der Woude, F. J. (2001) 'Treatment of chronic renal allograft rejection in rats with a low-molecular-weight heparin (reviparin).', *Transplantation*, 72(2), pp. 209–15.

Breton, C., Fournel-Gigleux, S. and Palcic, M. M. (2012) 'Recent structures, evolution and mechanisms of glycosyltransferases', *Current Opinion in Structural Biology*, 22(5), pp. 540–549.

Breuninger, L. M., Dempsey, W. L., Uhl, J. and Murasko, D. M. (1993) 'Hydrocortisone regulation of interleukin-6 protein production by a purified population of human peripheral blood monocytes.', *Clinical immunology and immunopathology*, 69(2), pp. 205–14.

Bui, C., Ouzzine, M., Talhaoui, I., Sharp, S., Prydz, K., Coughtrie, M. W. H. and Fournel-Gigleux, S. (2010) 'Epigenetics: methylation-associated repression of heparan sulfate 3-O-sulfotransferase gene expression contributes to the invasive phenotype of H-EMC-SS chondrosarcoma cells', *The FASEB Journal*, 24(2), pp. 436–450.

Bullock, S. L., Fletcher, J. M., Beddington, R. S. P. and Wilson, V. A. (1998) 'Renal agenesis in mice homozygous for a gene trap mutation in the gene encoding heparan sulfate 2-sulfotransferase', *Genes and Development*, 12(12), pp. 1894–1906.

Bunnag, S., Einecke, G., Reeve, J., Jhangri, G. S., Mueller, T. F., Sis, B., Hidalgo, L. G., Mengel, M., Kayser, D., Kaplan, B. and Halloran, P. F. (2009) 'Molecular Correlates of Renal Function in Kidney Transplant Biopsies', *Journal of the American Society of Nephrology*, 20(5), pp. 1149–1160.

Burton, C. J., Combe, C., Walls, J. and Harris, K. P. G. (1996) 'Fibronectin production by human tubular cells: The effect of apical protein', *Kidney International*, 50(3), pp. 760–767.

Carlsson, P., Presto, J., Spillmann, D., Lindahl, U. and Kjellén, L. (2008) 'Heparin/heparan sulfate biosynthesis: Processive formation of N-sulfated domains', *Journal of Biological Chemistry*, 283(29), pp. 20008–20014.

Castillo, G. M., Lukito, W., Wight, T. N. and Snow, A. D. (1999) 'The sulfate moieties of

glycosaminoglycans are critical for the enhancement of beta-amyloid protein fibril formation.', *Journal of neurochemistry*, 72(4), pp. 1681–7.

Caterson, B. and Melrose, J. (2018) 'Keratan sulfate, a complex glycosaminoglycan with unique functional capability', *Glycobiology*, 28(4), pp. 182–206.

Celie, J. W. A. M., Katta, K. K., Adepu, S., Melenhorst, W. B. W. H., Reijmers, R. M., Slot, E. M., Beelen, R. H. J., Spaargaren, M., Ploeg, R. J., Navis, G., Van Der Heide, J. J. H., Van Dijk, M. C. R. F., Van Goor, H. and Van Den Born, J. (2012) 'Tubular epithelial syndecan-1 maintains renal function in murine ischemia/reperfusion and human transplantation', *Kidney International*, 81(7), pp. 651–661.

Ceol, M., Vianello, D., Schleicher, E., Anglani, F., Barbanti, M., Bonfante, L., Bertaglia, G., Graziotto, R., D'Angelo, A., Del Prete, D. and Gambaro, G. (2003) 'Heparin reduces glomerular infiltration and TGF-b protein expression by macrophages in puromycin glomerulosclerosis', *Journal of Nephrology*, 16(2), pp. 210–218.

Chawla, L. S., Eggers, P. W., Star, R. A. and Kimmel, P. L. (2014) 'Acute Kidney Injury and Chronic Kidney Disease as Interconnected Syndromes', *New England Journal of Medicine*, 371(1), pp. 58–66.

Chen, S., Wassenhove-McCarthy, D. J., Yamaguchi, Y., Holzman, L. B., Van Kuppevelt, T. H., Jenniskens, G. J., Wijnhoven, T. J., Woods, A. C. and McCarthy, K. J. (2008) 'Loss of heparan sulfate glycosaminoglycan assembly in podocytes does not lead to proteinuria', *Kidney International*, 74(3), pp. 289–299.

Chevalier, R. L., Forbes, M. S. and Thornhill, B. A. (2009) 'Ureteral obstruction as a model of renal interstitial fibrosis and obstructive nephropathy', *Kidney International*, 75(11), pp. 1145–1152.

Clark, S. J., Keenan, T. D. L., Fielder, H. L., Collinson, L. J., Holley, R. J., Merry, C. L. R., van Kuppevelt, T. H., Day, A. J. and Bishop, P. N. (2011) 'Mapping the differential distribution of glycosaminoglycans in the adult human retina, choroid, and sclera.', *Investigative ophthalmology & visual science*, 52(9), pp. 6511–21.

Clayton, A., Thomas, J., Thomas, G. J., Davies, M. and Steadman, R. (2001) 'Cell surface heparan

sulfate proteoglycans control the response of renal interstitial fibroblasts to fibroblast growth factor-2.', *Kidney international*, 59(6), pp. 2084–2094.

Clegg, D. O., Reda, D. J., Harris, C. L., Klein, M. A., O'Dell, J. R., Hooper, M. M., Bradley, J. D., Bingham, C. O., Weisman, M. H., Jackson, C. G., Lane, N. E., Cush, J. J., Moreland, L. W., Schumacher, H. R., Oddis, C. V., Wolfe, F., Molitor, J. A., Yocum, D. E., Schnitzer, T. J., Furst, D. E., Sawitzke, A. D., Shi, H., Brandt, K. D., Moskowitz, R. W. and Williams, H. J. (2006) 'Glucosamine, Chondroitin Sulfate, and the Two in Combination for Painful Knee Osteoarthritis', *New England Journal of Medicine*, 354(8), pp. 795–808.

Cohen, J. L., Dayan, S. H., Brandt, F. S., Nelson, D. B., Axford-Gatley, R. A., Theisen, M. J. and Narins, R. S. (2013) 'Systematic Review of Clinical Trials of Small- and Large-Gel-Particle Hyaluronic Acid Injectable Fillers for Aesthetic Soft Tissue Augmentation', *Dermatologic Surgery*, 39(2), pp. 205–231.

Copeland, R., Balasubramaniam, A., Tiwari, V., Zhang, F., Bridges, A., Linhardt, R. J., Shukla, D. and Liu, J. (2008) 'Using a 3-O-Sulfated Heparin Octasaccharide To Inhibit the Entry of Herpes Simplex Virus Type 1 †', *Biochemistry*, 47(21), pp. 5774–5783.

Creely, J. J., Commers, P. A. and Haralson, M. A. (1988) 'Synthesis of type III collagen by cultured kidney epithelial cells.', *Connective tissue research*, 18(2), pp. 107–22.

Cribbs, R. K., Harding, P. A., Luquette, M. H. and Besner, G. E. (2002) 'Endogenous production of heparin-binding EGF-like growth factor during murine partial-thickness burn wound healing', *Journal of Burn Care and Rehabilitation*, 23(2), pp. 116–125.

Cripps, J. G., Crespo, F. A., Romanovskis, P., Spatola, A. F. and Fernández-Botrán, R. (2005) 'Modulation of acute inflammation by targeting glycosaminoglycan-cytokine interactions.', *International immunopharmacology*, 5(11), pp. 1622–32.

Czyzewski, A., Jenssen, H., Fjell, C., Waldbrook, M., Chongsiriwatana, N., Yuen, E., Hancock, R. and Barron, A. (2016) 'Characterization of Peptoids as Antimicrobial Agents', *PLoS ONE*, 11(2), p. e0135961.

Dai, Y., Yang, Y., MacLeod, V., Yue, X., Rapraeger, A. C., Shriver, Z., Venkataraman, G., Sasisekharan, R. and Sanderson, R. D. (2005) 'HSulf-1 and HSulf-2 are potent inhibitors of

myeloma tumor growth in vivo.', *The Journal of biological chemistry*, 280(48), pp. 40066–73.

Datta, P., Li, G., Yang, B., Zhao, X., Baik, J. Y., Gemmill, T. R., Sharfstein, S. T. and Linhardt, R. J. (2013) 'Bioengineered chinese hamster ovary cells with golgi-targeted 3-O-sulfotransferase-1 biosynthesize heparan sulfate with an antithrombin-binding site', *Journal of Biological Chemistry*, 288(52), pp. 37308–37318.

David, G., Bai, X. M., Van der Schueren, B., Cassiman, J. J. and Van den Berghe, H. (1992) 'Developmental changes in heparan sulfate expression: in situ detection with mAbs.', *The Journal of cell biology*, 119(4), pp. 961–75.

Daynes, R. A. and Araneo, B. A. (1989) 'Contrasting effects of glucocorticoids on the capacity of T cells to produce the growth factors interleukin 2 and interleukin 4.', *European journal of immunology*, 19(12), pp. 2319–25.

DePianto, D. J., Chandriani, S., Abbas, A. R., Jia, G., N'Diaye, E. N., Caplazi, P., Kauder, S. E., Biswas, S., Karnik, S. K., Ha, C., Modrusan, Z., Matthay, M. A., Kukreja, J., Collard, H. R., Egen, J. G., Wolters, P. J. and Arron, J. R. (2015) 'Heterogeneous gene expression signatures correspond to distinct lung pathologies and biomarkers of disease severity in idiopathic pulmonary fibrosis.', *Thorax*, 70(1), pp. 48–56.

Desai, U. R., Wang, H. M. and Linhardt, R. J. (1993) 'Substrate specificity of the heparin lyases from Flavobacterium heparinum.', *Archives of biochemistry and biophysics*, 306(2), pp. 461–8.

Diamond, J. R. and Karnovsky, M. J. (1986) 'Nonanticoagulant protective effect of heparin in chronic aminonucleoside nephrosis.', *Renal physiology*, 9(6), pp. 366–74.

Dogra, P., Martin, E. B., Williams, A., Richardson, R. L., Foster, J. S., Hackenback, N., Kennel, S. J., Sparer, T. E. and Wall, J. S. (2015) 'Novel heparan sulfate-binding peptides for blocking herpesvirus entry.', *PloS one*, 10(5), p. e0126239.

Dredge, K., Brennan, T., Brown, M. P., Lickliter, J. D., Bampton, D., Hammond, E., Lin, L., Yang, Y. and Millward, M. (2017) 'An open-label, multi-center phase I study of the safety and tolerability of the novel immunomodulatory agent PG545 in subjects with advanced solid tumors.', *Journal of Clinical Oncology*, 35(15_suppl), pp. 3083–3083.

Drexler, H. G. and Uphoff, C. C. (2002) ‘Mycoplasma contamination of cell cultures: Incidence, sources, effects, detection, elimination, prevention’, *Cytotechnology*, 39(2), pp. 75–90.

Edavettal, S. C., Carrick, K., Shah, R. R., Pedersen, L. C., Tropsha, A., Pope, R. M. and Liu, J. (2004) ‘A conformational change in heparan sulfate 3-O-sulfotransferase-1 is induced by binding to heparan sulfate.’, *Biochemistry*, 43(16), pp. 4680–8.

Edge, A. S. B. and Spiro, R. G. (1990) ‘Characterization of novel sequences containing 3-O-sulfated glucosamine in glomerular basement membrane heparan sulfate and localization of sulfated disaccharides to a peripheral domain’, *Journal of Biological Chemistry*, 265(26), pp. 15874–15881.

Edge, A. S. and Spiro, R. G. (2000) ‘A specific structural alteration in the heparan sulphate of human glomerular basement membrane in diabetes.’, *Diabetologia*, 43(8), pp. 1056–9.

Edward, D. P., Thonar, E. J., Srinivasan, M., Yue, B. J. and Tso, M. O. (1990) ‘Macular dystrophy of the cornea. A systemic disorder of keratan sulfate metabolism.’, *Ophthalmology*, 97(9), pp. 1194–200.

Einecke, G., Reeve, J., Sis, B., Mengel, M., Hidalgo, L., Famulski, K. S., Matas, A., Kasiske, B., Kaplan, B. and Halloran, P. F. (2010) ‘A molecular classifier for predicting future graft loss in late kidney transplant biopsies’, *Journal of Clinical Investigation*, 120(6), pp. 1862–1872.

El-Assal, O. N. and Besner, G. E. (2005) ‘HB-EGF enhances restitution after intestinal ischemia/reperfusion via PI3K/Akt and MEK/ERK1/2 activation’, *Gastroenterology*, 129(2), pp. 609–625.

El-Assal, O. N., Paddock, H., Marquez, A. and Besner, G. E. (2008) ‘Heparin-binding epidermal growth factor-like growth factor gene disruption is associated with delayed intestinal restitution, impaired angiogenesis, and poor survival after intestinal ischemia in mice’, *Journal of Pediatric Surgery*, 43(6), pp. 1182–1190.

Erturk, E. (2014) ‘Ischemia-reperfusion injury and volatile anesthetics’, *Biomed Res Int*, pp. 1–7.

Esko, J. D., Kimata, K. and Lindahl, U. (2009) ‘Proteoglycans and Sulfated Glycosaminoglycans’, in *Essentials of Glycobiology*, pp. 229–248.

Esko, J. D. and Linhardt, R. J. (2009) ‘Proteins that Bind Sulfated Glycosaminoglycans’, *Essentials of Glycobiology*, pp. 1–13.

Esko, J. D. and Selleck, S. B. (2002) ‘Order out of chaos: assembly of ligand binding sites in heparan sulfate.’, *Annual review of biochemistry*, 71, pp. 435–71.

Facchiano, A., Russo, K., Facchiano, A. M., De Marchis, F., Facchiano, F., Ribatti, D., Aguzzi, M. S. and Capogrossi, M. C. (2003) ‘Identification of a novel domain of fibroblast growth factor 2 controlling its angiogenic properties.’, *The Journal of biological chemistry*, 278(10), pp. 8751–60.

Fan, G., Xiao, L., Cheng, L., Wang, X., Sun, B. and Hu, G. (2000) ‘Targeted disruption of NDST-1 gene leads to pulmonary hypoplasia and neonatal respiratory distress in mice’, *FEBS Letters*, 467, pp. 7–11.

Fan, L., Li, W., Ying, S., Shi, L., Wang, Z., Chen, G., Ye, H., Wu, X., Wu, J., Liang, G. and Li, X. (2015) ‘A peptide derivative serves as a fibroblast growth factor 2 antagonist in human gastric cancer’, *Tumor Biology*, 36(9), pp. 7233–7241.

Farris, A. B. and Colvin, R. B. (2012) ‘Renal interstitial fibrosis: Mechanisms and evaluation’, *Current Opinion in Nephrology and Hypertension*, 21(3), pp. 289–300.

Fernandez-Botran, R., Gorantla, V., Sun, X., Ren, X., Perez-Abadia, G., Crespo, F. A., Oliver, R., Orhun, H. I., Quan, E. E., Maldonado, C., Ray, M. and Barker, J. H. (2002) ‘Targeting of glycosaminoglycan-cytokine interactions as a novel therapeutic approach in allotransplantation.’, *Transplantation*, 74(5), pp. 623–629.

Fernandez-Botran, R., Yan, J. and Justus, D. E. (1999) ‘Binding of interferon gamma by glycosaminoglycans: a strategy for localization and/or inhibition of its activity.’, *Cytokine*, 11(5), pp. 313–25.

Ferreras, L., Sheerin, N. S., Kirby, J. A. and Ali, S. (2015) ‘Mechanisms of Renal Graft Chronic Injury and Progression to Interstitial Fibrosis’, *Current Transplantation Reports*, 2(3), pp. 259–268.

Ferro, V. (2013) ‘Heparan sulfate inhibitors and their therapeutic implications in inflammatory illnesses.’, *Expert opinion on therapeutic targets*, 17(8), pp. 965–75.

Feyzi, E., Lustig, F., Fager, G., Spillmann, D., Lindahl, U. and Salmivirta, M. (1997) 'Characterization of heparin and heparan sulfate domains binding to the long splice variant of platelet-derived growth factor A chain.', *The Journal of biological chemistry*, 272(9), pp. 5518–24.

Ford, B. K., Hamza, M. and Rabenstein, D. L. (2013) 'Design, synthesis, and characterization of heparin-binding peptoids.', *Biochemistry*, 52(21), pp. 3773–80.

Forsberg, E., Pejler, G., Ringvall, M., Lunderius, C., Tomasini-Johansson, B., Kusche-Gullberg, M., Eriksson, I., Ledin, J., Hellman, L. and Kjellén, L. (1999) 'Abnormal mast cells in mice deficient in a heparin-synthesizing enzyme.', *Nature*, 400(6746), pp. 773–6.

Fox, C., Cocchiaro, P., Oakley, F., Howarth, R., Callaghan, K., Leslie, J., Luli, S., Wood, K. M., Genovese, F., Sheerin, N. S. and Moles, A. (2016) 'Inhibition of lysosomal protease cathepsin D reduces renal fibrosis in murine chronic kidney disease', *Scientific Reports*, 6(1), p. 20101.

Frantz, C., Stewart, K. M. and Weaver, V. M. (2010) 'The extracellular matrix at a glance', *Journal of Cell Science*, 123(24), pp. 4195–4200.

Fraser, J. R., Laurent, T. C. and Laurent, U. B. (1997) 'Hyaluronan: its nature, distribution, functions and turnover.', *Journal of internal medicine*, 242(1), pp. 27–33.

Freeman, C., Liu, L., Banwell, M. G., Brown, K. J., Bezos, A., Ferro, V. and Parish, C. R. (2005) 'Use of sulfated linked cyclitols as heparan sulfate mimetics to probe the heparin/heparan sulfate binding specificity of proteins', *Journal of Biological Chemistry*, 280(10), pp. 8842–8849.

Frese, M.-A., Milz, F., Dick, M., Lamanna, W. C. and Dierks, T. (2009) 'Characterization of the human sulfatase Sulf1 and its high affinity heparin/heparan sulfate interaction domain.', *The Journal of biological chemistry*, 284(41), pp. 28033–44.

Funderburgh, J. L. (2000) 'Keratan sulfate: structure, biosynthesis, and function', *Glycobiology*, 10(10), pp. 951–958.

Fuschiotti, P. (2011) 'Role of IL-13 in systemic sclerosis.', *Cytokine*, 56(3), pp. 544–9.

Fuschiotti, P., Larregina, A. T., Ho, J., Feghali-Bostwick, C. and Medsger, T. A. (2013)

‘Interleukin-13-producing CD8+ T cells mediate dermal fibrosis in patients with systemic sclerosis.’, *Arthritis and rheumatism*, 65(1), pp. 236–46.

Gabay, C., Medinger-Sadowski, C., Gascon, D., Kolo, F. and Finckh, A. (2011) ‘Symptomatic effects of chondroitin 4 and chondroitin 6 sulfate on hand osteoarthritis: A randomized, double-blind, placebo-controlled clinical trial at a single center’, *Arthritis & Rheumatism*, 63(11), pp. 3383–3391.

Ge, X. N., Ha, S. G., Rao, A., Greenberg, Y. G., Rushdi, M. N., Esko, J. D., Rao, S. P. and Sriramarao, P. (2014) ‘Endothelial and leukocyte heparan sulfates regulate the development of allergen-induced airway remodeling in a mouse model.’, *Glycobiology*, 24(8), pp. 715–27.

Ghaderian, S. B., Hayati, F., Shayanpour, S. and Beladi Mousavi, S. S. (2015) ‘Diabetes and end-stage renal disease; a review article on new concepts.’, *Journal of renal injury prevention*, 4(2), pp. 28–33.

Ghadiali, R. S., Guimond, S. E., Turnbull, J. E. and Pisconti, A. (2017) ‘Dynamic changes in heparan sulfate during muscle differentiation and ageing regulate myoblast cell fate and FGF2 signalling’, *Matrix Biology*, 59, pp. 54–68.

Gil, N., Goldberg, R., Neuman, T., Garsen, M., Zcharia, E., Rubinstein, A. M., Van Kuppevelt, T., Meirovitz, A., Pisano, C., Li, J. P., Van Der Vlag, J., Vlodavsky, I. and Elkin, M. (2012) ‘Heparanase is essential for the development of diabetic nephropathy in mice’, *Diabetes*, 61(1), pp. 208–216.

Gilbert, S. (2000) *Developmental Biology*. 6th editio. Sinauer Associates.

Girardin, E. P., HajMohammadi, S., Birmele, B., Helisch, A., Shworak, N. W. and De Agostini, A. I. (2005) ‘Synthesis of anticoagulantly active heparan sulfate proteoglycans by glomerular epithelial cells involves multiple 3-O-sulfotransferase isoforms and a limiting precursor pool’, *Journal of Biological Chemistry*, 280(45), pp. 38059–38070.

Girshovich, A., Vinsonneau, C., Perez, J., Vandermeersch, S., Verpont, M. C., Placier, S., Jouanneau, C., Letavernier, E., Baud, L. and Haymann, J. P. (2012) ‘Ureteral obstruction promotes proliferation and differentiation of the renal urothelium into a bladder-like phenotype’, *Kidney International*, 82(4), pp. 428–435.

Goedert, M., Jakes, R., Spillantini, M. G., Hasegawa, M., Smith, M. J. and Crowther, R. A. (1996) 'Assembly of microtubule-associated protein tau into Alzheimer-like filaments induced by sulphated glycosaminoglycans', *Nature*, 383(6600), pp. 550–553.

Gospodarowicz, D. and Moran, J. S. (1975) 'Mitogenic effect of fibroblast growth factor on early passage cultures of human and murine fibroblasts.', *The Journal of cell biology*, 66(2), pp. 451–7.

Gottmann, U., Mueller-Falcke, A., Schnuelle, P., Birck, R., Nickeleit, V., van der Woude, F. J., Yard, B. A. and Braun, C. (2007) 'Influence of hypersulfated and low molecular weight heparins on ischemia/reperfusion: injury and allograft rejection in rat kidneys', *Transplant International*, 20(6), pp. 542–549.

Greenfield, N. J. (2006) 'Using circular dichroism spectra to estimate protein secondary structure.', *Nature protocols*, 1(6), pp. 2876–90.

Grobe, K., Ledin, J., Ringvall, M., Holmborn, K., Forsberg, E., Esko, J. D. and Kjellén, L. (2002) 'Heparan sulfate and development: differential roles of the N-acetylglucosamine N-deacetylase/N-sulfotransferase isozymes.', *Biochimica et biophysica acta*, 1573(3), pp. 209–15.

Gschwandtner, M., Strutzmann, E., Teixeira, M. M., Anders, H. J., Diedrichs-Möhring, M., Gerlza, T., Wildner, G., Russo, R. C., Adage, T. and Kungl, A. J. (2017) 'Glycosaminoglycans are important mediators of neutrophilic inflammation in vivo', *Cytokine*, 91, pp. 65–73.

Guimond, S. E. and Turnbull, J. E. (1999) 'Fibroblast growth factor receptor signalling is dictated by specific heparan sulphate saccharides', *Current Biology*, 9(22), pp. 1343–1346.

Habuchi, H., Habuchi, O. and Kimata, K. (1995) 'Purification and Characterisation of Heparan Sulfate 6-Sulfotransferase from the Culture Medium of Chinese Hamster Ovary Cells', *The Journal of biological chemistry*, pp. 4172–9.

Habuchi, H. and Kimata, K. (2010) 'Mice Deficient in Heparan Sulfate 6-O-Sulfotransferase-1', *Progress in Molecular Biology and Translational Science*, 93, pp. 79–111.

Habuchi, H., Miyake, G., Nogami, K., Kuroiwa, A., Matsuda, Y., Kusche-Gullberg, M., Habuchi, O., Tanaka, M. and Kimata, K. (2003) 'Biosynthesis of heparan sulphate with diverse structures and functions: two alternatively spliced forms of human heparan sulphate 6-O-sulphotransferase-

2 having different expression patterns and properties.', *The Biochemical journal*, 371(Pt 1), pp. 131–142.

Habuchi, H., Nagai, N., Sugaya, N., Atsumi, F., Stevens, R. L. and Kimata, K. (2007) 'Mice deficient in heparan sulfate 6-O-sulfotransferase-1 exhibit defective heparan sulfate biosynthesis, abnormal placentation, and late embryonic lethality.', *The Journal of biological chemistry*, 282(21), pp. 15578–88.

Habuchi, H., Tanaka, M., Habuchi, O., Yoshida, K., Suzuki, H., Ban, K. and Kimata, K. (2000) 'The occurrence of three isoforms of heparan sulfate 6-O-sulfotransferase having different specificities for hexuronic acid adjacent to the targeted N-sulfoglucosamine.', *The Journal of biological chemistry*, 275(4), pp. 2859–68.

HajMohammadi, S., Enjyoji, K., Princivalle, M., Christi, P., Lech, M., Beeler, D., Rayburn, H., Schwartz, J. J., Barzegar, S., De Agostini, A. I., Post, M. J., Rosenberg, R. D. and Shworak, N. W. (2003) 'Normal levels of anticoagulant heparan sulfate are not essential for normal hemostasis', *Journal of Clinical Investigation*, 111(7), pp. 989–999.

Hammond, E., Handley, P., Dredge, K. and Bytheway, I. (2013) 'Mechanisms of heparanase inhibition by the heparan sulfate mimetic PG545 and three structural analogues', *FEBS Open Bio*, 3, pp. 346–351.

Haraldsson, B., Nystrom, J. and Deen, W. M. (2008) 'Properties of the Glomerular Barrier and Mechanisms of Proteinuria', *Physiological Reviews*, 88(2), pp. 451–487.

Hart, G. W. and Varki, A. (2015) *Future Directions in Glycosciences, Essentials of Glycobiology*. Cold Spring Harbor Laboratory Press.

Hasan, S., Hosseini, G., Princivalle, M., Dong, J.-C., Birsan, D., Cagide, C. and de Agostini, A. I. (2002) 'Coordinate expression of anticoagulant heparan sulfate proteoglycans and serine protease inhibitors in the rat ovary: a potent system of proteolysis control.', *Biology of reproduction*, 66(1), pp. 144–58.

Hasegawa, H. and Wang, F. (2008) 'Visualizing mechanosensory endings of TrkC-expressing neurons in HS3ST-2-hPLAP mice.', *The Journal of comparative neurology*, 511(4), pp. 543–56.

Hashimoto, Y., Orellana, A., Gil, G. and Hirschberg, C. B. (1992) 'Molecular cloning and expression of rat liver N-heparan sulfate sulfotransferase.', *The Journal of biological chemistry*, 267(22), pp. 15744–50.

Hellec, C., Delos, M., Carpentier, M., Denys, A. and Allain, F. (2018) 'The heparan sulfate 3-O-sulfotransferases (HS3ST) 2, 3B and 4 enhance proliferation and survival in breast cancer MDA-MB-231 cells', *PLoS ONE*, 13(3), p. e0194676.

Henrotin, Y., Mathy, M., Sanchez, C. and Lambert, C. (2010) 'Chondroitin sulfate in the treatment of osteoarthritis: from in vitro studies to clinical recommendations.', *Therapeutic advances in musculoskeletal disease*, 2(6), pp. 335–48.

Hesketh, E. E., Czopek, A., Clay, M., Borthwick, G., Ferenbach, D., Kluth, D. and Hughes, J. (2014) 'Renal ischaemia reperfusion injury: a mouse model of injury and regeneration.', *Journal of visualized experiments : JoVE*, 15(88), p. e51816.

Hewitson, T. D. and Becker, G. J. (1995) 'Interstitial myofibroblasts in IgA glomerulonephritis.', *American journal of nephrology*, 15(2), pp. 111–7.

Higashiyama, S., Abraham, J., Miller, J., Fiddes, J. and Klagsbrun, M. (1991) 'A heparin-binding growth factor secreted by macrophage-like cells that is related to EGF', *Science*, 251(4996), pp. 936–939.

Hijmans, R. S., Shrestha, P., Sarpong, K. A., Yazdani, S., El Masri, R., De Jong, W. H. A., Navis, G., Vivès, R. R. and Van Den Born, J. (2017) 'High sodium diet converts renal proteoglycans into pro-inflammatory mediators in rats', *PLoS ONE*. Edited by J. A. Joles, 12(6), p. e0178940.

Hirano, K., Sasaki, N., Ichimiya, T., Miura, T., van Kuppevelt, T. H. and Nishihara, S. (2012) '3-O-sulfated heparan sulfate recognized by the antibody HS4C3 contribute to the differentiation of mouse embryonic stem cells via fas signaling', *PLoS ONE*, 7(8), p. e43440.

Hirsch, R. J., Brody, H. J. and Carruthers, J. D. A. (2007) 'Hyaluronidase in the office: A necessity for every dermasurgeon that injects hyaluronic acid', *Journal of Cosmetic and Laser Therapy*, 9(3), pp. 182–185.

Holland, E. C. and Varmus, H. E. (1998) 'Basic fibroblast growth factor induces cell migration and

proliferation after glia-specific gene transfer in mice.', *Proceedings of the National Academy of Sciences of the United States of America*, 95(3), pp. 1218–23.

Homma, T., Sakai, M., Cheng, H. F., Yasuda, T., Coffey, R. J., Harris, R. C. and Harris, R. C. (1995) 'Induction of heparin-binding epidermal growth factor-like growth factor mRNA in rat kidney after acute injury.', *The Journal of clinical investigation*, 96(2), pp. 1018–25.

Horvath, L. Z., Friess, H., Schilling, M., Borisch, B., Deflorin, J., Gold, L. I., Korc, M. and Büchler, M. W. (1996) 'Altered expression of transforming growth factor-beta S in chronic renal rejection.', *Kidney international*, 50(2), pp. 489–98.

Hosgood, S. A., Thompson, E., Moore, T., Wilson, C. H. and Nicholson, M. L. (2018) 'Normothermic machine perfusion for the assessment and transplantation of declined human kidneys from donation after circulatory death donors', *British Journal of Surgery*, 105(4), pp. 388–394.

Van Den Hoven, M. J., Rops, A. L., Bakker, M. A., Aten, J., Rutjes, N., Roestenberg, P., Goldschmeding, R., Zcharia, E., Vlodavsky, I., Van Der Vlag, J. and Berden, J. H. (2006) 'Increased expression of heparanase in overt diabetic nephropathy', *Kidney International*, 70(12), pp. 2100–2108.

Van Den Hoven, M. J., Rops, A. L., Vlodavsky, I., Levidiotis, V., Berden, J. H. and Van Der Vlag, J. (2007) 'Heparanase in glomerular diseases', *Kidney International*, pp. 543–548.

Huang, G., Besner, G. E. and Brigstock, D. R. (2012) 'Heparin-binding epidermal growth factor-like growth factor suppresses experimental liver fibrosis in mice', *Laboratory Investigation*, 92(5), pp. 703–712.

Hull, E., Montgomery, M., Leyva, K., Hull, E. E., Montgomery, M. R. and Leyva, K. J. (2017) 'Epigenetic Regulation of the Biosynthesis & Enzymatic Modification of Heparan Sulfate Proteoglycans: Implications for Tumorigenesis and Cancer Biomarkers', *International Journal of Molecular Sciences*, 18(7), p. 1361.

Hynes, R. O. (2009) 'The extracellular matrix: Not just pretty fibrils', *Science*, 326(5957), pp. 1216–1219.

Ibrahimi, O. A., Zhang, F., Lang Hrstka, S. C., Mohammadi, M. and Linhardt, R. J. (2004) 'Kinetic Model for FGF, FGFR, and Proteoglycan Signal Transduction Complex Assembly †', *Biochemistry*, 43(16), pp. 4724–4730.

Iida, S., Miyajima, J., Suzuki Matsuoka M Inoue, K. K. and Noda, S. (1997) 'Expression of heparan sulfate proteoglycan mRNA in rat kidneys during calcium oxalate nephrolithiasis', *Urol Res*, 25, pp. 361–364.

Iozzo, R. V (2001) 'Heparan sulfate proteoglycans: intricate molecules with intriguing functions.', *The Journal of clinical investigation*, 108(2), pp. 165–7.

Iozzo, R. V and Schaefer, L. (2015) 'Proteoglycan form and function: A comprehensive nomenclature of proteoglycans', *Matrix Biology*, 42, pp. 11–55.

Itano, N. and Kimata, K. (2002) 'Mammalian Hyaluronan Synthases', *IUBMB Life (International Union of Biochemistry and Molecular Biology: Life)*, 54(4), pp. 195–199.

Iwata, M. and Zager, R. A. (1996) 'Myoglobin inhibits proliferation of cultured human proximal tubular (HK-2) cells', *Kidney International*, 50, pp. 796–804.

Javerzat, S., Auguste, P. and Bikfalvi, A. (2002) 'The role of fibroblast growth factors in vascular development.', *Trends in molecular medicine*, 8(10), pp. 483–9.

Jemth, P., Smeds, E., Do, A. T., Habuchi, H., Kimata, K., Lindahl, U. and Kusche-Gullberg, M. (2003) 'Oligosaccharide Library-based Assessment of Heparan Sulfate 6-O-Sulfotransferase Substrate Specificity', *Journal of Biological Chemistry*, 278(27), pp. 24371–24376.

Jenkins, M. (1906) 'Greffe de Reins au pli du coude par soudures arterielles et veineuses', *Lyon Med*, (107), p. 3.

Jin, K., Mao, X. O., Sun, Y., Xie, L., Jin, L., Nishi, E., Klagsbrun, M. and Greenberg, D. A. (2002) 'Heparin-Binding Epidermal Growth Factor-Like Growth Factor: Hypoxia-Inducible Expression In Vitro and Stimulation of Neurogenesis In Vitro and In Vivo', *The Journal of Neuroscience*, 22(13), pp. 5365–5373.

Jokiranta, T. S., Cheng, Z.-Z., Seeberger, H., Jòzsi, M., Heinen, S., Noris, M., Remuzzi, G.,

Ormsby, R., Gordon, D. L., Meri, S., Hellwage, J. and Zipfel, P. F. (2005) 'Binding of Complement Factor H to Endothelial Cells Is Mediated by the Carboxy-Terminal Glycosaminoglycan Binding Site', *The American Journal of Pathology*, 167(4), pp. 1173–1181.

Joladarashi, D., Salimath, P. V. and Chilkunda, N. D. (2011) 'Diabetes results in structural alteration of chondroitin sulfate/dermatan sulfate in the rat kidney: Effects on the binding to extracellular matrix components', *Glycobiology*, 21(7), pp. 960–972.

Jordan, R. E., Oosta, G. M., Gardner, W. T. and Rosenberg, R. D. (1980) 'The kinetics of hemostatic enzyme-antithrombin interactions in the presence of low molecular weight heparin.', *The Journal of biological chemistry*, 255(21), pp. 10081–90.

Jorpes, J. E. and Gardell, S. (1948) 'On heparin monosulfuric acid', *The Journal of biological chemistry*, 176(1), pp. 267–276.

Kalluri, R. and Zeisberg, M. (2006) 'Fibroblasts in cancer', *Nat Rev Cancer*, 6(5), pp. 392–401.

Kalus, I., Salmen, B., Viebahn, C., von Figura, K., Schmitz, D., D'Hooge, R. and Dierks, T. (2009) 'Differential involvement of the extracellular 6-O-endosulfatases Sulf1 and Sulf2 in brain development and neuronal and behavioural plasticity.', *Journal of cellular and molecular medicine*, 13(11–12), pp. 4505–21.

Kasiske, B. L., Andany, M. A. and Danielson, B. (2002) 'A thirty percent chronic decline in inverse serum creatinine is an excellent predictor of late renal allograft failure.', *American journal of kidney diseases : the official journal of the National Kidney Foundation*, 39(4), pp. 762–8.

Katta, K., Imran, T., Busse-Wicher, M., Grønning, M., Czajkowski, S. and Kusche-Gullberg, M. (2015) 'Reduced Expression of EXTL2, a Member of the Exostosin (EXT) Family of Glycosyltransferases, in Human Embryonic Kidney 293 Cells Results in Longer Heparan Sulfate Chains.', *The Journal of biological chemistry*, 290(21), pp. 13168–77.

Kawase, T., Shimizu, A., Adachi, E., Tojimbara, T., Nakajima, I., Fuchinoue, S. and Sawada, T. (2001) 'Collagen IV is upregulated in chronic transplant nephropathy', *Transplantation Proceedings*, 33(1–2), pp. 1207–1208.

Kaysen, G. A. (2017) 'Lipid-Lowering Therapy in CKD: Should We Use It and in Which Patients',

Blood Purification, 43(1–3), pp. 196–199.

Keshari, K. R., Sriram, R., Koelsch, B. L., Van Criekinge, M., Wilson, D. M., Kurhanewicz, J. and Wang, Z. J. (2013) 'Hyperpolarized 13C-pyruvate magnetic resonance reveals rapid lactate export in metastatic renal cell carcinomas', *Cancer Research*, 73(2), pp. 529–538.

Khan, S. R. (2010) 'Nephrocalcinosis in animal models with and without stones.', *Urological research*, 38(6), pp. 429–38.

Kim, B. T., Kitagawa, H., Tamura, J., Saito, T., Kusche-Gullberg, M., Lindahl, U. and Sugahara, K. (2001) 'Human tumor suppressor EXT gene family members EXTL1 and EXTL3 encode alpha 1,4- N-acetylglucosaminyltransferases that likely are involved in heparan sulfate/ heparin biosynthesis.', *Proceedings of the National Academy of Sciences of the United States of America*, 98(13), pp. 7176–81.

Kitagawa, H., Shimakawa, H. and Sugahara, K. (1999) 'The tumor suppressor EXT-like gene EXTL2 encodes an alpha1, 4-N-acetylhexosaminyltransferase that transfers N-acetylgalactosamine and N-acetylglucosamine to the common glycosaminoglycan-protein linkage region. The key enzyme for the chain initiation of he', *The Journal of biological chemistry*, 274(20), pp. 13933–7.

Klag, M. J., Whelton, P. K., Randall, B. L., Neaton, J. D., Brancati, F. L., Ford, C. E., Shulman, N. B. and Stamler, J. (1996) 'Blood Pressure and End-Stage Renal Disease in Men', *New England Journal of Medicine*, 334(1), pp. 13–18.

Knudsen, S. L. J., Wai Mac, A. S., Henriksen, L., Van Deurs, B. and Grøvdal, L. M. (2014) 'EGFR signaling patterns are regulated by its different ligands', *Growth Factors*, 32(5), pp. 155–163.

Kobayashi, S., Morimoto, K., Shimizu, T., Takahashi, M., Kurosawa, H. and Shirasawa, T. (2000) 'Association of EXT1 and EXT2, hereditary multiple exostoses gene products, in Golgi apparatus.', *Biochemical and biophysical research communications*, 268(3), pp. 860–7.

Koh, T. J. and DiPietro, L. A. (2011) 'Inflammation and wound healing: the role of the macrophage.', *Expert reviews in molecular medicine*, 13, p. e23.

Kramer, A. (2006) 'Induction of Glomerular Heparanase Expression in Rats with Adriamycin

Nephropathy Is Regulated by Reactive Oxygen Species and the Renin-Angiotensin System', *Journal of the American Society of Nephrology*, 17(9), pp. 2513–2520.

Kramer, A., van den Hoven, M., Rops, A., Wijnhoven, T., van den Heuvel, L., Lensen, J., van Kuppevelt, T., van Goor, H., van der Vlag, J., Navis, G. and Berden, J. H. M. (2006a) 'Induction of Glomerular Heparanase Expression in Rats with Adriamycin Nephropathy Is Regulated by Reactive Oxygen Species and the Renin-Angiotensin System', *Journal of the American Society of Nephrology*, 17(9), pp. 2513–2520.

Kramer, A., van den Hoven, M., Rops, A., Wijnhoven, T., van den Heuvel, L., Lensen, J., van Kuppevelt, T., van Goor, H., van der Vlag, J., Navis, G. and Berden, J. H. M. (2006b) 'Induction of Glomerular Heparanase Expression in Rats with Adriamycin Nephropathy Is Regulated by Reactive Oxygen Species and the Renin-Angiotensin System', *Journal of the American Society of Nephrology*, 17(9), pp. 2513–2520.

Kreisberg, J. I. and Karnovsky, M. J. (1983) 'Glomerular cells in culture.', *Kidney international*, 23(3), pp. 439–47.

Krenn, E. C., Wille, I., Gesslbauer, B., Poteser, M., van Kuppevelt, T. H. and Kungl, A. J. (2008) 'Glycanogenomics: A qPCR-approach to investigate biological glycan function', *Biochemical and Biophysical Research Communications*, 375(3), pp. 297–302.

Krusius, T., Finne, J., Margolis, R. K. and Margolis, R. U. (1986) 'Identification of an O-glycosidic mannose-linked sialylated tetrasaccharide and keratan sulfate oligosaccharides in the chondroitin sulfate proteoglycan of brain.', *The Journal of biological chemistry*, 261(18), pp. 8237–42.

Kumar, A. V., Gassar, E. S., Spillmann, D., Stock, C., Sen, Y. P., Zhang, T., Van Kuppevelt, T. H., Hulsewig, C., Kozlowski, E. O., Pavao, M. S. G., Ibrahim, S. A., Poeter, M., Rescher, U., Kiesel, L., Koduru, S., Yip, G. W. and Gotte, M. (2014) 'HS3ST2 modulates breast cancer cell invasiveness via MAP kinase-and Tcf4 (Tcf7l2)-dependent regulation of protease and cadherin expression', *International Journal of Cancer*, 135(11), pp. 2579–2592.

van Kuppevelt, T. H., Dennissen, M. A., van Venrooij, W. J., Hoet, R. M. and Veerkamp, J. H. (1998) 'Generation and application of type-specific anti-heparan sulfate antibodies using phage display technology. Further evidence for heparan sulfate heterogeneity in the kidney.', *The Journal*

of biological chemistry, 273(21), pp. 12960–6.

Kwon, Y.-U. and Kodadek, T. (2007) 'Quantitative evaluation of the relative cell permeability of peptoids and peptides.', *Journal of the American Chemical Society*, 129(6), pp. 1508–9.

de La Motte, C. A., Hascall, V. C., Drazba, J., Bandyopadhyay, S. K. and Strong, S. A. (2003) 'Mononuclear leukocytes bind to specific hyaluronan structures on colon mucosal smooth muscle cells treated with polyinosinic acid:polycytidylic acid: inter-alpha-trypsin inhibitor is crucial to structure and function.', *The American journal of pathology*, 163(1), pp. 121–33.

Lai, J., Chien, J., Staub, J., Avula, R., Greene, E. L., Matthews, T. A., Smith, D. I., Kaufmann, S. H., Roberts, L. R. and Shridhar, V. (2003) 'Loss of HSulf-1 Up-regulates Heparin-binding Growth Factor Signaling in Cancer', *Journal of Biological Chemistry*, 278(25), pp. 23107–23117.

Lamanna, W. C., Baldwin, R. J., Padva, M., Kalus, I., Ten Dam, G., van Kuppevelt, T. H., Gallagher, J. T., von Figura, K., Dierks, T. and Merry, C. L. R. (2006) 'Heparan sulfate 6-O-endosulfatases: discrete in vivo activities and functional co-operativity.', *The Biochemical journal*, 400(1), pp. 63–73.

Lamanna, W. C., Frese, M.-A., Balleininger, M. and Dierks, T. (2008) 'Sulf loss influences N-, 2-O-, and 6-O-sulfation of multiple heparan sulfate proteoglycans and modulates fibroblast growth factor signaling.', *The Journal of biological chemistry*, 283(41), pp. 27724–35.

Langford-Smith, A., Keenan, T. D. L., Clark, S. J., Bishop, P. N. and Day, A. J. (2014) 'The role of complement in age-related macular degeneration: heparan sulphate, a ZIP code for complement factor H?', *Journal of innate immunity*, 6(4), pp. 407–16.

Lanner, F. and Rossant, J. (2010) 'The role of FGF/Erk signaling in pluripotent cells', *Development*, 137(20), pp. 3351–3360.

Lawrence, R., Yabe, T., Hajmohammadi, S., Rhodes, J., McNeely, M., Liu, J., Lamperti, E. D., Toselli, P. A., Lech, M., Spear, P. G., Rosenberg, R. D. and Shworak, N. W. (2007) 'The principal neuronal gD-type 3-O-sulfotransferases and their products in central and peripheral nervous system tissues.', *Matrix biology*, 26(6), pp. 442–55.

Leali, D., Bianchi, R., Bugatti, A., Nicoli, S., Mitola, S., Ragona, L., Tomaselli, S., Gallo, G.,

Catello, S., Rivieccio, V., Zetta, L. and Presta, M. (2010) 'Fibroblast growth factor 2-antagonist activity of a long-pentraxin 3-derived anti-angiogenic pentapeptide.', *Journal of cellular and molecular medicine*, 14(8), pp. 2109–21.

Leask, A. and Abraham, D. J. (2004) 'TGF-beta signaling and the fibrotic response.', *FASEB journal : official publication of the Federation of American Societies for Experimental Biology*, 18(7), pp. 816–27.

Lechner, M. S. and Dressler, G. R. (1997) 'The molecular basis of embryonic kidney development', *Mechanisms of Development*, 62(2), pp. 105–120.

Lee, K. S., Park, J. H., Lee, S., Lim, H. J., Choi, H. E. and Park, H. Y. (2007) 'HB-EGF induces delayed STAT3 activation via NF-κB mediated IL-6 secretion in vascular smooth muscle cell', *Biochimica et Biophysica Acta - Molecular Cell Research*, 1773(11), pp. 1637–1644.

Lee, V. W. and Harris, D. C. (2011) 'Adriamycin nephropathy: A model of focal segmental glomerulosclerosis', *Nephrology*, 16(1), pp. 30–38.

Lerman, L. O., Schwartz, R. S., Grande, J. P., Sheedy, P. F. and Romero, J. C. (1999) 'Noninvasive evaluation of a novel swine model of renal artery stenosis.', *Journal of the American Society of Nephrology : JASN*, 10(7), pp. 1455–65.

Lerner, I., Hermano, E., Zcharia, E., Rodkin, D., Bulvik, R., Doviner, V., Rubinstein, A. M., Ishai-Michaeli, R., Atzmon, R., Sherman, Y., Meirovitz, A., Peretz, T., Vlodavsky, I. and Elkin, M. (2011) 'Heparanase powers a chronic inflammatory circuit that promotes colitis-associated tumorigenesis in mice', *Journal of Clinical Investigation*, 121(5), pp. 1709–1721.

Lewis, A., Steadman, R., Manley, P., Craig, K., de la Motte, C., Hascall, V. and Phillips, A. O. (2008) 'Diabetic nephropathy, inflammation, hyaluronan and interstitial fibrosis.', *Histology and histopathology*, 23(6), pp. 731–9.

Li, J., Li, Q., Xie, X., Ao, Y., Tie, C. and Song, R. (2009) 'Differential roles of dihydropyridine calcium antagonist nifedipine, nitrendipine and amlodipine on gentamicin-induced renal tubular toxicity in rats', *European Journal of Pharmacology*, 620(1–3), pp. 97–104.

Li, J. P., Gong, F., Hagner-McWhirter, Å., Forsberg, E., Åbrink, M., Kisilevsky, R., Zhang, X. and

Lindahl, U. (2003) ‘Targeted disruption of a murine glucuronyl C5-epimerase gene results in heparan sulfate lacking L-iduronic acid and in neonatal lethality’, *Journal of Biological Chemistry*, 278(31), pp. 28363–28366.

Li, J. P. and Kusche-Gullberg, M. (2016) ‘Heparan Sulfate: Biosynthesis, Structure, and Function’, *International Review of Cell and Molecular Biology*, 325, pp. 215–273.

Li, Y.-C., Ho, I.-H., Ku, C.-C., Zhong, Y.-Q., Hu, Y.-P., Chen, Z.-G., Chen, C.-Y., Lin, W.-C., Zulueta, M. M. L., Hung, S.-C., Lin, M.-G., Wang, C.-C. and Hsiao, C.-D. (2014) ‘Interactions that influence the binding of synthetic heparan sulfate based disaccharides to fibroblast growth factor-2.’, *ACS chemical biology*, 9(8), pp. 1712–7.

Lind, T., Tufaro, F., McCormick, C., Lindahl, U. and Lidholt, K. (1998) ‘The putative tumor suppressors EXT1 and EXT2 are glycosyltransferases required for the biosynthesis of heparan sulfate.’, *The Journal of biological chemistry*, 273(41), pp. 26265–8.

Lindahl, B., Eriksson, L., Spillmann, D., Caterson, B. and Lindahl, U. (1996) ‘Selective loss of cerebral keratan sulfate in Alzheimer’s disease.’, *The Journal of biological chemistry*, 271(29), pp. 16991–4.

Lindahl, U., Couchman, J., Kimata, K. and Esko, J. D. (2015) ‘Proteoglycans and Sulfated Glycosaminoglycans’, in *Essentials of Glycobiology*.

Linden, M. and Brattsand, R. (1994) ‘Effects of a corticosteroid, budesonide, on alveolar macrophage and blood monocyte secretion of cytokines: differential sensitivity of GM-CSF, IL-1 beta, and IL-6.’, *Pulmonary pharmacology*, 7(1), pp. 43–7.

Liu, C.-J., Lee, P.-H., Lin, D.-Y., Wu, C.-C., Jeng, L.-B., Lin, P.-W., Mok, K.-T., Lee, W.-C., Yeh, H.-Z., Ho, M.-C., Yang, S.-S., Lee, C.-C., Yu, M.-C., Hu, R.-H., Peng, C.-Y., Lai, K.-L., Chang, S. S.-C. and Chen, P.-J. (2009) ‘Heparanase inhibitor PI-88 as adjuvant therapy for hepatocellular carcinoma after curative resection: A randomized phase II trial for safety and optimal dosage’, *Journal of Hepatology*, 50(5), pp. 958–968.

Liu, J., Shworak, N. W., Fritze, L. M., Edelberg, J. M. and Rosenberg, R. D. (1996) ‘Purification of heparan sulfate D-glucosaminyl 3-O-sulfotransferase.’, *The Journal of biological chemistry*, 271(43), pp. 27072–82.

Liu, J. and Thorp, S. C. (2002) ‘Cell surface heparan sulfate and its roles in assisting viral infections.’, *Medicinal research reviews*, 22(1), pp. 1–25.

Liu, Y. (2004) ‘Epithelial to mesenchymal transition in renal fibrogenesis: pathologic significance, molecular mechanism, and therapeutic intervention.’, *Journal of the American Society of Nephrology : JASN*, 15(1), pp. 1–12.

Liu, Y. (2015) ‘Cellular and molecular mechanisms of renal fibrosis.’, *Nat Rev Nephrol.*, 7(12), pp. 684–96.

Loeven, M. A., Rops, A. L., Lehtinen, M. J., van Kuppevelt, T. H., Daha, M. R., Smith, R. J., Bakker, M., Berden, J. H., Rabelink, T. J., Jokiranta, T. S. and van der Vlag, J. (2016) ‘Mutations in Complement Factor H Impair Alternative Pathway Regulation on Mouse Glomerular Endothelial Cells in Vitro.’, *The Journal of biological chemistry*, 291(10), pp. 4974–81.

López-Novoa, J. M., Rodríguez-Peña, A. B., Ortiz, A., Martínez-Salgado, C. and López Hernández, F. J. (2011) ‘Etiopathology of chronic tubular, glomerular and renovascular nephropathies: Clinical implications’, *Journal of Translational Medicine*, 9(13), pp. 1–26.

Lortat-Jacob, H., Turnbull, J. E. and Grimaud, J. a (1995) ‘Molecular organization of the interferon gamma-binding domain in heparan sulphate.’, *Biochem. J.*, 310, pp. 497–505.

Lote, C. J. (2013) *Principles of renal physiology*, *Principles of Renal Physiology*. Springer.

Lu, J., Auduong, L., White, E. S. and Yue, X. (2014) ‘Up-regulation of heparan sulfate 6-O-sulfation in idiopathic pulmonary fibrosis’, *American Journal of Respiratory Cell and Molecular Biology*, 50(1), pp. 106–114.

Lyon, M., Rushton, G. and Gallagher, J. T. (1997) ‘The Interaction of the Transforming Growth Factor- s with Heparin/Heparan Sulfate Is Isoform-specific’, *Journal of Biological Chemistry*, 272(29), pp. 18000–18006.

Ma, R., Cui, Z., Hu, S.-Y., Jia, X.-Y., Yang, R., Zheng, X., Ao, J., Liu, G., Liao, Y.-H. and Zhao, M.-H. (2014) ‘The alternative pathway of complement activation may be involved in the renal damage of human anti-glomerular basement membrane disease.’, *PloS one*. Edited by S. H. M. Rooijakkers, 9(3), p. e91250.

Maccarana, M., Casu, B. and Lindahl, U. (1993) ‘Minimal sequence in heparin/heparan sulfate required for binding of basic fibroblast growth factor’, *Journal of Biological Chemistry*, 268(32), pp. 23898–23905.

Mack, J. A., Feldman, R. J., Itano, N., Kimata, K., Lauer, M., Hascall, V. C. and Maytin, E. V (2012) ‘Enhanced inflammation and accelerated wound closure following tetraphorbol ester application or full-thickness wounding in mice lacking hyaluronan synthases Has1 and Has3.’, *The Journal of investigative dermatology*, 132(1), pp. 198–207.

Majors, A. K., Austin, R. C., de la Motte, C. A., Pyeritz, R. E., Hascall, V. C., Kessler, S. P., Sen, G. and Strong, S. A. (2003) ‘Endoplasmic reticulum stress induces hyaluronan deposition and leukocyte adhesion.’, *The Journal of biological chemistry*, 278(47), pp. 47223–31.

Maleszewska, M., Moonen, J.-R. A. J., Huijkman, N., van de Sluis, B., Krenning, G. and Harmsen, M. C. (2013) ‘IL-1β and TGFβ2 synergistically induce endothelial to mesenchymal transition in an NFκB-dependent manner.’, *Immunobiology*, 218(4), pp. 443–54.

Mao, X., Gauche, C., Coughtrie, M. W. H., Bui, C., Gulberti, S., Merhi-Soussi, F., Ramalanjaona, N., Bertin-Jung, I., Diot, A., Dumas, D., De Freitas Caires, N., Thompson, A. M., Bourdon, J. C., Ouzzine, M. and Fournel-Gigleux, S. (2016) ‘The heparan sulfate sulfotransferase 3-OST3A (HS3ST3A) is a novel tumor regulator and a prognostic marker in breast cancer’, *Oncogene*, 35(38), pp. 5043–5055.

de Marchis, F., Ribatti, D., Giampietri, C., Lentini, A., Faraone, D., Scoccianti, M., Capogrossi, M. C. and Facchiano, A. (2002) ‘Platelet-derived growth factor inhibits basic fibroblast growth factor angiogenic properties in vitro and in vivo through its alpha receptor.’, *Blood*, 99(6), pp. 2045–53.

Marcum, J. A., Atha, D. H., Fritze, L. M. S., Nawroth, P., Stern, D. and Rosenberg, R. D. (1986) ‘Cloned bovine aortic endothelial cells synthesize anticoagulantly active heparan sulfate proteoglycan’, *Journal of Biological Chemistry*, 261(16), pp. 7507–7517.

Marcum, J. A. and Rosenberg, R. D. (1984) ‘Anticoagulantly active heparin-like molecules from the vascular tissue’, *Biochemistry*, 23(1), pp. 1730–1737.

Margosio, B., Marchetti, D., Vergani, V., Giavazzi, R., Rusnati, M., Presta, M. and Taraboletti, G.

(2003) ‘Thrombospondin 1 as a scavenger for matrix-associated fibroblast growth factor 2.’, *Blood*, 102(13), pp. 4399–406.

Martin, E. B., Williams, A., Heidel, E., Macy, S., Kennel, S. J. and Wall, J. S. (2013) ‘Peptide p5 binds both heparinase-sensitive glycosaminoglycans and fibrils in patient-derived AL amyloid extracts.’, *Biochemical and biophysical research communications*, 436(1), pp. 85–9.

Martinez, P., Denys, A., Delos, M., Sikora, A. S., Carpentier, M., Julien, S., Pestel, J. and Allain, F. (2015) ‘Macrophage polarization alters the expression and sulfation pattern of glycosaminoglycans’, *Glycobiology*, 25(5), pp. 502–513.

Masola, V., Zaza, G., Onisto, M., Lupo, A. and Gambaro, G. (2015) ‘Impact of heparanase on renal fibrosis’, *Journal of Translational Medicine*, 13(1), p. 181.

Masola, V., Zaza, G., Secchi, M. F., Gambaro, G., Lupo, A. and Onisto, M. (2014) ‘Heparanase is a key player in renal fibrosis by regulating TGF-β expression and activity.’, *Biochimica et biophysica acta*, 1843(9), pp. 2122–8.

El Masri, R., Seffouh, A., Lortat-Jacob, H. and Vivès, R. R. (2017) ‘The “in and out” of glucosamine 6-O-sulfation: the 6th sense of heparan sulfate’, *Glycoconjugate Journal*, 34(3), pp. 285–298.

Massena, S., Christoffersson, G., Hjertström, E., Zcharia, E., Vlodavsky, I., Ausmees, N., Rolny, C., Li, J.-P. and Phillipson, M. (2010) ‘A chemotactic gradient sequestered on endothelial heparan sulfate induces directional intraluminal crawling of neutrophils.’, *Blood*, 116(11), pp. 1924–31.

Matheson, P. J., Fernandez-Botran, R., Smith, J. W., Matheson, S. A., Downard, C. D., McClain, C. J. and Garrison, R. N. (2016) ‘Association Between MC-2 Peptide and Hepatic Perfusion and Liver Injury Following Resuscitated Hemorrhagic Shock.’, *JAMA surgery*, 151(3), pp. 265–72.

Matos, L. L. de, Trufelli, D. C., de Matos, M. G. L. and da Silva Pinhal, M. A. (2010) ‘Immunohistochemistry as an important tool in biomarkers detection and clinical practice.’, *Biomarker insights*, 5, pp. 9–20.

McCarthy, K. J., Abrahamson, D. R., Bynum, K. R., St John, P. L. and Couchman, J. R. (1994) ‘Basement membrane-specific chondroitin sulfate proteoglycan is abnormally associated with the

glomerular capillary basement membrane of diabetic rats.', *The journal of histochemistry and cytochemistry : official journal of the Histochemistry Society*, 42(4), pp. 473–84.

McCormick, C., Duncan, G., Goutsos, K. T. and Tufaro, F. (2000) 'The putative tumor suppressors EXT1 and EXT2 form a stable complex that accumulates in the Golgi apparatus and catalyzes the synthesis of heparan sulfate.', *Proceedings of the National Academy of Sciences of the United States of America*, 97(2), pp. 668–73.

McElvaney, O. J., O'Reilly, N., White, M., Lacey, N., Pohl, K., Gerlza, T., Bergin, D. A., Kerr, H., McCarthy, C., O'Brien, M. E., Adage, T., Kungl, A. J., Reeves, E. P. and McElvaney, N. G. (2015) 'The effect of the decoy molecule PA401 on CXCL8 levels in bronchoalveolar lavage fluid of patients with cystic fibrosis.', *Molecular immunology*, 63(2), pp. 550–8.

McKeehan, W. L., Wu, X. and Kan, M. (1999) 'Requirement for anticoagulant heparan sulfate in the fibroblast growth factor receptor complex', *Journal of Biological Chemistry*, 274(31), pp. 21511–21514.

McKenna, R. M., Takemoto, S. K. and Terasaki, P. I. (2000) 'Anti-HLA antibodies after solid organ transplantation.', *Transplantation*, 69(3), pp. 319–26.

Meng, X.-M., Nikolic-Paterson, D. J. and Lan, H. Y. (2014) 'Inflammatory processes in renal fibrosis.', *Nature reviews. Nephrology*, 10(9), pp. 493–503.

Meyer, K. and Chaffee, E. (1941) 'The mucopolysaccharides of skin.', *The Journal of Biological Chemistry*, 138(138), pp. 491–499.

Meyer, K., Davidson, E., Linker, A. and Hoffman, P. (1956) 'The acid mucopolysaccharides of connective tissue.', *Biochim Biophys Acta*, 21(3), pp. 506–518.

Meyer, K., Linker, A., Davidson, E. A. and Weissmann, B. (1953) 'The mucopolysaccharides of bovine cornea.', *The Journal of biological chemistry*, 205(2), pp. 611–616.

Meyer, K. and Palmer, J. W. (1934) 'the Polysaccharide of the Vitreous Humor', *The Journal of Biological*, 107(3), pp. 629–634.

Michos, O. (2009) 'Kidney development: from ureteric bud formation to branching

morphogenesis.', *Current opinion in genetics & development*, 19(5), pp. 484–90.

Middleton, J., Neil, S., Wintle, J., Clark-Lewis, I., Moore, H., Lam, C., Auer, M., Hub, E. and Rot, A. (1997) 'Transcytosis and surface presentation of IL-8 by venular endothelial cells.', *Cell*, 91(3), pp. 385–95.

Mikami, T. and Kitagawa, H. (2013) 'Biosynthesis and function of chondroitin sulfate', *Biochimica et Biophysica Acta (BBA) - General Subjects*, 1830(10), pp. 4719–4733.

Miner, J. H. (1999) 'Renal basement membrane components', *Kidney International*, 56(6), pp. 2016–2024.

Miyamoto, K., Asada, K., Fukutomi, T., Okochi, E., Yagi, Y., Hasegawa, T., Asahara, T., Sugimura, T. and Ushijima, T. (2003) 'Methylation-associated silencing of heparan sulfate D-glucosaminyl 3-O-sulfotransferase-2 (3-OST-2) in human breast, colon, lung and pancreatic cancers', *Oncogene*, 22(2), pp. 274–280.

Miyata, K., Yotsumoto, F., Fukagawa, S., Kiyoshima, C., Ouk, N. S., Urushiyama, D., Ito, T., Katsuda, T., Kurakazu, M., Araki, R., Sanui, A., Miyahara, D., Murata, M., Shirota, K., Yagi, H., Takono, T., Kato, K., Yaegashi, N., Akazawa, K., Kuroki, M., Yasunaga, S. and Miyamoto, S. (2017) 'Serum Heparin-binding Epidermal Growth Factor-like Growth Factor (HB-EGF) as a Biomarker for Primary Ovarian Cancer.', *Anticancer research*, 37(7), pp. 3955–3960.

Mochizuki, H., Yoshida, K., Gotoh, M., Sugioka, S., Kikuchi, N., Kwon, Y.-D., Tawada, A., Maeyama, K., Inaba, N., Hiruma, T., Kimata, K. and Narimatsu, H. (2003) 'Characterization of a heparan sulfate 3-O-sulfotransferase-5, an enzyme synthesizing a tetrasulfated disaccharide.', *The Journal of biological chemistry*, 278(29), pp. 26780–7.

Mochizuki, H., Yoshida, K., Shibata, Y. and Kimata, K. (2008) 'Tetrasulfated disaccharide unit in heparan sulfate: Enzymatic formation and tissue distribution', *Journal of Biological Chemistry*, 283(45), pp. 31237–31245.

Monfort, J., Pelletier, J.-P., Garcia-Giralt, N. and Martel-Pelletier, J. (2008) 'Biochemical basis of the effect of chondroitin sulphate on osteoarthritis articular tissues', *Annals of the Rheumatic Diseases*, 67(6), pp. 735–740.

Monslow, J., Sato, N., Mack, J. A. and Maytin, E. V (2009) ‘Wounding-induced synthesis of hyaluronic acid in organotypic epidermal cultures requires the release of heparin-binding egf and activation of the EGFR.’, *The Journal of investigative dermatology*, 129(8), pp. 2046–58.

Moon, A. F., Xu, Y., Woody, S. M., Krahn, J. M., Linhardt, R. J., Liu, J. and Pedersen, L. C. (2012) ‘Dissecting the substrate recognition of 3-O-sulfotransferase for the biosynthesis of anticoagulant heparin.’, *Proceedings of the National Academy of Sciences of the United States of America*, 109(14), pp. 5265–70.

Moreth, K., Brodbeck, R., Babelova, A., Gretz, N., Spieker, T., Zeng-Brouwers, J., Pfeilschifter, J., Young, M. F., Schaefer, R. M. and Schaefer, L. (2010) ‘The proteoglycan biglycan regulates expression of the B cell chemoattractant CXCL13 and aggravates murine lupus nephritis.’, *The Journal of clinical investigation*, 120(12), pp. 4251–72.

Moreth, K., Frey, H., Hubo, M., Zeng-Brouwers, J., Nastase, M. V., Hsieh, L. T. H., Haceni, R., Pfeilschifter, J., Iozzo, R. V and Schaefer, L. (2014) ‘Biglycan-triggered TLR-2- and TLR-4-signaling exacerbates the pathophysiology of ischemic acute kidney injury’, *Matrix Biology*, 35, pp. 143–151.

Morita, M., Uchigata, Y., Hanai, K., Ogawa, Y. and Iwamoto, Y. (2011) ‘Association of urinary type IV collagen with GFR decline in young patients with type 1 diabetes’, *American Journal of Kidney Diseases*, 58(6), pp. 915–920.

Mummery, R. S. and Rider, C. C. (2004) ‘Characterization of the Heparin-Binding Properties of IL-6’, *The Journal of Immunology*, 173(7), pp. 4755–4755.

Murphy, M., Drago, J. and Bartlett, P. F. (1990) ‘Fibroblast growth factor stimulates the proliferation and differentiation of neural precursor cells in vitro.’, *Journal of neuroscience research*, 25(4), pp. 463–75.

Murray, J. E., Merrill, J. P., Harrison, J. H., Wilson, R. E. and Dammin, G. J. (1984) ‘Prolonged survival of human-kidney homografts by immunosuppressive drug therapy.’, *Annals of plastic surgery*, 12(1), pp. 70–83.

Murray, J., Merrill, J. and Harrison, J. (1955) ‘Renal homotransplantation in identical twins’, *Surgical forum*, 6, pp. 432–436.

Nagai, N., Habuchi, H., Kitazume, S., Toyoda, H., Hashimoto, Y. and Kimata, K. (2007) 'Regulation of heparan sulfate 6-O-sulfation by beta-secretase activity.', *The Journal of biological chemistry*, 282(20), pp. 14942–51.

Nagamine, S., Tamba, M., Ishimine, H., Araki, K., Shiomi, K., Okada, T., Ohto, T., Kunita, S., Takahashi, S., Wismans, R. G. P., van Kuppevelt, T. H., Masu, M. and Keino-Masu, K. (2012) 'Organ-specific sulfation patterns of heparan sulfate generated by extracellular sulfatases Sulf1 and Sulf2 in mice.', *The Journal of biological chemistry*, 287(12), pp. 9579–90.

Nakamura, K., Yokohama, S., Yoneda, M., Okamoto, S., Tamaki, Y., Ito, T., Okada, M., Aso, K. and Makino, I. (2004) 'High, but not low, molecular weight hyaluronan prevents T-cell-mediated liver injury by reducing proinflammatory cytokines in mice', *Journal of Gastroenterology*, 39(4), pp. 346–354.

Nankivell, B. J., Borrows, R. J., Fung, C. L.-S., O'Connell, P. J., Allen, R. D. M. and Chapman, J. R. (2003) 'The natural history of chronic allograft nephropathy.', *The New England journal of medicine*, 349(24), pp. 2326–33.

Neugebauer, J. M., Cadwallader, A. B., Amack, J. D., Bisgrove, B. W. and Yost, H. J. (2013) 'Differential roles for 3-OSTs in the regulation of cilia length and motility', *Development*, 140(18), pp. 3892–3902.

Nigwekar, S. U., Tamez, H. and Thadhani, R. I. (2014) 'Vitamin D and chronic kidney disease–mineral bone disease (CKD–MBD)', *BoneKEy Reports*, 3, p. 498.

Nouwen, E. J., Dauwe, S., Van Der Biest, I. and De Broe, M. E. (1993) 'Stage- and segment-specific expression of cell-adhesion molecules N-CAM, A-CAM, and L-CAM in the kidney', *Kidney International*, 44(1), pp. 147–158.

O'Boyle, G., Mellor, P., Kirby, J. a and Ali, S. (2009) 'Anti-inflammatory therapy by intravenous delivery of non-heparan sulfate-binding CXCL12.', *FASEB journal*, 23(11), pp. 3906–16.

O'Donnell, C. D., Tiwari, V., Oh, M. J. and Shukla, D. (2006) 'A role for heparan sulfate 3-O-sulfotransferase isoform 2 in herpes simplex virus type 1 entry and spread', *Virology*, 346(2), pp. 452–459.

Oflaz, H., Turkmen, A., Kazancioglu, R., Kayacan, S. M., Bunyak, B., Genchallac, H., Erol, B., Mercanoglu, F., Umman, S. and Sever, M. S. (2003) 'The effect of calcineurin inhibitors on endothelial function in renal transplant recipients.', *Clinical transplantation*, 17(3), pp. 212–6.

Okonogi, H., Nishimura, M., Utsunomiya, Y., Hamaguchi, K., Tsuchida, H., Miura, Y., Suzuki, S., Kawamura, T., Hosoya, T. and Yamada, K. (2001) 'Urinary type IV collagen excretion reflects renal morphological alterations and type IV collagen expression in patients with type 2 diabetes mellitus.', *Clinical nephrology*, 55(5), pp. 357–64.

de Oliveira, S., Rosowski, E. E. and Huttenlocher, A. (2016) 'Neutrophil migration in infection and wound repair: Going forward in reverse', *Nature Reviews Immunology*, 16(6), pp. 378–391.

Pai, A., Leaf, E. M., El-Abbadi, M. and Giachelli, C. M. (2011) 'Elastin degradation and vascular smooth muscle cell phenotype change precede cell loss and arterial medial calcification in a uremic mouse model of chronic kidney disease', *American Journal of Pathology*, 178(2), pp. 764–773.

Paliogianni, F., Ahuja, S. S., Balow, J. P., Balow, J. E. and Boumpas, D. T. (1993) 'Novel mechanism for inhibition of human T cells by glucocorticoids. Glucocorticoids inhibit signal transduction through IL-2 receptor.', *Journal of immunology*, 151(8), pp. 4081–9.

Parthasarathy, N., Goldberg, I. J., Sivaram, P., Mulloy, B., Flory, D. M. and Wagner, W. D. (1994) 'Oligosaccharide sequences of endothelial cell surface heparan sulfate proteoglycan with affinity for lipoprotein lipase', *Journal of Biological Chemistry*, 269(35), pp. 22391–22396.

Patel, V. N., Lombaert, I. M. A., Cowherd, S. N., Shworak, N. W., Xu, Y., Liu, J. and Hoffman, M. P. (2014) 'Hs3st3-Modified Heparan Sulfate Controls KIT+ Progenitor Expansion by Regulating 3-O-Sulfotransferases', *Developmental Cell*, 29(6), pp. 662–673.

Pecly, I. M. D., Gonçalves, R. G., Rangel, E. P., Takiya, C. M., Taboada, F. S., Martinusso, C. A., Pavão, M. S. G. and Leite, M. (2006) 'Effects of low molecular weight heparin in obstructed kidneys: Decrease of collagen, fibronectin and TGF-β, and increase of chondroitin/ dermatan sulfate proteoglycans and macrophage infiltration', *Nephrology Dialysis Transplantation*, 21(5), pp. 1212–1222.

Pejler, G., Backstrom, G. and Lindahl, U. (1987) 'Structure and affinity for antithrombin of heparan sulfate chains derived from basement membrane proteoglycans', *Journal of Biological Chemistry*,

262(11), pp. 5036–5043.

Pempe, E. H., Xu, Y., Gopalakrishnan, S., Liu, J. and Harris, E. N. (2012) 'Probing structural selectivity of synthetic heparin binding to stabilin protein receptors', *Journal of Biological Chemistry*, 287(25), pp. 20774–20783.

Perollet, C., Han, Z. C., Savona, C., Caen, J. P. and Bikfalvi, A. (1998) 'Platelet factor 4 modulates fibroblast growth factor 2 (FGF-2) activity and inhibits FGF-2 dimerization.', *Blood*, 91(9), pp. 3289–99.

Peterson, S. B. and Liu, J. (2010) 'Unraveling the specificity of heparanase utilizing synthetic substrates.', *The Journal of biological chemistry*, 285(19), pp. 14504–13.

Petrella, R. and Wakeford, C. (2015) 'Pain relief and improved physical function in knee osteoarthritis patients receiving ongoing hylan G-F 20, a high-molecular-weight hyaluronan, versus other treatment options: data from a large real-world longitudinal cohort in Canada', *Drug Design, Development and Therapy*, 9, p. 5633.

Petrey, A. C. and de la Motte, C. A. (2014) 'Hyaluronan, a crucial regulator of inflammation', *Frontiers in Immunology*, 5, p. ART101.

Pettersson, I., Kusche, M., Unger, E., Wlad, H., Nylund, L., Lindahl, U. and Kjellén, L. (1991) 'Biosynthesis of heparin. Purification of a 110-kDa mouse mastocytoma protein required for both glucosaminyl N-deacetylation and N-sulfation.', *The Journal of biological chemistry*, 266(13), pp. 8044–9.

Pikas, D. S., Eriksson, I. and Kjellén, L. (2000) 'Overexpression of different isoforms of glucosaminyl N-deacetylase/N- sulfotransferase results in distinct heparan sulfate N-sulfation patterns', *Biochemistry*, 39(15), pp. 4552–4558.

Pinhal, M. A., Smith, B., Olson, S., Aikawa, J., Kimata, K. and Esko, J. D. (2001) 'Enzyme interactions in heparan sulfate biosynthesis: uronosyl 5-epimerase and 2-O-sulfotransferase interact in vivo.', *Proceedings of the National Academy of Sciences of the United States of America*, 98(23), pp. 12984–9.

Pomin, V. H. (2015) 'Keratan sulfate: An up-to-date review', *International Journal of Biological*

Macromolecules, 72, pp. 282–289.

Préchoux, A., Halimi, C., Simorre, J.-P., Lortat-Jacob, H. and Laguri, C. (2015) 'C $_5$ -Epimerase and 2- *O* -Sulfotransferase Associate *in Vitro* to Generate Contiguous Epimerized and 2- *O* -Sulfated Heparan Sulfate Domains', *ACS Chemical Biology*, 10(4), pp. 1064–1071.

Prestegard, J. H., Liu, J. and Widmalm, G. (2015) *Oligosaccharides and Polysaccharides*, *Essentials of Glycobiology*. Cold Spring Harbor Laboratory Press.

Princivalle, M., Hasan, S., Hosseini, G. and de Agostini, A. I. (2001) 'Anticoagulant heparan sulfate proteoglycans expression in the rat ovary peaks in preovulatory granulosa cells.', *Glycobiology*, 11(3), pp. 183–94.

Properzi, F., Lin, R., Kwok, J., Naidu, M., Van Kuppevelt, T. H., Ten Dam, G. B., Camargo, L. M., Raha-Chowdhury, R., Furukawa, Y., Mikami, T., Sugahara, K. and Fawcett, J. W. (2008) 'Heparan sulphate proteoglycans in glia and in the normal and injured CNS: Expression of sulphotransferases and changes in sulphation', *European Journal of Neuroscience*, 27(3), pp. 593–604.

Proudfoot, A. E., Fritchley, S., Borlat, F., Shaw, J. P., Vilbois, F., Zwahlen, C., Trkola, A., Marchant, D., Clapham, P. R. and Wells, T. N. (2001) 'The BBXB motif of RANTES is the principal site for heparin binding and controls receptor selectivity.', *The Journal of biological chemistry*, 276(14), pp. 10620–6.

Prozialeck, W. C., Lamar, P. C. and Appelt, D. M. (2004) 'Differential expression of E-cadherin, N-cadherin and beta-catenin in proximal and distal segments of the rat nephron.', *BMC physiology*, 4, p. 10.

Purkerson, M. L., Tollefsen, D. M. and Klahr, S. (1988) 'N-desulfated/acetylated heparin ameliorates the progression of renal disease in rats with subtotal renal ablation.', *Journal of Clinical Investigation*, 81(1), pp. 69–74.

Pye, D. A., Vives, R. R., Turnbull, J. E., Hyde, P. and Gallagher, J. T. (1998) 'Heparan sulfate oligosaccharides require 6-O-sulfation for promotion of basic fibroblast growth factor mitogenic activity.', *The Journal of biological chemistry*, 273(36), pp. 22936–42.

Qin, Y., Ke, J., Gu, X., Fang, J., Wang, W., Cong, Q., Li, J., Tan, J., Brunzelle, J. S., Zhang, C., Jiang, Y., Melcher, K., Li, J., Xu, H. E. and Ding, K. (2015) 'Structural and functional study of D-glucuronyl C5-epimerase.', *The Journal of biological chemistry*, 290(8), pp. 4620–30.

Queeley, G. L. and Campbell, E. S. (2018) 'Comparing treatment modalities for end-stage renal disease: A meta-analysis', *American Health and Drug Benefits*, 11(3), pp. 118–125.

Rabenstein, D. L. (2002) 'Heparin and heparan sulfate: structure and function', *Natural Product Reports*, 19(3), pp. 312–331.

Racusen, L. C., Monteil, C., Sgrignoli, A., Lucskay, M., Marouillat, S., Rhim, J. G. S. and Morin, J. P. (1997) 'Cell lines with extended in vitro growth potential from human renal proximal tubule: Characterization, response to inducers, and comparison with established cell lines', *Journal of Laboratory and Clinical Medicine*, 129(3), pp. 318–329.

Raman, R., Myette, J., Venkataraman, G., Sasisekharan, V. and Sasisekharan, R. (2002) 'Identification of structural motifs and amino acids within the structure of human heparan sulfate 3-O-sulfotransferase that mediate enzymatic function.', *Biochemical and biophysical research communications*, 290(4), pp. 1214–9.

Ricard-Blum, S. (2011) 'The Collagen Family', *Cold Spring Harbor Perspectives in Biology*, 3(1), pp. 1–19.

Ricard-Blum, S., Féraud, O., Lortat-Jacob, H., Rencurosi, A., Fukai, N., Dkhissi, F., Vittet, D., Imberty, A., Olsen, B. R. and van der Rest, M. (2004) 'Characterization of endostatin binding to heparin and heparan sulfate by surface plasmon resonance and molecular modeling: role of divalent cations.', *The Journal of biological chemistry*, 279(4), pp. 2927–36.

Rienstra, H., Katta, K., Celie, J. W. a M., Van Goor, H., Navis, G., Van Den Born, J. and Hillebrands, J. L. (2010) 'Differential expression of proteoglycans in tissue remodeling and lymphangiogenesis after experimental renal transplantation in rats', *PLoS ONE*, 5(2), p. e9095.

Rittirsch, D., Huber-Lang, M. S., Flierl, M. A. and Ward, P. A. (2009) 'Immunodesign of experimental sepsis by cecal ligation and puncture.', *Nature protocols*, 4(1), pp. 31–6.

Rong, J., Habuchi, H., Kimata, K., Lindahl, U. and Kusche-Gullberg, M. (2001) 'Substrate

specificity of the heparan sulfate hexuronic acid 2-O-sulfotransferase', *Biochemistry*, 40(18), pp. 5548–5555.

Rops, A. L., van den Hoven, M. J., Bakker, M. A., Lensen, J. F., Wijnhoven, T. J., van den Heuvel, L. P., van Kuppevelt, T. H., van der Vlag, J. and Berden, J. H. (2007) 'Expression of glomerular heparan sulphate domains in murine and human lupus nephritis', *Nephrology Dialysis Transplantation*, 22(7), pp. 1891–1902.

Rops, A., Loeven, M. A., van Gemst, J. J., Eversen, I., Van Wijk, X. M., Dijkman, H. B., van Kuppevelt, T. H., Berden, J. H. M., Rabelink, T. J., Esko, J. D. and van der Vlag, J. (2014) 'Modulation of heparan sulfate in the glomerular endothelial glycocalyx decreases leukocyte influx during experimental glomerulonephritis.', *Kidney international*, 86(5), pp. 932–42.

Rosenberg, R. D. and Damus, P. S. (1973) 'The Purification and Mechanism of Action of Human Antithrombin-Heparin Cofactor', *Journal of biological chemistry*, 248(18), pp. 6490–6505.

Rot, A. (1993) 'Neutrophil attractant/activation protein-1 (interleukin-8) induces in vitro neutrophil migration by haptotactic mechanism.', *European journal of immunology*, 23(1), pp. 303–6.

Rullo, A. and Nitz, M. (2010) 'Importance of the spatial display of charged residues in heparin-peptide interactions.', *Biopolymers*, 93(3), pp. 290–8.

Ryan, M. J., Johnson, G., Kirk, J., Fuerstenberg, S. M., Zager, R. A. and Torok-Storb, B. (1994) 'HK-2: An immortalized proximal tubule epithelial cell line from normal adult human kidney', *Kidney International*, 45(1), pp. 48–57.

Sagoo, P., Perucha, E., Sawitzki, B., Tomiuk, S., Stephens, D. a, Miqueu, P., Chapman, S., Craciun, L., Sergeant, R., Brouard, S., Rovis, F., Jimenez, E., Ballow, A., Giral, M., Rebollo-Mesa, I., Le Moine, A., Braudeau, C., Hilton, R., Gerstmayer, B., Bourcier, K., Sharif, A., Krajewska, M., Lord, G. M., Roberts, I., Goldman, M., Wood, K. J., Newell, K., Seyfert-Margolis, V., Warrens, A. N., Janssen, U., Volk, H.-D., Soulillou, J.-P., Hernandez-Fuentes, M. P. and Lechler, R. I. (2010) 'Development of a cross-platform biomarker signature to detect renal transplant tolerance in humans.', *The Journal of clinical investigation*, 120(6), pp. 1848–61.

Sakai, M., Zhang, M. Z., Homma, T., Garrick, B., Abraham, J. A., McKanna, J. A. and Harris, R. C. (1997) 'Production of heparin binding epidermal growth factor-like growth factor in the early

phase of regeneration after acute renal injury: Isolation and localization of bioactive molecules', *Journal of Clinical Investigation*, 99(9), pp. 2128–2138.

Samson, S. C., Ferrer, T., Jou, C. J., Sachse, F. B., Shankaran, S. S., Shaw, R. M., Chi, N. C., Tristani-Firouzi, M. and Yost, H. J. (2013) '3-OST-7 Regulates BMP-Dependent Cardiac Contraction', *PLoS Biology*. Edited by S. M. Hughes, 11(12), p. e1001727.

Sano, M., Fukuda, K., Kodama, H., Takahashi, T., Kato, T., Hakuno, D., Sato, T., Manabe, T., Tahara, S. and Ogawa, S. (2000) 'Autocrine/paracrine secretion of IL-6 family cytokines causes angiotensin II-induced delayed STAT3 activation', *Biochemical and Biophysical Research Communications*, 269(3), pp. 798–802.

Sappino, A. P., Schürch, W. and Gabbiani, G. (1990) 'Differentiation repertoire of fibroblastic cells: expression of cytoskeletal proteins as marker of phenotypic modulations.', *Laboratory investigation; a journal of technical methods and pathology*, 63(2), pp. 144–61.

Sasisekharan, R., Shriver, Z., Venkataraman, G. and Narayanasami, U. (2002) 'Roles of heparan-sulphate glycosaminoglycans in cancer.', *Nature reviews. Cancer*, 2(7), pp. 521–8.

Sato, N., Ohsawa, I., Nagamachi, S., Ishii, M., Kusaba, G., Inoshita, H., Toki, A., Horikoshi, S., Ohi, H., Matsushita, M. and Tomino, Y. (2011) 'Significance of glomerular activation of the alternative pathway and lectin pathway in lupus nephritis', *Lupus*, 20(13), pp. 1378–1386.

Saweirs, W. W. M. and Goddard, J. (2007) 'What are the best treatments for early chronic kidney disease?: A Background Paper prepared for the UK Consensus Conference on Early Chronic Kidney Disease', *Nephrology Dialysis Transplantation*, 22(Supplement 9), pp. ix31-ix38.

Schaefer, L. (2011) 'Small Leucine-Rich Proteoglycans in Kidney Disease', *Journal of the American Society of Nephrology*, 22(7), pp. 1200–1207.

Schaefer, L., Babelova, A., Kiss, E., Hausser, H.-J., Baliova, M., Krzyzankova, M., Marsche, G., Young, M. F., Mihalik, D., Götte, M., Malle, E., Schaefer, R. M. and Gröne, H.-J. (2005) 'The matrix component biglycan is proinflammatory and signals through Toll-like receptors 4 and 2 in macrophages.', *The Journal of clinical investigation*, 115(8), pp. 2223–33.

Schaefer, L., Macakova, K., Raslik, I., Micegova, M., Gröne, H.-J., Schönherr, E., Robenek, H.,

Echtermeyer, F. G., Grässel, S., Bruckner, P., Schaefer, R. M., Iozzo, R. V. and Kresse, H. (2002) 'Absence of Decorin Adversely Influences Tubulointerstitial Fibrosis of the Obstructed Kidney by Enhanced Apoptosis and Increased Inflammatory Reaction', *The American Journal of Pathology*, 160(3), pp. 1181–1191.

Schlessinger, J., Plotnikov, a N., Ibrahimi, O. a, Eliseenkova, a V, Yeh, B. K., Yayon, a, Linhardt, R. J. and Mohammadi, M. (2000) 'Crystal structure of a ternary FGF-FGFR-heparin complex reveals a dual role for heparin in FGFR binding and dimerization.', *Molecular cell*, 6, pp. 743–750.

Schlieper, G., Aretz, A., Verberckmoes, S. C., Kruger, T., Behets, G. J., Ghadimi, R., Weirich, T. E., Rohrmann, D., Langer, S., Tordoir, J. H., Amann, K., Westenfeld, R., Brandenburg, V. M., D'Haese, P. C., Mayer, J., Ketteler, M., McKee, M. D. and Floege, J. (2010) 'Ultrastructural Analysis of Vascular Calcifications in Uremia', *Journal of the American Society of Nephrology*, 21(4), pp. 689–696.

Schmidt, E. P., Overdier, K. H., Sun, X., Lin, L., Liu, X., Yang, Y., Ammons, L. A., Hiller, T. D., Suflita, M. A., Yu, Y., Chen, Y., Zhang, F., Cothren Burlew, C., Edelstein, C. L., Douglas, I. S. and Linhardt, R. J. (2016) 'Urinary Glycosaminoglycans Predict Outcomes in Septic Shock and Acute Respiratory Distress Syndrome.', *American journal of respiratory and critical care medicine*, 194(4), pp. 439–49.

Schmidt, E. P., Yang, Y., Janssen, W. J., Gandjeva, A., Perez, M. J., Barthel, L., Zemans, R. L., Bowman, J. C., Koyanagi, D. E., Yunt, Z. X., Smith, L. P., Cheng, S. S., Overdier, K. H., Thompson, K. R., Geraci, M. W., Douglas, I. S., Pearse, D. B. and Tuder, R. M. (2012) 'The pulmonary endothelial glycocalyx regulates neutrophil adhesion and lung injury during experimental sepsis', *Nature Medicine*, 18(8), pp. 1217–1223.

Scotton, C. and Chambers, R. (2007) 'Molecular targets in pulmonary fibrosis - The myofibroblast in focus', *CHEST*, 132(4), pp. 1311–1321.

Selbi, W., de la Motte, C. A., Hascall, V. C., Day, A. J., Bowen, T. and Phillips, A. O. (2006) 'Characterization of hyaluronan cable structure and function in renal proximal tubular epithelial cells.', *Kidney international*, 70(7), pp. 1287–95.

Sepulveda-Diaz, J. E., Alavi Naini, S. M., Huynh, M. B., Ouidja, M. O., Yanicostas, C., Chantepie,

S., Villares, J., Lamari, F., Jospin, E., Van Kuppevelt, T. H., Mensah-Nyagan, A. G., Raisman-Vozari, R., Soussi-Yanicostas, N. and Papy-Garcia, D. (2015) 'HS3ST2 expression is critical for the abnormal phosphorylation of tau in Alzheimer's disease-related tau pathology', *Brain*, 138(5), pp. 1339–1354.

Severin, I. C., Gaudry, J.-P., Johnson, Z., Kungl, A., Jansma, A., Gesslbauer, B., Mulloy, B., Power, C., Proudfoot, A. E. I. and Handel, T. (2010) 'Characterization of the chemokine CXCL11-heparin interaction suggests two different affinities for glycosaminoglycans.', *The Journal of biological chemistry*, 285(23), pp. 17713–24.

Shah, M. M., Sakurai, H., Sweeney, D. E., Gallegos, T. F., Bush, K. T., Esko, J. D. and Nigam, S. K. (2010) 'Hs2st mediated kidney mesenchyme induction regulates early ureteric bud branching', *Developmental Biology*, 339(2), pp. 354–365.

Sharma, A. K., Mauer, S. M., Kim, Y. and Michael, A. F. (1993) 'Interstitial fibrosis in obstructive nephropathy', *Kidney International*, 44(4), pp. 774–788.

Sheng, G. J., Oh, Y. I., Chang, S. K. and Hsieh-Wilson, L. C. (2013) 'Tunable heparan sulfate mimetics for modulating chemokine activity', *Journal of the American Chemical Society*, 135, pp. 10898–10901.

Sheng, J., Liu, R., Xu, Y. and Liu, J. (2011) 'The dominating role of N-deacetylase/N-sulfotransferase 1 in forming domain structures in heparan sulfate.', *The Journal of biological chemistry*, 286(22), pp. 19768–76.

Sherwood, E. R. and Toliver-Kinsky, T. (2004) 'Mechanisms of the inflammatory response', *Best Practice and Research: Clinical Anaesthesiology*, 18(3), pp. 385–405.

Shively, J. E. and Conrad, H. E. (1976) 'Formation of anhydrosugars in the chemical depolymerization of heparin.', *Biochemistry*, 15(18), pp. 3932–42.

Shukla, D., Liu, J., Blaiklock, P., Shworak, N. W., Bai, X., Esko, J. D., Cohen, G. H., Eisenberg, R. J., Rosenberg, R. D. and Spear, P. G. (1999) 'A novel role for 3-O-sulfated heparan sulfate in herpes simplex virus 1 entry.', *Cell*, 99(1), pp. 13–22.

Shukla, D., Liu, J., Blaiklock, P., Shworak, N. W., Bai, X., Esko, J. D., Cohen, G. H., Eisenberg,

R. J., Rosenberg, R. D. and Spear, P. G. (1999) ‘A novel role for 3-O-sulfated heparan sulfate in herpes simplex virus 1 entry’, *Cell*, 99(1), pp. 13–22.

Shworak, N. W., Hajmohammadi, S., De Agostini, A. I. and Rosenberg, R. D. (2003) ‘Mice deficient in heparan sulfate 3-O-sulfotransferase-1: Normal hemostasis with unexpected perinatal phenotypes’, *Glycoconjugate Journal*, 19, pp. 355–361.

Shworak, N. W., Liu, J., Petros, L. M., Zhang, L., Kobayashi, M., Copeland, N. G., Jenkins, N. A. and Rosenberg, R. D. (1999) ‘Multiple isoforms of heparan sulfate D-glucosaminyl 3-O-sulfotransferase: Isolation, characterization, and expression of human cDNAs and identification of distinct genomic loci’, *Journal of Biological Chemistry*, 274(8), pp. 5170–5184.

Sikora, A. S., Delos, M., Martinez, P., Carpentier, M., Allain, F. and Denys, A. (2016) ‘Regulation of the Expression of Heparan Sulfate 3-O-Sulfotransferase 3B (HS3ST3B) by Inflammatory Stimuli in Human Monocytes’, *Journal of Cellular Biochemistry*, 117(7), pp. 1529–1542.

Silbert, J. E. and Sugumaran, G. (2002) ‘Biosynthesis of Chondroitin/Dermatan Sulfate’, *IUBMB Life (International Union of Biochemistry and Molecular Biology: Life)*, 54(4), pp. 177–186.

Simon, R. J., Kania, R. S., Zuckermann, R. N., Huebner, V. D., Jewell, D. A., Banville, S., Ng, S., Wang, L., Rosenberg, S. and Marlowe, C. K. (1992) ‘Peptoids: a modular approach to drug discovery.’, *Proceedings of the National Academy of Sciences of the United States of America*, 89(20), pp. 9367–71.

Situmorang, G. R. and Sheerin, N. S. (2018) ‘Ischaemia reperfusion injury: mechanisms of progression to chronic graft dysfunction’, *Pediatric Nephrology*, pp. 1–13.

Smits, N. C., Kobayashi, T., Srivastava, P. K., Skopelja, S., Ivy, J. A., Elwood, D. J., Stan, R. V., Tsongalis, G. J., Sellke, F. W., Gross, P. L., Cole, M. D., DeVries, J. T., Kaplan, A. V., Robb, J. F., Williams, S. M. and Shworak, N. W. (2017) ‘HS3ST1 genotype regulates antithrombin’s inflammomodulatory tone and associates with atherosclerosis’, *Matrix Biology*, 63, pp. 69–90.

Solez, K., Colvin, R. B., Racusen, L. C., Haas, M., Sis, B., Mengel, M., Halloran, P. F., Baldwin, W., Banfi, G., Collins, a. B., Cosio, F., David, D. S. R., Drachenberg, C., Einecke, G., Fogo, a. B., Gibson, I. W., Glotz, D., Iskandar, S. S., Kraus, E., Lerut, E., Mannon, R. B., Mihatsch, M., Nankivell, B. J., Nickeleit, V., Papadimitriou, J. C., Randhawa, P., Regele, H., Renaudin, K.,

Roberts, I., Seron, D., Smith, R. N. and Valente, M. (2008) 'Banff 07 classification of renal allograft pathology: Updates and future directions', *American Journal of Transplantation*, 8, pp. 753–760.

Song, K., Li, Q., Jiang, Z.-Z., Guo, C.-W. and Li, P. (2011) 'Heparan sulfate D-glucosaminyl 3-O-sulfotransferase-3B1, a novel epithelial-mesenchymal transition inducer in pancreatic cancer', *Cancer Biology & Therapy*, 12(5), pp. 388–398.

Spillmann, D., Witt, D. and Lindahl, U. (1998) 'Defining the interleukin-8-binding domain of heparan sulfate.', *The Journal of biological chemistry*, 273(25), pp. 15487–93.

Spinetti, G., Camarda, G., Bernardini, G., Romano Di Peppe, S., Capogrossi, M. C. and Napolitano, M. (2001) 'The Chemokine CXCL13 (BCA-1) Inhibits FGF-2 Effects on Endothelial Cells', *Biochemical and Biophysical Research Communications*, 289(1), pp. 19–24.

Spinetti, G., Kraenkel, N., Emanueli, C. and Madeddu, P. (2008) 'Diabetes and vessel wall remodelling: From mechanistic insights to regenerative therapies', *Cardiovascular Research*, pp. 265–273.

Staples, G. O. and Zaia, J. (2011) 'Analysis of Glycosaminoglycans Using Mass Spectrometry.', *Current proteomics*, 8(4), pp. 325–336.

Steer, D. L., Shah, M. M., Bush, K. T., Stuart, R. O., Sampogna, R. V., Meyer, T. N., Schwesinger, C., Bai, X., Esko, J. D. and Nigam, S. K. (2004) 'Regulation of ureteric bud branching morphogenesis by sulfated proteoglycans in the developing kidney', *Developmental Biology*, 272(2), pp. 310–327.

Steer, J. H., Vuong, Q. and Joyce, D. (1997) 'Suppression of human monocyte tumour necrosis factor-alpha release by glucocorticoid therapy: relationship to systemic monocytopaenia and cortisol suppression.', *British journal of clinical pharmacology*, 43(4), pp. 383–389.

Stefanska, A., Eng, D., Kaverina, N., Pippin, J. W., Gross, K. W., Duffield, J. S. and Shankland, S. J. (2016) 'Cells of renin lineage express hypoxia inducible factor 2α following experimental ureteral obstruction.', *BMC nephrology*, 17(5), pp. 1–11.

Stern, R. (2004) 'Hyaluronan catabolism: a new metabolic pathway', *European Journal of Cell*

Biology, 83(7), pp. 317–325.

Stoler-Barak, L., Petrovich, E., Aychek, T., Gurevich, I., Tal, O., Hatzav, M., Ilan, N., Feigelson, S. W., Shakhar, G., Vlodavsky, I. and Alon, R. (2015) 'Heparanase of murine effector lymphocytes and neutrophils is not required for their diapedesis into sites of inflammation.', *FASEB journal : official publication of the Federation of American Societies for Experimental Biology*, pp. 1–12.

Sugar, T., Wassenhove-Mccarthy, D. J., Esko, J. D., Van Kuppevelt, T. H., Holzman, L. and Mccarthy, K. J. (2014) 'Podocyte-specific deletion of NDST1, a key enzyme in the sulfation of heparan sulfate glycosaminoglycans, leads to abnormalities in podocyte organization in vivo', *Kidney International*, 85(2), pp. 307–318.

Sugaya, N., Habuchi, H., Nagai, N., Ashikari-Hada, S. and Kimata, K. (2008) '6-O-sulfation of heparan sulfate differentially regulates various fibroblast growth factor-dependent signalings in culture', *Journal of Biological Chemistry*, 283, pp. 10366–10376.

Süsal, C. and Opelz, G. (2002) 'Kidney graft failure and presensitization against HLA class I and class II antigens.', *Transplantation*, 73(8), pp. 1269–73.

Susztak, K., Raff, A. C., Schiffer, M. and Böttinger, E. P. (2006) 'Glucose-Induced Reactive Oxygen Species Cause Apoptosis of Podocytes and Podocyte Depletion at the Onset of Diabetic Nephropathy', *Diabetes*, 55, pp. 225–233.

Takeda, K., Hashimoto, K., Uchikawa, R., Tegoshi, T., Yamada, M. and Arizono, N. (2010) 'Direct effects of IL-4/IL-13 and the nematode Nippostrongylus brasiliensis on intestinal epithelial cells in vitro.', *Parasite immunology*, 32(6), pp. 420–9.

Takemura, T., Yoshida, Y., Kiso, S., Saji, Y., Ezaki, H., Hamano, M., Kizu, T., Egawa, M., Chatani, N., Furuta, K., Kamada, Y., Iwamoto, R., Mekada, E., Higashiyama, S., Hayashi, N. and Takehara, T. (2013) 'Conditional knockout of heparin-binding epidermal growth factor-like growth factor in the liver accelerates carbon tetrachloride-induced liver injury in mice', *Hepatology Research*, 43(4), pp. 384–393.

Talsma, D. T., Daha, M. R. and Van Den Born, J. (2017) 'The bittersweet taste of tubulo-interstitial glycans', *Nephrology Dialysis Transplantation*, pp. 611–619.

Tátrai, P., Egedi, K., Somorácz, Á., Van Kuppevelt, T. H., Ten Dam, G., Lyon, M., Deakin, J. A., Kiss, A., Schaff, Z. and Kovalszky, I. (2010) 'Quantitative and qualitative alterations of heparan sulfate in fibrogenic liver diseases and hepatocellular cancer', *Journal of Histochemistry and Cytochemistry*, 58(5), pp. 429–441.

Tecle, E., Diaz-Balzac, C. A. and Bülow, H. E. (2013) 'Distinct 3-O-sulfated heparan sulfate modification patterns are required for kal-1-dependent neurite branching in a context-dependent manner in Caenorhabditis elegans.', *G3 (Bethesda, Md.)*, 3(3), pp. 541–52.

Terada, T., Mizobata, M., Kawakami, S., Yabe, Y., Yamashita, F. and Hashida, M. (2006) 'Basic fibroblast growth factor-binding peptide as a novel targeting ligand of drug carrier to tumor cells', *Journal of Drug Targeting*, 14(8), pp. 536–545.

Thacker, B. E., Seamen, E., Lawrence, R., Parker, M. W., Xu, Y., Liu, J., Vander Kooi, C. W. and Esko, J. D. (2016a) 'Expanding the 3-O-Sulfate Proteome - Enhanced Binding of Neuropilin-1 to 3-O-Sulfated Heparan Sulfate Modulates Its Activity', *ACS Chemical Biology*, 11(4), pp. 971–980.

Thacker, B. E., Seamen, E., Lawrence, R., Parker, M. W., Xu, Y., Liu, J., Vander Kooi, C. W. and Esko, J. D. (2016b) 'Expanding the 3-O-Sulfate Proteome - Enhanced Binding of Neuropilin-1 to 3-O-Sulfated Heparan Sulfate Modulates Its Activity', *ACS Chemical Biology*, 11(4), pp. 971–980.

Thacker, B. E., Xu, D., Lawrence, R. and Esko, J. D. (2014) 'Heparan sulfate 3-O-sulfation: a rare modification in search of a function.', *Matrix biology*, 35, pp. 60–72.

Thadhani, R., Pascual, M. and Bonventre, J. V. (1996) 'Acute Renal Failure', *New England Journal of Medicine*, 334(22), pp. 1448–1460.

Tiwari, V., O'Donnell, C. D., Oh, M. J., Valyi-Nagy, T. and Shukla, D. (2005) 'A role for 3-O-sulfotransferase isoform-4 in assisting HSV-1 entry and spread', *Biochemical and Biophysical Research Communications*, 338(2), pp. 930–937.

Traeger, T., Koerner, P., Kessler, W., Cziupka, K., Diedrich, S., Busemann, A., Heidecke, C.-D. and Maier, S. (2010) 'Colon Ascendens Stent Peritonitis (CASP) - a Standardized Model for Polymicrobial Abdominal Sepsis', *Journal of Visualized Experiments*, (46), p. e2299.

Trowbridge, J. M. and Gallo, R. L. (2002) 'Dermatan sulfate: new functions from an old

glycosaminoglycan', *Glycobiology*, 12(9), pp. 117–125.

Turnbull, J. E., Fernig, D. G., Ke, Y., Wilkinson, M. C. and Gallagher, J. T. (1992) 'Identification of the basic fibroblast growth factor binding sequence in fibroblast heparan sulfate', *Journal of Biological Chemistry*, 267(15), pp. 10337–10341.

Ullman, E. (1914) 'Tissue and organ transplantation', *Annals of surgery*, 60(2), pp. 195–219.

Vanderheyden, T., Kumar, S. and Fisk, N. M. (2003) 'Fetal renal impairment', *Seminars in Neonatology*, 8(4), pp. 279–289.

Vanheule, V., Janssens, R., Boff, D., Kitic, N., Berghmans, N., Ronsse, I., Kungl, A. J., Amaral, F. A., Teixeira, M. M., Van Damme, J., Proost, P. and Mortier, A. (2015) 'The positively charged COOH-terminal glycosaminoglycan-binding CXCL9(74-103) peptide inhibits CXCL8-induced neutrophil extravasation and monosodium urate crystal-induced gout in mice', *Journal of Biological Chemistry*, 290(35), pp. 21292–21304.

Vanpouille, C., Deligny, A., Delehedde, M., Denys, A., Melchior, A., Liénard, X., Lyon, M., Mazurier, J., Fernig, D. G. and Allain, F. (2007) 'The heparin/heparan sulfate sequence that interacts with cyclophilin B contains a 3-O-sulfated N-unsubstituted glucosamine residue', *Journal of Biological Chemistry*, 282(33), pp. 24416–24429.

Vaughan, E. D., Marion, D., Poppas, D. P. and Felsen, D. (2004) 'Pathophysiology of unilateral ureteral obstruction: studies from Charlottesville to New York.', *The Journal of urology*, 172(6 Pt 2), pp. 2563–9.

Vivès, R. R., Seffouh, A. and Lortat-Jacob, H. (2014) 'Post-Synthetic Regulation of HS Structure: The Yin and Yang of the Sulfs in Cancer', *Frontiers in Oncology*, 3, p. 331.

Vlieghe, P., Lisowski, V., Martinez, J. and Khrestchatisky, M. (2010) 'Synthetic therapeutic peptides: science and market', *Drug Discovery Today*, 15(1–2), pp. 40–56.

Wall, J. S., Richey, T., Stuckey, A., Donnell, R., Macy, S., Martin, E. B., Williams, A., Higuchi, K. and Kennel, S. J. (2011) 'In vivo molecular imaging of peripheral amyloidosis using heparin-binding peptides.', *Proceedings of the National Academy of Sciences of the United States of America*, 108(34), pp. E586-94.

Wang, L., Fuster, M., Sriramarao, P. and Esko, J. D. (2005) 'Endothelial heparan sulfate deficiency impairs L-selectin- and chemokine-mediated neutrophil trafficking during inflammatory responses.', *Nature immunology*, 6(9), pp. 902–910.

Weber, M., Hauschild, R., Schwarz, J., Moussion, C., de Vries, I., Legler, D. F., Luther, S. A., Bollenbach, T. and Sixt, M. (2013) 'Interstitial dendritic cell guidance by haptotactic chemokine gradients.', *Science*, 339(6117), pp. 328–32.

Wei, Q. and Dong, Z. (2012) 'Mouse model of ischemic acute kidney injury: technical notes and tricks', *American journal of physiology. Renal physiology*, 303(11), pp. 1487–1494.

Wells, A. F., Larsson, E., Tengblad, A., Fellström, B., Tufveson, G., Klareskog, L. and Laurent, T. C. (1990) 'The localization of hyaluronan in normal and rejected human kidneys.', *Transplantation*, 50(2), pp. 240–3.

Westergren-Thorsson, G., Hedström, U., Nybom, A., Tykesson, E., Åhrman, E., Hornfelt, M., Maccarana, M., van Kuppevelt, T. H., Dellgren, G., Wildt, M., Zhou, X.-H., Eriksson, L., Bjermer, L. and Hallgren, O. (2017) 'Increased deposition of glycosaminoglycans and altered structure of heparan sulfate in idiopathic pulmonary fibrosis', *The International Journal of Biochemistry & Cell Biology*, 83, pp. 27–38.

Wiggins, R. C. (2007) 'The spectrum of podocytopathies: A unifying view of glomerular diseases', *Kidney International*, 71(12), pp. 1205–1214.

Wijnhoven, T. J. M., Geelen, J. M., Bakker, M., Lensen, J. F. M., Rops, A. L. W. M. M., Kramer, A. B., Navis, G., Van Den Hoven, M. J. W., Van Der Vlag, J., Berden, J. H. M., Wetzels, J. F. M., Van Den Heuvel, L. P. W. J., Monnens, L. A. H. and Van Kuppevelt, T. H. (2007) 'Adult and paediatric patients with minimal change nephrotic syndrome show no major alterations in glomerular expression of sulphated heparan sulphate domains', *Nephrology Dialysis Transplantation*, 22(10), pp. 2886–2893.

Wijnhoven, T. J. M., Lensen, J. F. M., Rops, A. L. W. M. M., van der Vlag, J., Kolset, S. O., Bangstad, H.-J., Pfeffer, P., van den Hoven, M. J. W., Berden, J. H. M., van den Heuvel, L. P. W. J. and van Kuppevelt, T. H. (2006) 'Aberrant Heparan Sulfate Profile in the Human Diabetic Kidney Offers New Clues for Therapeutic Glycomimetics', *American Journal of Kidney Diseases*,

48(2), pp. 250–261.

Woodhouse, S., Batten, W., Hendrick, H. and Malek, P. A. (2006) 'The Glomerular Filtration Rate: An Important Test for Diagnosis, Staging, and Treatment of Chronic Kidney Disease', *Laboratory Medicine*, 37(4), pp. 244–246.

Wynn, T. A. (2007) 'Common and unique mechanisms regulate fibrosis in various fibroproliferative diseases', *Journal of Clinical Investigation*, 117(3), pp. 524–529.

Xia, G., Chen, J., Tiwari, V., Ju, W., Li, J.-P., Malmstrom, A., Shukla, D. and Liu, J. (2002) 'Heparan sulfate 3-O-sulfotransferase isoform 5 generates both an antithrombin-binding site and an entry receptor for herpes simplex virus, type 1.', *The Journal of biological chemistry*, 277(40), pp. 37912–9.

Xiong, J., Wang, Y., Zhu, Z., Liu, J., Wang, Y., Zhang, C., Hammes, H.-P., Lang, F. and Feng, Y. (2007) 'NG2 proteoglycan increases mesangial cell proliferation and extracellular matrix production', *Biochemical and Biophysical Research Communications*, 361(4), pp. 960–967.

Xu, C., Chang, A., Hack, B. K., Eadon, M. T., Alper, S. L. and Cunningham, P. N. (2014) 'TNF-mediated damage to glomerular endothelium is an important determinant of acute kidney injury in sepsis.', *Kidney international*, 85(1), pp. 72–81.

Xu, D., Tiwari, V., Xia, G., Clement, C., Shukla, D. and Liu, J. (2005) 'Characterization of heparan sulphate 3-O-sulphotransferase isoform 6 and its role in assisting the entry of herpes simplex virus type 1.', *The Biochemical journal*, 385(Pt 2), pp. 451–9.

Yang, J., Su, Y., Zhou, Y. and Besner, G. E. (2014) 'Heparin-binding EGF-like growth factor (HB-EGF) therapy for intestinal injury: Application and future prospects.', *Pathophysiology : the official journal of the International Society for Pathophysiology*, 21(1), pp. 95–104.

Yayon, A., Aviezert, D., Safrant, M., Grosst, J. L., Heldman, Y., Cabilly, S., Givolt, D. and Katchalski-Katzir, E. (1993) 'Isolation of peptides that inhibit binding of basic fibroblast growth factor to its receptor from a random phage-epitope library', *Proc. Natl. Acad. Sci. USA*, 90, pp. 10643–10647.

Ye, S., Luo, Y., Lu, W., Jones, R. B., Linhardt, R. J., Capila, I., Toida, T., Kan, M., Pelletier, H.

and McKeehan, W. L. (2001) ‘Structural basis for interaction of FGF-1, FGF-2, and FGF-7 with different heparan sulfate motifs’, *Biochemistry*, 40(48), pp. 14429–14439.

Yin, F., Li, P., Zheng, M., Chen, L., Xu, Q., Chen, K., Wang, Y. Y., Zhang, Y. Y. and Han, C. (2003) ‘Interleukin-6 family of cytokines mediates isoproterenol-induced delayed STAT3 activation in mouse heart’, *Journal of Biological Chemistry*, 278(23), pp. 21070–21075.

Yu, L., Border, W. A., Huang, Y. and Noble, N. A. (2003) ‘TGF-β isoforms in renal fibrogenesis’, *Kidney International*, 64(3), pp. 844–856.

Yuan, Y., Zhang, F., Wu, J., Shao, C. and Gao, Y. (2015) ‘Urinary candidate biomarker discovery in a rat unilateral ureteral obstruction model.’, *Scientific reports*, 5, p. 9314.

Yue, B. (2014) ‘Biology of the extracellular matrix: An overview’, *Journal of Glaucoma*, 23(8), pp. S20–S23.

Yue, X., Li, X., Nguyen, H. T., Chin, D. R., Sullivan, D. E. and Lasky, J. A. (2008) ‘Transforming growth factor-beta1 induces heparan sulfate 6-O-endosulfatase 1 expression in vitro and in vivo.’, *The Journal of biological chemistry*, 283(29), pp. 20397–407.

Yue, X., Lu, J., Auduong, L., Sides, M. D. and Lasky, J. A. (2013) ‘Overexpression of Sulf2 in idiopathic pulmonary fibrosis.’, *Glycobiology*, 23(6), pp. 709–19.

Zhang, L., Lawrence, R., Schwartz, J. J., Bai, X., Wei, G., Esko, J. D. and Rosenberg, R. D. (2001) ‘The effect of precursor structures on the action of glucosaminyl 3-O-sulfotransferase-1 and the biosynthesis of anticoagulant heparan sulfate.’, *The Journal of biological chemistry*, 276(31), pp. 28806–13.

Zhang, L., Song, K., Zhou, L., Xie, Z., Zhou, P., Zhao, Y., Han, Y., Xu, X. and Li, P. (2015) ‘Heparan sulfate D-glucosaminyl 3-O-sulfotransferase-3B1 (HS3ST3B1) promotes angiogenesis and proliferation by induction of VEGF in acute myeloid leukemia cells’, *Journal of Cellular Biochemistry*, 116(6), pp. 1101–1112.

Zhang, W., Moskowitz, R. W., Nuki, G., Abramson, S., Altman, R. D., Arden, N., Bierma-Zeinstra, S., Brandt, K. D., Croft, P., Doherty, M., Dougados, M., Hochberg, M., Hunter, D. J., Kwoh, K., Lohmander, L. S. and Tugwell, P. (2008) ‘OARSI recommendations for the management of hip

and knee osteoarthritis, Part II: OARSI evidence-based, expert consensus guidelines', *Osteoarthritis and Cartilage*, 16(2), pp. 137–162.

8 Appendices

8.1 Oral presentations

Development of Heparin and HS Glycotherapeutics, workshop, Vietnam 2018

New findings and potential use of Heparan Sulfate in kidney diseases

Laura Ferreras, Jeremy E. Turnbull, Edwin A Yates, Neil S. Sheerin, Simi Ali

UK GAGs and PGs meeting, UK 2017

Heparan Sulfate sulfation in renal fibrosis

Laura Ferreras, John A Kirby, Neil S Sheerin, Simi Ali

Glycans & Proteoglycans: The Sweet and Smart Molecules, workshop, France 2017

Modulation of Heparan Sulfate sulfation in renal fibrosis.

Laura Ferreras, Anna Moles, Rana el Masri, Romain R. Vivès, Neil S. Sheerin, Simi Ali

International Proteoglycans conference, Italy 2017

Heparan sulfate in renal fibrosis: what role for the 3-O-sulfotransferases?

Laura Ferreras, Neil S Sheerin, Anna Moles, Marion Kusche-Gullberg, Katie Cooke, Simi Ali

10th North East Renal Research mini-symposium, UK 2017

Heparan sulfate sulfation in renal fibrosis

Laura Ferreras, John A Kirby, Neil S Sheerin, Simi Ali

ICM Research Seminar, UK 2017

Heparan sulfate 3-O sulfotransferases in renal fibrosis

Laura Ferreras, Neil S Sheerin, Marion Kusche-Gullberg, Simi Ali

Proteoglycans Gordon Research Seminar, USA 2016

Investigating the role of heparin sulfate 3-O-sulfotransferases in renal fibrosis

Laura Ferreras, Neil S Sheerin, Marion Kusche-Gullberg, Simi Ali

4th North East Renal Research mini-symposium, UK 2015

The role of Heparan Sulfate in chronic renal rejection

Laura Ferreras, John A Kirby, Neil S Sheerin, Simi Ali

8.2 Poster presentation

BSMB Spring Meeting, UK 2017

Heparan sulfate 3-O sulfotransferases in renal fibrosis.

Laura Ferreras, Neil S Sheerin, Anna Moles, Marion Kusche-Gullberg, Katie Cooke, Simi Ali

Proteoglycans Gordon Research Conference, USA 2016

Investigating the role of heparin sulfate 3-O-sulfotransferases in renal fibrosis

Laura Ferreras, Neil S Sheerin, Marion Kusche-Gullberg, Simi Ali

North East Kidney Patient and family/Career Day, UK 2015

Understanding and preventing renal graft loss: The role of Heparan sulfate

Laura Ferreras, Neil S Sheerin, John A Kirby, Simi Ali

8.3 Awards

Best Oral Presentation award, International Proteoglycans conference, Italy 2017

Best Poster Presentation award BSMB spring meeting, Oxford 2017

Best Poster Presentation award prICM Poster event, Newcastle University 2017

EMBO short term fellowship 2016 (1687.4€, ASTF No: 251)

ISMB international travel award 2017 (400€)

Newcastle University travel award 2017 (£500)

Biochemical Society travel award 2017 (£400)

BSI travel award 2016 (£1000)

8.4 Publications

From this work:

Ferreras L., Moles A., Situmorang G. R., el Masri R., Wilson I. L., Cooke K., Kusche-Gullberg M., Vivès R. R., Sheerin N. S., Ali S. Heparan sulfate in chronic kidney diseases: exploring the role of 3-O-sulfation (*submitted to Biochimica et Biophysica Acta general subjects October 2018*)

Ferreras L., Sheerin N. S., Moles A., Kusche-Gullberg M., Ali S., British Society for Matrix Biology Spring 2017 Meeting. Heparan sulfate 3-O sulfotransferases in renal fibrosis. International Journal of Experimental Pathology vol. 98 issue 3 pp: A1-A23 (2017).

Ferreras, L., Sheerin, N. S., Kirby, J. A., Ali, S. Mechanisms of Renal Graft Chronic Injury and Progression to Interstitial Fibrosis. Current Transplantation Reports. 2, 259–268 (2015).

From previous work:

Reynaud C., **Ferreras L**., DiMauro P., Kan C., Croset M., Bonnelye E., Pez F., Thomas C., Aimont G., Karnoub A.E., Brevet M., Clezardin P. Lysyl oxidase is a strong determinant of tumor cell colonization in bone. Cancer Research; 77, 2 (2016).

Bochaton, T., Crola-Da-Silva, C., Pillot B., Villedieu, C., **Ferreras, L.**, Alam, M.R., Thibault, H., Strina, M., Gharib, A., Ovize, M., Baetz, D. Inhibition of myocardial reperfusion injury by ischemic postconditioning requires sirtuin 3-mediated deacetylation of cyclophilin D. J Mol Cell Cardiol. 84, 61 (2015).

8.5 Published review

Curr Transpl Rep (2015) 2:259–268
DOI 10.1007/s40472-015-0069-2

IMMUNOLOGY (R FAIRCHILD, SECTION EDITOR)

Mechanisms of Renal Graft Chronic Injury and Progression to Interstitial Fibrosis

Laura Ferreras[1] · Neil S. Sheerin[1] · John A. Kirby[1] · Simi Ali[1]

Published online: 27 June 2015

Abstract Following transplantation, the kidney is exposed to many different injuries which result in inflammation, overproduction of extracellular matrix, interstitial fibrosis and progressive loss of renal function. To date, treatment options for patients with progressive graft dysfunction are very limited. The development of new therapies requires a better understanding of the pathogenesis of transplant interstitial fibrosis and specific biomarkers to identify patients with progressive transplant fibrosis and monitor response to new therapies. Here, we review our current understanding of how and why extracellular matrix accumulates and the relationship between fibrosis and inflammation. In particular, we focus on the role of heparan sulphate that regulates recruitment, migration and differentiation of interstitial cells and also acts as a reservoir for multiple cytokines and growth factors.

This article is part of the Topical Collection on *Immunology*

✉ Simi Ali
simi.ali@ncl.ac.uk

Laura Ferreras
laura.ferreras@ncl.ac.uk

Neil S. Sheerin
neil.sheerin@ncl.ac.uk

John A. Kirby
john.kirby@ncl.ac.uk

[1] Applied Immunobiology and Transplantation Group, Institute of Cellular Medicine, Medical School, Newcastle University, Newcastle Upon Tyne NE2 4HH, UK

Keywords Kidney transplantation · Chemokines · Heparan sulphate · Migration · Inflammation · Interstitial fibrosis · Glycosaminoglycan

Introduction

Clinical Summary

Renal transplantation is the best option for patients with end-stage kidney disease. In 2012, at least 77,800 kidney transplants were performed worldwide [1]. In the UK, graft survival rate after renal transplantation is 85–95 % after 1 year, 70–80 % after 5 years and 50–60 % after 15 years. Ten years after kidney transplantation, over 50 % of patients will have evidence of progressive chronic graft dysfunction [2]. In order to reduce injury and prolong organ survival, a clear understanding of the different physiological events occurring before, during and after transplantation is essential.

Risk Factors for Interstitial Fibrosis/Tubular Atrophy

Before transplantation, the integrity of the organ depends on the donor. Cadaveric transplantation, donor vascular pathology and age of the donor are important factors that impact early and long-term graft function. Transplantation involves a period of ischemia, followed by reperfusion, during which there is an oxidative burst with increased production of reactive oxygen and nitrogen species, pH changes, an increase in mitochondrial calcium and, if severe, cell death. Haemodynamic changes after

transplantation are also important with glomerular hypertension and angiotensin II-mediated remodelling leading to impaired kidney function. Additionally, after transplantation, urinary infection and drug toxicity, in particular, the pro-fibrotic effects of calcineurin inhibitors are also associated with graft dysfunction.

Classification of Interstitial Fibrosis

In the past, research in renal transplant was hindered by a lack of a common classification of renal transplant pathology. The Banff classification is an international standard classification of renal transplant pathology that was introduced to overcome this problem. This classification takes into account different stages in the evolution of graft inflammation and fibrosis. Since 2007, the classification considers five categories as shown in Table 1.

Interstitial Fibrosis/Tubular Atrophy: an Active Matrix-Cell Interaction

Initiation: Chemokines and Inflammation: a Glycosaminoglycan-Dependant Phenomenon

Interstitial fibrosis tubular atrophy (IFTA) can result from chronic rejection and is frequently associated with infiltration of inflammatory cells. The interaction between these inflammatory cells and the extracellular matrix (ECM) is an important factor in the development of the inflammatory response and tissue injury. Glycosaminoglycans (GAG), also known as mucopolysaccharides, are glucosidic macromolecules composed of repeating disaccharide entities. Chondroitin sulphate, dermatan sulphate, keratan sulphate and heparin/heparan sulphate (HS) are the main GAGs found in tissue. HS is synthesised by all mammalian cells; it can be found covalently attached to various protein cores and is a major component of the ECM. HS is composed of a 10–200 disaccharide subunits with a hexuronic acid that could either be D-glucuronic acid or L-iduronic acid (IdoA) linked to a D-glucosamine (GlcN). Uronyl C-5-epimerase converts D-glucuronic acid into L-iduronic acid. The resulting IdoA can be sulphated at the 2-O position by a glucosaminyl 2-O-sulfotransferase (HS2ST). GlcN can be sulphated at the 3–O, 6-O or N positions by seven glucosaminyl 3-O-sulfotransferase (HS3STs), three glucosaminyl 6-O-sulphotransferases (HS6ST) and four glucosaminyl N-deacetylase/N-sulphotransferases, respectively (NDST). Following its synthesis, HS is associated with a protein to form HS proteoglycans (HSPG) that have multiple functions in cell physiology [4].

At present, around 50 chemokines and 20 chemokine receptors have been discovered. Chemokines consist of three antiparallel beta strands and an alpha helical region at the C-terminus. They are classified based on the position of the first two N-terminal cysteines. They can bind to specific G-protein-coupled receptors to induce migratory responses.

Chemokine signalling promotes neuronal migration and vascular remodelling and attracts cancer cells to distant sites during metastasis. During allograft rejection, chemokine expression follows a temporal pattern and their expression varies inside the graft itself [5]. Chemokines also undergo post-translational modifications during inflammation [6], for example nitration, which can alter their biological function including leukocyte recruitment [7].

Chemokines can bind to GAGs on cell surfaces and within the ECM. HS protects chemokines from degradation, enhances receptor binding and therefore regulates activity of chemokines, but most importantly, HS is responsible for the

Table 1 Classification of renal allograft rejection[a]

1	Normal	No rejection detected
2	Antibody-mediated rejection	Antibody-mediated graft injury with C4d staining in the glomerulus and peri-tubular capillaries. Associated with capillary, vascular or glomerular inflammation, acute tubular necrosis or chronic injury (including IFTA)
3	Borderline changes	Interstitial lymphocyte infiltrates with minor tubulitis and no intimal arteritis
4	T cell-mediated rejection	Significant interstitial, tubular inflammation and/or intimal inflammation. Chronic arteriopathy also included
5	Interstitial fibrosis and tubular atrophy (IFTA)	In the absence of another pathology. Grade I mild 25 % of cortical area, grade II 26 to 50 % cortical area and grade III when more of 50 % of cortical area is affected
6	Other	Changes that are not caused by rejection

[a] This classification reflects the different events that lead to graft dysfunction

Data from [3]

chemokine gradient that attracts immune cells [8••]. The chemokine-GAG interaction is required for leukocyte binding to the endothelium and transmigration across the endothelium [9] and chemotaxis to the site of tissue injury [8••] as illustrated in Fig. 1. This review will focus on the role of HS in the development of graft inflammation and fibrosis.

Gradient Creation and Leukocyte Migration

Leukocyte recruitment is initiated by endothelial cell activation and chemokine presentation to leukocytes. However, the presence of chemokines alone is not sufficient to trigger leukocyte diapedesis. The spatial and temporal organisation of chemokines during inflammation is critical for leukocyte migration [5]. A higher chemokine concentration in the vessel wall and extravascular space generates a chemokine gradient along which leukocytes travel through the vessel wall and into the ECM [8••, 11, 12].

The binding of leukocytes to endothelial cells has been extensively studied. HS is important for the selectin-mediated binding of neutrophils to the endothelium. P- and E-selectin expression on endothelial cells and L-selectin on neutrophils are important for neutrophil migration. Mice that lack an enzyme important for HS biosynthesis (NDST1) in endothelial cells and leukocytes demonstrate weak L-selectin-mediated binding and a reduced rolling velocity [13].

The ECM is vital in generating and maintaining the chemokine gradient required for the cell migration, that occurs in graft rejection, embryonic development, formation of metastasis and infection. For example, in mouse skin, dendritic cells are guided toward lymphatic vessels by an endogenous gradient of CCL21. Dissociation of CCL21 from matrix HS using heparitinase diminishes the migration by disrupting the chemokine gradient [8••]. In another study, Massena et al. [12] analysed neutrophil migration in heparanase transgenic animals (hpa-tg mice). Overexpression of heparanase significantly reduced directional migration of neutrophils which was replaced by random crawling. These experiments highlight the importance of HS for leukocyte migration.

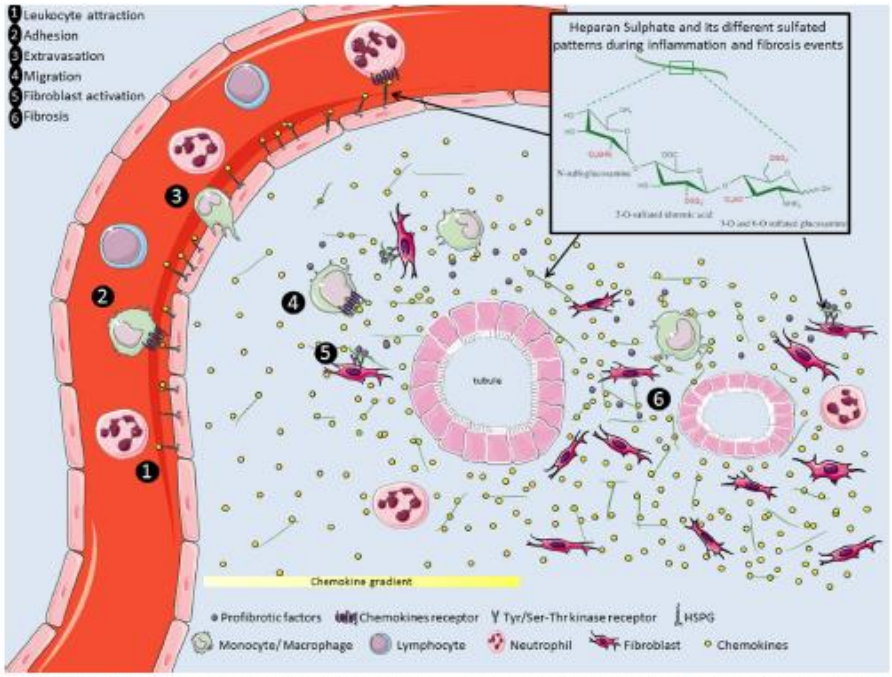

Fig. 1 The role of HS in the multistep processes leading to inflammation and fibrosis. During inflammation, immune cells such as neutrophils and monocytes are attracted to the site of inflammation (*1*) and adhere to the activated endothelium (*2*). HS promotes adhesion to the vessel wall through chemokine gradient formation and presentation (2) and selectin interaction (not shown). Following basal lamina transmigration (*3*), the immune cells migrate via a chemokine gradient established by HS and reach the matrix surrounding the tubules (*4*). Secretion of pro-fibrotic factors by immune cells will activate fibroblasts (*5*) and lead to fibrosis and later tubular atrophy (*6*). *Top right image*—HS structure and its multiple sulfation sites. *HSPG* heparan sulphate proteoglycans, *Tyr/Ser-Thr* tyrosine or serine-threonine kinase receptor, *HS* heparan sulphate. Figure was produced using Servier medical kit [10]

GAGs Protect Chemokines from Enzymatic Degradation

Proteolysis in the ECM is an active process responsible for matrix remodelling that also controls activity of non-matrix proteins. Chemokine degradation by metalloproteinases or peptidases would impact on the generation of an effective gradient and therefore leukocyte infiltration. The binding of chemokines to HS can protect them from proteolysis, increasing their half-life in the ECM and therefore supporting a higher chemokine concentration that is essential for leukocyte migration. For example, HS protects CXCL12 from degradation by the peptidase CD26/dipeptidyl peptidase IV [14].

Regulation of Chemokines Activity by GAGs

HS is crucial for the activity of many chemokines and growth factors. HS does not only bind chemokines and growth factors but can also act as a scaffold for the assembly and presentation of ligands to their receptors [15], increasing their activity at low concentrations [16]. Chemokines can be monomeric or form oligomers in solution. The monomeric form can bind its receptor and induce cell migration [17]. However, oligomerized chemokines can be more active than the monomeric form, and for some, it is an absolute requirement for their function in vivo [18]. Physiological activity of CCL5 relies on GAG binding-induced oligomerization [19], and disrupting oligomerisation has been proposed as a novel therapeutic strategy to inhibit chemokine function.

These findings show that HS not only protects chemokines from degradation and helps create a gradient but also enhances ligand-receptor interactions of many molecules implicated in the development of IFTA. It triggers the activation of many signalling pathways by increasing the ability of chemokines and growth factors to bind their target receptors.

Interstitial Fibrosis

Once in the injured tissue, leukocytes such as macrophages, T cells and mast cells are important mediators of interstitial fibrosis. The degree of renal fibrosis is correlated with the extent of leukocyte infiltration. M2 macrophages, mast cells and T cells can release pro-fibrotic mediators (insulin-like growth factor-1, fibroblast growth factor 2 and transforming growth factor-β1) [20•]. Therefore, the presence of leukocytes in the renal interstitium promotes fibroblast activation and proliferation (see Fig. 1).

Interstitial fibroblasts can be derived from several sources including resident fibroblasts, bone marrow-derived fibrocytes and epithelial cells by the processes of epithelial to mesenchymal transition (EMT) [21] and endothelial to mesenchymal transition [22, 23]. Fibroblast proliferation and activation will lead to an increase in matrix biosynthesis which is also controlled by growth factors such as TGF-β and FGF2.

GAGs have a key role in controlling the fibrotic response as a consequence of the interaction between GAGs and growth factors. HS is implicated in the initiation of the signalling pathway of pro-fibrotic factors. Several studies that explored the interaction of TGF-β and HSPGs demonstrate that HSPG binds to the latent TGF-β-binding protein (LTBP) [24•]. TGF-β is initially synthesised as an inactive precursor which is cleaved to form the mature, active peptide. Two mature peptides are associated with two molecules of another protein, latency-associated peptide (LAP), to form a small latent complex. This is then covalently bound to the LTBP. This whole complex (the large latent complex) is then secreted from the cell where it can bind to the ECM, specifically HSPGs. Therefore, the ECM acts as a reservoir to TGFβ which can be activated in response to injury, and in the kidney, it contributes to progressive fibrosis [24•]. Furthermore, studies have demonstrated that HSPG expression on the cell surface is crucial for FGF2-induced renal fibroblast proliferation which is a prominent factor during interstitial fibrosis [25].

Modification of GAGs During Matrix Remodelling

Biosynthesis, post-translational modifications and degradation of ECM proteins are key processes in tissue homeostasis and contribute to the development of irreversible fibrosis. As discussed above, the ECM is not simply a product of the fibrotic response, instead the biochemistry of the matrix can alter severity and type of injury.

HS proteoglycan expression can vary during embryonic development and ageing and during the development of disease [26]. In the kidney, the level of N-sulphated-HS is significantly increased during acute rejection [27] and 6-O-sulfation is increased in fibrotic renal disease [28]. Expression of the HSPG perlecan shows a significant increase in the glomeruli of rat renal allografts compared with isografts and non-transplanted kidneys [29]. These changes in the profile of tissue HSPGs may be the consequence of disease but, as discussed above, may then alter the outcome of injury. HSPGs could also have a protective role in transplantation. Increased syndecan-1 expression after transplantation is associated with low levels of proteinuria and lower serum creatinine. There is evidence that syndecan-1 is not simply a biomarker of renal function but has a causal role in protecting the allograft. Syndecan-1-deficient mice have worse renal function, tubular damage, and an increase in interstitial macrophages and myofibroblasts compared with wild-type mice following bilateral renal ischemia/reperfusion [30•].

There is conflicting evidence that HS can either drive inflammation or have a protective role in transplantated kidneys. There are two explanations for those observations. Firstly,

different matrix proteins can undergo post-translation modification by the addition of HS groups. Secondly, HS function will vary depending on the level and state of sulfation. Different enzymes regulate HS post-translational modification such as the addition of a sulphate group (sulfation) or an acetyl group (acetylation). Both modifications play a role in chemokine and growth factor binding and therefore in leukocyte recruitment and tissue fibrosis. Specific regions of HS selectively interact with chemokines and growth factors, and sulfation and acetylation at these sites will affect HS function. Sulfation generates a high negative charge on HS (see red groups Fig. 1) allowing positively charged molecules such as FGF-2 to bind with a low dissociation constant (Kd), and different sulfation patterns will modify the affinity of HS with FGF2 [31]. Heparin promotes the interaction between FGF and FGFR. Within the HS molecule, 2-O-sulfation is necessary for binding whereas 6-O-sulfation is required for FGF2-FGFR1 signalling [32–34]. A low Kd allows a very high affinity between these molecules which implies that a low concentration of FGF2 will be able to activate its signalling pathway. Therefore, cells having highly sulphated HS will be more sensitive to FGF2.

Enzymes Involved in HS Modification

After transplantation, there can be differential expression of HS-modifying enzymes, and this could modify HS-chemokine and growth factor interactions and therefore cell infiltration and the fibrotic response. The expression of HS-modifying enzymes could impact multiple steps implicated in the development of IFTA (see Table 2).

Modifying HS impacts on early events in fibrosis. Recently, Massola V. et al. published two papers showing that, in human renal proximal tubular cell line (HK2), the silencing of heparanase, an enzyme that cleaves HSPG, inhibits EMT induced by FGF-2 and reduces TGF-β expression. The function of heparanase can vary depending on the scenario studied (see Table 2) [49]. As an example, mice overexpressing the enzyme show a drop in leukocyte recruitment; however, patients with ulcerative colitis, characterised by significant inflammatory cell infiltration, have an increase in heparanase expression [50]. Heparanase overexpression in these patients might be a response by the body to disrupt the chemokine gradient created by HS.

Taken together, these results show that the modulation of HS in the ECM and on cell membranes is crucial for the initiation of inflammation and fibrosis. However, if we look into inflammation and matrix remodelling processes, young patients with juvenile idiopathic arthritis have similar HS plasma and urinary concentrations compared to healthy controls [51]. It is probable that it is not only the presence of HS that determines function but also its sulfation pattern. HS sulfation modification will determine the ability of the transplant to recruit leukocytes, support inflammation and trigger fibrosis (see Table 2).

HS N-Sulfation and Acetylation Patterns

The N-sulfation pattern increases the negative charge present on HS and therefore increases its affinity for positively charged molecules such as chemokines and growth factors. The expression of N-sulphated HS is increased in acutely rejecting kidney. This observation can be explained by the effect that pro-inflammatory cytokines have on the expression of the two isoforms of N-deacetylase-sulphotransferase NDST [1, 2] increasing expression of both [52]. Also, it was found that following aortic transplantation in a mouse model, inflammatory cell invasion was significantly reduced in transplants from NDST-1-deficient donors [53]. Thus, it appears that the modulation of NDST expression by pro-inflammatory cytokines can modulate leukocyte infiltration, impact the capacity of HS to bind pro-fibrotic factors and, therefore, increase inflammation and fibrosis.

HS O-Sulfation Patterns

The level of O-sulfation of HS varies in the transplanted kidney. In human renal allograft, the use of specific antibodies targeting sulphate groups at N-, 6-O and 2-O positions show an increase in HS sulfation during chronic rejection [28], a pattern that has been found important for FGF2 activity [54]. Additionally, N- and O-sulfation seems to modulate HSPG affinity to different growth factors [55].

Furthermore, one isoform of HS3ST enzyme, the heparan sulphate D-glucosaminyl 3-*O*-sulfotransferase-3B1, when overexpressed in a pancreatic cell line promotes EMT [40]. The cells used in this study show, after transfection, a fibroblastic morphology, a decrease in E cadherin and b-catenin (epithelial markers), and an increase in mesenchymal markers. These results agree with the previous conclusion that the modulation of HS enzymes within an allograft can enhance the fibrotic response (see Table 2). However, it has been found that another isoform, HS3ST1, is overexpressed in tolerant, drug-free renal transplant recipients [41]. Little is known about the 3-O-sulphation of HS, and our current work is trying to resolve the mystery of the double-edged sword that is HS 3-O-sulfation.

Therapeutic Opportunities

Mutant Chemokines

Knowledge of the interaction between HS and chemokines and growth factors [31, 56] allows design of compounds that do not bind HS [57–59]. These would interfere with gradient

Table 2 Enzymes implicated in HS sulfation: modulated expression and impacts

Enzyme studied	Model	Methods/analysis	Observations	Ref
NDST (1–4) *N*-deacetylase-sulfotransferase	Mice NDST1−/− endothelial cell specific	Acute peritonitis, contact dermatitis	Impaired inflammatory responses. Decreased neutrophil infiltration	[13]
	Mice NDST1−/− endothelial cell and leukocytes specific	Antiglomerular basement membrane nephritis	Decrease in granulocyte and macrophage influx. Improved renal function and reduced glomerular injuries (creatinine blood urea nitrogen; glomerular hyalinosis)	[35•]
		Acute inflammatory reaction (induced by IP thioglycollate); air pouch model	Decrease in chemokine presentation, migration and neutrophil influx	[13]
		Repetitive allergen exposure analyses of airway remodelling	Less macrophage infiltration and peribronchial fibrosis compared to WT	[36]
	NDST1−/− mice	Generation of NDST1 null mice	Non-viable, neonatal death due to lung defects	[37]
	NDST2−/− mice	Intraperitoneal injection of IgE followed by anti IgE antibodies injection	No significant difference in neutrophil influx in the peritoneum compared to NDST2+/+ mice but have decreased number of connective tissue mast cells	[38]
HS2ST 2-*O*-sulfotransferase	Mice HS2ST−/− endothelial cell specific	Acute peritonitis	Increase in neutrophils and monocyte infiltration, enhanced chemokine binding and number of neutrophils attached to the endothelial cell surface	[39]
HS3ST 1-3A, 3B-6 3-*O*-sulfotransferase	HS3ST3B overexpression in pancreatic cell line	Analysis of epithelial-mesenchymal markers	EMT processes promoted	[40]
	Tolerant patients (renal transplantation)	Blood samples analysis	Increased expression of HS3ST1	[41]
HS6ST-1,2,36-6-*O*-sulfotransferase	Human renal allografts	Histology	Increased HS 6-*O*-sulfation on tubular epithelial cells from patient with chronic rejection and in mice with fibrotic kidney	[28]
	Murine model of fibrosis			
	Human lung samples idiopathic pulmonary fibrosis	Histology	Increased HS 6-*O*-sulfation, HS6ST1/2 overexpression. No difference in N and 2-*O*-sulfation	[42]
Endosulphatases (SULF1,2)	Idiopathic pulmonary fibrosis patient	Lung samples analysis	Sulf2 mRNA overexpression	[43]
	Sulf2 KO type II alveolar epithelial cells	TGF beta stimulation	Increase in TGF-β1 target gene expression	[43]
	Sulf1/2 double KO MEFs	FGF2 stimulation	Increase in FGF2 response compared to WT	[44]
Heparanase (hps)	Mice overexpressing hps	Neutrophil chemoattraction into cremaster muscle	Drop in leukocyte recruitment	[12]
	Colon samples from ulcerative colitis; Hps tg mice	Histology, mouse model of colitis	Hps overexpression. Compared to WT, elevated hps in colonic epithelium have similar leukocyte infiltration during acute phase and increased mucosal infiltration during chronic phase	[45]
	Hps−/− mice	LPS injection	Inhibition of neutrophil adhesion to pulmonary microvasculature	[46]
	Hps-silenced tubular cells	Pro-fibrotic stimulation	Reduced TGFβ synthesis, no change in EMT	[47]
	Hps−/− effector T cells	Injection of Hps−/− effector T cells in WT mice with lymph node or skin inflammation	Hps not essential for lymphocyte extravasation through inflamed lymph nodes and inflamed skin vessels.	[48]
	Hps −/− mice	Zymosan-induced peritonitis	Hps contributes to monocyte but not neutrophil entry to inflammation site	[48]

WT wild type, *KO* knock out; *IP* intraperitoneal; *LPS* lipopolysaccharides

formation. For example, O'Boyle et al. analysed a non-HS-binding mutant (mt) CXCL12. In vivo, intravenous administration of a wild-type and mtCXCL12 mixture resulted in abolition of the chemotactic potential of the wild-type chemokine to recruit leukocytes in a murine air pouch model. In vitro, the ability of wtCXCL12 to induce peripheral blood mononuclear cells to migrate across an endothelial monolayer was abolished when mtCXCL12 was mixed with wild-type CXCL12 [58]. Following isograft skin transplantation, injection of a non-GAG-binding CCL7 inhibits leukocyte infiltration [60]. In rat allograft, skin transplantation, administration of synthetic octapeptides derived from the murine-binding sequence of interferon gamma blocks the binding of the whole protein and some chemokines to HS and delays rejection [61, 62].

In another approach, mutant chemokines with an increased ability for binding GAG [63] and sometimes with also a decreased ability for receptor activation [64•] are also being studied. Recently, one of these mutants for CXCL8 named PA401 that displays increased binding to HS but no binding to the receptor and therefore displaces the WT CXCL8 from ECM was shown in vitro to decrease CXCL8 levels in airway fluid from patients suffering from cystic fibrosis and to reduce neutrophil chemotaxis [65].

Chemokines acting as chemokine receptor antagonists are also under study. As an example, Met-CCL5 is a methionylated form of the chemokine CCL5 and is a ligand for CCR1, CCR3, CCR5, CCR9 and ACKR1 in humans. In a renal transplant model, rats treated with Met-CCL5 injection have a significant decrease in tubular damage, leukocyte and macrophages infiltration and vascular injury [66, 67].

Viral Chemokines

The study of viruses led to the discovery of viral chemokines that have the ability to modify the chemokine network. Viral chemokine-binding proteins such as myxoma virus protein M-T7 are of great interest as they can interfere with the chemokine-GAG binding domains, although the molecular mechanism underlying MT7 action is still under investigation [68]. Several studies using M-T7 show that interfering with the GAG-binding domain of chemokines is an effective way of diminishing vascular inflammation and cell invasion. In a murine model of renal transplantation, M-T7 treatment increases allograft survival [53] and can prevent chronic rejection [69]. Furthermore, following vascular balloon injury, intimal hyperplasia was inhibited by MT7 protein infusion [70]. It was hypothesised that the effect of M-T7 activity on vascular inflammation is due to its interaction with sulphated HS located on endothelial cells. In support of this in an aortic allograft model, MT7 only affects intimal inflammation and thickness in wild-type mice but not in mice deficient in NDST1. Similarly in a mouse peritoneal ascites model, M-T7 treatment decreased cell invasion in WT but not in NDST1−/− mouse [53]. This highlights again the major role of sulphated HS-chemokine interactions in inflammation. Thus, the GAG binding of chemokines appears to be the potential target for future therapies for allograft inflammation and IFTA.

Evasins

The discovery of inhibitory effects of tick saliva on pro-inflammatory cytokines led to the detection of small proteins (60–79 amino acids) named Evasins [71] that can bind chemokines and inhibit cell recruitment in vitro and have anti-inflammatory activities in murine models [72]. They can inspire synthetic peptides for chemokine neutralising and are now of great interest to define the binding sequence [73].

HS Mimetics

Small HS mimetics can be developed to better understand HS sulphation patterns required for pro- [74] and anti-inflammatory activities considering the impact on heparanase action [75] and chemokine/growth factor binding [76]. Depending on their composition and length, these small mimetics have been found to be effective in inhibiting the interaction between fibroblast growth factor-1, FGF2 and vascular endothelial growth factor with immobilised heparin [76]. Furthermore, the use of a trisulphated HS mimetic can inhibit CCL5 chemotactic action in vitro [77].

Biomarkers

Non-invasive techniques to diagnose rejection in allograft kidneys require representative biomarkers of the graft's immune status. Biomarkers that could serve as predictive tools for rejection might help to stratify patients for individualised treatment and allow early intervention. Increasing understanding and screening of specific mRNA in renal transplant recipients have provided various candidate biomarkers [78]. HS enzymes have been proposed as biomarkers of tolerance [41] and chemokines for acute rejection [79]. A cleavage product of the proteoglycan agrin named CAF (C-terminal agrin fragment) has been found to be significantly correlated with delayed graft function at 1–3 days post-renal transplantation. Furthermore, the serum concentration of CAF drops faster than creatinine which makes it a potential biomarker for renal recovery after transplantation [80••]. An elevated serum level of LG3, a C-terminal fragment of perlecan, is associated with graft loss in patients with acute vascular rejection [81]. In kidney transplant recipients, the glomerular filtration rate has been found to be inversely associated with elevated concentrations of heparanase in the urine [82].

Conclusion

Heparan sulphate is potentially a major player in the events leading to inflammation and fibrosis. However, it could play both pro-inflammatory and anti-inflammatory roles. As one enzyme involved in HS sulfation is overexpressed in tolerant patients (HS3ST1) [41], it might be of interest to look at other enzymes/isoforms present in different patient samples. This may lead to the development of new biomarkers that could differentiate tolerant patient from a patient with chronic graft rejection.

Acknowledgments This work was supported by a Marie Curie Grant from the European Commission FP7 in the framework of the POSAT ITN (Prolong Organ Survival After Transplantation, Initial Training Networks, 606979).

Compliance with Ethics Guidelines

Conflict of Interest Laura Ferreras, Neil S. Sheerin, and John A. Kirby declare that they have no conflict of interest.

Simi Ali had a European patent application-07450189.1-2406 (filing date: 27.12.07), SDF-1 based glycosaminoglycan antagonists and methods of using the same (Kungl A, Werner, I, Slingsby, J, Ali, S, Kirby, JA) issued. It was a joint patent with Austrian SME which has now closed its business.

Human and Animal Rights and Informed Consent This article does not contain any studies with human or animal subjects performed by any of the authors.

References

Papers of particular interest, recently published have been highlighted:
• Of importance
•• Of major importance

1. Those 2012 data are based on the Global Observatory on Donation and Transplantation (GODT) data, produced by the WHO-ONT collaboration n.d. http://www.transplant-observatory.org/Pages/Facts.aspx. Accessed 15 Feb 2015
2. Nankivell BJ, Borrows RJ, Fung CL-S, O'Connell PJ, Allen RDM, Chapman JR. The natural history of chronic allograft nephropathy. N Engl J Med. 2003;349:2326–33. doi:10.1056/NEJMoa020009.
3. Solez K, Colvin RB, Racusen LC, Haas M, Sis B, Mengel M, et al. Banff 07 classification of renal allograft pathology: updates and future directions. Am J Transplant. 2008;8:753–60. doi:10.1111/j.1600-6143.2008.02159.x.
4. Bishop JR, Schuksz M, Esko JD. Heparan sulphate proteoglycans fine-tune mammalian physiology. Nature. 2007;446:1030–7. doi:10.1038/nature05817.
5. Colvin BL, Thomson AW. Chemokines, their receptors, and transplant outcome. Transplantation. 2002;74:149–55. doi:10.1097/00007890-200207270-00001.
6. Barker CE, Ali S, O'Boyle G, Kirby JA. Transplantation and inflammation: implications for the modification of chemokine function. Immunology. 2014;143:138–45. doi:10.1111/imm.12332.
7. Molon B, Ugel S, Del Pozzo F, Soldani C, Zilio S, Avella D, et al. Chemokine nitration prevents intratumoral infiltration of antigen-specific T cells. J Exp Med. 2011;208:1949–62. doi:10.1084/jem.20101956.
8. •• Weber M, Hauschild R, Schwarz J, Moussion C, de Vries I, Legler DF, et al. Interstitial dendritic cell guidance by haptotactic chemokine gradients. Science. 2013;339:328–32. doi:10.1126/science.1228456. **This paper demonstrates for the first time in living tissue the existence of a chemokine gradient guiding immune cells.**
9. Ferro V. Heparan sulfate inhibitors and their therapeutic implications in inflammatory illnesses. Expert Opin Ther Targets. 2013;17:965–75. doi:10.1517/14728222.2013.811491.
10. Banque d'images PowerPoint Servier n.d. http://smart.servier.fr/servier-medical-art. Accessed 22 Feb 2015.
11. Kay RR, Langridge P, Traynor D, Hoeller O. Changing directions in the study of chemotaxis. Nat Rev Mol Cell Biol. 2008;9:455–63. doi:10.1038/nrm2419.
12. Massena S, Christoffersson G, Hjertström E, Zcharia E, Vlodavsky I, Ausmees N, et al. A chemotactic gradient sequestered on endothelial heparan sulfate induces directional intraluminal crawling of neutrophils. Blood. 2010;116:1924–31. doi:10.1182/blood-2010-01-266072.
13. Wang L, Fuster M, Sriramarao P, Esko JD. Endothelial heparan sulfate deficiency impairs L-selectin- and chemokine-mediated neutrophil trafficking during inflammatory responses. Nat Immunol. 2005;6:902–10. doi:10.1038/ni1233.
14. Sadir R, Imberty A, Baleux F, Lortat-Jacob H. Heparan sulfate/heparin oligosaccharides protect stromal cell-derived factor-1 (SDF-1)/CXCL12 against proteolysis induced by CD26/dipeptidyl peptidase IV. J Biol Chem. 2004;279:43854–60. doi:10.1074/jbc.M405392200.
15. Xu D, Esko JD. Demystifying heparan sulfate-protein interactions. Annu Rev Biochem. 2014;83:129–57. doi:10.1146/annurev-biochem-060713-035314.
16. Ali S, Palmer ACV, Banerjee B, Fritchley SJ, Kirby JA. Examination of the function of RANTES, MIP-1 α, and MIP-1β following interaction with heparin-like glycosaminoglycans. J Biol Chem. 2000;275:11721–7. doi:10.1074/jbc.275.16.11721.
17. Paavola CD, Hemmerich S, Grunberger D, Polsky I, Bloom A, Freedman R, et al. Monomeric monocyte chemoattractant protein-1 (MCP-1) binds and activates the MCP-1 receptor CCR2B. J Biol Chem. 1998;273:33157–65. doi:10.1074/jbc.273.50.33157.
18. Proudfoot AEI, Handel TM, Johnson Z, Lau EK, LiWang P, Clark-Lewis I, et al. Glycosaminoglycan binding and oligomerization are essential for the in vivo activity of certain chemokines. Proc Natl Acad Sci U S A. 2003;100:1885–90. doi:10.1073/pnas.0334864100.
19. Johnson Z, Kosco-Vilbois MH, Herren S, Cirillo R, Muzio V, Zaratin P, et al. Interference with heparin binding and oligomerization creates a novel anti-inflammatory strategy targeting the chemokine system. J Immunol. 2004;173:5776–85. doi:10.4049/jimmunol.173.9.5776.
20. • Meng X-M, Nikolic-Paterson DJ, Lan HY. Inflammatory processes in renal fibrosis. Nat Rev Nephrol. 2014;10:493–503. doi:10.1038/nrneph.2014.114. **A recent overview on renal fibrosis.**
21. Kalluri R, Neilson EG. Epithelial-mesenchymal transition and its implications for fibrosis. J Clin Invest. 2003;112:1776–84. doi:10.1172/JCI20530.
22. Curci C, Castellano G, Stasi A, Divella C, Loverre A, Gigante M, et al. Endothelial-to-mesenchymal transition and renal fibrosis in ischaemia/reperfusion injury are mediated by complement anaphylatoxins and Akt pathway. Nephrol Dial Transplant. 2014;29:799–808. doi:10.1093/ndt/gft516.

54. Seffouh A, Milz F, Przybylski C, Laguri C, Oosterhof A, Bourcier S, et al. HSulf sulfatases catalyze processive and oriented 6-O desulfation of heparan sulfate that differentially regulates fibroblast growth factor activity. FASEB J. 2013;27:2431–9. doi:10.1096/fj.12-226373.
55. Katta K, Boersema M, Adepu S, Rienstra H, Celie JWAM, Mencke R, et al. Renal heparan sulfate proteoglycans modulate fibroblast growth factor 2 signaling in experimental chronic transplant dysfunction. Am J Pathol. 2013;183:1571–84. doi:10.1016/j.ajpath.2013.07.030.
56. Poluri KM, Joseph PRB, Sawant KV, Rajarathnam K. Molecular basis of glycosaminoglycan heparin binding to the chemokine CXCL1 dimer. J Biol Chem. 2013;288:25143–53. doi:10.1074/jbc.M113.492579.
57. Cripps JG, Crespo FA, Romanovskis P, Spatola AF, Fernández-Botrán R. Modulation of acute inflammation by targeting glycosaminoglycan-cytokine interactions. Int Immunopharmacol. 2005;5:1622–32. doi:10.1016/j.intimp.2005.04.010.
58. O'Boyle G, Mellor P, Kirby JA, Ali S. Anti-inflammatory therapy by intravenous delivery of non-heparan sulfate-binding CXCL12. FASEB J. 2009;23:3906–16. doi:10.1096/fj.09-134643.
59. Anders H-J, Ninichuk V, Schlöndorff D. Progression of kidney disease: blocking leukocyte recruitment with chemokine receptor CCR1 antagonists. Kidney Int. 2006;69:29–32. doi:10.1038/sj.ki.5000053.
60. Ali S, O'Boyle G, Hepplewhite P, Tyler JR, Robertson H, Kirby JA. Therapy with nonglycosaminoglycan-binding mutant CCL7: a novel strategy to limit allograft inflammation. Am J Transplant. 2010;10:47–58. doi:10.1111/j.1600-6143.2009.02868.x.
61. Fernandez-Botran R, Yan J, Justus DE. Binding of interferon gamma by glycosaminoglycans: a strategy for localization and/or inhibition of its activity. Cytokine. 1999;11:313–25. doi:10.1006/cyto.1998.0438.
62. Fernandez-Botran R, Gorantla V, Sun X, Ren X, Perez-Abadia G, Crespo FA, et al. Targeting of glycosaminoglycan-cytokine interactions as a novel therapeutic approach in allotransplantation. Transplantation. 2002;74:623–9. doi:10.1097/00007890-200209150-00007.
63. Brandner B, Rek A, Diedrichs-Möhring M, Wildner G, Kungl AJ. Engineering the glycosaminoglycan-binding affinity, kinetics and oligomerization behavior of RANTES: a tool for generating chemokine-based glycosaminoglycan antagonists. Protein Eng Des Sel. 2009;22:367–73. doi:10.1093/protein/gzp013.
64.• Adage T, Piccinini AM, Falsone A, Trinker M, Robinson J, Gesslbauer B, et al. Structure-based design of decoy chemokines as a way to explore the pharmacological potential of glycosaminoglycans. Br J Pharmacol. 2012;167:1195–205. doi:10.1111/j.1476-5381.2012.02089.x. **The authors describe the CellJammer approach. They provide structure and action mechanisms informations about decoy chemokines.**
65. McElvaney OJ, O'Reilly N, White M, Lacey N, Pohl K, Gerlza T, et al. The effect of the decoy molecule PA401 on CXCL8 levels in bronchoalveolar lavage fluid of patients with cystic fibrosis. Mol Immunol. 2015;63:550–8. doi:10.1016/j.molimm.2014.10.013.
66. Gröne HJ, Weber C, Weber KS, Gröne EF, Rabelink T, Klier CM, et al. Met-RANTES reduces vascular and tubular damage during acute renal transplant rejection: blocking monocyte arrest and recruitment. FASEB J. 1999;13:1371–83.
67. Song E, Zou H, Yao Y, Proudfoot A, Antus B, Lui S, et al. Early application of Met-RANTES ameliorates chronic allograft nephropathy. Kidney Int. 2002;61:676–85. doi:10.1046/j.1523-1755.2002.00148.x.
68. Bartee MY, Chen H, Dai E, Liu LY, Davids JA, Lucas A. Defining the anti-inflammatory activity of a potent myxomaviral chemokine modulating protein, M-T7, through site directed mutagenesis. Cytokine. 2014;65:79–87. doi:10.1016/j.cyto.2013.10.005.
69. Bédard ELR, Kim P, Jiang J, Parry N, Liu L, Wang H, et al. Chemokine-binding viral protein M-T7 prevents chronic rejection in rat renal allografts. Transplantation. 2003;76:249–52. doi:10.1097/01.TP.0000061604.57432.E3.
70. Liu L, Lalani A, Dai E, Seet B, Macauley C, Singh R, et al. The vital anti-inflammatory chemokine-binding protein M-T7 reduces intimal hyperplasia after vascular injury. J Clin Invest. 2000;105:1613–21. doi:10.1172/JCI8934.
71. Frauenschuh A, Power CA, Déruaz M, Ferreira BR, Silva JS, Teixeira MM, et al. Molecular cloning and characterization of a highly selective chemokine-binding protein from the tick Rhipicephalus sanguineus. J Biol Chem. 2007;282:27250–8. doi:10.1074/jbc.M704706200.
72. Déruaz M, Frauenschuh A, Alessandri AL, Dias JM, Coelho FM, Russo RC, et al. Ticks produce highly selective chemokine binding proteins with antiinflammatory activity. J Exp Med. 2008;205:2019–31. doi:10.1084/jem.20072689.
73. Bonvin P, Dunn SM, Rousseau F, Dyer DP, Shaw J, Power CA, et al. Identification of the pharmacophore of the CC chemokine-binding proteins Evasin-1 and −4 using phage display. J Biol Chem. 2014;289:31846–55. doi:10.1074/jbc.M114.599233.
74. Teng L, Fu H, Wang M, Deng C, Song Z, Chen J. Immunomodulatory activity of heparan sulfate mimetics from Escherichia coli K5 capsular polysaccharide in vitro. Carbohydr Polym. 2015;115:643–50. doi:10.1016/j.carbpol.2014.08.119.
75. Hammond E, Handley P, Dredge K, Bytheway I. Mechanisms of heparanase inhibition by the heparan sulfate mimetic PG545 and three structural analogues. FEBS Open Bio. 2013;3:346–51. doi:10.1016/j.fob.2013.07.007.
76. Freeman C, Liu L, Banwell MG, Brown KJ, Bezos A, Ferro V, et al. Use of sulfated linked cyclitols as heparan sulfate mimetics to probe the heparin/heparan sulfate binding specificity of proteins. J Biol Chem. 2005;280:8842–9. doi:10.1074/jbc.M410769200.
77. Sheng GJ, Oh YI, Chang SK, Hsieh-Wilson LC. Tunable heparan sulfate mimetics for modulating chemokine activity. J Am Chem Soc. 2013;135:10898–901. doi:10.1021/ja4027727.
78. Suthanthiran M, Schwartz JE, Ding R, Abecassis M, Dadhania D, Samstein B, et al. Urinary-cell mRNA profile and acute cellular rejection in kidney allografts. N Engl J Med. 2013;369:20–31. doi:10.1056/NEJMoa1215555.
79. Hricik DE, Nickerson P, Formica RN, Poggio ED, Rush D, Newell KA, et al. Multicenter validation of urinary CXCL9 as a risk-stratifying biomarker for kidney transplant injury. Am J Transplant. 2013;13:2634–44. doi:10.1111/ajt.12426.
80.•• Steubl D, Hettwer S, Vrijbloed W, Dahinden P, Wolf P, Luppa P, et al. C-terminal agrin fragment-a new fast biomarker for kidney function in renal transplant recipients. Am J Nephrol. 2014;38:501–8. doi:10.1159/000356969. **Demonstrate for the first time that CAF could be a more sensitive marker than creatinine for renal function in transplanted patients.**
81. Soulez M, Pilon E-AA, Dieudé M, Cardinal H, Brassard N, Qi S, et al. The perlecan fragment LG3 is a novel regulator of obliterative remodeling associated with allograft vascular rejection. Circ Res. 2012;110:94–104. doi:10.1161/CIRCRESAHA.111.250431.
82. Shafat I, Agbaria A, Boaz M, Schwartz D, Baruch R, Nakash R, et al. Elevated urine heparanase levels are associated with proteinuria and decreased renal allograft function. PLoS One. 2012;7:e44076. doi:10.1371/journal.pone.0044076.

23. Zeisberg EM, Tarnavski O, Zeisberg M, Dorfman AL, McMullen JR, Gustafsson E, et al. Endothelial-to-mesenchymal transition contributes to cardiac fibrosis. Nat Med. 2007;13:952–61. doi:10.1038/nm1613.
24.• Willet JDP, Pichitsiri W, Jenkinson SE, Brain JG, Wood K, Alhasan AA, et al. Kidney transplantation: analysis of the expression and T cell-mediated activation of latent TGF-β. J Leukoc Biol. 2013;93:471–8. doi:10.1189/jlb.0712324. **This recent study showed increased level of the Latent TGF-β binding protein-1 and Heparan Sulfate around tubules and within interstitium in patients with chronic inflammation and IF/TA.**
25. Clayton A, Thomas J, Thomas GJ, Davies M, Steadman R. Cell surface heparan sulfate proteoglycans control the response of renal interstitial fibroblasts to fibroblast growth factor-2. Kidney Int. 2001;59:2084–94. doi:10.1046/j.1523-1755.2001.00723.x.
26. Rabenstein DL. Heparin and heparan sulfate: structure and function. Nat Prod Rep. 2002;19:312–31. doi:10.1039/b100916h.
27. Ali S, Hardy LA, Kirby JA. Transplant immunobiology: a crucial role for heparan sulfate glycosaminoglycans? Transplantation. 2003;75:1773–82. doi:10.1097/01.TP.0000065805.97974.93.
28. Alhasan AA, Spiekhofer J, Kusche-Gullberg M, Kirby JA, Ali S. Role of 6-O-sulfated heparan sulfate in chronic renal fibrosis. J Biol Chem. 2014;289:20295–306. doi:10.1074/jbc.M114.554691.
29. Rienstra H, Katta K, Celie JWAM, Van Goor H, Navis G, Van Den Born J, et al. Differential expression of proteoglycans in tissue remodeling and lymphangiogenesis after experimental renal transplantation in rats. PLoS One 2010;5. doi:10.1371/journal.pone.0009095.
30.• Celie JWAM, Katta KK, Adepu S, Melenhorst WBWH, Reijmers RM, Slot EM, et al. Tubular epithelial syndecan-1 maintains renal function in murine ischemia/reperfusion and human transplantation. Kidney Int. 2012;81:651–61. doi:10.1038/ki.2011.425. **This paper provides in vivo and in vitro evidences that better graft function and prolonged allograft survival is correlated to tubular epithelial cells syndecan 1 increased expression.**
31. Li Y-C, Ho I-H, Ku C-C, Zhong Y-Q, Hu Y-P, Chen Z-G, et al. Interactions that influence the binding of synthetic heparan sulfate based disaccharides to fibroblast growth factor-2. ACS Chem Biol. 2014;9:1712–7. doi:10.1021/cb500298q.
32. Sugaya N, Habuchi H, Nagai N, Ashikari-Hada S, Kimata K. 6-O-sulfation of heparan sulfate differentially regulates various fibroblast growth factor-dependent signalings in culture. J Biol Chem. 2008;283:10366–76. doi:10.1074/jbc.M705948200.
33. Schlessinger J, Plotnikov AN, Ibrahimi OA, Eliseenkova AV, Yeh BK, Yayon A, et al. Crystal structure of a ternary FGF-FGFR-heparin complex reveals a dual role for heparin in FGFR binding and dimerization. Mol Cell. 2000;6:743–50. doi:10.1016/S1097-2765(00)00073-3.
34. Pye DA, Vives RR, Turnbull JE, Hyde P, Gallagher JT. Heparan sulfate oligosaccharides require 6-O-sulfation for promotion of basic fibroblast growth factor mitogenic activity. J Biol Chem. 1998;273:22936–42.
35.• Rops LWMM, Loeven MA, van Gemst JJ, Eversen I, van Wijk XM, Dijkman HB, et al. Modulation of heparan sulfate in the glomerular endothelial glycocalyx decreases leukocyte influx during experimental glomerulonephritis. Kidney Int. 2014;86:932–42. doi:10.1038/ki.2014.115. **The authors showed in vitro evidences that altering sulfation of HS leads to a reduced glomerular leukocyte influx and better renal function in glomerulonephritis.**
36. Ge XN, Ha SG, Rao A, Greenberg YG, Rushdi MN, Esko JD, et al. Endothelial and leukocyte heparan sulfates regulate the development of allergen-induced airway remodeling in a mouse model. Glycobiology. 2014;24:715–27. doi:10.1093/glycob/cwu035.
37. Fan G, Xiao L, Cheng L, Wang X, Sun B, Hu G. Targeted disruption of NDST-1 gene leads to pulmonary hypoplasia and neonatal respiratory distress in mice. FEBS Lett. 2000;467:7–11. doi:10.1016/S0014-5793(00)01111-X.
38. Forsberg E, Pejler G, Ringvall M, Lunderius C, Tomasini-Johansson B, Kusche-Gullberg M, et al. Abnormal mast cells in mice deficient in a heparin-synthesizing enzyme. Nature. 1999;400:773–6. doi:10.1038/23488.
39. Axelsson J, Xu D, Kang BN, Nussbacher JK, Handel TM, Ley K, et al. Inactivation of heparan sulfate 2-O-sulfotransferase accentuates neutrophil infiltration during acute inflammation in mice. Blood. 2012;120:1742–51. doi:10.1182/blood-2012-03-417139.
40. Song K, Li Q, Jiang Z-Z, Guo C-W, Li P. Heparan sulfate D-glucosaminyl 3-O-sulfotransferase-3B1, a novel epithelial-mesenchymal transition inducer in pancreatic cancer. Cancer Biol Ther. 2011;12:388–98. doi:10.4161/cbt.12.5.15957.
41. Sagoo P, Perucha E, Sawitzki B, Tomiuk S, Stephens DA, Miqueu P, et al. Development of a cross-platform biomarker signature to detect renal transplant tolerance in humans. J Clin Invest. 2010;120:1848–61. doi:10.1172/JCI39922.
42. Lu J, Auduong L, White ES, Yue X. Up-regulation of heparan sulfate 6-O-sulfation in idiopathic pulmonary fibrosis. Am J Respir Cell Mol Biol. 2014;50:106–14. doi:10.1165/rcmb.2013-0204OC.
43. Yue X, Lu J, Auduong L, Sides MD, Lasky JA. Overexpression of Sulf2 in idiopathic pulmonary fibrosis. Glycobiology. 2013;23:709–19. doi:10.1093/glycob/cwt010.
44. Lamanna WC, Frese M-A, Balleininger M, Dierks T. Sulf loss influences N-, 2-O-, and 6-O-sulfation of multiple heparan sulfate proteoglycans and modulates fibroblast growth factor signaling. J Biol Chem. 2008;283:27724–35. doi:10.1074/jbc.M802130200.
45. Lerner I, Hermano E, Zcharia E, Rodkin D, Bulvik R, Doviner V, et al. Heparanase powers a chronic inflammatory circuit that promotes colitis-associated tumorigenesis in mice. J Clin Invest. 2011;121:1709–21. doi:10.1172/JCI43792.
46. Schmidt EP, Yang Y, Janssen WJ, Gandjeva A, Perez MJ, Barthel L, et al. The pulmonary endothelial glycocalyx regulates neutrophil adhesion and lung injury during experimental sepsis. Nat Med. 2012;18:1217–23. doi:10.1038/nm.2843.
47. Masola V, Zaza G, Secchi MF, Gambaro G, Lupo A, Onisto M. Heparanase is a key player in renal fibrosis by regulating TGF-β expression and activity. Biochim Biophys Acta. 1843;2014:2122–8. doi:10.1016/j.bbamcr.2014.06.005.
48. Stoler-Barak L, Petrovich E, Aychek T, Gurevich I, Tal O, Hatzav M, et al. Heparanase of murine effector lymphocytes and neutrophils is not required for their diapedesis into sites of inflammation. FASEB J 2015:1–12. doi:10.1096/fj.14-265447.
49. Goldberg R, Meirovitz A, Hirshoren N, Bulvik R, Binder A, Rubinstein AM, et al. Versatile role of heparanase in inflammation. Matrix Biol. 2013;32:234–40. doi:10.1016/j.matbio.2013.02.008.
50. Waterman M, Ben-Izhak O, Eliakim R, Groisman G, Vlodavsky I, Ilan N. Heparanase upregulation by colonic epithelium in inflammatory bowel disease. Mod Pathol. 2007;20:8–14. doi:10.1038/modpathol.3800710.
51. Winsz-Szczotka K, Kuźnik-Trocha K, Komosińska-Vassev K, Wisowski G, Gruenpeter A, Lachór-Motyka I, et al. Plasma and urinary glycosaminoglycans in the course of juvenile idiopathic arthritis. Biochem Biophys Res Commun. 2015. doi:10.1016/j.bbrc.2015.02.018.
52. Carter NM, Ali S, Kirby JA. Endothelial inflammation: the role of differential expression of N-deacetylase/N-sulphotransferase enzymes in alteration of the immunological properties of heparan sulphate. J Cell Sci. 2003;116:3591–600. doi:10.1242/jcs.00662.
53. Dai E, Liu L-Y, Wang H, McIvor D, Sun YM, Macaulay C, et al. Inhibition of chemokine-glycosaminoglycan interactions in donor tissue reduces mouse allograft vasculopathy and transplant rejection. PLoS One. 2010;5, e10510. doi:10.1371/journal.pone.0010510.

8.6 Article submitted to *Biochimica et Biophysica Acta* general subjects

Heparan sulfate in chronic kidney diseases: exploring the role of 3-O-sulfation

Laura Ferreras [a], Anna Moles [a,1], Gerhard R Situmorang [a,2], Rana el Masri [b], Imogen L Wilson [a], Katie Cooke [a], Marion Kusche-Gullberg [c], Romain R Vivès [b], Neil S Sheerin [a,d], Simi Ali [a]

[a] Institute of Cellular Medicine, Faculty of Medical Sciences, Newcastle University, NE2 4HH, UK
[b] Univ. Grenoble Alpes, CNRS, CEA, IBS, Grenoble, France
[c] University of Bergen, Department of Biomedicine, Jonas Lies vei 91, N-5009 Bergen, Norway
[d]Newcastle upon Tyne Hospitals NHS Foundation Trust and NIHR Newcastle Biomedical Research Centre

Running title: HS 3-O-sulfation in renal fibrosis

Corresponding author:
Professor Simi Ali
Institute of Cellular Medicine
3rd floor William Leech Building
Faculty of Medical Sciences
Newcastle University
NE2 4HH
UK
simi.ali@ncl.ac.uk
+44 (0) 191 208 7158

Abstract

One of the main feature of chronic kidney disease is the development of renal fibrosis. Heparan Sulfate (HS) is involved in disease development by modifying the function of growth factors and cytokines and creating chemokine gradients. In this context, we aimed to understand the function of HS sulfation in renal fibrosis. Using a mouse model of renal fibrosis, we found that total HS 2-O-sulfation was increased in damaged kidneys, whilst, tubular staining of HS 3-O-sulfation was decreased. The expression of HS modifying enzymes significantly correlated with the development of fibrosis with HS3ST1 demonstrating the strongest correlation. The pro-fibrotic factors TGFβ1 and TGFβ2/IL1β significantly downregulated HS3ST1 expression in both renal epithelial cells and renal fibroblasts. To determine the implication of HS3ST1 in growth factor binding and signaling, we generated an *in vitro* model of renal epithelial cells overexpressing HS3ST1 (HKC8-HS3ST1). Heparin Binding EGF like growth factor (HB-EGF) induced rapid, transient STAT3 phosphorylation in control HKC8 cells. In contrast, a prolonged response was demonstrated in HKC8-HS3ST1 cells. Finally, we showed that both HS 3-O-sulfation and HB-EGF tubular staining were decreased with the development of fibrosis. Taken together, these data suggest that HS 3-O-sulfation is modified in fibrosis and highlight HS3ST1 as an attractive biomarker of fibrosis progression with a potential role in HB-EGF signaling.

1. Introduction

Chronic kidney disease (CKD) is a worldwide health problem affecting 8-16% of the world's population [1]. CKD is characterised by glomerulosclerosis and interstitial fibrosis and is caused by a wide range of pathologies including metabolic disease, inflammation and vascular damage which finally lead to the accumulation of extracellular matrix [2]. There is currently no treatment that can reverse renal fibrosis, therefore finding new biomarkers and treatments is one of the major challenges in medicine [2,3].

Heparan Sulfate (HS) is a sulfated polysaccharide with a structure consisting of repeating units of uronic acid (UA) linked to a N-acetyl- or N-sulfo-D-glucosamine (GlcNAc, GlcNS), which can vary in length and degree of sulfation. HS is an abundant component of extracellular matrices and cell surfaces, where it is found covalently bound to the core protein of HS proteoglycans (HSPG) [4]. HSPGs regulate the function of growth factors and chemokines by preventing their proteolysis, regulating receptor activation and anchoring them to the extracellular matrix and to the cell surface [5–7]. Due to its role in leukocyte recruitment and in the binding and modulation of pro-fibrotic factors such as TGFβ [8], HS plays a crucial role in the development of fibrosis [9,10]. Furthermore, HS has been associated with renal tissue remodelling as expression of HSPGs including Collagen XVIII and perlecan is increased in interstitial fibrosis of kidney isografts and allografts in rats [11]. In addition, we have previously shown increased HS sulfation on the tubular epithelial cell membranes and in the interstitium of kidneys in patients with chronic rejection [12].

HS can be sulfated at the N, 2-O, 3-O and 6-O position. These modifications are key to its function, as the negative charge provided by the sulfation modulates HS binding to proteins. HS sulfation in the glomerular basement membrane (GBM) has been extensively studied but the role of HS in the glomerular filtration is still not fully understood [13,14]. However, it is evident that there is a fundamental change in HS composition in pathological conditions [14,15]. In diabetic patients, disaccharide analysis of the glomerular basement membrane revealed a decrease in 3-O-sulfation [16]. Biopsies from patients with glomerulopathies such as lupus nephritis, membranous glomerulonephritis, minimal change disease and diabetic nephropathy showed a decrease in HS by indirect immunofluorescence staining [15]. In contrast, patients with proliferative lupus nephritis had a significant increase of N- and 2-O-sulfated HS in their glomeruli [17].

Several enzymes are responsible for the biosynthesis and sulfation of HS. The exostosin (EXT) enzymes EXT1 and EXT2 are involved in HS polymerisation [18], while the sulfotransferases add sulfate groups to the carbohydrate backbone. There are four isoforms of N-deacetylase/N-sulfotransferase (NDST), one 2-O-sulfotransferase (HS2ST), seven isoforms of 3-O sulfotransferase (HS3ST) and three isoforms of 6-O sulfotransferase (HS6ST) [19–21]. Additionally, HS can be 6-O-desulfated by two endogenous sulfatases (SULF) [22]. Changes in the expression of enzymes involved in HS biosynthesis are associated with the development of renal dysfunction [23]. Podocyte specific NDST1 knockout led to the development of glomerular hypertrophy together with an increase in mesangial area at 6 months [24]. Additionally, podocyte specific EXT1 knockout mice showed hypertrophic glomeruli and a decrease in highly sulfated HS on the glomerular capillary endothelium [25]. Furthermore, heparanase, an enzyme that cleaves HS from HSPG and releases biologically active oligosaccharide fragments, is also important in the development of renal diseases [26,27]. Heparanase expression is increased in rats with Adriamycin nephropathy [28] and in patients with overt diabetic nephropathy [29]. Heparanase KO mice were protected against the development of diabetic nephropathy [30].

Although HS 3-O sulfation composition and localisation in the kidney have been previously studied [31,32], very little is known about its biological role and possible effects on growth factor function [33]. HS3STs are known to generate the binding motif for antithrombin III and HS herpes simplex virus 1 gD protein, but their activity and substrate specificity are still being studied [34]. These enzymes are not homogeneously expressed in the body and there is increasing evidence that their expression changes during the development of disease. HS3ST2 and HS3ST4 are mainly expressed in the brain [35,36] and there has been interest in HS3ST2 in tauopathies, with its expression increasing in the hippocampus of patients with Alzheimer's disease [37]. HS3ST3 and HS3ST1 are more widely expressed with HS3ST1 mostly expressed in the brain, heart, lung, spleen, stomach, small intestine, colon, testis and the kidney [35,36]. HS3ST1 expression is regulated by a number of factors, with LPS and TNFα reducing its expression in human microvascular endothelial cells [38], whereas expression is increased by IL-4 and IL-13 treatment of intestinal epithelial cells [39] and FGF10 treatment of salivary gland epithelia [40]. Reports describing the expression of HS3ST1 during renal transplantation show that it is overexpressed in tolerant patients [41] and in failing grafts [42]. While the first study examined blood samples, the latter analysed tissue expression, which may explain the discrepant findings. These studies did not investigate the mechanism underlying the changes in HS3ST1 expression.

In this study, we have investigated changes in HS sulfation during the development of renal interstitial fibrosis *in vivo* and determined whether these changes were mirrored by the expression of HS modifying enzymes. Furthermore, we identified factors that modulate the expression of HS3ST1 in renal cells *in vitro*. Finally, we analysed the implications of the changes in HS3ST1 expression on HB-EGF signalling, a growth factor known to stimulate tubular epithelial cells repair [43], cell motility [44] and is expressed in renal transplants [45,46].

2. Materials and Methods

2.1. Animal work

All experiments were carried out under UK Home Office regulations (PPL60/4521) at the Comparative Biology Centre (CBC) in Newcastle University. C57BL/6 mice aged 8-10 weeks were subjected to Unilateral Ureteral Obstruction (UUO). The non-ligated kidney was used as control. Mice kidneys were harvested at 5 and 10 days post-UUO with 6 animals per group. Each kidney collected was dissected for paraffin embedded sections, frozen sections, RNA extraction and HS disaccharide analysis.

2.2. Cells culture and treatments

All media were supplemented with 2 mM L-Glutamine, 100 U/mL Penicillin, 100 µg/mL Streptomycin (Sigma). The immortalised renal tubular epithelial cell line HK2 (ATCC) was grown in Dulbecco's Modified Eagle Medium (DMEM, Sigma, D5671) supplemented with 10% heat inactivated Fetal Bovine Serum (FBS). The second cell line of immortalised renal epithelial cells studied was HKC8 [47]. They were cultured in DMEM-F12 (Sigma, D6421) supplemented with 5% FBS. NKR-49F were cultured in DMEM supplemented with 5% FBS. All cells were grown in a humidified incubator with 5% CO_2 at 37°C.

Cell were seeded in complete media until 80% confluent then in starving medium supplemented with 0.5% FBS for 16-24 hours. For Western Blot studies, cells were treated with 10 ng/mL HB-EGF (Sigma E4643). For HS3ST1 expression study, all recombinant human cytokines were purchased from PeproTech and were active in both human and rats. Cells were treated with either 5 ng/mL TGFβ1 (100-21C), 10 ng/mL TGFβ2 (100-35B) + 10 ng/mL IL1β (200-01B).

Human kidney primary proximal tubular epithelial cells (primary PTECs) were isolated from macroscopically normal parts of nephrectomy specimens removed for oncological indications (ethical approval 13/EM/0311). The resected kidney tissue was collected in sterile RPMI 1640 media (Sigma-Aldrich) supplemented with 5% FBS and Penicillin (100U/mL) / Streptomycin (100 µg/ml), and was immediately transferred to 4°C for subsequent cell isolation procedure. Primary PTECs were isolated using Percoll gradient centrifugation protocol as previously reported [48]. Briefly, samples were enzymatically digested with collagenase, mechanically sieved and

centrifuged with two discontinuous Percoll gradients (1.04 gram/mL and 1.07 gram/mL). This method yielded 1.5 to 2 million cells/gram wet weight of tissue specimen. Primary PTECs were maintained in DMEM/HAM F-12 media (Lonza) supplemented with insulin, hydrocortisone, GA-1000, adrenaline, T3, transferrin, foetal bovine serum, and human epithelial growth factor. Preliminary experiments to characterise the isolated cells showed positive staining of epithelial cell markers, such as ZO-1, E-cadherin, K-cadherin and Cytokeratin. The isolated cells did not express mesenchymal markers, such as α-SMA, Vimentin or Collagen type-1. Under light microscope, the cells were hexagonal in shape, and showed "cobblestone-like" appearance with the occasional presence of hemicysts or "dome" formation when grown to form a confluent monolayer. Moreover, scanning electron microscope images of the isolated cells revealed the presence of brush borders, which is a typical feature of kidney tubular epithelial cells. These epithelial characteristics were evident up to the first three passages. Only cells in passage two were used in our experiments.

2.3. RNAs extraction and quantitative RT-PCR

In this study, two methods of RNA extraction were used. A column-based method using the Qiagen RNeasy Plus Mini Kit for cells following manufacturer's instructions and a Trizol/Chloroform method for mouse tissue. Briefly, mouse kidney tissue was homogenised in TRI reagent (Ambion) using the Tissue Lyser II by Qiagen. RNA was isolated separated from the protein by adding chloroform (AnalaR) and mixed by inversion. Samples were centrifuged, and the aqueous phase mixed with isopropanol. The RNAs pellet was suspended in 1mL of 70% ethanol and air dried before being suspended in 30μL of RNAse free water (Ambion). To avoid gDNA contamination 1 μg of sample was treated with RQ1 DNAse (Promega) for 30 minutes at 37°C. Next, samples were treated with DNase stop solution (Promega) 10 minutes 65°C. Complementary DNA (cDNA) was generated using Tetro cDNA synthesis kit (Bioline, BIO-65043) following the manufacturer's instruction. TaqMan probes (Thermofisher) were used to amplify cDNA (see supplementary data, table 1). HPRT was used as housekeeping gene to normalize CT values. Samples were analysed using the comparative ΔΔCT method.

2.4. HS disaccharide analysis from cells

Subconfluent HKC8 cells were cultured with 200 μCi/ml $Na_2{}^{35}SO_4$ (Perkin Elmer) for 24 hrs at 37°C. After incubation, the culture medium was removed and frozen at –20 °C for further use. The

cell layer was washed twice with cold PBS and solubilized at 4°C for 60 min in 1% Triton TX-100, 50 mM Tris/HCl pH (7.4), 0,15 M NaCl and proteinase inhibitors. After centrifugation, the supernatant was collected and an aliquot (100µl) was removed for protein determination using the BCA protein determination kit (Pierce). The remaining supernatant was used for purification of the ^{35}S-labeled polysaccharides. Polysaccharide chains were released from the core protein by treatment with 0.5 M NaOH over night at 4°C. After completed ß-elimination, the samples were neutralized with 4 M HCl. Samples were adjusted to 0.15 M NaCl and applied to a 0.5 ml DEAE-Sephacel column equilibrated in 0.15 M NaCl, 0.05 M Tris-HCl pH 7.4, 0.1% Triton X-100. The column was washed with the equilibration buffer, followed by 0.15 M NaCl, 0.05 M acetate buffer pH 4.0, 0.1% Triton X-100 and 0.05 M Tris/HCl pH 7.5. Finally, the labeled GAG chains were eluted with 1.5 M NaCl and desalted by gel chromatography using PD-10 columns (Sephadex G-25, Amersham Biosciences) in H_2O. Purified ^{35}S-labeled HS chains were cleaved at N-sulfated GlcN residues by deamination with nitrous acid at pH 1.5 followed by reduction with $NaBH_4$. Labeled deamination products were fractionated by gel chromatography on Sephadex G-15 (1 cm x 180 cm) in 0.2 M NH_4HCO_3. Fractions corresponding to oligo- and disaccharides were collected and desalted by lyophilization. HS disaccharides analysis was performed with HPLC using a Whatman Partisil 10-SAX column eluted with aqueous KH_2PO_4 of stepwise increasing concentration at a rate of 1 ml/min.

2.5. HS disaccharide analysis from renal samples

Pooled frozen kidney tissue were collected to generate four groups (D5 Control, D5 UUO, D10 Control, D10 UUO) with each group containing between 35 to 62 mg of frozen tissue. Samples were lysed, digested, purified and analysed as previously described [49]. Briefly, all samples were mechanically lysed in 50 mM Tris Buffered Saline, 2 mM EDTA, 6 M Urea and dialysed against 25 mM Tris, 5 mM EDTA pH 7.8. Following protein degradation in 2 mg/ml of pronase 24h at 37°C and two treatments with 5% v/v trichloroacetic acid, supernatants were washed with 50% v/v diethylether and run onto a DEAE-Sephacel column equilibrated in 20 mM phosphate pH 6.5. Samples were eluted in 20 mM phosphate, 1 M NaCl pH 6.5 and desalted with a PD-10 column. Finally, GAG chains were digested with 10 mU of heparinase I (Grampian enzymes) overnight at 30°C, then with 10 mU heparinase II and 10 mU heparinase III (Grampian enzymes) for 24h at 37°C. Disaccharides analysis was performed by reverse-phase ion-pair high-performance liquid chromatograph [49] in triplicate.

2.6. Stable transfectants

Plasmid EX-TO223-M13 containing flag tagged HS3ST1 enzyme sequence was purchased from GeneCopoeia. Bacterial transformation of *E.coli DH5α* (Invitrogen) was performed using the heat shock method. Bacterial cells lysis and plasmid purification were performed using Plasmid Mini Kits (Qiagen). To generate an empty plasmid (plasmid without HS3ST1 sequence), 3 µg of plasmid were digested with 30U of BsrGI (Bsp 1407I, ThermoFisher). The digested plasmid was extracted using QIAquick Gel Extraction Kit Plasmid extraction. The final plasmid was ligated 3h at room temperature using T4 DNA ligase.

Cells transfections were performed using Effectene Reagent (Qiagen) in combination with an enhancer and a DNA-condensation buffer. The following day, fresh media containing 200 µg/mL of selective antibiotic G418 was added to the transfected cells. Colonies were isolated using cloning cylinders.

2.7. Western Blotting

Cellular proteins were extracted using CelLytic M (Sigma) complemented with protease (Complete Mini Protease Inhibitor Cocktail, Roche) and phosphatase (Roche) inhibitors. Between 10 to 50 µg of protein extract samples were denaturated and electrophoretically separated by Sodium Dodecyl Sulfate (SDS) Polyacrylamide gel electrophoresis, then transferred by semi dry transfer (BioRad) to nitrocellulose membranes (BioRad). Membranes were blocked for 1h at room temperature in 0.1% Tween Tris-buffered saline (TBS) with 5% fat free milk or 5% Bovine Serum Albumin (BSA) when looking at phosphorylated proteins and probed overnight at 4°C using the following primary antibodies diluted in blocking buffer (STAT3 Y705 ab76315 Abcam 1:20 000, alpha tubulin T6074 Sigma 1:4000). Following overnight incubation, membranes were washed in TBS 0.1% Tween and incubated with the corresponding secondary antibodies conjugated with HorseRadish Peroxidase (R&D 1:1000), for 1 hour at room temperature. Finally, membranes were washed again, and bands were visualized by enhanced chemiluminescence and exposed to X-ray films.

2.8. Staining

Cells were fixed in ice-cold methanol for 5 minutes at -20°C, gradually rehydrated with PBS, blocked with 5% BSA in PBS for 2 hours at room temperature and incubated overnight with

primary antibodies (Flag Tag 2368 Cell Signalling 1:3000, GM130 Abcam 1:70). Slides were washed with PBS, then incubated for 2h at room temperature with the corresponding secondary antibody (anti-mouse Alexa fluor 488 ThermoFisher 1:100, anti-rabbit Dylight550, Immunoreagents 1:100). Finally, slides were washed in PBS and mounted with liquid mounting medium containing DAPI (Vectashield).

The use of fluorescently labeled Antithrombin III (AT) for detecting HS 3-O-sufation has been previously described [31]. Fluorescently labeled AT with Alexa fluor 647 was generated following manufacturer's instructions (ThermoFisher Scientific, A20173). Staining specificity was assessed with heparin competition. Cryosections of 7 μm thickness were fixed in acetone and blocked with 1% BSA in PBS for 20 minutes at room temperature. Slides were incubated for 1 hour with labeled antithrombin III and washed three times with blocking buffer. Slides were mounted using Diamond antifade with Dapi.

Mouse kidneys were dissected and fixed in 10% formalin solution and embedded in paraffin. Serial tissue sections of 4 μm thickness were cut and mounted onto slides. Peptide retrieval was performed by microwaving the slides in EDTA buffer. Sections were blocked 10 minutes with 2% FBS in PBS and incubated overnight at 4°C with primary antibody (HB-EGF ab192545 Abcam 1:200, HS4C3 1:5 given by Toin van Kuppevelt, Radboud University, Netherlands). The next day, sections were washed in PBS, then incubated with secondary antibody (anti VSV C7706 sigma, Dylight 550 Immunoreagent) diluted in PBS for 1-2 hours at room temperature. Sections were then washed in PBS, incubated with Sudan Black for 20 minutes in the dark at room temperature and finally washed in PBS before mounting with VECTA shield DAPI liquid mounting medium.

Sirius red and Haematoxylin Eosin staining were performed following standard procedures.

All images were analysed using Fiji software. Fluorescent imaging was performed using Leica LCM microscope, Zeiss Axioimager, Nicon A1R confocal microscope. For Sirius red quantification, images were analysed using LeicaQWin analysis software with 10 cortex fields analysed per section for each kidney.

2.9. Software

Graphs were created using Microsoft Excel and GraphPad Prism 6.0. Diagrams were generated using Servier Medical Art images (http://servier.com/Powerpoint-image-bank).

2.10. Statistical Analysis

Results are expressed as mean ± Standard Deviation. Statistical evaluations were performed using GraphPad Prism 6.0. Significant results were considered when $P<0.05$ (*), $P<0.01$ (**) and $P<0.001$ (***). P values were calculated using two tailed unpaired student's t-test with Welch's correction.

3. Results

3.1. Unilateral Ureteral Obstruction induces interstitial fibrosis and modulates HS sulfation

To assess the structural changes and fibrosis development in the UUO model, kidney sections were stained with H&E and Sirius red. Sections from day 5 (D5) and 10 (D10) showed tubular dilatation and tubulointerstitial expansion (figure 1A). Additionally, there was a significant increase in interstitial fibrosis as assessed by Sirius red staining when compared with control kidneys at D5 and D10 UUO ($p<0.05$ and $p<0.001$ respectively) (figure 1B-C). To further address the relevance of the UUO model for HS studies, HS sulfation was evaluated. As shown in figure 1D total HS O-sulfation, measured by reverse-phase ion-pair HPLC, increased in UUO by 13.7% at D5 and 6.5% at D10. Assessment of the pattern of HS sulfation showed an increase of total 2-O-sulfation by 45.3% at D5 and 19.2% at D10 (figure 1E). HS disaccharide composition (supplementary data, figure 1) revealed an increase of the disulfated disaccharides ΔUA.2S-GlcNS but a decrease in the monosulfated disaccharides ΔUA-GlcNAc.6S and in the disulfated disaccharides ΔUA-GlcNS.6S at D5 and D10 UUO. Overall, these results show that UUO-induced renal fibrosis results in changes in HS disaccharide sulfation patterns which could potentially translate in altered protein binding.

3.2. HS sulfotransferases and sulfatases mRNA expressions are altered in UUO

In order to investigate whether the increase in HS sulfation was mirrored by a change in the levels of HS sulfotransferases and sulfatases, their expression levels in control and UUO kidneys was analysed by real time qPCR. RNA expression analysis was chosen over protein analysis as endogenous protein levels can be difficult to measure with the antibodies currently available [50]. The increase of HS 2-O-sulfation was reflected by a significant increase of HS2ST1 expression at D10 of UUO ($p<0.01$) (figure 2A). Additionally, there was an increase of SULF1 at D5 ($p<0.05$) (figure 2B). The level of HS3ST3A expression shown in figure 2C decreased at D5 and D10 but only significantly at D5 ($p<0.05$). There was a significant increase in expression of HS3ST1 at both D5 and D10 UUO (figure 2D) ($p<0.001$). Furthermore, HS3ST1 expression correlated significantly with the degree of fibrosis assessed by Sirius red staining, Pearson correlation coefficient $r=0.7881$ with $p<0.001$ (figure 2E). The other enzymes, HS2ST1, HS3ST3A and SULF1 also showed a correlation with Sirius red staining (supplementary data, figure 2). Taken together, these results suggest that there is an association between the level of fibrosis and the expression of HS modifying

enzymes. Because of the highest correlation between HS3ST1 and fibrosis, we then explored the functional implication of this change.

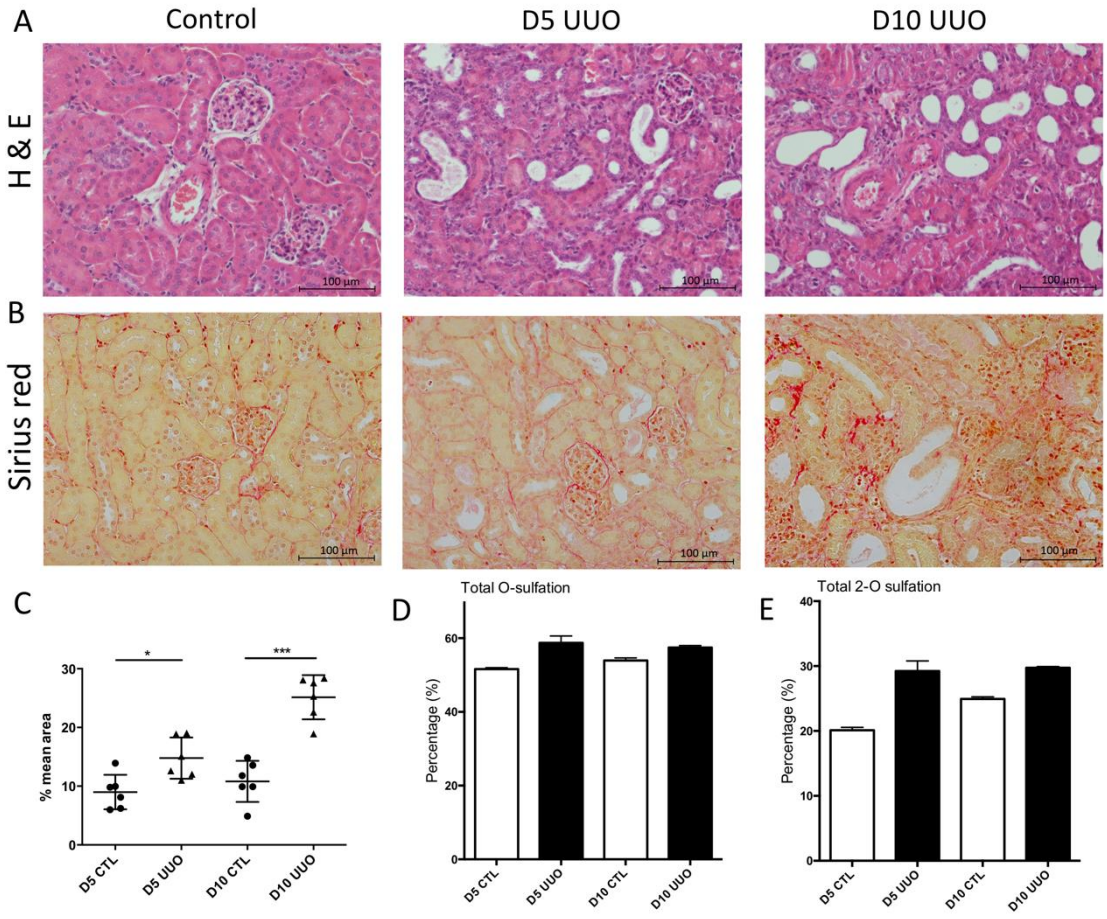

Figure 1. The development of interstitial fibrosis at D5 and D10 of UUO is accompanied by a change in HS sulfation. Representative images of Haematoxylin and Eosin staining (A) and Sirius red staining (B) of cortex from control unobstructed kidney, D5 UUO and D10 UUO. Scale bars represent 100 µm. Interstitial fibrosis was assessed by Sirius red staining (C). N=6 with 10 cortex fields analysed per section for each kidney, two-tailed unpaired t test, $p<0.05$ (*), $p<0.001$ (***). HS sulfation of 6 pooled control unobstructed kidney, D5 UUO and D10 UUO is represented as percentage of total disaccharides with error bars from technical replicates. Total O-sulfation (D) and total 2-O-sulfation (E). Results are represented as mean ±SD.

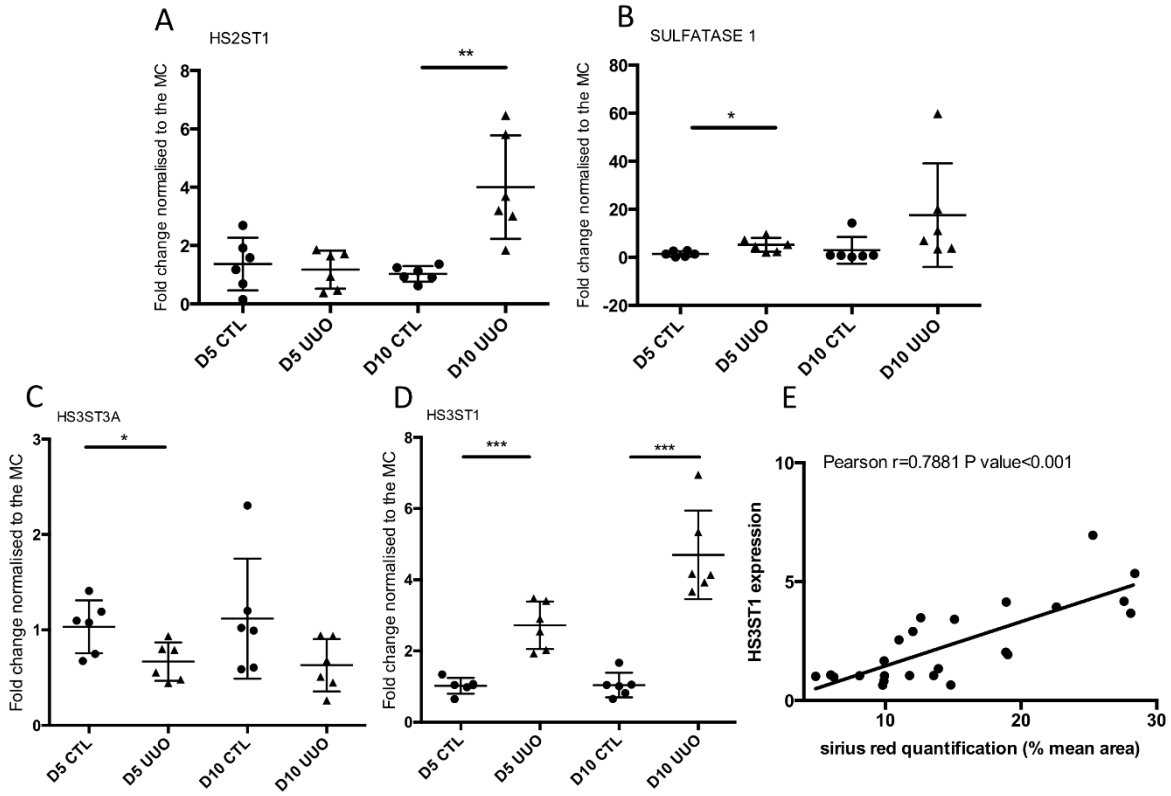

Figure 2. HS sulfotransferases are modulated at D5 and D10 UUO. Expression was adjusted to HPRT1 expression and normalised to the mean of controls (MC) N=6. Two-tailed unpaired t test with Welch's correction with $p<0.05$ (*), $p<0.01$ (**) $p<0.001$ (***). The Pearson's correlation coefficient was generated with the data from HS3ST1 expression and results from Sirius red staining.

3.3. Localisation of antithrombin binding HS within control and fibrotic kidneys

The purpose of analysing antithrombin III binding to the kidney was to localise HS 3-O-sulfation specifically resulting from HS3ST1 and HS3ST5 activity. As HS3ST5 is expressed at very low levels in the kidney, AT binding can be used as a surrogate marker of HS3ST1 activity. AT binding was seen in the luminal surface of blood vessels, on tubules, around Bowman's capsule and at the vascular pole of the glomerulus (figure 3). In D5 UUO kidney AT binding was not changed in blood vessels and could be observed within the expanded tubulointerstitium (figure 3D). The overall tubular staining decreased. The specificity of AT binding was assessed by competition with soluble heparin, which blocked AT binding to tissue sections (supplementary data, figure 3). The reduced tubular binding of AT, and by implication reduced 3-O sulfated HS, is despite the

increased expression of HS3ST1 seen in UUO kidneys. The increase of HS3ST1 expression might originate from other cells within the kidney including endothelial that produce AT binding HS [51] or M2 macrophages that express high levels of HS3ST1 [52,53] and are prominent in the UUO model [54]. However, the decrease in HS 3-O-sulfation observed in the tubular compartment was unexpected and further studied.

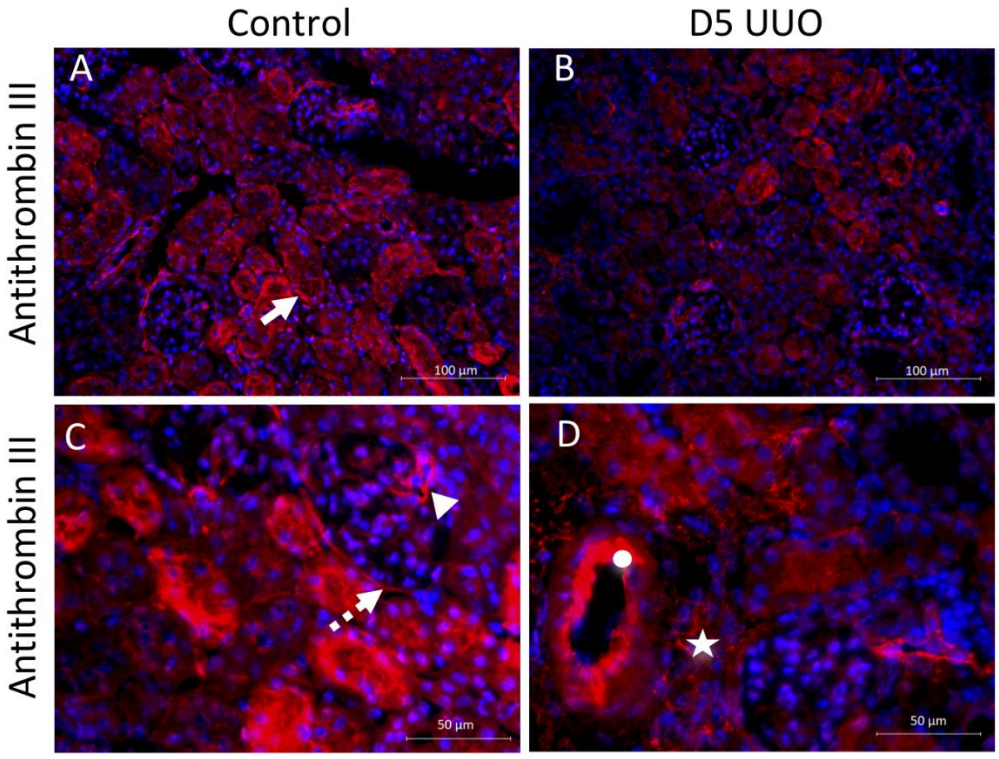

Figure 3. HSPG staining in control and fibrotic renal sections. Representative images of antithrombin III (AT) staining on cryosections from control kidney (A, C) and D5 UUO (B, D). AT was labelled with Alexa fluor 647. AT binding was detectable around Bowman's capsule (⇢), on blood vessels (❍), on the tubular basement membrane (➞), at the vascular pole of the glomerulus (▵) and in the expanded interstitium at D5 UUO (☆). N=6 with at least 5 cortex fields analysed per section for each kidney. Scale bars represent 100 and 50 µm.

3.4. Modulation of HS3ST1 expression by TGFβ1, TGFβ2/IL1β in renal epithelial cells and renal fibroblasts

To better understand the role of HS3ST1 in the development of fibrosis, we studied factors influencing HS3ST1 expression in the kidney. Primary human tubular epithelial cells screened for expression of HS3ST-family members by real time qPCR showed that HS3ST1 was the predominant enzyme, followed by HS3ST3A. HS3ST6 and HS3ST3B were expressed at low levels (figure 4A). To understand what modulates HS3ST1 expression in renal tubular epithelial cells, HK2 cells were treated with 5ng/mL TGFβ1. HS3ST1 expression was downregulated after 6 hours ($p<0.05$) and 48 hours ($p<0.05$) of treatment. HK2 cells treated with a pro-fibrotic combination of TGFβ2 (10 ng/mL) and IL1β (10 ng/mL) [55], also showed significant downregulation of HS3ST1 after 6 hours ($p<0.05$) and 24 hours ($p<0.01$) of treatment. This downregulation in the expression of HS3ST1 in tubular cells in response to pro-fibrotic stimuli is consistent with the reduced AT binding evident within the tubular compartment during the development of fibrotic disease. The down regulation of HS3ST1 expression was more pronounced in the renal fibroblast cell line NRK-49F (figure 5), with a significant decrease at 6 hours and 24 hours with both TGFβ1 and combined TGFβ2/IL1β ($p<0.05$ and $p<0.01$ respectively). In view of the reduction in tubular H3ST1 expression and the reduction in 3-O sulfation that is likely to result from this change, we next explored the function of 3-O sulfated HS in tubular cells.

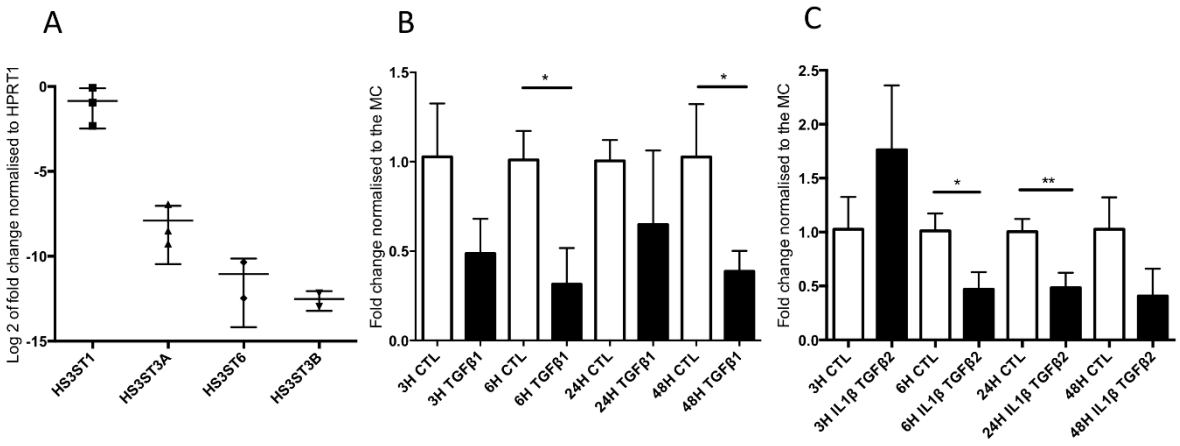

Figure 4. HS3ST1 expression in primary tubular epithelial cells isolated from human kidneys and immortalised renal epithelial cells HK2. Primary tubular epithelial cells were isolated from macroscopically healthy parts of the kidney N≥2. Results are displayed as log 2 of HS3ST1 fold

change normalised to HPRT1 (A). HK2 cells were incubated 24h in 0.5% FBS and treated for 3, 6 24 and 48 hours with 5 ng/mL TGFβ1 (B) and 10 ng/mL TGFβ2 IL1β (C) or maintained in media alone (CTL). Results are expressed by mean ±SD N=3 and were normalised to the mean of controls (MC). Two-tailed unpaired t test with Welch's correction with $p<0.05$ (*), $p<0.01$ (**).

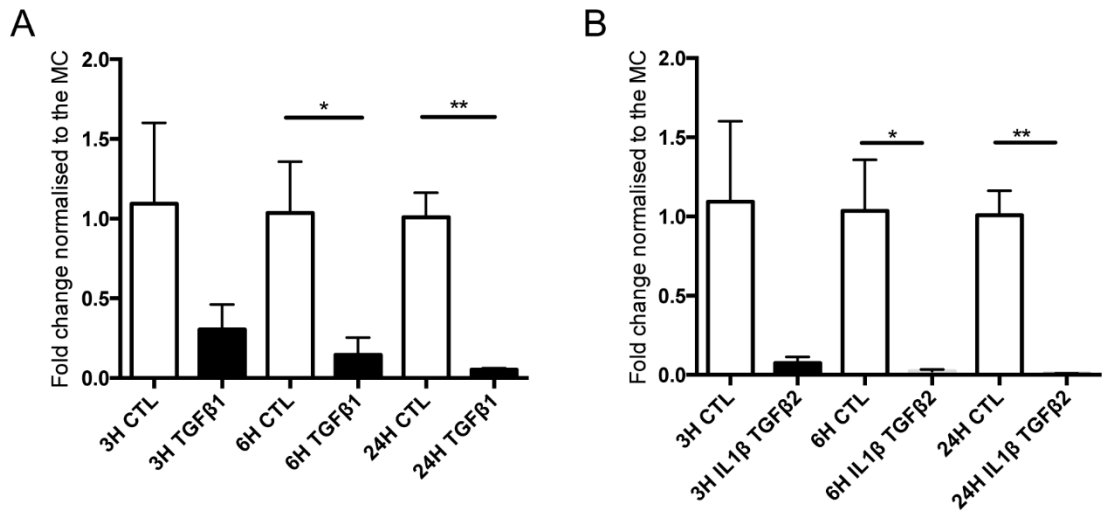

Figure 5. HS3ST1 expression is decreased in immortalised rat fibroblast NRK-49F cells following profibrotic treatments. Cells were incubated 24 hours in 0.5% FBS and treated for 3, 6 and 24 hours with 5 ng/mL TGFβ1 (A) and 10 ng/mL TGFβ2 IL1β (B) or maintained in media alone (CTL). Results are expressed by mean ±SD N=3 and were normalised to the mean of controls (MC). Two-tailed unpaired t test with Welch's correction with $p<0.05$ (*), $p<0.01$ (**).

3.5. Identification of HB-EGF as a potential growth factor modulated by HS 3-O-sulfation

The renal epithelial cell line HKC8 was stably transfected with either an empty plasmid (HKC8-CTL) or with a plasmid containing the HS3ST1 sequence (HKC8-HS3ST1). HKC8-CTL and HKC8-HS3ST1 were screened for protein expression and localisation by immunofluorescence (figure 6A). HS3ST1-flag co-localised with the cis Golgi and around the nucleus. To address the functionality of the HS3ST1 present in the HKC8-HS3ST1 cells, HS disaccharide analysis was performed after metabolic labeling of HKC8-CTL and HKC8-HS3ST1 (figure 6B). There was no detectable HS 3-O-sulfation in the HKC8-CTL but 3.7% (figure 6B) and 1.6% (supplementary data, figure 4) HS 3-O-sulfation in two clones of HKC8-HS3ST1. HB-EGF is known to bind to HSPG and can signal through STAT3. The signalling pattern was studied by assessing the phosphorylation of STAT3 (Y705). HB-EGF induced phosphorylation of STAT3 after 5 minutes

of stimulation, which then diminished by 1 hour in HKC8-CTL. However, HKC8-HS3ST1 showed a strong signal at 5 minutes, with continued phosphorylation at 1 hour in two clones (figure 6C). Taken together, these data show that the overexpression of HS3ST1 can affect HB-EGF signalling. The relevance of this finding *in vivo* was further studied using the UUO model.

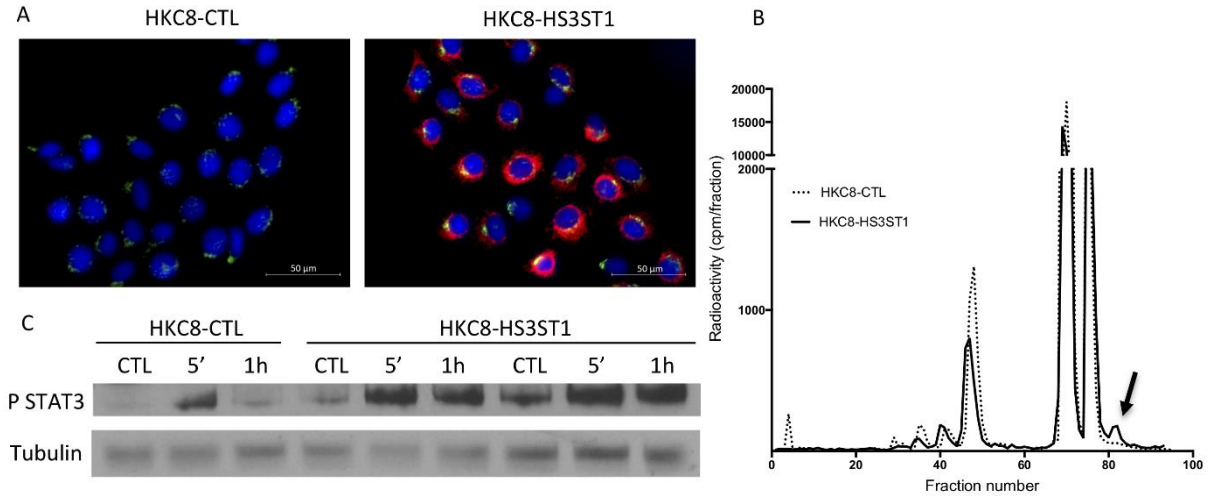

Figure 6. HS3ST1 overexpressing cells have more HS 3-O-sulfation and a different HB-EGF signalling. In stably transfected HKC8 cells, HS3ST1 expression was assessed by immunofluorescence (A) HS3ST1-FLAG is shown in red and GM130, a cis Golgi membrane marker, in green. Scale bar represents 50 µm. HS disaccharide analysis (B) showed no 3-O-sulfation in the mock (HKC8-CTL) and a small amount in the transfected cells HKC8-HS3ST1 (➔). HB-EGF signalling via P-STAT3 was analysed at 5 minutes and 1 hour in transfected cells HKC8-CTL and HKC8-HS3ST1 at 5 minutes and 1 hour, N=3 (C).

3.6. Total HS 3-O-sulfation and HB-EGF staining in renal fibrosis

HB-EGF staining was predominantly found on the basement membranes of tubules. The staining was not uniform, with some cortical tubules, most likely proximal tubules, staining more strongly than others (figure 7). A similar staining was observed at D5 and D10 UUO, but with a noticeable decrease in intensity (figure 7). Total HS 3-O-sulfation was analysed using the phage display antibody HS4C3, which recognises highly sulfated HS when 3-O-sulfation is present. The staining was similar to the AT staining but with a more intense staining in the glomerulus. Furthermore, and in agreement with the results from the AT staining (figure 3), the staining for HS 3-O-sulfation decreased during the development of fibrosis. In conclusion, both HB-EGF and HS 3-O-sulfation

are present on the tubular basement membrane and both are decreased during the development of fibrosis.

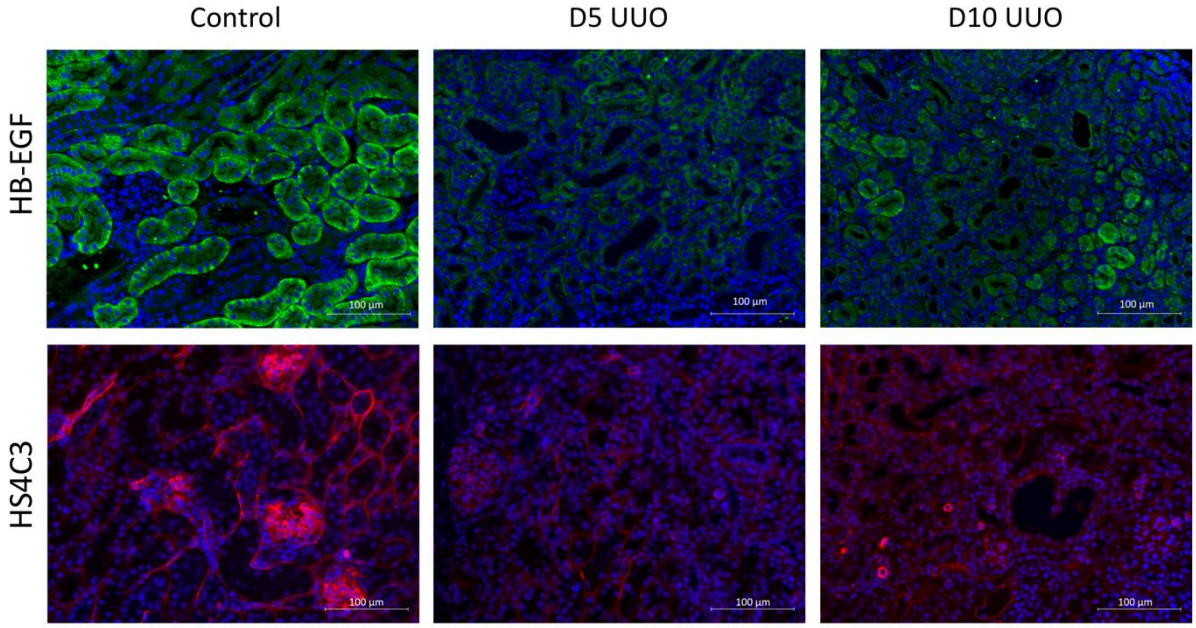

Figure 7. Staining of HB-EGF and total HS 3-O-sulfation. Representative images of HB-EGF and HS4C3 staining on paraffin embedded sections of control tissues, D5 UUO and D10 UUO. HB-EGF staining was mainly present on the tubular basement membrane. The HS4C3 antibody, which stains heavily sulfated HS, showed glomerular, vascular and tubular staining. N=6 with 10 cortex fields analysed per section for each kidney. Scale bars represent 100 µm.

4. Discussion

We hypothesise that, changes in HS O-sulfation in diseased kidneys alters growth factor binding and activity, potentially promoting either repair or fibrosis. We have shown here that there are changes in the pattern of HS sulfation during the development of renal fibrosis. Total HS O-sulfation was increased mainly due to an increase in 2-O-sulfation. Our results are consistent with the increase of HS 2-O-sulfation observed in tissue from patients with idiopathic pulmonary fibrosis [56] in which its role during tissue remodelling was proposed. 2-O-sulfation is known to be important for binding multiple growth factors for example members of the FGF family [57,58]. Due to the lack of HS 3-O-sulfation standards for the tissue disaccharides analysis, we could not analyse 3-O-sulfation during the evolution of UUO. Altered HS expression may be an attempt to increase growth factor activity and promote repair. However, in the context of persistent or repeated injury, the outcome may be fibrosis and loss of function.

The increase in HS 2-O-sulfation was mirrored by an increase in HS2ST1 expression. Surprisingly the HS sulfatase SULF1, that removes 6-O-sulfate groups, was also increased in UUO tissue. The increase in SULF1 expression can be explained by the presence of TGFβ1 in fibrotic tissue, a growth factor known to induce SULF1 expression [59]. Furthermore, HS3ST3A expression was decreased in renal fibrosis while HS3ST1 expression was increased and showed a strong correlation with the amount of fibrosis. SULF1 and HS3ST1 expression were previously found to be increased in fibrotic liver and in patients with hepatocellular carcinoma [60]. Taken together, these data highlight the potential of HS enzymes as markers of disease development.

Recently, there has been an increased interest in the function of HS 3-O-sulfation. In mouse embryos, HS 3-O-sulfation supported stem cell differentiation [61]. In the brain, HS3STs were found to regulate axonal growth cone collapse in mice [62] and neuronal development in *Caenorhabditis elegans* [63]. Furthermore, HS3STs have been extensively studied in cancer [64–66]. The impact of the increase of HS3ST1 expression was analysed with staining for 3-O-sulfation. There was an overall decrease in HS 3-O-sulfation in UUO tissue, particularly in the tubular compartment. There are several potential explanations for this decrease. First, the decrease in 3-O-sulfation might be explained by the presence of highly 2-O sulfated disaccharides that prevent HS3ST1 action and therefore by a low level of suitable HS precursor disaccharides as has been described in glomerular epithelial cells [31]. The increase of HS3ST1 mRNA might be an

unsuccessful attempt to increase the level of HS 3-O-sulfation. Second, HS 3-O-sulfation was only analysed by immunofluorescence and potentially the 3-O-sulfation was masked by growth factors bound to it. Lastly, an increase in HS3ST1 expression may occur in endothelial or infiltrating immune cells such as macrophages, masking a reduction in tubular cell HS3ST1 expression. HS3ST1 expression could be increased in some cells but decreased in others.

This study also aimed to identify regulators of HS3ST1 expression. TGFβ1 is known to be a pro-fibrotic factor [67] and TGFβ2/IL1β are implicated in endothelial to mesenchymal transition, a mechanism that contributes to fibrosis [55]. Both treatments downregulated HS3ST1 expression in renal fibroblasts and renal epithelial cells. Other enzymes such as SULF1 and SULF2 have been shown to be modulated by TGFβ1 [59] and heparanase is implicated in the regulation of TGFβ1 expression in tubular cells [68]. Taken together, these data show a relationship between TGFβ signalling and the expression of HS modifying enzymes. HS sulfation is known to influence protein binding and it is not surprising that pro fibrotic factors would be implicated in its regulation. Although we have looked at two different cell types, expression in tissues will be influenced by other cell types as well. Indeed, previous studies have shown that HS3ST enzyme expression by endothelial cells [38] and immune cells [69] is controlled by pro-inflammatory factors.

In order to study the effect of HS3ST1 expression on growth factor binding, we developed an *in vitro* model of renal epithelial cells overexpressing HS3ST1. Overexpression of HS3ST1 had an effect on HS disaccharide composition including an increase in HS 3-O-sulfation (up to 3.7%). This level of sulfation might seem low, but HS 3-O sulfation is a rare modification. In previous work on anticoagulant HS chains, 3-O sulfated glucosamine residues represented around 1% in porcine endothelial cells [51] and 6% in follicular fluid [70]. In CHO cells overexpressing HS3ST1, HS containing AT binding site represented 4% of the total HS [71].

Very little is known about the effect of 3-O-sulfated HS on growth factor function. HB-EGF can bind EGF receptor and induce STAT phosphorylation [72]. This happens rapidly and in control cells the response diminishes by 1 hour. In contrast, in cells overexpressing HS3ST1 the STAT phosphorylation is evident at 1 hour, suggesting that the cellular response to HB-EGF is altered by the presence of HS 3-O-sulfation. The mechanism of this delayed response remains to be elucidated, but a previous paper suggested that a delayed response to HB-EGF could be mediated by a second messenger such as IL-6 [73]. HB-EGF plays a role in cellular repair [43] and was

found to be protective in the development of liver fibrosis [74,75]. A decrease in tubular 3-O-sulfated HS staining was seen together with a decrease in HB-EGF during UUO. This could affect the capacity for tubular repair and worsen the severity of injury. It is also possible that in addition to reduced 3-O-sulfation, other structural changes in HS such as the increase in 2-O-sulfation are affecting HB-EGF binding. Further studies are required to elucidate precisely which HS structures can modify HB-EGF binding.

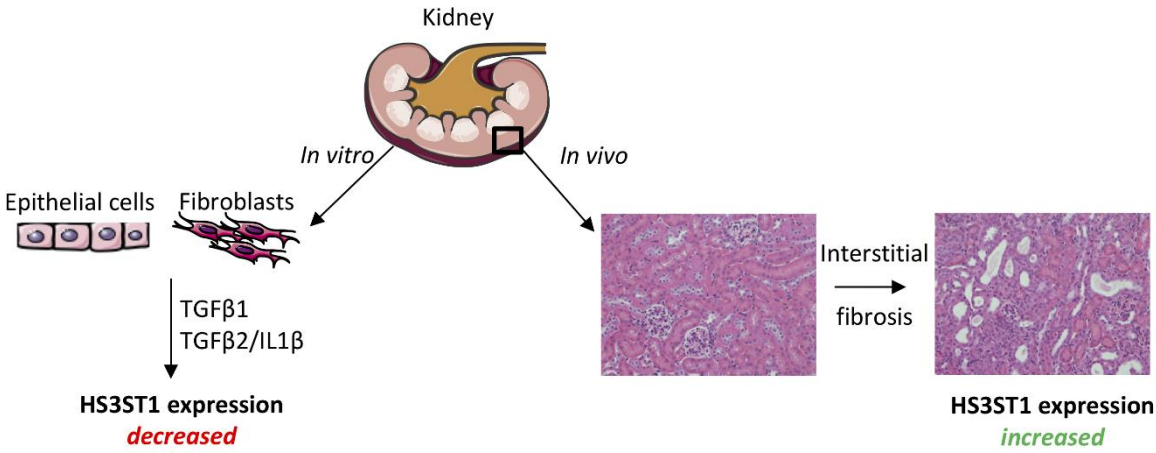

Figure 8. The complex regulation of HS3ST1 in fibrosis. HS3ST1 expression is strongly modulated in fibrosis. While *in vivo* data showed a strong correlation between HS3ST1 expression and the development of fibrosis, *in vitro* data showed a decreased expression following TGFβ1 and TGFβ2/IL1β treatment. Graphical illustrations were produced using Servier Medical Art (www.servier.com).

In conclusion, we believe this study has highlighted the complexity of the regulation of HS 3-O-sulfation and its potential role in renal fibrosis (figure 8). The strong correlation between the increase of HS3ST1 expression and the development of fibrosis, the changes in sulfation patterns during disease and the functional consequences of these changes all highlight the importance of studying HS 3-O- sulfation. A better understanding of HS biology may lead to more effective strategies to measure or modify sulfation for diagnostic or therapeutic benefit.

Acknowledgements

This work was funded by the European Commission FP7 in the framework of the Prolong Organ Survival After Transplantation, Initial Training Networks, 606979, by the Northern Counties Kidney Research Fund and by the French National Agency for Research (ANR-12-BSV8-0023). The Research was also supported by NIHR Newcastle Biomedical Research Centre. The authors would like to thank Dr Jeremy Palmer, Newcastle University, for the AT labeling help and the Bioimaging facility, Newcastle University for their support in imaging. The authors are grateful to Mona Gronning, University of Bergen for HS compositional analyses of cells and Toin van Kuppevelt, Radboud University Medical Center for providing the HS4C3 antibody.

Declarations of interest: none.

References

1 Jha V, Garcia-Garcia G, Iseki K, et al. Chronic kidney disease: Global dimension and perspectives. Lancet 2013;382:260–272.

2 Breyer MD, Susztak K. The next generation of therapeutics for chronic kidney disease. Nat Rev Drug Discov 2016;15:568–588.

3 Genovese F, Manresa AA, Leeming DJ, et al. The extracellular matrix in the kidney: a source of novel non-invasive biomarkers of kidney fibrosis? Fibrogenesis Tissue Repair 2014;7:4.

4 Bishop JR, Schuksz M, Esko JD. Heparan sulphate proteoglycans fine-tune mammalian physiology. Nature 2007;446:1030–1037.

5 Ferreras L, Sheerin NS, Kirby JA, et al. Mechanisms of Renal Graft Chronic Injury and Progression to Interstitial Fibrosis. Curr Transplant Reports 2015;2:259–268.

6 Iozzo R V, Schaefer L. Proteoglycan form and function: A comprehensive nomenclature of proteoglycans. Matrix Biol 2015;42:11–55.

7 Iozzo R V. Heparan sulfate proteoglycans: intricate molecules with intriguing functions. J Clin Invest 2001;108:165–167.

8 Lyon M, Rushton G, Gallagher JT. The Interaction of the Transforming Growth Factor- s with Heparin/Heparan Sulfate Is Isoform-specific. J Biol Chem 1997;272:18000–18006.

9 Ali S, Hardy L, Kirby J. Transplant immunobiology: a crucial role for heparan sulfate glycosaminoglycans? Transplantation 2003;75:1773–1782.

10 Massena S, Christoffersson G, Hjertström E, et al. A chemotactic gradient sequestered on endothelial heparan sulfate induces directional intraluminal crawling of neutrophils. Blood 2010;116:1924–1931.

11 Rienstra H, Katta K, Celie JW a M, et al. Differential expression of proteoglycans in tissue remodeling and lymphangiogenesis after experimental renal transplantation in rats. PLoS One 2010;5:e9095.

12 Alhasan AA, Spielhofer J, Kusche-Gullberg M, et al. Role of 6-O-sulfated heparan sulfate in chronic renal fibrosis. J Biol Chem 2014;289:20295–20306.

13 Goldberg S, Harvey SJ, Cunningham J, et al. Glomerular filtration is normal in the absence of both agrin and perlecan-heparan sulfate from the glomerular basement membrane. Nephrol Dial Transplant 2009;24:2044–2051.

14 Borza DB. Glomerular basement membrane heparan sulfate in health and disease: A regulator of local complement activation. Matrix Biol 2017;57–58:299–310.

15 Van Den Born J, Van Den Heuvel LPWJ, Bakker MA, et al. Distribution of GBM heparan sulfate proteoglycan core protein and side chains in human glomerular diseases. Kidney Int

1993;43:454–463.

16 Edge AS, Spiro RG. A specific structural alteration in the heparan sulphate of human glomerular basement membrane in diabetes. Diabetologia 2000;43:1056–1059.

17 Rops AL, van den Hoven MJ, Bakker MA, et al. Expression of glomerular heparan sulphate domains in murine and human lupus nephritis. Nephrol Dial Transplant 2007;22:1891–1902.

18 Busse M, Feta A, Presto J, et al. Contribution of EXT1, EXT2, and EXTL3 to heparan sulfate chain elongation. J Biol Chem 2007;282:32802–32810.

19 Rabenstein DL. Heparin and heparan sulfate: structure and function. Nat Prod Rep 2002;19:312–331.

20 El Masri R, Seffouh A, Lortat-Jacob H, et al. The "in and out" of glucosamine 6-O-sulfation: the 6th sense of heparan sulfate. Glycoconj J 2017;34:285–298.

21 Li JP, Kusche-Gullberg M. Heparan Sulfate: Biosynthesis, Structure, and Function. Int Rev Cell Mol Biol 2016;325:215–273.

22 Vivès RR, Seffouh A, Lortat-Jacob H. Post-Synthetic Regulation of HS Structure: The Yin and Yang of the Sulfs in Cancer. Front Oncol 2014;3:331.

23 Talsma DT, Katta K, Ettema MAB, et al. Endothelial heparan sulfate deficiency reduces inflammation and fibrosis in murine diabetic nephropathy. Lab Invest 2018;98:427–438.

24 Sugar T, Wassenhove-Mccarthy DJ, Esko JD, et al. Podocyte-specific deletion of NDST1, a key enzyme in the sulfation of heparan sulfate glycosaminoglycans, leads to abnormalities in podocyte organization in vivo. Kidney Int 2014;85:307–318.

25 Chen S, Wassenhove-McCarthy DJ, Yamaguchi Y, et al. Loss of heparan sulfate glycosaminoglycan assembly in podocytes does not lead to proteinuria. Kidney Int 2008;74:289–299.

26 Van Den Hoven MJ, Rops AL, Vlodavsky I, et al. Heparanase in glomerular diseases. Kidney Int 2007;72:543–548.

27 Masola V, Zaza G, Onisto M, et al. Impact of heparanase on renal fibrosis. J Transl Med 2015;13:181.

28 Kramer A. Induction of Glomerular Heparanase Expression in Rats with Adriamycin Nephropathy Is Regulated by Reactive Oxygen Species and the Renin-Angiotensin System. J Am Soc Nephrol 2006;17:2513–2520.

29 Van Den Hoven MJ, Rops AL, Bakker MA, et al. Increased expression of heparanase in overt diabetic nephropathy. Kidney Int 2006;70:2100–2108.

30 Gil N, Goldberg R, Neuman T, et al. Heparanase is essential for the development of diabetic nephropathy in mice. Diabetes 2012;61:208–216.

31 Girardin EP, HajMohammadi S, Birmele B, et al. Synthesis of anticoagulantly active heparan sulfate proteoglycans by glomerular epithelial cells involves multiple 3-O-sulfotransferase isoforms and a limiting precursor pool. J Biol Chem 2005;280:38059–38070.

32 Edge ASB, Spiro RG. Characterization of novel sequences containing 3-O-sulfated glucosamine in glomerular basement membrane heparan sulfate and localization of sulfated disaccharides to a peripheral domain. J Biol Chem 1990;265:15874–15881.

33 Thacker BE, Xu D, Lawrence R, et al. Heparan sulfate 3-O-sulfation: a rare modification in search of a function. Matrix Biol 2014;35:60–72.

34 Wang Z, Hsieh PH, Xu Y, et al. Synthesis of 3-O-Sulfated Oligosaccharides to Understand the Relationship between Structures and Functions of Heparan Sulfate. J Am Chem Soc 2017;139:5249–5256.

35 Mochizuki H, Yoshida K, Shibata Y, et al. Tetrasulfated disaccharide unit in heparan sulfate: Enzymatic formation and tissue distribution. J Biol Chem 2008;283:31237–31245.

36 Shworak NW, Liu J, Petros LM, et al. Multiple isoforms of heparan sulfate D-glucosaminyl 3-O-sulfotransferase. Isolation, characterization, and expression of human cdnas and identification of distinct genomic loci. J Biol Chem 1999;274:5170–5184.

37 Sepulveda-Diaz JE, Alavi Naini SM, Huynh MB, et al. HS3ST2 expression is critical for the abnormal phosphorylation of tau in Alzheimer's disease-related tau pathology. Brain 2015;138:1339–1354.

38 Krenn EC, Wille I, Gesslbauer B, et al. Glycanogenomics: a qPCR-approach to investigate biological glycan function. Biochem Biophys Res Commun 2008;375:297–302.

39 Takeda K, Hashimoto K, Uchikawa R, et al. Direct effects of IL-4/IL-13 and the nematode Nippostrongylus brasiliensis on intestinal epithelial cells in vitro. Parasite Immunol 2010;32:420–429.

40 Patel VN, Lombaert IMA, Cowherd SN, et al. Hs3st3-Modified Heparan Sulfate Controls KIT+ Progenitor Expansion by Regulating 3-O-Sulfotransferases. Dev Cell 2014;29:662–673.

41 Sagoo P, Perucha E, Sawitzki B, et al. Development of a cross-platform biomarker signature to detect renal transplant tolerance in humans. J Clin Invest 2010;120:1848–1861.

42 Einecke G, Reeve J, Sis B, et al. A molecular classifier for predicting future graft loss in late kidney transplant biopsies. J Clin Invest 2010;120:1862–1872.

43 Sakai M, Zhang MZ, Homma T, et al. Production of heparin binding epidermal growth factor-like growth factor in the early phase of regeneration after acute renal injury: Isolation and localization of bioactive molecules. J Clin Invest 1997;99:2128–2138.

44 Takemura T, Hino S, Okada M, et al. Role of membrane-bound heparin-binding epidermal growth factor-like growth factor (HB-EGF) in renal epithelial cell branching. Kidney Int

2002;61:1968–1979.

45 Celie JWAM, Katta KK, Adepu S, et al. Tubular epithelial syndecan-1 maintains renal function in murine ischemia/reperfusion and human transplantation. Kidney Int 2012;81:651–661.

46 Talsma DT, Daha MR, Van Den Born J. The bittersweet taste of tubulo-interstitial glycans. Nephrol Dial Transplant 2017;32:611–619.

47 Racusen LC, Monteil C, Sgrignoli A, et al. Cell lines with extended in vitro growth potential from human renal proximal tubule: Characterization, response to inducers, and comparison with established cell lines. J Lab Clin Med 1997;129:318–329.

48 Brown CDA, Sayer R, Windass AS, et al. Characterisation of human tubular cell monolayers as a model of proximal tubular xenobiotic handling. Toxicol Appl Pharmacol 2008;233:428–438.

49 Hijmans RS, Shrestha P, Sarpong KA, et al. High sodium diet converts renal proteoglycans into pro-inflammatory mediators in rats. PLoS One 2017;12:e0178940.

50 Sembajwe LF, Katta K, Grønning M, et al. The exostosin family of glycosyltransferases: mRNA expression profiles and heparan sulphate structure in human breast carcinoma cell lines. Biosci Rep 2018;38.

51 Marcum JA, Atha DH, Fritze LMS, et al. Cloned bovine aortic endothelial cells synthesize anticoagulantly active heparan sulfate proteoglycan. J Biol Chem 1986;261:7507–7517.

52 Martinez P, Denys A, Delos M, et al. Macrophage polarization alters the expression and sulfation pattern of glycosaminoglycans. Glycobiology 2015;25:502–513.

53 Martinez FO, Gordon S, Locati M, et al. Transcriptional profiling of the human monocyte-to-macrophage differentiation and polarization: new molecules and patterns of gene expression. J Immunol 2006;177:7303–7311.

54 Pan B, Liu G, Jiang Z, et al. Regulation of renal fibrosis by macrophage polarization. Cell Physiol Biochem 2015;35:1062–1069.

55 Maleszewska M, Moonen J-RAJ, Huijkman N, et al. IL-1β and TGFβ2 synergistically induce endothelial to mesenchymal transition in an NFκB-dependent manner. Immunobiology 2013;218:443–454.

56 Westergren-Thorsson G, Hedström U, Nybom A, et al. Increased deposition of glycosaminoglycans and altered structure of heparan sulfate in idiopathic pulmonary fibrosis. Int J Biochem Cell Biol 2017;83:27–38.

57 Ashikari-Hada S, Habuchi H, Kariya Y, et al. Characterization of Growth Factor-binding Structures in Heparin/Heparan Sulfate Using an Octasaccharide Library. J Biol Chem 2004;279:12346–12354.

58 Turnbull JE, Fernig DG, Ke Y, et al. Identification of the basic fibroblast growth factor

binding sequence in fibroblast heparan sulfate. J Biol Chem 1992;267:10337–10341.

59 Yue X, Li X, Nguyen HT, et al. Transforming growth factor-beta1 induces heparan sulfate 6-O-endosulfatase 1 expression in vitro and in vivo. J Biol Chem 2008;283:20397–20407.

60 Tátrai P, Egedi K, Somorácz Á, et al. Quantitative and qualitative alterations of heparan sulfate in fibrogenic liver diseases and hepatocellular cancer. J Histochem Cytochem 2010;58:429–441.

61 Hirano K, Sasaki N, Ichimiya T, et al. 3-O-sulfated heparan sulfate recognized by the antibody HS4C3 contribute to the differentiation of mouse embryonic stem cells via fas signaling. PLoS One 2012;7:e43440.

62 Thacker BE, Seamen E, Lawrence R, et al. Expanding the 3-O-Sulfate Proteome - Enhanced Binding of Neuropilin-1 to 3-O-Sulfated Heparan Sulfate Modulates Its Activity. ACS Chem Biol 2016;11:971–980.

63 Tecle E, Diaz-Balzac CA, Bülow HE. Distinct 3-O-sulfated heparan sulfate modification patterns are required for kal-1-dependent neurite branching in a context-dependent manner in Caenorhabditis elegans. G3 (Bethesda) 2013;3:541–552.

64 Kumar AV, Gassar ES, Spillmann D, et al. HS3ST2 modulates breast cancer cell invasiveness via MAP kinase-and Tcf4 (Tcf7l2)-dependent regulation of protease and cadherin expression. Int J Cancer 2014;135:2579–2592.

65 Hellec C, Delos M, Carpentier M, et al. The heparan sulfate 3-O-sulfotransferases (HS3ST) 2, 3B and 4 enhance proliferation and survival in breast cancer MDA-MB-231 cells. PLoS One 2018;13:e0194676.

66 Mao X, Gauche C, Coughtrie MWH, et al. The heparan sulfate sulfotransferase 3-OST3A (HS3ST3A) is a novel tumor regulator and a prognostic marker in breast cancer. Oncogene 2016;35:5043–5055.

67 Leask A, Abraham DJ. TGF-beta signaling and the fibrotic response. FASEB J 2004;18:816–827.

68 Masola V, Zaza G, Secchi MF, et al. Heparanase is a key player in renal fibrosis by regulating TGF-β expression and activity. Biochim Biophys Acta 2014;1843:2122–2128.

69 Sikora AS, Delos M, Martinez P, et al. Regulation of the Expression of Heparan Sulfate 3-O-Sulfotransferase 3B (HS3ST3B) by Inflammatory Stimuli in Human Monocytes. J Cell Biochem 2016;117:1529–1542.

70 De Agostini AI, Dong JC, Arrighi CDV, et al. Human follicular fluid heparan sulfate contains abundant 3-O-sulfated chains with anticoagulant activity. J Biol Chem 2008;283:28115–28124.

71 Datta P, Li G, Yang B, et al. Bioengineered chinese hamster ovary cells with golgi-targeted 3-O-sulfotransferase-1 biosynthesize heparan sulfate with an antithrombin-binding site. J Biol Chem 2013;288:37308–37318.

72 Knudsen SLJ, Wai Mac AS, Henriksen L, et al. EGFR signaling patterns are regulated by its different ligands. Growth Factors 2014;32:155–163.

73 Lee KS, Park JH, Lee S, et al. HB-EGF induces delayed STAT3 activation via NF-κB mediated IL-6 secretion in vascular smooth muscle cell. Biochim Biophys Acta - Mol Cell Res 2007;1773:1637–1644.

74 Takemura T, Yoshida Y, Kiso S, et al. Conditional knockout of heparin-binding epidermal growth factor-like growth factor in the liver accelerates carbon tetrachloride-induced liver injury in mice. Hepatol Res 2013;43:384–393.

75 Huang G, Besner GE, Brigstock DR. Heparin-binding epidermal growth factor-like growth factor suppresses experimental liver fibrosis in mice. Lab Investig 2012;92:703–712.

Supplementary data

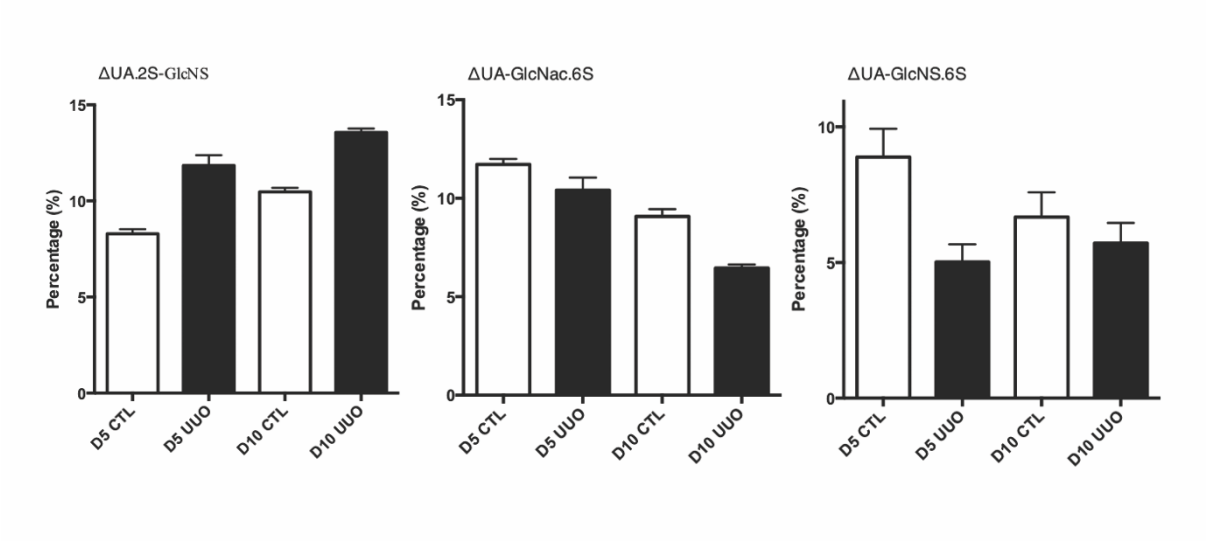

Supplementary figure 1. HS sulfation of 6 pooled control unobstructed kidney, D5 UUO and D10 UUO is represented as percentage of total disaccharides with error bars from technical replicates.

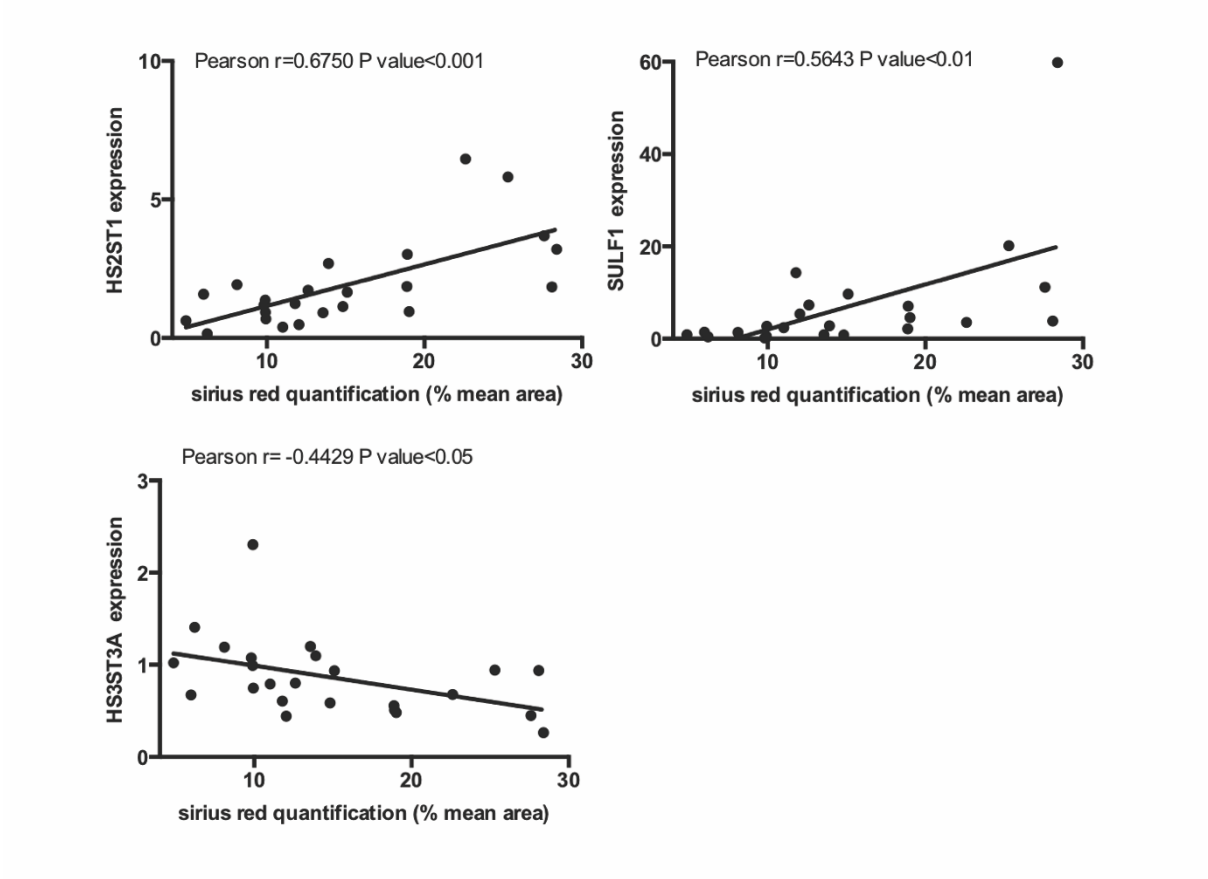

Supplementary figure 2. HS modifying enzymes correlation to Sirius red staining.

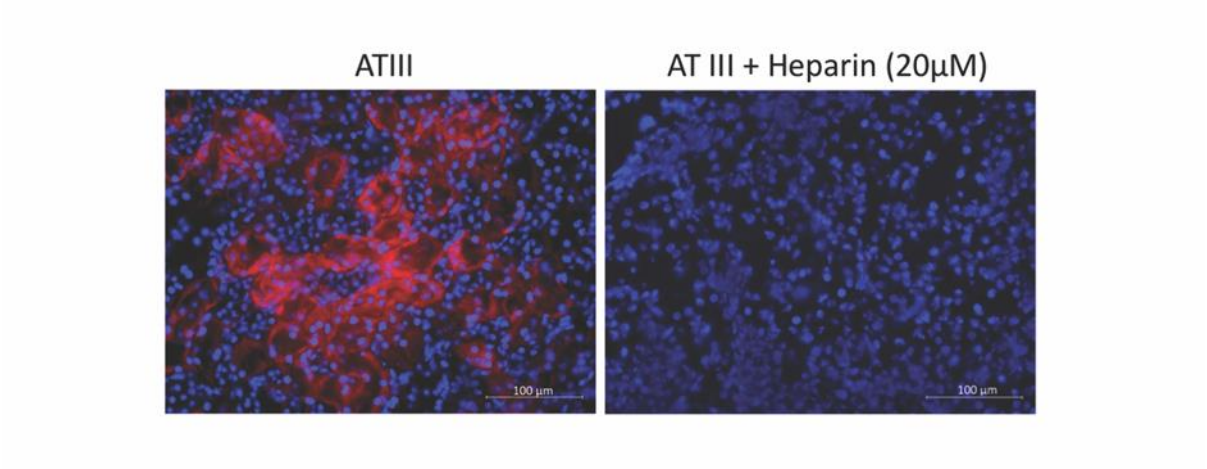

Supplementary figure 3. Antithrombin III staining specificity was assessed on mouse kidney tissue by incubating 1 hour with labelled ATIII or with ATIII and 20 µM heparin. The ATIII staining was abolished by incubating with 20 µM of heparin. Scale bars represent 100 µm.

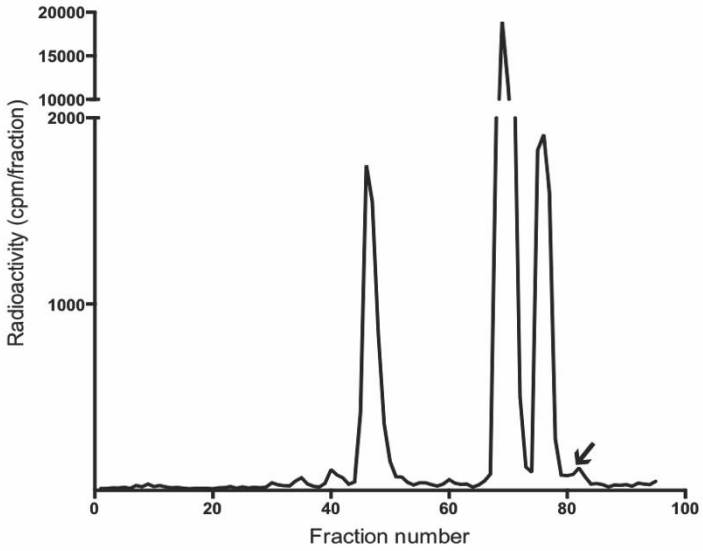

Supplementary figure 4. HS disaccharide analysis of a different overexpressing cellular clone than shown in figure 6B showed 1.6% HS 3-O-sulfation (➔)

Species	Gene name	Gene Symbol	Reference
Human	Heparan sulfate-glucosamine 3-O-sulfotransferase 3B1	HS3ST3B1	Hs01391447_m1
Human	Heparan sulfate-glucosamine 3-O-sulfotransferase 1	HS3ST1	Hs00245421_s1
Human	Heparan sulfate-glucosamine 3-O-sulfotransferase 3A1	HS3ST3A	Hs00925624_s1
Human	Hypoxanthine guanine phosphoribosyl transferase	HPRT1	Hs02800695_m1
Human	Heparan sulfate-glucosamine 3-O-sulfotransferase 1	HS3ST1 (for plasmid)	Hs01099196_m1
Human	Heparan sulfate-glucosamine 3-O-sulfotransferase 6	HS3ST6	Hs03007244_m1
Mouse	Heparan sulfate (glucosamine) 3-O-sulfotransferase 1	HS3ST1	Mm01964038_s1
Mouse	Heparan sulfate (glucosamine) 3-O-sulfotransferase 3A	HS3ST3A1	Mm000780907_s1
Mouse	Hypoxanthine guanine phosphoribosyl transferase	HPRT	Mm03024075_m1
Mouse	Sulfatase 1	SULF1	Mm00552283_m1
Mouse	Heparan Sulfate 2-O-sulfotransferase 1	HS2ST1	Mm00478684_m1

Supplementary table 1. Gene expression was determined using TaqMan probes from ThermoFisher. Hs: Homo sapiens, Mm: Mus musculus. Suffix m indicates probes that are designed between two exons whereas s defines probes that bind within a single exon.